

## **A Biomechanical Characterisation of Eccentric and Concentric Loading of the Triceps Surae Complex.**

Chaudhry, Saira

The copyright of this thesis rests with the author and no quotation from it or information derived from it may be published without the prior written consent of the author

For additional information about this publication click this link.

<http://qmro.qmul.ac.uk/jspui/handle/123456789/8401>

Information about this research object was correct at the time of download; we occasionally make corrections to records, please therefore check the published record when citing. For more information contact [scholarlycommunications@qmul.ac.uk](mailto:scholarlycommunications@qmul.ac.uk)

# **A Biomechanical Characterisation of Eccentric and Concentric Loading of the Triceps Surae Complex**

A thesis submitted for the degree of Doctor of Philosophy

by

Saira Chaudhry

School of Engineering and Material Science

Centre for Sports and Exercise Medicine

Queen Mary University of London

December 2012

## **Abstract**

This thesis presents a biomechanical characterisation of eccentric (EL) and concentric loading (CL) of the triceps surae. EL is commonly adopted as an effective treatment for Achilles tendinopathy, with notably better treatment success compared with CL. However, there is a lack of consensus about the most appropriate protocols for completing triceps surae exercises. Exercise parameters such as speed and load are important and may affect the stimuli sensed by the muscle-tendon unit and thus influence repair. This thesis aims to biomechanically characterise and compare EL and CL as a basis for trying to understand treatment effects.

A measuring system comprising motion tracking, 2D ultrasound, force plates and EMG was adopted and a semi-automatic tracking algorithm developed to track the muscle-tendon junction throughout the loading cycle (Chapter 3). Having validated the accuracy of measurements (Chapter 4), the effect of variables such as speed of exercise (chapter 5) and addition of load (Chapter 6) were assessed on Achilles tendon force, stiffness, stress, strain and force perturbations as well as muscle activation and contraction frequency (Chapter 7), in healthy subjects.

It was found that EL and CL do not differ in terms of tendon force, stiffness or strain. However, EL is characterised by lower muscle activation and by 10 Hz perturbations present within the tendon. These perturbations were found to be significantly dependent on movement speed and load applied during EL movements only. However, no effect of speed was found on tendon force, stiffness and strain during either exercise movement. Finally, temporo-spatial analysis of the calf revealed region specific variations in muscle activation during both EL and CL, with 10 Hz perturbations coming predominantly from medial soleus and medial gastrocnemius muscle activity.

These studies provide new information about the biomechanics of EL or CL, which should enhance understanding, and development, of conservative Achilles tendinopathy management.

## Acknowledgment

*Thanks to Almighty Allah and His prophet Muhammad (PBUH) and my Sarkar Mubarak to whom I would like to dedicate this thesis.*

I would like to give my sincere thanks to my supervisors, Dr. Hazel Screen and Dr. Dylan Morrissey for their guidance and much valued advice throughout the study. They have been a great source of inspiration. I am grateful for the freedom offered to explore my ideas and their continual encouragement to think beyond the limits. I could not have wished for better, more encouraging supervisors and I find myself indebted to them more than they know. Without their encouragement and effort, this thesis would not have been possible.

I would like to express thanks to Professor Roger Woledge, for introducing me to the field of biomechanics and developing my knowledge of MatLab. His generous support and optimism throughout my PhD remained a great source of inspiration in developing confidence in my abilities. His great experience in the field of biomechanics helped me greatly to understand and explore analytical skills and mathematical models to analyse huge amount of data. I would also like to give a special thanks to Professor Dan Bader for his continual support, encouragement and analytical thoughts towards the project.

These studies would not have been possible without the subjects who gave willingly of their time and Centre for Sports and Exercise medicine that helped with recruiting. My colleagues and friends were always there to discuss and help – Richard, Mark, Hassan, Ali and others were a great source of inspiration and encouragement. I would also like to thank three fellow students Dr Billy Leung for sketching the line drawings of the lower leg for this thesis, Dr Liz Sweeney and Jennifer Graham for helping in recruitment and data collection.

And finally for their love, dedication and belief in me, I owe great thanks to my family, my spiritual mother Api Jan, my mother, my sister, my daughter Hafsa, son Muhammad Haseeb and my husband Amir. I certainly would not have gotten this far without them.

## Table of Contents

Table of Contents .....	iv
List of Figures .....	viii
List of Tables .....	xvii
List of Abbreviations .....	xviii
<b>1 Chapter 1: Introduction and Literature Review .....</b>	<b>1</b>
1.1 Introduction .....	2
1.2 Anatomy .....	4
1.2.1 Triceps surae complex .....	4
1.2.2 Achilles tendon .....	6
1.2.3 Tendon composition .....	9
1.2.4 Tendon microstructure .....	10
1.2.5 Ankle .....	12
1.2.6 Joint coordinate system .....	13
1.3 Tendon mechanics .....	15
1.3.1 Mechanical Properties .....	16
1.4 Tendon pathology .....	19
1.4.1 Tendon strain injury .....	19
1.4.2 Tendon rupture .....	19
1.4.3 Tendinopathy .....	20
1.5 Achilles Tendinopathy Diagnosis .....	23
1.6 Tendinopathy Management .....	25
1.7 Loading of the triceps surae complex .....	29
1.8 Eccentric Loading .....	29
1.9 Eccentric vs Concentric Loading .....	32
1.10 Biomechanics of Eccentric training .....	34
1.10.1 Tendon Loading .....	34
1.10.2 Muscle activation .....	35
1.10.3 Force Perturbations .....	37
1.11 Optimal application of Eccentric loading? .....	39
1.11.1 Speed .....	45
1.11.2 Load .....	48
1.11.3 Dose .....	49
1.12 Conclusions .....	52
<b>2 Chapter 2: Aims and Objectives .....</b>	<b>53</b>
2.1 Aims .....	54
2.2 Objectives .....	54
2.3 Hypotheses .....	55
<b>3 Chapter 3: Materials and Methods .....</b>	<b>57</b>
3.1 Introduction .....	58
3.2 Experimental techniques and equipment .....	58
3.2.1 Electromyography .....	59
3.2.1.1 General background .....	59
3.2.1.2 Current study .....	61
3.2.2 Force Plates .....	63
3.2.2.1 General background .....	63
3.2.2.2 Current study .....	64
3.2.3 Motion tracking system .....	66
3.2.3.1 General background .....	66
3.2.3.2 Current study .....	66

3.2.3.3	Motion analysis software .....	70
3.2.4	Ultrasound.....	70
3.2.4.1	General background .....	70
3.2.4.2	Current study .....	72
3.2.4.3	Synchronising device.....	73
3.3	Experimental procedure .....	74
3.3.1	Subjects .....	75
3.3.2	Movement protocol.....	76
3.3.3	Measurement of Achilles tendon Force.....	77
3.3.4	Measurements of tendon cross sectional area .....	79
3.3.5	Measurement of tendon elongation .....	80
3.3.5.1	Ultrasound probe tracking accuracy .....	81
3.3.5.2	Tracking of the muscle-tendon junction .....	82
3.3.5.3	Semi-Automatic tracking .....	85
3.3.5.4	Total tendon length change.....	88
3.3.5.5	Technique accuracy .....	90
3.4	Data analysis .....	90
3.4.1	Registration .....	91
3.4.2	EMG analysis .....	92
3.4.3	Stress and strain .....	94
3.4.4	Stiffness .....	94
3.4.5	Measurement of perturbations.....	94
3.4.5.1	FFT optimisation .....	95
3.4.5.2	FFT of EMG .....	96
3.4.6	Statistical analysis.....	98
3.5	Results.....	98
3.5.1	Marker position .....	98
3.5.2	Achilles tendon force .....	100
3.5.3	EMG.....	100
3.5.4	Accuracy of US tracking.....	101
3.5.4.1	US and motion analysis tracking comparison .....	101
3.5.4.2	Image software and automatic tracking comparison .....	102
3.5.4.3	Reproducibility of the automatic tracking .....	103
3.5.4.4	Calcaneus and MTJ displacement.....	103
3.5.4.5	Error in ATL .....	106
3.6	Conclusions .....	106
<b>4</b>	<b>Chapter 4: Eccentric and concentric loading of the triceps surae: an <i>in vivo</i> study of biomechanical parameters .....</b>	<b>107</b>
4.1	Introduction .....	108
4.1.1	Hypotheses .....	108
4.2	Methods.....	109
4.2.1	Overview.....	109
4.2.2	Subjects .....	110
4.2.3	Data collection .....	111
4.2.3.1	Measurement of muscle activation .....	112
4.2.3.2	Measurement of tendon force.....	112
4.2.3.3	Measurement of tendon elongation.....	113
4.2.3.4	Measurement of perturbations .....	113
4.2.4	Repeated measures.....	113
4.2.5	Data analysis .....	113
4.2.6	Statistical analysis.....	115

4.3	Results.....	115
4.3.1	Achilles tendon force.....	115
4.3.2	Achilles tendon length.....	117
4.3.2.1	MTJ tracking.....	117
4.3.3	Achilles tendon force-length relationship.....	121
4.3.4	Muscle activation.....	124
4.3.5	Summary results for ATF and EMG.....	125
4.3.6	Force perturbations.....	127
4.3.7	EMG perturbations.....	132
4.3.8	Correlation between force and EMG perturbations.....	133
4.3.9	Reliability.....	134
4.4	Discussion.....	134
4.5	Conclusions.....	139
<b>5</b>	<b>Chapter 5: The effect of eccentric and concentric loading speed on the biomechanical parameters of the triceps surae.....</b>	<b>140</b>
5.1	Introduction.....	141
5.1.1	Hypotheses.....	143
5.2	Methods.....	143
5.2.1	Subjects.....	143
5.2.2	Exercise protocol.....	144
5.2.3	Data collection.....	144
5.2.3.1	Measurement of muscle activation.....	144
5.2.3.2	Measurement of tendon force.....	145
5.2.3.3	Measurement of tendon elongation.....	145
5.2.3.4	Measurement of perturbations.....	145
5.2.4	Repeated measures.....	145
5.2.5	Data analysis.....	146
5.2.6	Statistical analysis.....	147
5.3	Results.....	148
5.3.1	Normality.....	148
5.3.2	Raw data - marker position.....	148
5.3.3	Range of motion and speed.....	149
5.3.4	Achilles tendon force.....	152
5.3.5	Achilles tendon force-length relationship.....	154
5.3.6	Force perturbations.....	157
5.3.7	Muscle activation.....	159
5.3.8	Reliability.....	162
5.3.8.1	Intra-tester reliability.....	162
5.3.8.2	Inter-tester Reliability.....	162
5.4	Discussion.....	162
5.5	Conclusions.....	166
<b>6</b>	<b>Chapter 6: The biomechanical effects of varying applied load and exercise dose during eccentric and concentric triceps surae exercises.....</b>	<b>167</b>
6.1	Introduction.....	168
6.1.1	Hypotheses.....	169
6.2	Methods.....	169
6.2.1	Subjects.....	169
6.2.2	Exercise protocol- Effect of load.....	169
6.2.3	Exercise protocol- Effect of load and speed.....	170
6.2.4	Exercise protocol - Effect of varying dose.....	170
6.2.5	Data collection.....	171

6.2.6	Data analysis .....	171
6.2.7	Statistical analysis .....	171
6.3	Results.....	172
6.3.1	Effect of load .....	172
6.3.1.1	Achilles tendon force .....	172
6.3.1.2	Muscle activation .....	174
6.3.2	Effect of speed and load.....	175
6.3.3	Effect of dose.....	177
6.3.3.1	Achilles tendon force .....	178
6.3.3.2	Force perturbations .....	180
6.3.3.3	Muscle activation .....	181
6.4	Discussion .....	181
6.5	Conclusions .....	185
<b>7</b>	<b>Chapter 7: Low density high surface area electromyography of the calf during eccentric and concentric loading.....</b>	<b>186</b>
7.1	Introduction .....	187
7.1.1	Hypotheses.....	190
7.2	Methods.....	190
7.2.1	Subjects .....	190
7.2.2	Exercise protocol .....	191
7.2.3	Data collection .....	192
7.2.4	Data analysis .....	194
7.2.5	Statistical analysis .....	197
7.3	Results.....	197
7.3.1	Muscle activation maps .....	197
7.3.1.1	Mean Group Data.....	198
7.3.2	Muscle perturbations maps.....	204
7.4	Discussion .....	210
7.5	Conclusions .....	213
<b>8</b>	<b>Chapter 8: Discussion.....</b>	<b>214</b>
8.1	Introduction .....	215
8.2	Study Limitations .....	216
8.3	Hypotheses 1 and 2 .....	218
8.3.1	Method development and the Differences between EL and CL.....	218
8.4	Hypothesis 3 .....	220
8.4.1	Changing exercise speed will not influence the pattern of tendon mechanics, EMG activity or tendon perturbations. ....	220
8.5	Hypothesis 4 .....	222
8.5.1	Changing the applied load during exercise will not influence the pattern of tendon mechanics, EMG activity or tendon perturbations .....	222
8.6	Hypothesis 5 .....	226
8.6.1	Different patterns of muscle activation will be observed across different regions of the triceps surae during exercise .....	226
8.7	Future work.....	229
8.8	Conclusions .....	231
	<b>References.....</b>	<b>233</b>
	<b>Appendix I .....</b>	<b>252</b>
	<b>Appendix II .....</b>	<b>258</b>



## List of Figures

- Figure 1.1:** Anatomy of the right triceps surae muscle group and the Achilles tendon from the posterior view, A: Achilles tendon, B: Gastrocnemius incorporating i) lateral gastrocnemius head, and ii) medial gastrocnemius head, C: Soleus muscle..... 5
- Figure 1.2:** The triceps surae is an example of second class lever; here the load lies between the effort and the fulcrum. Such leverage allows us to walk, or raise or lower our body. .... 6
- Figure 1.3:** Photograph of a Human Achilles tendon..... 7
- Figure 1.4:** Human tendon showing the discrete levels of organisation modified from Screen et al 2004 with permission. .... 11
- Figure 1.5:** Description of the ankle joint showing the bones, tendons and ligaments..... 13
- Figure 1.6:** Illustration of the ankle joint complex coordinate system in the neutral position. The tibia/fibula coordinate system is denoted as XYZ whereas the calcaneus is denoted as xyz (modified from Wu et al., 2002). MC = Tibia Medial Condyle; LC = Tibia Lateral Condyle; IC = inter condyle point; TT = Tibial tuberosity; LM = Lateral Malleolus; MM = Medial Malleolus; IM = inter Malleolus. .... 14
- Figure 1.7:** Schematic drawing of the tendon mechanical response to tensile loading, indicating the typically reported range of strain values for each region (Thorpe et al., 2012, Rigby et al., 1959, Wren et al., 2001). .... 16
- Figure 1.8:** An pathology continuum model from (Cook and Purdam, 2009). This model shows the transition from a normal to degenerative tendon and possible pathways for returning the tissue to normal tendon. The potential for reversibility is reduced if the degenerative stage is reached..... 22
- Figure 1.9:** Mechanical and activation characteristics of eccentric and concentric muscle activation in triceps surae loading. During isometric loading, load torque is equal to muscle torque, during eccentric loading, load torque is greater, causing the lengthening of the muscle tendon unit. In contrast, during concentric loading, muscle torque is higher resulting in the shortening of the muscle tendon unit. ... 29
- Figure 1.10:** Three main potential factors included in eccentric loading effectiveness..... 34
- Figure 1.11:** Schematic indicating the differences in the muscle activation required to provide a certain force during EL and CL. Muscle is consistently activated more during CL, with an increasing differential at higher forces (Bigland and Lippold, 1954)..... 36
- Figure 1.12:** The amplitude of muscle force is higher during eccentric loading (EL) but unchanged with load velocity. By contrast, the amplitude of EMG is higher during concentric loading (CL) and increases with increasing velocity (Bigland and Lippold, 1954, Westing et al., 1988)..... 46
- Figure 3.1:** Diagram showing the experiment setup and the synchronization of the collection. An ultrasound probe was used to track the muscle-tendon junction (MTJ), motion analysis to track the lower limbs and ultrasound probe movements, force plates to measure the ground reaction force, and surface electromyography to measure muscle activation. To synchronise the force, EMG and motion data collected using CODA motion software with the ultrasound data, a synchronisation switch was developed. The placement of each piece of equipment on the leg is shown in the top right..... 59

- Figure 3.2:** Block diagram of the EMG setup. Muscle activation is recorded for the lower leg muscles, with a reference electrode on the lateral malleolus, and then amplified within the on-body EMG device. A transmission card is used to transfer the data over a wireless network to a PC mounted receiver. .... 62
- Figure 3.3:** Kistler Force plate coordinate axes where  $dx = 120\text{mm}$ ,  $dy = 200\text{mm}$   $dz = 54\text{mm}$  for the 9281 Force plate ( $400 \times 600$ ). Four pressure sensors named as 1, 2, 3 and 4 are used to measure the force. .... 64
- Figure 3.4:** Schematic of the CODA motion analysis system with four cameras (C1-4) receiving signals from a single active marker placed arbitrarily, in this case, within the volume. Motion analysis is generally combined with force plate data to acquire forces during movement. In such a setup, cameras are aligned to an origin between the two force platforms. The motion analysis coordinate system (XYZ) is also shown. .... 67
- Figure 3.5:** Marker placement: H = greater trochanter; FM = Femur Medial epicondyle; FL = Femur Lateral epicondyle; MC = Tibia Medial Condyle; LC = Tibia Lateral Condyle; IC = inter condyle point (virtual Marker shown in white); TT = Tibial tuberosity; LM = Lateral Malleolus; MM = Medial Malleolus; IM = inter Malleolus (virtual Marker shown in white); AT = Achilles tendon; CA = Calcaneus;  $MT_1$  = Metatarsal 1;  $MT_5$  = Metatarsal 5. The coordinate systems for tibia\fibula (XYZ) and calcaneus (xyz) are also shown..... 69
- Figure 3.6:** Block diagram of a standard ultrasound imaging system..... 72
- Figure 3.7:** Schematic diagram of the synchronization system developed for synchronising the motion analysis, force plates (FPs), EMG and US data. Manual integration (MI) of US was achieved with a switch which triggered the CODA active hub through electrical integration ( $EI_1$ ). The hub (shown with a yellow dotted line) was further electronically integrated ( $EI_2$ ,  $EI_3$ ) with the Force plates and wireless electromyography (EMG) system. .... 74
- Figure 3.8:** The exercise was performed on a wooden box placed on a recessed force plate. EMG was recorded by electrodes placed on the calf muscle and joint motion was tracked by placing CODA markers on the leg joints. An US probe tracked the MTJ, with motion tracking markers attached to monitor its position. .... 75
- Figure 3.9:** Eccentric and concentric loading of the Achilles tendon. (A) Image shows the starting position for concentric loading. Concentric loading involves shortening of the triceps surae muscle and lifting to the position in image B. (B) Image shows the starting position of EL, the triceps surae lengthens as the heel is lowered below the level of the forefoot to the position in image A during eccentric loading (open crosses show EMG electrode placed on the medial side of the leg)..... 77
- Figure 3.10:** Illustration of some of the forces acting on the foot. .... 78
- Figure 3.11:** Schematic illustration of the ATF calculation. ATF was calculated by dividing the ankle joint external moment ( $GrF \times q$ ) by the moment arm between the AT and the ankle joint centre ( $d$ ). .... 79
- Figure 3.12:** An example of the measurement of the Achilles tendon area. Image J software was used to analyse the area. The image in transverse mode was taken and the CSA is shown as area bounded between the red and yellow lines shown above. 80
- Figure 3.13:** Set up used for MTJ tracking to establish Achilles tendon length. C and C' denote the calcaneus position at full plantarflexion and dorsiflexion respectively. MTJ and MTJ' is the location of the muscle-tendon junction at full dorsiflexion

and plantarflexion. The distance between the two positions is defined as Achilles tendon length change. Tendon length at each time point was defined as the distance between C and the MTJ..... 81

**Figure 3.14:** Illustration of a wand immersed in a gel container being imaged by an ultrasound probe with motion markers attached. The position of the coil relative to the laboratory coordinate system was tracked by the motion analysis markers and also with the ultrasound probe. The tracking results from the two were compared..... 82

**Figure 3.15:** Algorithm steps for tracking MTJ displacement. The MTJ was found throughout the movement, by taking the median of the 64 intersection points as a result of 8 brightest lines on each side of the junction. .... 86

**Figure 3.16:** A) An MTJ image. B) A schematic description of the Radon transform, applied to calculate the MTJ in each frame of the US video. .... 88

**Figure 3.17:** Schematic illustration of the tracking of MTJ. The junction was imaged by ultrasound whilst synchronously determining the position and orientation of the ultrasound image. The origin was initially defined at marker 1 which was then redefined at the top left corner of the image. The distance between middle of the US probe and the corner of probe was 16 mm in the negative x direction. The distance between the marker and the skin was found to be 25mm in the negative y direction, while the thickness of the probe was 10mm in the z direction. The image was embedded into the lab coordinates. The distance between the new origin and the calcaneus marker was measured. The MTJ displacement, as measured by the algorithm, was taken away from this length and the Euclidean distance defined as the AT length was measured. .... 89

**Figure 3.18:** Manual tracking of the MTJ was carried out using Image J software. The intersection of the two lines (shown with a red star) was considered as the MTJ. The lines were drawn manually on each frame and the x, y pixel of their intersection was taken..... 90

**Figure 3.19:** Data registration was carried out with respect to the heel height. Red stars represent the minimum and maximum heel height and the green line plotted between them shows the region of single leg support taken for further analysis. .... 91

**Figure 3.20:** Description of the data registration. (A) Single leg phase data were isolated by checking the ground reaction force under the untested leg (thin red line). Z component of GrF under the test leg (bold red line) and x, y components (blue, green) are also shown. Body weight (black line) is also plotted. (B) The point of application of the force is shown including the x, y (blue, green) and z (red) components. .... 92

**Figure 3.21:** Graphs showing the sequence of analysis of EMG data for the soleus (Sol), lateral gastrocnemius (GL), medial gastrocnemius (GM) and tibialis anterior (TA) during concentric loading. (A) Raw EMG, (B) Rectified EMG, (C) Smooth EMG with a smoothing window size = 10, (D) Smoothed EMG with a smoothing window: size = 2000. .... 93

**Figure 3.22:** Description of FFT. (A) Test signal (B) Fourier transform of the signal..... 95

**Figure 3.23:** Description of the signal variance. Signal maximum variance should be equal to the cumulative summed power of that signal. Here cumulative sum power =  $VarX = 2.5359$  and maximum variance =  $SV = 2.5347$ . .... 96

- Figure 3.24:** Graphical description of the effect of smoothing the EMG signal on the resulting signal FFT. (A) Test EMG signal (B) smoothed EMG signal with a window size of 121, and its resulting FFT. Frequency components of the original signal are heavily diminished. (C) Unsmoothed EMG signal with a window size of 1 and its resulting FFT. The frequency components present in original signal can be seen here..... 97
- Figure 3.25:** Representation of all the 15 markers used on the lower leg and US probe seen perpendicular to the plane of action. The large arcs in red and green indicate the movement of 1<sup>st</sup> and 5<sup>th</sup> metatarsal with a red or green dot showing the centroid of these circles. Small arcs in black and blue represent motion of the tendon and calcaneum, whereas the big black arc is the point of application of force. Black arcs at the top are the movements of the lateral and medial tibial condyle. The US markers are shown in cyan, yellow and pink and these markers indicate any movement of probe. .... 99
- Figure 3.26:** Description of AT force (ATF) calculation. (A) ATF for two cycles of EL (blue) and ground reaction force (green) with registration of single leg and double leg support (black lines). (B) ATF during two cycles (isolated for the time points of single leg support) drawn against ankle angle (red and pink) and against heel height (blue and black). .... 100
- Figure 3.27:** EMG data during EL. Single leg phase EMG data was isolated by aligning it with the single phase data (blue) and double leg (green) of GrF and AT force (ATF). (A) ATF plotted as data points. (B) EMG data from the four muscles. .... 101
- Figure 3.28:** Relationship between the US and motion analysis tracking of the phantom. 102
- Figure 3.29:** Relationship between Automatic tracking, and tracking done using Image software..... 102
- Figure 3.30:** Relationship between tracking analyses of the same video by two different users (try 1 and try 2). .... 103
- Figure 3.31:** An example of the calcaneus movement data. Both x and y components are shown. .... 104
- Figure 3.32:** An example of the measurement of MTJ displacement using the algorithm developed. Both x and y components are shown. .... 104
- Figure 3.33:** Raw MTJ displacement (L) and force measurement. Note that the period of single leg support and double leg support (highlighted by the vertical dividing lines) are separated by the zero ground reaction force under the untested leg to ensure only the single support data is further analysed. .... 105
- Figure 4.1:** The total range of movement is shown for a typical subject during set of 2 cycles of EL. The data is shown in the laboratory coordinates system. The first and second cycle of loading selected for analysis are marked. .... 110
- Figure 4.2:** Flowchart for methods describing the data collection process for each subject. .... 111
- Figure 4.3:** Normalised AT force (ATF) plotted against ankle angle showing all repeats of each subject. A separate plot is shown for each subject. CL data is in blue and EL in red. .... 116
- Figure 4.4:** (A) Mean change in AT force (ATF) (normalised to body weight) for each subject, showing EL data in yellow and CL in cyan. The overall mean AT force is shown in red for EL and blue for CL. (B) For each subjects, the AT force during CL and EL are

- compared giving a difference value (CL - EL). The mean difference across all points is calculated (black line) and plotted with the 95% confidence intervals (white lines). ..... 117
- Figure 4.5:** MTJ tracking results for 80 videos. The X component of the movement is shown in blue whereas the y component is shown in green. Frame number is on the x axis and pixels are on y axis. .... 119
- Figure 4.6:** Achilles tendon length (ATL) and Achilles tendon force (ATF) data for all the repetitions by a single subject, plotted against time. The single leg support phase is shown in red for EL (A) and (C) and in blue for CL (B) and (D). A and B report the change in ATF with time and C and D report the change in ATL with time. .... 120
- Figure 4.7:** Mean Achilles tendon length (mATL) and mean Achilles tendon force (mATF) data for all the repetitions of the single subject in Figure 4.6, plotted against time. The single leg support phase is shown in red for EL (A) and (C) and in blue for CL (B) and (D). A and B report the change in mean ATF with time. C and D report the change in ATL. Double leg support phase is shown in green. .... 120
- Figure 4.8:** Mean plot of Achilles tendon force (ATF) against Achilles tendon length (ATL) for one subject, comparing EL (red) and CL (blue). The periods of double leg support are shown in green (EL) and black (CL). .... 121
- Figure 4.9:** Mean AT force-length graphs for each subject comparing EL data (filled red circles) and CL data (filled blue circles). .... 122
- Figure 4.10:** Summary results for mean Achilles tendon length ( $ATL \pm SE$ ) and Achilles tendon force ( $ATF \pm SE$ ) against heel height (A, B) and against ankle angle (C, D). .... 123
- Figure 4.11:** EMG is plotted against normalised time for a group of 10 subjects (each shown in a different colour). The top four panels show activity during EL and bottom four show CL data. Four muscles are shown: Sol = Soleus, GL = Lateral Gastrocnemius, GM = Medial gastrocnemius, TA = tibialis anterior. Muscle activation was higher for all calf muscles during CL as compared to during EL. 124
- Figure 4.12:** Ratios of mean EMG during EL to mean EMG during CL for each subject. (A) Soleus muscle (Sol). (B) Lateral Gastrocnemius (GL). (C) Medial Gastrocnemius (GM). (D) Tibialis anterior (TA). The red dotted line is drawn at a ratio of 1 as a reference line. .... 125
- Figure 4.13:** (A) Mean Achilles tendon force ( $ATF \pm SE$ ) and (B) Achilles tendon length ( $ATL \pm SE$ ) across all subjects and (C) resulting Force-length curve for EL (red circles) and CL (blue circles). Parallel to that, EMG data ( $\pm SE$ ) is also shown (D) for the anterior compartment during EL (red triangles) and CL (blue triangle) and the posterior compartment during EL (red circles) and CL (blue circles). .... 126
- Figure 4.14:** (A) Raw data for the normalised ATF (red and pink) and GrF/Body weight (blue and cyan) before (higher traces) and after de-trending (lower traces) during EL. (B) The corresponding amplitude of the FFT for each de-trended signal. (C) The corresponding amplitude within 1Hz bins. (D) Fourier cumulative power, from which a straight line is drawn at the maximum variance for each record, to show that the cumulative sum is equal to the variance. .... 127
- Figure 4.15:** FFT amplitude of the GrF (in  $N^2$  on y axis) within 1Hz bin for all the subjects. All repeats for each subject are shown on separate graphs. EL data is in red and CL in blue. .... 129

- Figure 4.16:** (A) All subject FFT mean data for the GrF for EL (red) and CL (blue) ( $\pm$  SE yellow for EL, cyan for CL) and (B) mean difference between the power of EL and CL for each subject (CL- EL). The mean difference across all points is calculated (black line) and plotted with the 95% confidence intervals (in white). ..... 131
- Figure 4.17:** (A) All subject FFT mean data for the ATF for EL (red) and CL (blue) ( $\pm$  SE yellow for EL, cyan for CL) and (B) mean difference between the power of EL and CL (CL- EL). The mean difference across all points is calculated (black line) and plotted with the 95% confidence intervals (in white). ..... 131
- Figure 4.18:** The differences between EMG FFT data for EL and CL, showing CL – EL for each subject, with the mean difference in black with 95 % confidence intervals in white, for the TA = tibialis anterior, Sol = Soleus, GM = medial gastrocnemius and GL = lateral gastrocnemius..... 132
- Figure 4.19:** The correlation between the FFT of the GrF and that of the TA = tibialis anterior, Sol = Soleus, GM = medial gastrocnemius and GL = lateral gastrocnemius during EL (red) and CL (blue). The red line is drawn at 5% to indicate significance level..... 133
- Figure 5.1:** Representation of all 15 markers used on the lower leg and US probe seen perpendicular to the plane of action during fast CL. The big arcs in red and green indicate the movement (centre of rotation) of 1<sup>st</sup> and 5<sup>th</sup> metatarsal with red and green dots denoting the centre of the projected circles. Small arcs in black and blue represents motion (Centre of rotation) of the tendon and calcaneum, whereas the large black arc is the point of application of force. Black arcs at the top are the movements from the lateral and medial tibia condyle. The US markers are shown (black box) in cyan, yellow and pink, monitoring any movement of probe. .... 149
- Figure 5.2:** Illustrative example of ROM (ankle angle) and GrF for a typical subject comparing EL and CL at fast (F) and slow (S) speeds..... 151
- Figure 5.3:** Normalised Achilles tendon force (ATF) data for all subjects, comparing fast eccentric (red), slow eccentric (pink), fast concentric (blue) and slow concentric (cyan). ..... 153
- Figure 5.4:** A comparison of the mean normalised Achilles tendon force (ATF) across all subjects during EL and CL at two loading speeds (CS = slow concentric, CF = fast concentric, ES = slow eccentric, EF = fast eccentric). ..... 154
- Figure 5.5:** Typical graphs for one subject, showing raw Achilles tendon force and Achilles tendon length with time (s) for (A) eccentric loading: fast in blue and slow in red and green is the double-leg support phase (B) concentric loading: fast in blue and slow in red and green shows double leg support (C) raw mean AT force-length curve for a single subject, during EL and CL at two loading speeds, EF (red), ES (pink), CF (blue) and CS (cyan). ..... 155
- Figure 5.6:** Typical graphs for one subject, showing raw Achilles tendon force and Achilles tendon length with time (s) for (A) eccentric loading: fast in blue and slow in red and green shows double leg support (B) concentric loading: fast in blue and slow in red and green shows double leg support (C) raw mean AT force-length curve for a single subject, during EL and CL at two loading speeds, EF (red), ES (pink), CF (blue) and CS (cyan). ..... 156

- Figure 5.7:** Mean power densities comparison for all subjects, during fast eccentric (red) and concentric (blue) movements, and slow eccentric (pink) and concentric (cyan) movements. .... 158
- Figure 5.8:** Mean Power density spectrums, comparing the relative magnitudes of perturbations for eccentric loading at fast (EF) and slow speeds (ES), and concentric loading at fast (CF) and slow (CS). Error bars represent the standard error of the mean. .... 159
- Figure 5.9:** Graphs of the mean EMG data for the TA= tibialis anterior, GM = medial gastrocnemius, GL = lateral gastrocnemius, Sol = Soleus for five different subjects (each shown in a different colour) during each exercise regime. The 2 panels on the far right show mean Achilles tendon force (ATF) and heel height (HHT) for the same subjects during exercise. .... 160
- Figure 5.10:** Mean EMG data for the posterior compartment consisting of the soleus (Sol), medial gastrocnemius (GM) and lateral gastrocnemius (GM) and anterior compartment consisting of tibialis anterior (TA) comparing EL and CL at fast and slow loading speeds. (CS = slow concentric, CF = fast concentric, ES = slow eccentric, EF = fast eccentric). .... 161
- Figure 6.1:** A comparison of the normalised mean AT force (ATF) ( $\pm$  SE) during EL and CL at the two loads at medium speed (The test group with the additional load were described as heavy eccentric or concentric loading (HEL or HCL). .... 172
- Figure 6.2:** Typical graph showing mean change in AT force (ATF) against change in AT length (ATL) for repeats by a single subject, during EL and CL with and without load ( $\pm$  SD) (The test group with the additional load were described as heavy eccentric or concentric loading (HEL or HCL). .... 173
- Figure 6.3:** Mean ( $\pm$  SE) power of the ground reaction force summed over 1Hz windows, comparing eccentric and concentric loading at heavy load and body weight during (A) slow, (B) medium and (C) fast speeds exercise. The test groups with the additional load are described as heavy eccentric or concentric loading (HEL or HCL). Note the increasing scale of the y axes, as the magnitude of perturbations increases with exercise speed. .... **Error! Bookmark not defined.**
- Figure 6.4:** Mean EMG ( $\pm$  SE) data from the Soleus (Sol), lateral gastrocnemius (GL), medial gastrocnemius (GM) and tibialis anterior (TA) during eccentric and concentric loading, with and without additional load. The test groups with the additional load were described as heavy eccentric or concentric loading (HEL or HCL). .... 175
- Figure 6.5:** Representation of all 15 markers used on the lower leg, and the US probe (seen perpendicular to the plane of action) during 11 repeats of CL. The big arcs in red and green indicate the movement (centre of rotation) of the 1<sup>st</sup> and 5<sup>th</sup> metatarsal, with red and green dots at the centre of these circles. Small arcs in black and blue represent motion in the tendon and calcaneum, whereas the big cyan arc is the point of application of force. The black arcs at the top are the movements from the lateral and medial tibia condyle. .... 177
- Figure 6.6:** Description of the consistency in heel height and speed of loading between the 11 repetitions during CL. A plot of the GrF under the contralateral leg (z in red, x in green and y in blue) is also shown to ensure that only the data during one leg support was analysed. The single leg loading data is marked with green lines for first cycle. .... 178

<b>Figure 6.7:</b> An example data set, showing the ATF for each repeat of EL or CL by a single subject. ....	179
<b>Figure 6.8:</b> Data for the first and last cycle of exercise are isolated to show more clearly the change in ATF over 11 repeats of exercise for (A) EL and HEL and (B) CL and HCL. The test groups with the additional load were described as heavy eccentric or concentric loading (HEL or HCL). ....	179
<b>Figure 6.9:</b> A typical record of GrF perturbations over the 1 <sup>st</sup> and 11 <sup>th</sup> cycles of exercise for a subject completing EL and CL with and without additional load. High magnitude perturbations are evident at 10 - 12 Hz during HEL at both cycle 1 and 11. ....	180
<b>Figure 7.1:</b> EMG electrode and motion marker arrangement, set up on the lower leg. Motion markers are attached to each of 16 pairs of sEMG electrodes to enable tracking of position as well as muscle activation. In addition the usual lower limb maker protocol is applied. ....	187
<b>Figure 7.2:</b> Schematic drawing of the calf muscle showing the positioning and orientation of the 16 channel dual EMG set up. A motion tracking marker was placed on each electrode pair to track the position in space. ....	193
<b>Figure 7.3:</b> The raw EMG signal (blue), alongside the rectified and smoothed data (red) from all 16 channels across the triceps surae during three cycles of CL. ....	194
<b>Figure 7.4:</b> Colour representation of each channel of EMG activity across the calf muscle, with an intensity indicator. ....	195
<b>Figure 7.5:</b> (a) Calf colour map during CL and (b) stick figure with the colour map representing calf muscle activation shown in the correct location. All in the laboratory coordinates. ....	196
<b>Figure 7.6:</b> Colour maps depicting EMG activity across the triceps surae muscle during 3 cycles (C1-3) of EL for a single subject. Only the loading phase is depicted, as indicated by the coloured dots in the top left schematic. The guide to relative colour map intensities is also shown on the bottom left, where 1 is high and 0 is low. ....	199
<b>Figure 7.7:</b> Colour maps depicting EMG activity across the triceps surae muscle during 3 cycles (C1-3) of CL for a single subject. Only the loading phase is depicted, as indicated by the coloured dots in the top left schematic. The guide to the relative colour map intensities is also shown on the bottom left, where 1 is high and 0 is low. ....	200
<b>Figure 7.8:</b> Mean EMG map data during EL and CL for all subjects. The guide to relative colour map intensities is also shown at the bottom, where 1 is high and 0 is low. ....	201
<b>Figure 7.9:</b> Mean standard deviation of muscle activity data between either a single subject repeats (within subjects) or across subject mean data (between subjects) shown with respect to range of movement. ....	204
<b>Figure 7.10:</b> Two typical records of GrF perturbations for a subject completing EL and CL. High magnitude perturbations are evident at around 10 - 12 Hz during EL. ....	205
<b>Figure 7.11:</b> A series of typical FFT outputs, from the EMG signal in each of the 16 channels attached on the triceps surae during EL. The Y axis indicates the Power of the signal ( $mV^2$ ) and the X-axis indicated the frequency in Hz. Channel numbers are shown above each graph. The point of peak power, taken as a mean of both cycles from each channel, is marked with red lines. ....	206



- Figure 7.12:** A series of typical FFT outputs, from the EMG signal in each of the 16 channels attached on the triceps surae during CL. The Y axis indicates the Power of the signal ( $mV^2$ ) and the X-axis indicated the frequency in Hz. Channel numbers are shown above each graph. The point of peak power, taken as a mean of both cycles, from each channel is marked with red lines..... 207
- Figure 7.13:** The FFT of the EMG from each channel across the triceps surae was taken, and the magnitude of each signal frequency (shown below each map: 2 - 30Hz) shown pictorially during EL..... 208
- Figure 7.14:** The FFT of the EMG from each channel across the triceps surae was taken, and the magnitude of each signal frequency (shown below each map: 2 - 30Hz) shown pictorially during CL..... 209
- Figure 8.1:** Schematic showing how perturbation magnitude and frequencies may vary during EL with tendon (A) load and (B) speed. Tendon stiffness can be increased by either increasing exercise speed, or exercise load, leading to higher magnitude, more tuned perturbations in the tendon during fast, heavy eccentric loading. .... 225
- Figure 8.2:** Schematic of the triceps surae muscle, in which the site of mid-portion Achilles tendinopathy is highlighted in red, whereas the location of the ~ 10 - 12 Hz perturbations are highlighted in green. It is speculated that EL may facilitate tendon repair in response to a combination of two biomechanical phenomenon, applied strain originating predominantly from the connection of medial gastrocnemius, and perturbations mainly originating at the site of medial soleus. Current findings indicate that perturbations may be focused on the free tendon and site of tendinopathy; a possible mechanism behind EL effectiveness as compared to CL..... 228

## List of Tables

<b>Table 1.1:</b> List of those treatments available for tendinopathy which have been investigated with controlled studies. ....	26
<b>Table 1.2:</b> Details of the range of reported EL studies highlighting dose parameters. ....	42
<b>Table 1.3:</b> Summary of the differences between the EL protocol employed, derived from Table 1.2. ....	45
<b>Table 1.4:</b> Review of the notable studies conducted to investigate the effect of exercise variables during EL and CL. Note that most studies have measured isometric, only one study has investigated clinically relevant loading conditions.....	51
<b>Table 3.1:</b> Summary of the studies outlining a biomechanical analysis of the Achilles tendon/Gastrocnemius tendon.....	84
<b>Table 4.1:</b> Parameters extracted and calculated from the data.,.....	110
<b>Table 4.2:</b> Subject characteristics .....	110
<b>Table 4.3:</b> Order of exercise as determined by each subject making a blind selection from an envelope. ....	112
<b>Table 4.4:</b> Summary of the mechanical properties of the AT during CL and EL.....	123
<b>Table 5.1:</b> Summary of the GrF and range of motion for CL and EL at each speed.....	150
<b>Table 5.2:</b> Summary of the mechanical properties of the AT during CL and EL at the two loading speeds.....	156
<b>Table 6.1:</b> Summary of the results comparing eccentric and concentric loading at two loads. ....	174
<b>Table 7.1:</b> Demographic data for each participant and detail of the order in which they completed the testing exercises .....	191
<b>Table 7.2:</b> Group mean EMG data at selected ankle angle .....	202
<b>Table 7.3:</b> Group mean EMG data at selected ankle angle .....	202
<b>Table 8.1:</b> Summary of thesis findings.....	232

## List of Abbreviations

AT	Achilles tendon
ATL	Achilles tendon length
ATF	Achilles tendon force
BWt	Body weight
CL	Concentric loading
CSA	Cross-sectional area
EL	Eccentric loading
EMG	Electromyography
FFT	Fast Fourier transforms
FOV	Field of view
GrF	Ground reaction force
GL	Lateral gastrocnemius
GM	Medial gastrocnemius
HCL	Heavy concentric loading
HEL	Heavy eccentric loading
K	stiffness
$L$	Muscle tendon junction change
$\Delta L_i$	Change in length
MTJ	muscle-tendon junction
$\text{rad.s}^{-1}$	radian per second
ROM	range of movement
SD	Standard deviation
SE	Standard error
Sol	Soleus
TA	Tibialis anterior
$\epsilon$	Strain
fc	Cut-off frequency

## **Chapter 1: Introduction and Literature Review**

## **1.1 Introduction**

Achilles tendinopathy is a painful condition occurring in and around the Achilles tendon (AT), thought to be a failed healing response (Maffulli et al., 1998, Cook and Purdam, 2009). It is often characterized by disruption of collagen fibres, an increase in non-collagenous matrix and random proliferation of tenocytes, as shown by tendon thickening, disordered tendon fibrils and neo-vascularisation on ultrasound imaging. Excessive repetitive overloading - often after a period of relative under load - of the Achilles is considered one of the main stimuli leading to tendinopathy. As such it is common in athletes, accounting for 6 - 18 % of all running injuries (Longo et al., 2009). It has been reported that the incident rate of Achilles tendinopathy is 2.35 per 1000 Dutch general practitioner registered adult patients with 35% of the cases related to sport activity (de Jonge et al., 2011b). However, it also occurs in non-athletes, with around 33 % of tendinopathic presentations occurring in sedentary individuals (Kingma et al., 2007).

Achilles tendinopathy is prone to recurrence, as current treatments are only partially successful. The main conservative treatment of choice is heavy load eccentric loading (EL) of the triceps surae (Rowe et al., 2012), shown to be effective in various controlled clinical trials and systemic reviews, with a variable success rate of 60 - 82 % (Fahlstrom et al., 2003, Sayana and Maffulli, 2007, Kingma et al., 2007). The EL protocol was first proposed by Stanish et al back in 1986 (Stanish et al., 1986), and the first controlled trial carried out by Alfredson in 1998 (Alfredson et al., 1998) confirming the superior outcomes of EL over concentric loading (CL). Since this time, a number of studies have evaluated the efficacy of EL, providing a sufficient level of evidence to support this treatment method (Rowe et al., 2012)

Eccentric loading involves the lengthening of the muscle-tendon unit during the application of load. This is the opposite of CL where the muscle-tendon unit shortens during use, and also differs from isometric exercise, in which the muscle-tendon unit length remains unchanged. EL has been shown to result in positive clinical outcomes for Achilles and other tendinopathies, improving pain, patient satisfaction and function when compared with CL (Rowe et al., 2012, Yu et al., 2012). However, it is unclear why EL results in better therapeutic outcomes than CL, nor are the mechanisms underlying symptomatic improvement well understood. In addition, there has been inadequate reporting - and even more limited investigation - of variations in training parameters such as frequency, speed of movement, load, dose and painful limits.

The effect of training protocol variations on tendon adaptation and remodelling are unclear, but it is reasonable to predict that the different mechanical stimuli resulting from such variations may induce different therapeutic stimuli. Force is generated by the contractile machinery of the muscles, and is transferred to bones via tendons. This process is necessary to produce moments about joints and is required in order to make joint movement possible (Nigg and Herzog, 2007). Muscles, bones and tendons work together in the lower leg to bear the stresses associated with walking, running and jumping (Kirkendall and Garrett, 1997). This chapter explores, evaluates and discusses the research literature of importance for a thesis that is focussed on biomechanical and physiological investigation of the mechanisms underpinning the main conservative treatment method for tendinopathy. The main focus is on the role of EL in managing tendinopathy and knowledge we have about the use of this particular exercise regime. Initially, the anatomy of the investigated muscles and tendon is discussed, followed by tendon disorders and their management.

## 1.2 **Anatomy**

This section gives a brief overview of the anatomy of the triceps surae muscle, Achilles tendon and ankle.

### 1.2.1 **Triceps surae complex**

'Triceps' is Latin for three heads and 'surae' means calf, hence the triceps surae (TS) complex describes the combination of the two heads of the gastrocnemius muscle and one head of the soleus muscle. The gastrocnemius and soleus shape the posterior part of the leg known as the calf, and insert via the common Achilles tendon into the calcaneus of the heel (Jozsa and Kannus, 1997). The gastrocnemius originates above the knee joint, from the distal part of the femur (*Figure 1.1*). It is a superficial muscle (*Figure 1.1*) with two prominent bellies that form the proximal curve of the calf, arising from a lateral and medial head. The lateral head originates from the lateral surface of the lateral femoral condyle and the medial head from the popliteal surface above the medial condyle. The lateral head contains a sesamoid bone which articulates with the lateral femoral condyle, the fabella, in about 25 % of people (Cunningham and Romanes, 1986). The two muscle bellies remain separate from each other, with the medial being larger and longer than the lateral belly. Both heads end near the middle of the leg on the posterior surface of a common thin tendon (Jamieson et al., 1971). This tendon then fuses with the calcaneus to form the 'tendo calcaneus' or, as it is more commonly named, the Achilles tendon (*Figure 1.1*).

The soleus originates from the lower leg and is deep to the gastrocnemius, on the posterior surface of the calf (Jamieson et al., 1971) (*Figure 1.1*). It originates in an extensive cone shape from the superior tibia, fibula and interosseous membrane. The muscle between the gastrocnemius and soleus is the plantaris muscle. It is a small muscle and arises from the

popliteal surface of the femur. The plantaris is usually hidden under the lateral head of the gastrocnemius and is occasionally absent (Cunningham and Romanes, 1986).

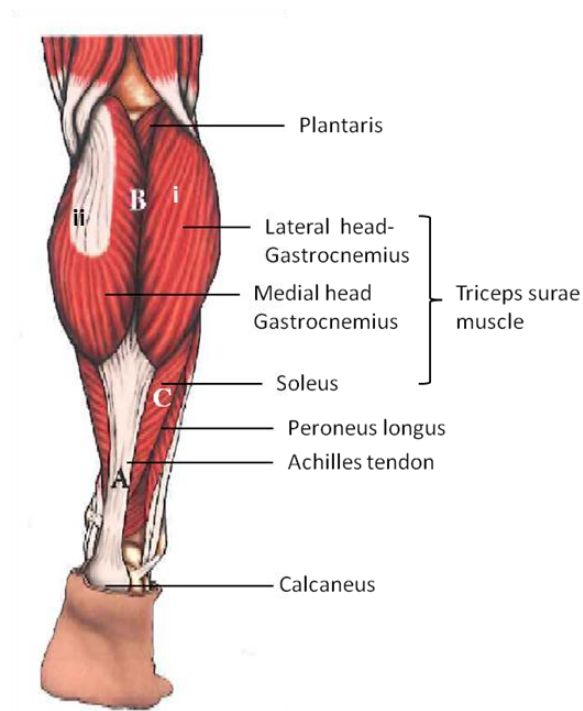


**Figure 1.1:** Anatomy of the right triceps surae muscle group and the Achilles tendon from the posterior view, A: Achilles tendon, B: Gastrocnemius incorporating i) lateral gastrocnemius head, and ii) medial gastrocnemius head, C: Soleus muscle.

Like all muscles, the triceps surae has a very good blood supply, and plays an important part in returning the venous blood from the lower limb. The soleus also contains considerable venous plexi (Cunningham and Romanes, 1986).

The actions of the triceps surae are to pull the heel up and thus extend the distal foot downward, therefore providing the propelling force in running and jumping. The triceps surae is classified as a second class lever as the load lies between the fulcrum and the effort. The main function of the triceps surae is to overcome the resistance of the load (body weight) with the effort being produced by calf muscle contraction. The muscles act around the fulcrum of the metatarsal heads to raise the weight of the body on to the toes



(Figure 1.2). The gastrocnemius has a particular role in high force activities, while the soleus is more active during endurance activity such as walking. Both muscles act with the dorsiflexors of the ankle joint to stabilize the ankle, while the gastrocnemius is also involved in knee flexion. When the knee is bent the gastrocnemius becomes ineffective as a plantar flexor of the ankle, at which point the soleus becomes the main muscle concerned (Cunningham, 1986).

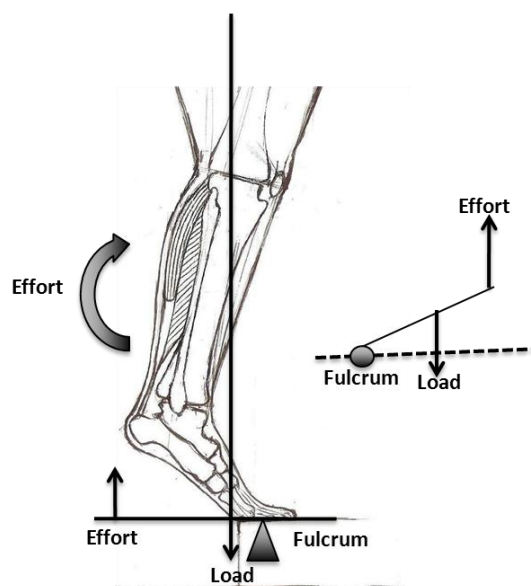


**Figure 1.2:** The triceps surae is an example of second class lever; here the load lies between the effort and the fulcrum. Such leverage allows us to walk, or raise or lower our body.

### 1.2.2 Achilles tendon

Achilles, the hero of Homer's 'Iliad', lends his name to the Achilles tendon (O'Brien, 1992). In an attempt to make him immortal, Achilles' mother dipped him in the river Styx. However, he was left vulnerable at the heel, where she held him. This part became the cause of his death, when a poisoned arrow fired by the Trojan prince Paris embedded in his heel (Shampo and Kyle, 1992). This has given rise to the figure of speech that maintains that the Achilles tendon is a person's weakest point.

The Achilles tendon (AT) is the thickest and strongest tendon in the human body (O'Brien, 1992). It is the fibrous tendon that connects the gastrocnemius and soleus muscles to the heel (*Figure 1.1*), hence if the tendon is ruptured, it causes severe locomotor disability (Pagenstert et al., 2010). The most proximal part of the AT arises from the two heads of the gastrocnemius muscle, to form a flat and broad band of connective tissue. Moving distally along its length, it becomes more rounded and begins to narrow (Doral et al., 2010), as the soleus muscle fibres insert on its anterior/ventral surface. The small plantaris muscle also connects to the AT in some individuals, or runs alongside it. The distal part of the AT attaches to the calcaneal bone through a fibro-cartilaginous region, known as the teno-osseous junction. The healthy AT is brilliant white in colour and has an elastic texture (Jozsa and Kannus, 1997). It is alternatively known as the heel cord, heel tendon or calcaneal tendon (*Figure 1.3*).



**Figure 1.3:** Photograph of a Human Achilles tendon.

The AT is one of the most highly loaded tendons in the human body, facing high stresses during locomotion (Komi et al., 1992). It is therefore is one of the most frequently ruptured tendons (Pagenstert et al., 2010). Achilles tendon injuries usually cause severe pain and disability and there are indications that the incidence of rupture has been rising in Western society during recent years (Maffulli et al., 2010b).

Muscle and tendon work together to make joint movement possible; the inclusion of tendon plays a role in efficient transfer of muscular force with minimal energy loss (Alexander and Bennet-Clark, 1977). It provides the capacity to modulate muscle activity and allows the muscle belly to be situated away from the bone where there is more space.

Tendon has a specialised structure at its insertion with either muscle or bone. The site of the attachment of the muscle and tendon is known as the myotendinous junction (muscle-tendon junction) while tendon attachment with bone is named the teno-osseous, osteo-tendinous or teno-periosteal junction. At the osteo-tendinous junction, the structures changes from tendon to fibrocartilage, mineralised fibrocartilage and finally bone (Benjamin et al., 1986).

Tendon is often isolated from its surroundings by a connective tissue sheath, which provides protection and reduces friction during gliding. If the sheath is absent, tendon is commonly covered in a loose connective tissue called paratenon; a structure of gliding membranes continuous with the fascial envelope of the muscle proximal to the tendon (Kannus, 2000). Lubrication is provided by the synovial cells of the paratenon, and the paratenon functions as an elastic sleeve, allowing the tendon to move freely from surrounding tissues (Hess et al., 1989).

The epitendon is deep to the paratenon, being a fine connective tissue layer which covers the entire tendon. Contiguous with the epitendon is the endotenon, which surrounds the bundles of fascicles which constitute the tendon (Kastelic et al., 1978). Each of these layers carries blood vessels, lymphatic vessels and nerves, which normally pass up and down through the body of the tendon (Elliott, 1965, Hess et al., 1989). Tendons are quite poorly

vascularised in comparison to many other tissues, such as skeletal muscle. However, blood capillaries usually enter the tendon through the endotendon and paratendon, from the myotendinous junction region (Vailas et al., 1978). The Achilles tendon has three blood supply sources, the myotendinous junction, vessels in surrounding connective tissues and the osteo-tendinous junction (Doral et al., 2010).

### **1.2.3 Tendon composition**

Tendon consists of collagen and elastin fibres embedded within a proteoglycan rich matrix. This matrix is sometimes referred to as ground substance, and in addition to proteoglycans, it contains a wide range of other, small molecules. Type I collagen constitutes at least 60 % of the dry mass of the tissue and approximately 95 % of the total collagen, while elastin accounts for approximately 1-2 % of the dry mass of tendon (Riley et al., 1994, Hess et al., 1989). Other collagens found in small quantities in tendon include types II, III, V, VI, IX, X and XI many of which are particularly found in specialised areas such as the fibrocartilage at the insertion, where they may function to dissipate stress concentrations at the hard tissue interface (Waggett et al., 1998). Collagen provides tendon with its tensile strength, whereas elastin is thought to contribute to the positional recovery of the crimped collagen fibres, following tendon extension (Butler et al., 1978) .

Tendon is approximately 70 % water by wet weight. Water plays a vital role in keeping the tendon hydrated which enables the sliding of the tendon with its sheath or surrounding tissue (Blevins et al., 1997). Proteoglycans are of particular importance for maintaining hydration. These are negatively charged hydrophilic molecules, that can entrap up to fifty times their weight in water (Doral et al., 2010). If soft tissues becomes dehydrated (*in vitro*), there is an increase in its stiffness and a concomitant dramatic reduction in the

mechanical strength of the tendon (Hoffman et al., 2005, Nicolle and Paliarne, 2010). Water in tendon also assists in tissue nutrition and provides protection from the compressive forces surrounding the tendon.

Tendons consist of a number of different cells, mainly tenocytes and tenoblasts which account for approximately 90 - 95 % of the total cell count. The remaining cells are chondrocytes at the osteotendinous junction, synovial cells in the sheath and also endothelial cells and smooth muscle cells (Jozsa and Kannus, 1997). As the tendon matures, the collagen fibres increase in size and increase in thermal stability, leading to a subsequent decrease in elasticity (Vogel, 1983). It is possible that these changes are responsible for the increased risk of injury in mature tendon. Some of these changes may be counteracted by eccentric exercise (Langberg et al., 2007), although there is also evidence that mature tendons have limited capacity for alteration and may even be damaged by exercise (Jarvinen et al., 2001, Smith et al., 1999). It is evident that some tendons have high physical demands placed upon them; however the demands on tendons vary significantly. Tendons from particular sites, such as the elbow, knee, ankle and shoulder experience the highest loads, are most likely to demonstrate degenerative changes, which increase in severity with age (Thorpe et al., 2010).

#### **1.2.4 Tendon microstructure**

The physical properties of tendon are dependent on its micro structure (Hess et al., 1989). The main matrix component, collagen, has fibres which are packed closely together, parallel to the direction of force (Riley, 2004). They are arranged in a highly organised hierarchy of successively larger structural units (*Figure 1.4*), bound together by collagen cross-links and interspersed with blood vessels and nerve fibres (Kastelic et al., 1978). The

collagen molecule is the smallest structural unit and these align end-to-end in a quarter-staggered array to build fibrils. Fibrils have a diameter of 10 to 500 nm depending on the age, location and species from which the tendon is sampled (Parry et al., 1978, Moore and De Beaux, 1987). Fibrils join together to form fibres, which in turn aggregate to form 'fascicles', which are bound together by a thin layer of loose connective tissue known as the endotenon. While the majority of collagen fibres run parallel to the load axis a small proportion of fibres run transversely, and there are spirals and plait-like formations in many tendons (Jozsa and Kannus, 1997), to provide resistance against transverse, shear or rotational forces that may act on the tendon. The hierarchical composite organisation of the fibres acts as a fail-safe system, by which failure of one or a few fibre bundles does not extensively reduce the strength of the whole tendon (Riley, 2004).

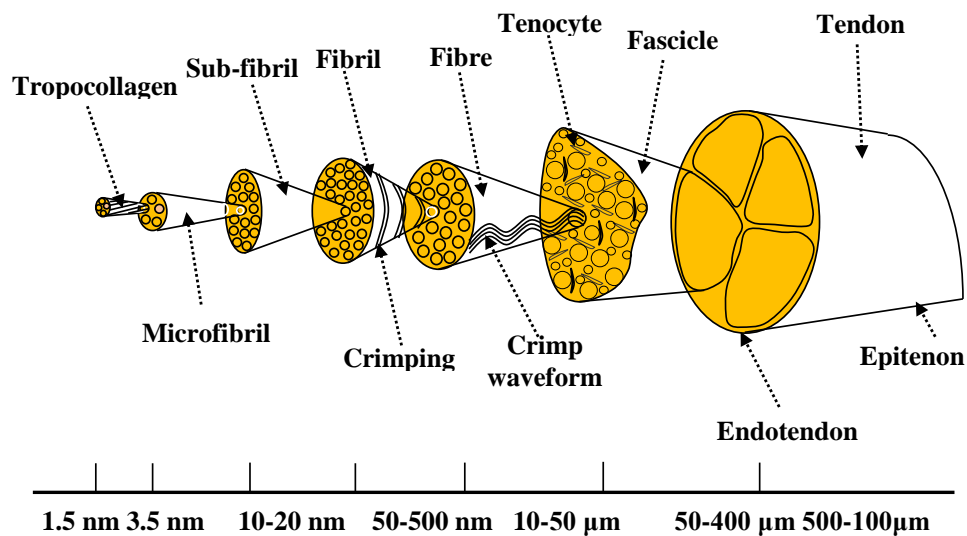


**Figure 1.4:** Human tendon showing the discrete levels of organisation modified from Screen et al 2004 with permission.

### 1.2.5 Ankle

The ankle is a complex articulation consisting of bones, ligaments, tendons and muscles (*Figure 1.5*). The joint acts like a hinge, and consists of four bones; the calcaneus, talus, tibia, and fibula. The tibia and fibula are the long bones of the lower leg, and the fibula, a relatively thinner bone, is lateral to the tibia (Jamieson et al., 1971). These two bones are bound together by the ligaments and the interosseous membrane. The talus is a wedge-shaped bone that fits into the mortise formed by the bound tibia and fibula. The tibia, fibula and talus are the bones involved in talo-crural articulation, which enables dorsiflexion and plantarflexion. The key ankle muscles are the calf muscles (gastrocnemius and soleus) which connect to the calcaneus by the AT, and the peroneals (the posterior tibialis and anterior tibialis) which are on the outside edge of the ankle (Jamieson et al., 1971).

The tibialis anterior, extensor digitorum longus, extensor hallucis longus and peroneus tertius are the main muscles responsible for dorsiflexion, while the gastrocnemius, soleus, tibialis posterior, fibularis brevis and longus, flexor hallucis longus, flexor digitorum longus and plantaris act during plantarflexion. Multiple ligamentous attachments, muscular attachments and a fibrous capsule maintain the articulation of all three bones (Jamieson et al., 1971). The ankle joint is also supported by nearby tendons, the largest of these tendons being the AT. The ankle joint complex has two major functional axes, the subtalar joint axis, determined by the talus and calcaneus, and the ankle joint axis, determined by talus and tibia.

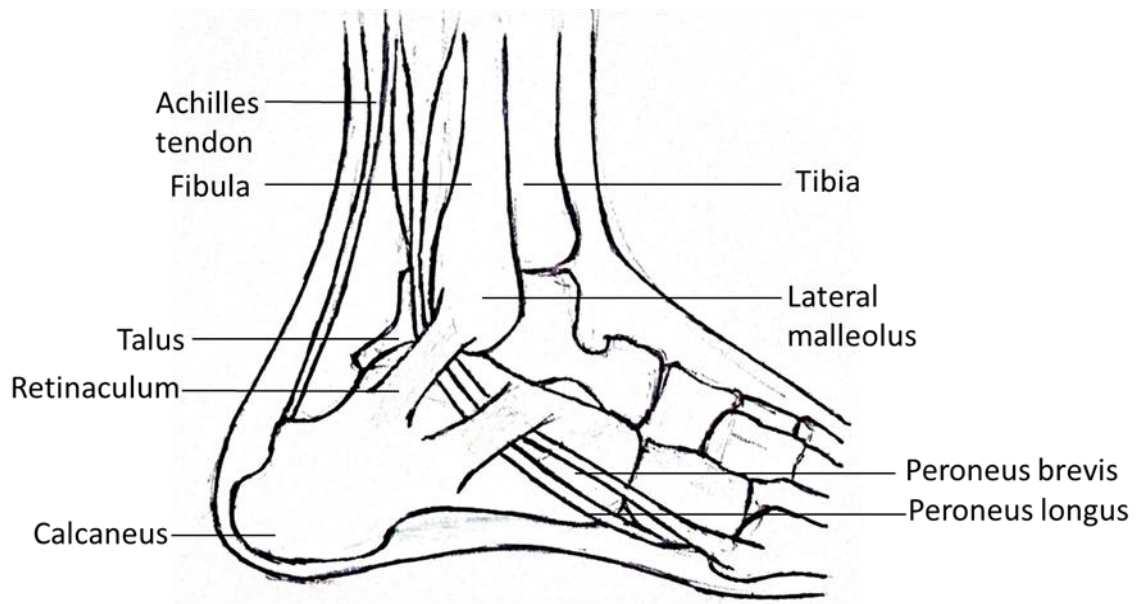


**Figure 1.5:** Description of the ankle joint showing the bones, tendons and ligaments.

### **1.2.6 Joint coordinate system**

According to The Standardization and Terminology Committee (STC) of the International Society of Biomechanics (ISB), a general reporting standard for joint kinematics is in use for the lower limb (Wu et al., 2002). This standard was first proposed by Grood and Suntay, based on the Joint Coordinate System (JCS) for the knee (Grood and Suntay, 1983). *Figure 1.6* shows the two main coordinate systems for the fibula/tibia and calcaneus when in the neutral position.



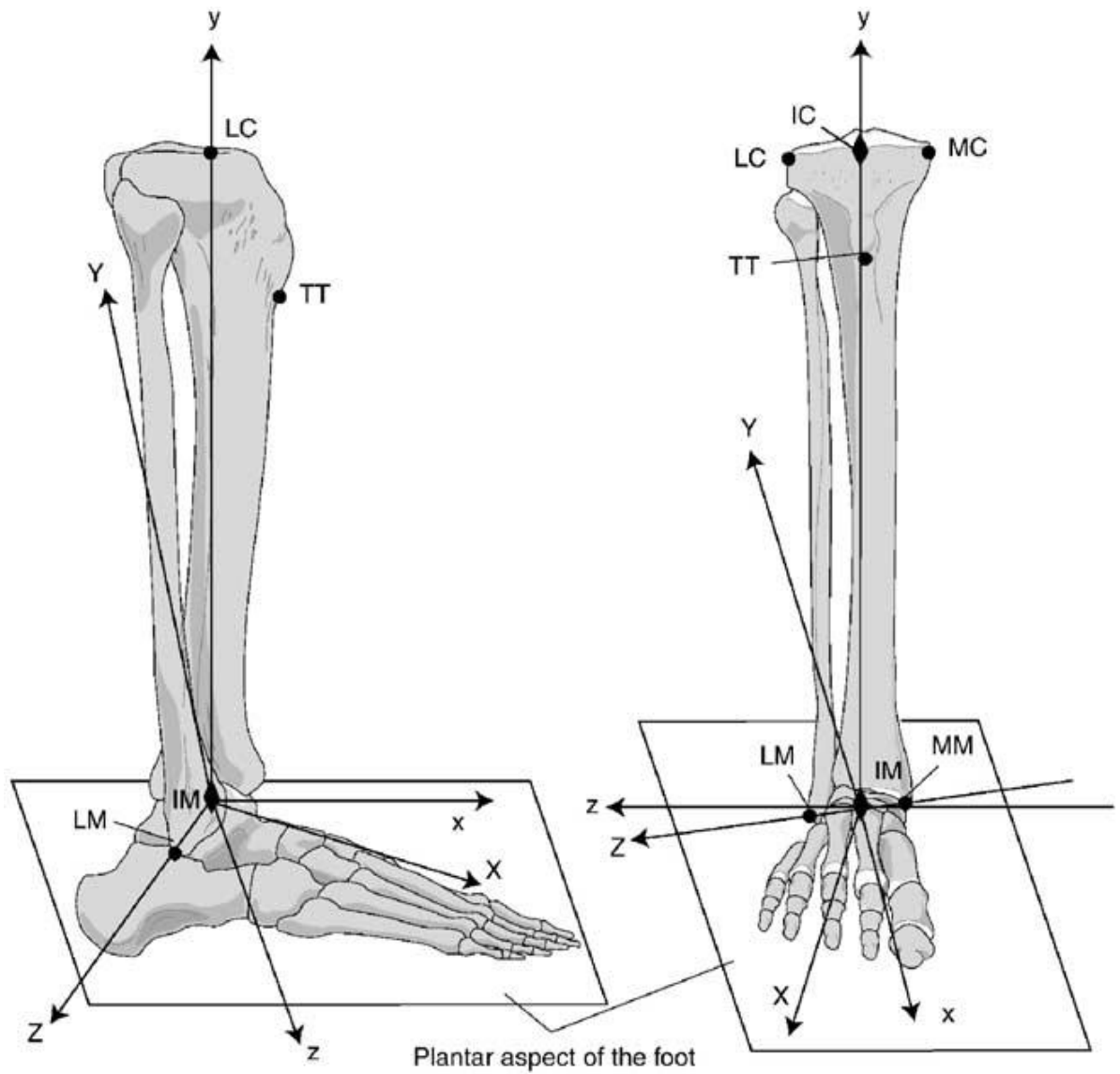


**Figure 1.6:** Illustration of the ankle joint complex coordinate system in the neutral position. The tibia/fibula coordinate system is denoted as XYZ whereas the calcaneus is denoted as xyz (modified from Wu et al., 2002). MC = Tibia Medial Condyle; LC = Tibia Lateral Condyle; IC = inter condyle point; TT = Tibial tuberosity; LM = Lateral Malleolus; MM = Medial Malleolus; IM = inter Malleolus.

### 1.3 Tendon mechanics

Tendons play a role protecting muscle fibres from tensile injury. Tendons exhibit both elastic and time-dependant characteristics, enabling them to modulate their strain response to different loading conditions (Fukunaga et al., 2002). Although it is evident that tendon characteristics contribute to the complex mechanics of joint movement, there is limited knowledge on *in vivo* human tendon adaptation under the full spectrum of loading conditions (Magnusson et al., 2008). Tendon responds and adapts to changes in its mechanical environment (Benjamin and Ralphs, 1997). When a healthy adult tendon is exposed to a tensile load, it shows a typical stress strain curve, as shown in *Figure 1.7*.

The tendon stress-strain curve can be sub divided into three regions (Butler et al., 1978). At low strains of  $\sim 3\%$ , tendon shows a nonlinear behaviour, known as the toe region (Joza and Kannus, 1997). In this region, tendon responds to load with straightening of the crimped collagen fibres and improved alignment of the planar organisation of collagen. The region beyond the toe region is the linear elastic region in which strains of up to  $\sim 6 - 12\%$  have been reported (Wren et al., 2001, Lichtwark and Wilson, 2005b). Beyond the linear region permanent deformation occurs. Failure properties are highly variable between tendons, with the actual strain level required to induce damage in tendon varying significantly and being dependant on various factors such as matrix cross-linking, species and age. Nominal failure strains for tendon are reported to be in the range of  $12 - 22\%$  (Thorpe et al., 2012, Rigby et al., 1959, Wren et al., 2001).

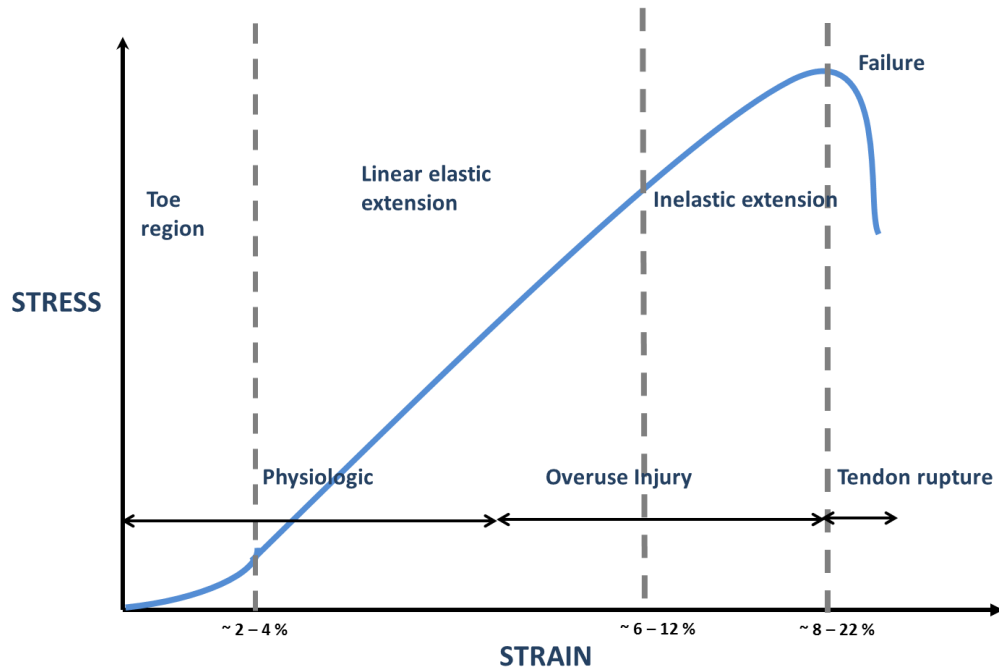


**Figure 1.7:** Schematic drawing of the tendon mechanical response to tensile loading, indicating the typically reported range of strain values for each region (Thorpe et al., 2012, Rigby et al., 1959, Wren et al., 2001).

### 1.3.1 Mechanical Properties

The mechanical properties of the tendon help to characterise tendon behaviour under different loading conditions and have been investigated *in vitro* (Abrahams, 1967, Zajac, 1989, Wren et al., 2001) as well as *in vivo* (Mahieu et al., 2008, Westh et al., 2008, Reeves et al., 2003a, Coupe et al., 2008, Magnusson et al., 2008, Lichtwark and Wilson, 2005b, Carroll et al., 2008, Reeves et al., 2003b, Maganaris, 2002). Normalised force-extension behaviour is normally reported to facilitate comparison between tendons, using the following parameters:

- **Stress:** defined as the force per unit area.

$$\text{Stress } (\sigma) = \frac{\text{Force}(F)}{\text{Area (CSA)}}$$

**Equation 1.1**

- **Strain:** defined as tendon extension with respect to its original length.

$$\text{Strain } (\epsilon) = \frac{\text{displacement } (\Delta L)}{\text{Original length } (L)} \quad \text{Equation 1.2}$$

- **Stiffness:** is defined as the slope of the force-displacement curve, and indicates the magnitude of tendon resistance on application of force.

$$\text{Stiffness } (K) = \frac{\text{Force } (F)}{\text{displacement } (\Delta L)} \quad \text{Equation 1.3}$$

- **Modulus:** is a measure of the material stiffness relative to its dimensions. It tells the magnitude of material deformation for a given stress.

$$\text{Modulus } (E) = \frac{\text{Stress } (\sigma)}{\text{Strain } (\epsilon)} \quad \text{Equation 1.4}$$

In addition, tendons show viscoelastic behaviour, exhibiting typical time dependent properties, as outlined below:-

- **Creep:** describes the increasing deformation of a sample when held under constant load. This contrasts with an elastic material which does not exhibit increase deformation no matter how long the load is applied.
- **Stress relaxation:** describes how stress will reduce or relax when a sample is held under a constant deformation.
- **Hysteresis:** If a viscoelastic material is loaded and unloaded, the unloading curve will not follow the loading curve. The difference between the two curves represents the hysteresis loss, or amount of energy that is dissipated during loading.

Numerous *in vitro* mechanical tests have been carried out on tendons, investigating a wide range of parameters, including tensile strength, viscoelasticity and the effects of repetitive loading on tendon strength. Most of this *in vitro* work has been carried out in cadaveric animals. As such, the material properties may be influenced by the freezing or preservation of tissue (Smith et al., 1996), while sample gripping artefacts and different test protocols may also influence the resulting data (Ker, 1981), making it difficult to carry out appropriate sample comparison. Failure stress values for tendon samples *in vitro* have been reported to be in the range of 20 MPa to 140 MPa (Wren et al., 2001, Elliott, 1965) whilst modulus values derived for various mammalian tendons range from 1.25 GPa to 1.65 GPa (Bennett et al, 1986). The failure strain for tendon at the bone attachment has been reported to be higher than the tendon substance (Wren et al., 2001).

*In vivo* measurement of tendon mechanical properties usually involves ultrasound or MRI imaging of tendon extension whilst performing isometric muscle contractions on a dynamometer (Maganaris and Paul, 2002, Maganaris, 2002, Hof, 1998). Such studies have reported tendon strains of around 5 - 10 % during isometric exercise, and forces well below those seen in many dynamic movements (Finni et al., 2003, Maganaris and Paul, 2002, Muramatsu et al., 2001). However, recent technical advances have made it possible to measure strain during dynamic movements. Currently, measurements of the proximal displacement of the muscle-tendon junction (MTJ) in relation to an external marker are usually employed to understand AT mechanics (Lichtwark and Wilson, 2005b, Arampatzis et al., 2007b, Arampatzis et al., 2010). Furthermore studies involving patients with Achilles tendinopathy have employed dynamometers to measure mechanical properties of the tendon (Child et al., 2010). The results obtained from *in vivo* settings vary greatly. In young sedentary adults, for example, tendon stiffness has been shown to vary between 17 and 760 N/mm, Young's modulus between 0.3 and 1.4 GPa and mechanical hysteresis between 11 and 19 % (Maganaris et al., 2008). The variation in properties seen can be due to the different testing protocols employed and also differences in the task during which the mechanical properties are measured.

## **1.4 Tendon pathology**

### **1.4.1 Tendon strain injury**

While the main function of tendon is to transfer forces generated by muscle to bone, it also acts as a buffer by absorbing external shocks in order to reduce muscle damage. This function places a high demand on tendon mechanical strength and elasticity (Kirkendall and Garrett, 1997), and if a given tendon cannot withstand the necessary high strains, tendon injury can occur.

Tendon injuries can be due to sudden trauma or repetitive use. Excessive loading of tendons during various activities beyond the physiological range is considered to be the main pathological stimulus for degeneration (Selvanetti et al., 1997), but tendon injuries are caused by intrinsic and extrinsic factors. Intrinsic factors involve factors such as age, gender, body mass index, ankle instability, calf muscle dysfunction; these factors predominate in chronic disorders. Extrinsic factors may include the effect of footwear, training surfaces condition, change of use, training patterns and techniques, inactivity and indirect violence (Jarvinen et al., 2005).

### **1.4.2 Tendon rupture**

When tendons are exposed to repetitive loading or overload beyond the physiological threshold they respond with either degeneration of the matrix, inflammation of the tendon sheath or in some cases both phenomena have been observed (Benazzo and Maffulli, 2000, Jarvinen et al., 2005). If fatigue damage is not actively repaired, tendons will weaken and eventually rupture (Fredberg et al., 2008).

The aetiology of tendon rupture remains unclear (Williams, 1986, Maffulli et al., 2011a). Degenerative changes are commonly found in histological findings in spontaneous ruptures.

Degenerative changes were reported by Arner et al in all the patients with Achilles tendon rupture, thought to be due to intrinsic abnormalities (Arner et al., 1959). In another study, degenerative changes were found in 97 % tendons showing spontaneous ruptures, whereas 33 % of the control tendons also showed degenerative changes (Kannus and Jozsa, 1991). More recently, greater degeneration has been found in ruptured Achilles tendons as compared to chronically painful tendons (Tallon et al., 2001). The tensile strength of the tendon may decrease as a result of degenerative changes, which can then result in tendon rupture. The Achilles tendon is heavily loaded during sports activity and is therefore highly prone to rupture (Pagenstert et al., 2010). It has been estimated that 60 - 75 % of Achilles tendon ruptures occur during sports activities, particularly badminton (52 % (Cetti et al., 1993)), basketball, track and field and soccer (Jarvinen et al., 2001). Achilles tendon ruptures are most commonly seen between the 3<sup>rd</sup> and 5<sup>th</sup> decades of life. The ruptures are usually associated with higher activity and exercise. Acute rupture occurs more frequently in older athletes as the tendon structure and composition changes with age. However re-rupture rates are highest amongst younger patients (Moller et al., 1996). Healing from tendon tears takes place in three stages: inflammation, repair and remodelling (Pfefer et al., 2009). The inflammatory response starts directly after the injury occurs and a hematoma is formed, initiating growth of a capillary network over a period of about 2 - 7 days. In the repair phase, continuing for 5 - 21 days, cells produce type III collagen. Finally, the remodelling phase is initiated, which involves the alignment and organisation of the collagen and a change in collagen type to type I. The elasticity and tensile strength of the tendon improves during remodelling, and progressive tensile loading is often offered as a treatment in this phase of tendon healing (Sharma and Maffulli, 2005).

### **1.4.3 *Tendinopathy***

Tendinopathies are a major cause of morbidity in athletes (Knobloch et al., 2008b). Tendinopathy is characterised by local tenderness, swelling, pain and subsequent diminished performance (Maffulli

et al., 1998). Other terms and conditions include tendinosis, tendinitis, paratendinitis and paratendinitis with tendinosis (Khan et al., 1999, van Dijk et al., 2011). Tendinopathy is thought to occur as a result of the inability of a tendon to achieve normal homeostatic balance between damage and repair. It is quite common in sports, with tendinopathies accounting for around 30 - 50 % of all sport injuries (Jarvinen et al., 2001). It is prevalent in runners, representing 6 - 18 % of all running injuries (Longo et al., 2009). However, its precise aetiology and treatment remained elusive.

While the aetiology of tendinopathy remains unclear (Longo et al., 2009), there are a number of hypotheses relating to its initiation. There are mechanical, neural and vascular theories for the cause of the degenerative changes in the tendon. In addition to extrinsic and intrinsic factors, increasing age and gender are also background factors that can influence tendinopathy development (Kannus, 1997).

Tendon pathology has been characterized by abnormal collagen, ground substance, tenocytes, and vasculature (van Dijk et al., 2011). Early studies of tendinopathy considered that inflammation may be involved, but an assessment of the fluid around the tendon indicates no inflammatory markers (Alfredson et al., 1999, Khan et al., 2000). There are, however, signs of neurogenic inflammation (Cook and Purdam, 2009). Nevertheless, it is important to consider that the absence of inflammatory modulators at the end stage of a chronic disease does not confirm their absence at the start.

Disorganized, failed and ineffective healing is a constant feature of chronic tendinopathy (Tan and Chan, 2008). While normal tendon is composed mostly of type I collagen, tendinopathic tendons have a greater proportion of type III collagen, which is associated with tendon rupture and less uniformity in collagen orientation (Riley, 2004). Thus the main factors that result in tendinopathy may involve failed or inadequate healing of the tendon matrix in response to mechanical strain or



repeated micro-trauma. The combination of pain, swelling and impaired performance and failed healing response indicates the clinical diagnosis tendinopathy (van Dijk et al., 2011). However, the pathogenesis of tendinopathy is difficult to investigate, because tendon biopsies are not often taken before tendon rupture.

More recently it has been proposed that there is a continuum in the pathology of the tendon with three key stages: reactive tendinopathy, tendon disrepair and tendon degeneration (Cook and Purdam, 2009). Reactive tendinopathy is a non-inflammatory proliferative response in the cell and matrix that occurs because of the overload. This causes a short term reduction in stress as a result of an increase in cross sectional area. At this stage continual tendon use can lead to tendon disrepair but equally proper training and rehabilitation can lead back to the normal tendon (*Figure 1.8*).

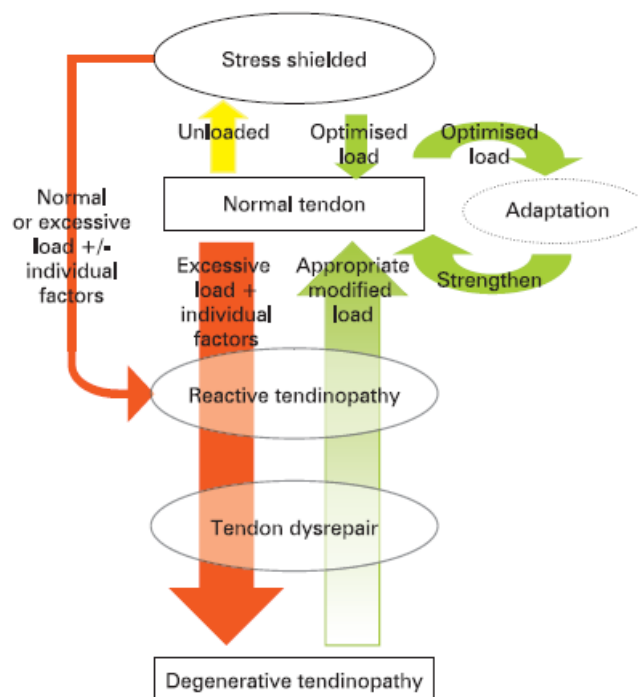


**Figure 1.8:** An pathology continuum model from (Cook and Purdam, 2009). This model shows the transition from a normal to degenerative tendon and possible pathways for returning the tissue to normal tendon. The potential for reversibility is reduced if the degenerative stage is reached.

It has been reported that the incidence of tendinopathy is higher in individuals who are overweight and diabetic (BATTERY and MAFFULLI, 2011). Prolonged systematic inflammation and impaired insulin sensitivity are one of the risk factors for a failed healing response and predispose to the advancement of chronic overuse tendinopathies (DEL BUONO et al., 2011a).

Recently it has been shown that tendinopathy weakens the mechanical and material properties of the Achilles tendon (ARYA and KULIG, 2010). Modulus, strain and cross sectional area in 12 individuals with AT and 12 matched controls were investigated using real time ultrasound imaging and a dynamometer. Tendinopathic tendons showed a significantly reduced modulus and higher cross sectional area. Furthermore, another study with male athletes has shown significantly higher Achilles tendon-aponeurosis strains in subjects with Achilles tendinopathy, as compared to a control group (CHILD et al., 2010). Such findings suggest that alteration in mechanical properties may be the cause or correlate of dysfunction during tendinopathy.

### **1.5 Achilles Tendinopathy Diagnosis**

If Achilles tendinopathy occur in the main body of the tendon, it is known as mid-portion tendinopathy and if these symptoms occur at the insertion of the tendon at calcaneus, it is known as insertional tendinopathy.

A correct clinical diagnosis can often be established solely by clinical examination. This involves palpating the lower leg for tenderness, swelling, nodules, warmth, and decrease in mass (atrophy). It also involves excluding a tendon tear using the Simmond's test (mostly known as the 'calf squeeze' test), or Thompson's tests, during which the patient kneels or lies prone, the examiner squeezes the calf, normally producing plantarflexion of the ankle, but not if the tendon is ruptured. The 'angle of

the dangle' is also considered a reliable test for Achilles rupture. Here, the patient lies prone with their foot hanging free over the examination couch; if the tendon is ruptured, the foot will show abnormal dorsiflexion. If a clinical diagnosis is not clear or requires confirmation, ultrasonography or MRI can be used to reveal the pathology within the tendon (Wijesekera et al., 2011). In tendon, imaging abnormalities include hypoechoic regions seen on ultrasound and areas with high signal intensity seen on MRI (Tumilty et al., 2008, Kountouris and Cook, 2007). These regions correspond with areas of altered collagen fibre structure, and increased interfibrillar proteoglycans. Colour and power Doppler have recently added a new dimension to standard ultrasound tendon imaging (Wijesekera et al., 2011). These imaging technologies can show clear colour images of blood flow in tissues, highlighting tendinopathic areas of increased vascularisation. Studies in various tendons have shown that clinical outcomes are not always dependent on tendon images (Khan et al., 2003). In addition, imaging gives only anatomical, but not functional or symptomatic information. Thus, imaging should not be the only guide for diagnostic or clinical decisions.

The severity of the condition can be assessed by the VISA-A (Victorian Institute of Sports Assessment—Achilles) Score. This is the best validated and most widely used clinical questionnaire for tendinopathy assessment, and was developed following the VISA-P questionnaire for patellar tendinopathy in Melbourne, Australia, by the Victorian Institute of Sport Assessment (Visentini et al., 1998). The score assesses symptoms, ability to play sport and function in everyday life. The VISA-A questionnaire has been shown to be reliable and valid when used in patients with a range of severities of Achilles tendinopathy as well as control subjects, and has proven sensitivity to change in the condition (Robinson et al., 2001). In addition, visual analogue scales are used for pain assessment. However, these assessments alone also cannot make a reliable diagnosis.

## 1.6 *Tendinopathy Management*

Tendon healing takes a long time as tendon has a slow metabolic rate and there are no rapid effective treatments. Conservative treatment is recommended as the initial strategy by most researchers (Kader et al., 2002, Maffulli et al., 2010). This is commonly a multi-oriented approach, including the correction of aetiological factors, complete or modified rest, medication like analgesics and aprotinin injections, orthotics such as a heel lift, change of shoes, stretching and massage, and eccentric strengthening exercises (Alfredson and Lorentzon, 2000).

There is currently a lack of consensus about the treatment of choice for tendinopathy as conservative modalities are generally lacking in suitable evidence. More than twenty treatments have been offered to manage Achilles tendinopathy, but the rationale behind the use of these is generally anecdotal and based on limited scientific evidence. Empirical research indicates strong evidence for EL and shock wave therapy and moderate evidence for low level laser therapy (Rowe et al., 2012, Sussmilch-Leitch et al., 2012). Tendinopathy management techniques that have been investigated with controlled trials are shown in *Table 1.1*. The treatments have been arranged according to the number of evidence based studies, with the most studied at the top.

In a recent study (Humphrey et al., 2010) high volume image guided injections (HVIGI) deep to but not into the main body of the Achilles tendon were found to be effective at improving symptoms in resistant tendinopathy; reducing neovascularisation, and decreasing maximal tendon thickness at short-term follow-up. This study does not have a control group, so the outcomes of this treatment cannot be compared with the other available modalities. However, it is interesting to note that these all patients in this study were non-respondent to other conservative treatments.

**Table 1.1:** List of those treatments available for tendinopathy which have been investigated with controlled studies.

<b>Treatment</b>	<b>Studies</b>
<b>Eccentric training</b> <i>Stretching of the affected muscle-tendon unit. Dose varies. Mostly carried out with additional weight.</i>	(Yelland et al., 2011, Gardin et al., 2010, Knobloch et al., 2007, Knobloch et al., 2010, Sayana and Maffulli, 2007, Maffulli et al., 2008b, Herrington and McCulloch, 2007, Langberg et al., 2007, Norregaard et al., 2007, Silbernagel et al., 2001)
<b>Extracorporeal Shockwave Therapy</b> <i>Low level energy is generated from a shock wave generator and transmitted through the patient's skin as a shock wave using a standard commercially available ultrasound gel.</i>	(Rompe et al., 2009, Rompe et al., 2007, Furia, 2008, Cacchio et al., 2011, Costa et al., 2005)
<b>Low level laser therapy</b> <i>Uses a low level laser or light emitting diode to alter cellular function.</i>	(Stasinopoulos et al., 2009, Stergioulas et al., 2008, Tumilty et al., 2008, Tumilty et al., 2010)
<b>Glyceryltrinitrate patches</b> <i>Nitric oxide is delivered transcutaneously to the area of painful tendinopathy using commercially available glyceryltrinitrate patches.</i>	(Paoloni and Murrell, 2007, Paoloni et al., 2005, Paoloni et al., 2004, Kane et al., 2008)
<b>Injections treatment</b> <i>Corticosteroids, Polidocanol, autologous blood, platelet-rich plasma, high-volume injections, hyperosmolar dextrose, brisement, aprotinin and low-dose heparin. Inject directly into the site of injury.</i>	(de Jonge et al., 2011a, Creaney et al., 2011, Kon et al., 2009, Willberg et al., 2011, Willberg et al., 2008, Alfredson and Ohberg, 2005)
<b>Therapeutic Ultrasound</b> <i>Pulsed ultrasound applied to the symptomatic area of the painful tendon.</i>	(Stasinopoulos and Stasinopoulos, 2004, Chester et al., 2008, Warden et al., 2008, Finnoff et al., 2011)
<b>Splinting</b> <i>A device to support or immobilize the affected limb is used.</i>	(de Vos et al., 2007b, de Jonge et al., 2010, Roos et al., 2004)
<b>Air heel Bracing</b> <i>Air cells located under the heel and above the calcaneus apply pulsating compression with every step as well immobilizing the limb.</i>	(Petersen et al., 2007, Knobloch et al., 2008a)
<b>Message</b> <i>Deep friction massage of the calf</i>	(Stasinopoulos and Stasinopoulos, 2004, Brosseau et al., 2002)
<b>Active rest</b> <i>Patients prevented from performing any activity involving tendon loading.</i>	(Silbernagel et al., 2011)

The use of platelet-rich plasma (PRP) has also been gaining popularity in the management of tendon injury in sports (Mei-Dan et al., 2010). It is hypothesised that PRP may accelerate tissue healing and

regeneration as a result of proliferative and anabolic cellular response. However, there are few studies which show no superior results in chronic Achilles tendinopathy over a placebo or saline injections (de Vos et al., 2010, de Jonge et al., 2011a). Indeed very few studies have made an attempt to investigate the potential mechanism of action, therefore more scientific based control studies are required to investigate its role in tendinopathy treatment (Del Buono et al., 2011b).

A recent review of the treatment of tendinopathy concluded that current data is in support of the use of eccentric loading, sclerotherapy, shock wave therapy, platelet rich plasma injections and nitric oxide patches, whereas the results for ultrasound, massage, active rest, and laser therapy are inconsistent (Magnussen et al., 2009, Rowe et al., 2012). However, these conclusions are of limited value due to the low volume and quality of the evidence available.

If conservative treatment fails, surgical procedures may be adopted. Various surgical techniques involve the exposure of the tendon and removal of fibrotic adhesions, or the removal of the intratendinous degeneration (Maffulli et al., 2004). Multiple longitudinal tenotomies have been shown to stimulate neo-angiogenesis in the Achilles tendon and increase blood flow (Friedrich et al., 2001). Surgery has been considered an acceptable choice among patients who fail to respond to nonoperative treatment. Recently, it has been suggested that percutaneous repair of the AT is a good choice for elite athletes, allowing a safe and prompt return to sports (Maffulli et al., 2011a).

However, recovery after surgery takes a long time regardless of the surgical technique. The majority of data for surgical interventions has come from uncontrolled retrospective studies and there have been very few randomised controlled trials. Satisfactory outcomes have been shown to range from 67 % to 87 % and appear to depend on the severity of the tendinopathy (Andres and Murrell, 2008).

Worse results have been shown among women (Maffulli et al., 2008a) in terms of prolonged healing times, slow return to activity level and higher risk of further surgery.

Achilles tendon disorders are considered troublesome to treat. In addition, because of individual sport cultures and different sport habits across countries, management protocol varies and thus national epidemiologic studies are of importance in each individual country (Maffulli et al., 2003). Many treatments are offered to patients with painful tendons, but the scientific evidence for most of the conservative and surgical treatments remains unclear (Alfredson, 2003, Maffulli et al., 2010).

One of the vital aspects of tendinopathy management is to know how we can stimulate a chronic tendinopathy to recover quickly and allow the individual to return to activity safely and quickly. Active prevention measures and participation in physical activity can play a key role in decreasing the (re-) injury rate and can lead to increased athletic performance (Maffulli et al., 2011b). Indeed, tendon loading has been shown to be effective as a treatment for tendinopathy (Silbernagel et al., 2011). Kjaer and co-workers reported a good healing response in diseased tendon with loading (Kjaer et al., 2003) and it has been reported in various studies that human tendons respond to exercise induced mechanical loading by increasing collagen synthesis and the cross sectional area of tendon. However, excess loading can cause microscopic injuries to collagen fibres and make the tendon more susceptible to failure (Brown et al., 2006). For a clear approach to the treatment of tendinopathy, a greater knowledge of the tendon matrix and its changes in response to loading is required.

## 1.7 Loading of the triceps surae complex

Human motion is facilitated by muscles, exerting forces against objects and supporting surfaces. In *Figure 1.9*, for example, the triceps surae can exert a torque to control the rotation of the ankle about the ankle joint and thereby move the load represented as body weight. When the muscle and load torques are equivalent under such conditions, the load does not move, and the triceps surae performs an isometric (constant length) contraction. However, when two torques are different, the load is either raised or lowered. When the muscle torque exceeds the load torque, the triceps surae and tendon unit shorten and perform a concentric contraction to raise the load (*Figure 1.9A*) referred as concentric loading (CL). In contrast, when the muscle torque is less than the load torque, the activated muscle tendon unit is lengthened and performs an eccentric contraction to lower the load (*Figure 1.9B*) referred as eccentric loading (EL).

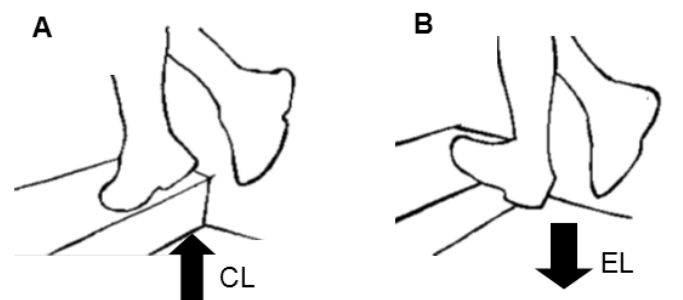


**Figure 1.9:** Mechanical and activation characteristics of eccentric and concentric muscle activation in triceps surae loading. During isometric loading, load torque is equal to muscle torque, during eccentric loading, load torque is greater, causing the lengthening of the muscle tendon unit. In contrast, during concentric loading, muscle torque is higher resulting in the shortening of the muscle tendon unit.

## 1.8 Eccentric Loading

Of all available treatments for tendinopathy, EL has found to be effective even when rest, change of shoes, orthoses, NSAIDs, physical therapy and other ordinary training programmes have failed. EL success rates in the management of Achilles tendinopathy are 50 - 60 % in sedentary patients



(Sayana and Maffulli, 2007) and 60 % - 82 % in athletes. *Table 1.2* details a literature survey of training programmes which employed EL as the main treatment protocol.

EL was first applied as a training regime to treat Achilles tendinopathy in 1986. Stanish et al first introduced the concept and reported that 6 weeks of an eccentric exercise programme, consisting of once daily exercise bout with a progressive increase in the speed of movement, led to complete relief of pain in 44 % of their 200 patients with Achilles tendinopathy and marked improvement of symptoms in 43 % (Stanish et al., 1986) . Unfortunately this study did not have a control group and lacked strong methodology. However, in 1998 Alfredson confirmed the efficacy of eccentric loading with a prospective controlled, non-randomized study comparing heavy load eccentric calf muscle loading with surgical treatment in patients with Achilles tendinopathy (Alfredson et al., 1998). Alfredson also modified the EL protocol and proposed three sets of 15 repetitions with an extended knee and three sets with a flexed knee twice a day, every day, for 12 weeks. The subjects were encouraged to use additional loads to increase the load torque during the training and the exercise was performed at a relatively controlled and slow speed. The group reported 100 % improvement in pain. Since then a number of studies have quantified the efficacy of eccentric loading and have produced a body of evidence to support the use of eccentric training in the treatment of mid portion Achilles tendinopathy (Woodley et al., 2007, Roos et al., 2004, Grigg et al., 2009, Chester et al., 2008, Maffulli et al., 2008b, Knobloch et al., 2008a, Rompe et al., 2009, Rompe et al., 2007, Langberg et al., 2007, Shalabi et al., 2004b, Satyendra and Byl, 2006, Stergioulas et al., 2008, Gardin et al., 2010, Mafi et al., 2001, Croisier et al., 2001). Alfredson and co-workers have also provided different algorithms for tendinopathy management centred on eccentric training (Alfredson, 2003, Alfredson and Cook, 2007). Although there are some critics who have questioned the quality of some of the trials (Woodley et al., 2007), there is still a body of evidence that EL provides promising results in the treatment of tendinopathy.

Most of the studies of EL have shown success in treating mid-portion Achilles tendinopathy, while results have been disappointing in patients with insertional Achilles tendinopathy. Fahlstrom et al., 2003 reported that only 32 % of patients with insertional tendinopathy responded to EL as compared to 89 % for mid-portion Achilles tendinopathy. Indeed, EL efficacy in insertional tendinopathy is generally considered unsatisfactory (Kearney and Costa, 2010), and attempts have been made to modify the protocol to optimise the treatment for insertional tendinopathy (Jonsson et al., 2008). The proposed insertional tendinopathy specific protocol incorporates only the plantar flexion phase of loading, and showed a success rate of 67 %, but the study lacked a control group to assess efficacy (Jonsson et al., 2008). Overall, there is a lack of understanding concerning the mechanism of efficacy in a standard EL protocol; consequently it is difficult to draw conclusions on the possible pathways through which EL may function.

The EL modality has been evaluated in different controlled clinical trials and systematic reviews (Kindermann et al., 2010). Rompe et al reported better clinical outcomes in an eccentric strengthening group compared to a “wait and see” group at 4 months (Rompe et al., 2007) and imaging of the Achilles tendon before and after a 12-week EL protocol showed thinning and normalization of the tendon structure both on ultrasound and MRI (Courville et al., 2009, Kon et al., 2009).

Eccentric exercise has also been shown to increase the tendon strength and endurance (Silbernagel et al., 2006, Silbernagel et al., 2001). It has also been reported by Knobloch that daily EL is a safe and easy measure and provides beneficial effects on microcirculation in tendon without any evident adverse effects in both mid-portion and insertional Achilles tendinopathy (Knobloch, 2007). In the longer term, an EL program has also been shown to increase type I collagen production (Gardin et al., 2010, Langberg et al., 2007). Ultrasonographic imaging has shown that patients with Achilles

tendinosis, treated with eccentric calf muscle training, benefit from a localised decrease in tendon thickness and partially normalised tendon structure (Ohberg et al., 2004).

The effect of repetitive stretching, which cause the lengthening of the muscle-tendon unit, may also have an impact on the capacity of the muscle-tendon unit to effectively absorb load (Petersen et al., 2007). Another possible mechanism of EL action relates to mechanical insult of the nerves that produce pain in Achilles tendinopathy. As the nerve structures found in painful human tendons lie in close proximity to the tendon vessels and these vessels disappear with muscle stretch and contraction, the alteration of neovascularisation and subsequent changes to the accompanying nerves may result in good clinical effects with eccentric training (Courville et al., 2009). Indeed, other studies indicate that neovascularisation is decreased by an eccentric training intervention, as demonstrated by colour Doppler sonography (Courville et al., 2009). However, that observation could also be the result of other stimuli that influence pain and neovascular obliteration, so no definite conclusions can be drawn from these studies.

Although the effectiveness of eccentric exercise can be explained with a number of theories, none have been fully investigated. Many important questions concerning the use and effectiveness of EL in the management of the Achilles tendon disorders are still unanswered (Knobloch, 2009). It is still unclear why EL works in tendinopathy (Peers and Lysens, 2005, Maffulli and Longo, 2008), and how it results in clinical and mechanical changes.

### **1.9 *Eccentric vs Concentric Loading***

Concentric exercises still feature in rehabilitation programmes as an important component of strength training. There is no set protocol for CL, but it has been employed in various doses

depending on applied clinical reasoning. CL is the reverse of eccentric action; that is, the muscle-tendon unit gets shorter as the muscle works (*Figure 1.9A*). The clinical studies which have compared the efficacy of eccentric versus concentric contractions report that EL consistently results in a superior outcome (Kongsgaard et al., 2009, Richards et al., 2010). Accordingly, comparing CL and EL could help establish EL specific effects. In a 12-week course of eccentric strengthening exercises study, EL was found to be more effective than a traditional concentric strengthening program for treating Achilles and patellar tendinopathy in recreational athletes. In the Achilles tendinopathy study, 82 % of the patients randomised to the eccentric strengthening protocol described improvement in pain levels, compared with 36 % in the concentric training group. Eight weeks of 50 minutes daily dose of EL has resulted in reduction in pain and improved function in patient with Achilles tendinopathy (Yu et al., 2012). However the mechanism behind this is not known. A study of 74 healthy volunteers has shown that a 6-week eccentric training programme changes the dorsiflexion range of motion which was significantly higher only in the eccentric training group, however, no change in stiffness was observed for both EL and CL group (Mahieu et al., 2008). In contrast, another study has shown 6 week period of eccentric training resulted in decreased stiffness of the Achilles tendon, as compared to the concentric training in healthy subjects (Morrissey et al., 2011). However the patients in the later study had different baseline activity levels, making a direct comparison of EL and CL difficult. A few studies have, within the past few years, taken a more explanatory and mechanistic approach to understand EL, coupling clinical findings of eccentric training in tendinopathy with an investigation into the structural, functional and molecular effects of the loading regime (Courville et al., 2009, Flint et al., 2009, Slater et al., 2010, Kulig et al., 2009). In one study conducted using MRI, Shalabi et al have shown that a single bout of exercise increases tendon volume and signal intensity on MRI after both EL and CL (Shalabi et al., 2004a). However, another study has shown that performing EL or CL with addition of 20 % bodyweight result in greater reduction in Achilles tendon thickness immediately after EL with full recovery in the same time course as CL (Grigg et al., 2009).

In a recent review, it was reported that EL may result in reduction in pain and increase in strength as compared to other available modalities, however, the mechanisms are still unclear (Wasielowski and Kotsko, 2007) emphasising the need for more research in order to compare EL with other available treatments, particularly CL.

### 1.10 *Biomechanics of Eccentric training*

Investigating the biomechanical effects of EL, to determine why EL may be a more effective tendinopathy treatment, is important, as the data will assist in the formation of improved and more concise EL protocols, which could be more effective and efficient. This section will discuss the biomechanics of triceps surae loading and the factors that can influence it. A literature survey shows that three main mechanical stimuli have been hypothesised to be involved in the possible effectiveness of EL (*Figure 1.10*).

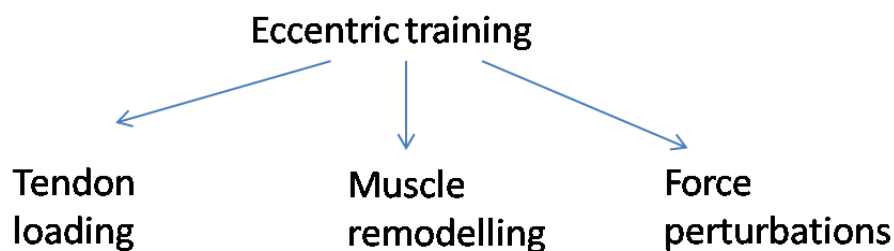


*Figure 1.10: Three main potential factors included in eccentric loading effectiveness.*

#### 1.10.1 *Tendon Loading*

One possible hypothesis concerning EL efficacy comes from Stanish and Curwin, 1986. They suggested that during EL the tendon is subjected to greater forces than during CL, leading to a greater remodelling stimulus. This hypothesis was supported by the fact that EL lengthens the

muscle-tendon unit, which they suggested would lead to higher strains on the tendon during motion. However, no evidence was presented to suggest that tendon mechanical parameters, such as stiffness and strain vary. A few studies have studied the EL effect on tendon stiffness, reporting mixed results (Morrissey et al., 2011, Mahieu et al., 2008). However, the details of the tendon forces, material properties as well as muscle activation during the course of exercise were not reported.

### **1.10.2 Muscle activation**

It is well known that EL is characterized by lower EMG than CL (*Figure 1.11*), reflecting a lower level of muscle activation (Qi et al., 2011a, Bigland and Lippold, 1954). This lower EMG probably indicates reduced recruitment of motor units. In addition there may be selective recruitment of particular types of motor units, as larger motor units are preferentially recruited across the motoneuron population (Moritani et al., 1987). It is evident from previous work that selective recruitment of higher threshold motor units occurs more in EL than CL (Moritani et al., 1987, Nardone et al., 1989). Initial studies using functional MRI have shown inhomogeneous activation during sub-maximal concentric-eccentric contractions against an elastic load (Laidlaw D., 1994). There is evidence of differences in the recruitment order, discharge rate and recruitment threshold of motor units during the different types of muscle contractions. For example, selective activation of high-threshold motor units in the gastrocnemius muscle was found when plantar flexor muscles performed EL as compared to CL at moderate to fast speeds (Nardone et al., 1989). In addition, lower discharge rate of the motoneurons was reported during EL with relatively sparse action potentials discharged at any one time, in contrast to the prolonged trains of action potentials seen during CL thus emphasising that recruitment order is altered during EL (Howell et al., 1995).

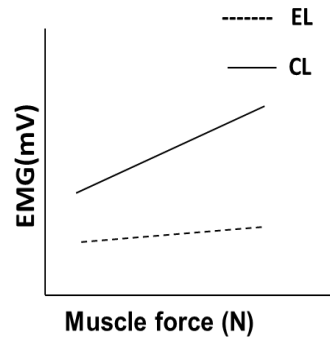


**Figure 1.11:** Schematic indicating the differences in the muscle activation required to provide a certain force during EL and CL. Muscle is consistently activated more during CL, with an increasing differential at higher forces (Bigland and Lippold, 1954).

A number of more recent studies have attempted to explain the difference in muscle activation seen during EL and CL (Enoka, 1996, Ono et al., 2010, Westing et al., 1991, Vaczi et al., 2011). Accumulating evidence suggest that different control strategies are provided by the central nervous system (CNS) for EL and CL activities (Enoka, 1996).

In isolated muscles which are fully activated (i.e. all fibres are stimulated at a frequency which maximally activates the contractile apparatus) the force during lengthening is much greater than during shortening at the same speed (Woledge et al., 1985). It follows that we should expect less muscle recruitment to be needed to meet the relatively constant load that is applied during both dynamic EL and CL in-vivo. According to the cross-bridge theory of muscle contraction, force is generated by muscle as a result of the interaction of actin and myosin. In a normal cross-bridge cycle, adenosine triphosphate molecules are hydrolysed when acto-myosin links break during the crossbridge cycle (Jones et al., 2004), whereas during EL, lengthening of the muscle occurs by breaking of acto-myosin links with less ATP hydrolysis (Woledge et al., 1985). There are therefore different force generation and modulation mechanism in play during the two loading types, resulting in a higher force per unit muscle activation during EL.

Changes in EMG amplitude measured using multichannel EMG have revealed that during the course of an isometric contraction, the active parts of the muscle vary (Grassme et al., 2003, Kleine et al., 2000, Scholle et al., 1992). Regional differences in muscle hypertrophy after sustained resistance training are attributed to the regional differences in muscle activation during the exercise (Wyndow et al., 2012). However, to date, there is no information on regional activation during clinically relevant EL and CL exercise protocols. Temporo-spatial mapping of the triceps surae during EL and CL can reveal an insight into the activation patterns and regional differences between the two types of loadings. Further triceps surae EMG mapping studies are required to find region specific differences in muscle behaviour during EL and CL.

### **1.10.3 Force Perturbations**

It is shown recently, in a study of sixteen healthy subjects, that EL was characterised by higher frequency content in the range of 8 - 12 Hz (Henriksen et al., 2009). Perturbations may arise through the mechanical tendency for body parts to oscillate at particular frequencies. These perturbations are considered multifactorial in origin, however a few studies have reported that they may originate from rhythmic neural activity in the central nervous system (Marsden et al., 1967b). Perturbations at around 10 Hz are often described as being primarily associated with muscle activity, and are classified as physiological tremor (McAuley and Marsden, 2000). Three main factors have been identified in increased perturbation amplitude, which include stress, fatigue and strength of contraction (McAuley and Marsden, 2000, Marsden et al., 1967a). Mean firing rates increase with the strength of contraction (McAuley and Marsden, 2000), so the amplitude of perturbations can be effected by varying the speed, load and intensity of muscle use. However, there is lack of research in this area and no data is available on the effect of these perturbations, or how they may be influenced by varying exercise variables.



Perturbations in a range of body tissues have shown to have positive and negative effects. At a cellular level, loading frequency is known to influence matrix metabolism in a number of connective tissues. For example, high frequency perturbations applied *in vitro* have been shown to result in increased bone density (Bacabac et al., 2006) while *in vivo* they increase muscle strength (Verschueren et al., 2004) and reduce the firing rate of motor units (Bongiovanni et al., 1990). The mechanism by which high frequency perturbations may influence tissue homeostasis is poorly understood. However, these perturbations may be perceived by cells as a fluctuating strain environment, initiating a range of metabolic mechano-transduction pathways.

In a recent study, Rees et al investigated the mechanism behind EL and reported no differences in Achilles tendon force for subjects carrying out EL and CL. This study was limited by the small sample size of 7 subjects (Rees et al., 2008) but similar results were reported in another study which investigated tendon force during one-legged full weight bearing ankle plantar and dorsiflexion exercises (Henriksen et al., 2009). In neither instance was the tendon stiffness reported.

Both of these studies have suggested that the mechanism of action by which eccentric loading effectively treats Achilles tendinopathy is through the perturbations seen during loading cycles rather than the absolute magnitude of the force (Rees et al., 2008, Henriksen et al., 2009). However, this hypothesis require further investigation; Rees et al., (2008) could not provide any details concerning the Achilles tendon perturbation frequencies, and while Henriksen at al., (2009) did report a higher GRF frequency content in the 8 -12 Hz range, measurements were done during one-legged full weight bearing ankle plantar and dorsiflexion exercises. Such a movement differs significantly from the typical EL protocol in which a single leg eccentric phase is followed by a concentric contraction of the other limb, making it difficult to draw clinically relevant conclusions (Alfredson et al., 1998). Furthermore neither of the study investigated tendon stiffness or the origin

of the perturbations. The mechanical properties of a tissue are known to influence these perturbations (McAuley and Marsden, 2000). Quantitative techniques have demonstrated that physiological tremor is not a pure 10 Hz perturbation, but is best defined as the summing of a number of perturbations across a frequency range (Halliday and Redfearn, 1956). However, no data exists to support that perturbations observed during EL are related to the tendon stiffness.

### **1.11 *Optimal application of Eccentric loading?***

Most EL protocols are based on early work by Alfredson (Alfredson et al., 1998). However, there is no consensus on the optimal dose of EL. A number of studies have attempted to further develop eccentric loading regimes by using overload devices, further loading the tendon during loading. For example, eccentric training on a 25 degree decline board has shown superior results in patellar tendinopathy as compared to squatting on horizontal surface (Young et al., 2005). There is considerable variation among the EL protocols adopted by various groups with many modifications to the Stanish or Alfredson protocols reported. Main parameters like loading speed, dose and use of additional load are not standardised. These parameters are important to understand as in a recent study it has been reported that the mechanical properties of triceps surae tendon and aponeurosis do not show a graded response with the sport activity intensity. It was shown that the range of applied strain, amplitude and frequency should be above a given threshold in order to trigger adaptational effects (Arampatzis et al., 2007a).

Mechanical conditioning is one of the drivers to enhance tendon healing (Bacaba et al 2006). It is well known that cells can convert mechanical stimuli into biochemical signals through mechanotransduction and it has been shown previously that tendons actively respond to mechanical conditioning by changing their chemical composition, metabolism and structure (Wang, 2006). Tendon cells, mainly tenocytes, are responsible for this adaption, and various studies show that

tenocytes respond to mechanical stimuli by altering their gene expression and cell phenotype (Wang et al., 2003).

A review of the disparate literature concerning EL shows that there are a number of potentially marked differences in the exercise programmes used, with no clarity concerning the most appropriate parameters. Variations in test protocols include; fast or slow loading, exercising into the pain or remaining short of pain, loading during the eccentric phase only or both phases of the movement, and progressing either load, speed or both. *Table 1.2* provides an overview of the literature concerning the range of EL protocols employed in various studies. There are three main parameters for defining the loading:-

- **Speed/Velocity** of the loading- ‘slow’ or ‘fast’ pace
- **Load** – ‘light’ (body weight) or ‘heavy’ (additional load) mass
- **Intensity** – number of repetitions; single or multiple.

The resultant force in the muscle tendon unit depends on an interaction between acceleration and load employed during the loading:-

$$F = ma \qquad \text{Equation 1.5}$$

where,

F = force exerted by the muscle

m = mass of the body to be raised or lowered

a = acceleration of the mass

According to this equation if either the acceleration during exercising or the total mass moved varies, the resultant force passing through the muscle tendon unit will vary, potentially altering the

remodelling stimuli and subsequent therapeutic results. As evident from the *Table 1.2*, there is lack of consistency in the employed speed, load and dose. None of the studies provide the rationale behind the protocol employed, perhaps reflecting the lack of understanding of the effect of these parameters on the resulting stiffness, strain and perturbation magnitude and frequencies.

**Table 1.2:** Details of the range of reported EL studies highlighting dose parameters.

Authors	Study Type	Study group	Control group	T stage	Speed	Load	Intensity	P	CG Intervention	Output measures	Results
(Stanish et al., 1986)	SI	200	N/A	18 m	progressive	with pain	EL followed by CL 3 x 10 repetition	6 w		pain	87% ↓
(Alfredson et al., 1998)	CS	recreational athletes 12 male 3 female mage: 44	recreational athletes 11 male 4 female, mage:40	3 m	slow speed	with pain	3 x 15 rep twice a day (KS+KB)	SG:12w CG:24w	conventional treatment	VAS  Concentric plantar flexion torque Eccentric plantar flexion torque	SG: before:81.4 after 4.8 (12w)  CG: before 71.8 after 21.2 (24w) SG: before 69.1 after 76.9,CG: before 70.3 after 73.6 SG: before 152 after 179.2,CG:before 146 after 144.3
(Mafi N, 2001)	RCS	active patients 22, mage:48	Active in sports 22,mage:48	SG:18m CG:23m	slow speed	with pain	3 x 15 rep twice a day (KS+KB)	12w	CL	VAS	SG: 82 % satisfied  CG:36% satisfied
(Alfredson and Lorentzon, 2003)	SI	4 male, 2female, mage:48	N/A	22 m	slow speed		3 x15 rep twice a day (KS+KB)	12w	N/A	VAS Glutamate level	before 69 after 17 unchanged
(Ohberg et al., 2004)	SI	19 male, mage:55 6 female, mage:55	N/A	17 m	slow speed	with pain	3 x15 rep twice a day (KS+KB)	12w	N/A	tendon thickness	before: 8.8 after 7.6 mm
(Shalabi et al., 2004b)	SI	mix  16 male mage:51 9 female, mage:51	N/A	18m	slow speed	with pain	3 x15 rep twice a day (KS+KB)	12w	N/A	tendon volume  interatendinous signal	before 6.6 ± 3.1 cm <sup>3</sup> after 5.8 ± 2.3 cm <sup>3</sup> before 227 ± 77 after 170 ± 83
(Petersen et al., 2007)	RCS	recreational athletes 23 male, mage: 42  14 female, mage: 42	recreational athletes CG1:20 male, 15 female, mage,42 CG2:17 male, 11 female, mage: 43	SG: 7m CG1: 7m  CG2: 7m	slow speed	with pain	3 x 15 rep a day (KS+KB)	12w	CG1: Airheel braces  CG2: Airheel brace + EL	VAS	SG: 60% ↓  CG1:56%↓  CG2:36%↓

T: tendinopathy stage; P: exercise period; CG: control group; SI: Single intervention; CS: control study; RCS: randomised control study; mage: mean age; w: week; m: month; KS: knee straight; KB: Knee bend; PRP: platelet rich plasma; LLLT: low level laser therapy; BW: body weight; R: reduction; SG: study group; RLSWT: repetitive low-energy shock wave therapy; US : ultrasound;

Authors	Study Type	Study group	Control group	T	Speed	Load	Intensity	P	CG Intervention	Output measures	Results
(de Vos et al., 2007b)	RCS	Active in sports 20 male mage: 44.1 12 female mage: 44.1	Active in sports 17male, mage: 45.1 14 female, mage: 45.1	SG: 34 m CG: 28m	slow speed	with pain	3 x 15 rep twice a day (KS+KB)	12w	EL + night splint	VISA-A  patient satisfaction	SG: Before 50.1; after 68.8  CG: before 49.4; after 67.0  SG: 63%, CG: 63%
(Rompe et al., 2007)	RCS	Mix 9male, mage: 48  16 female, mage: 48	Mix 11male, 14 female, mage: 51 9male,16 female, mage: 46	>6 m	Slow: w 1,4-6  Fast: w 2 ,3, 7-12	x 5kg- week 4- 12	1 x 10 rep twice a day - 1st w (KS+KB)  3 x15 rep twice a day - 11w (KS+KB)	12w	CG1: RLSWT  CG2: Wait and see	VISA-A	SG: before 51; after 76  CG1: before 50; after 70 CG2: before 48; after 55
(Langberg et al., 2007)	CS	elite soccer player  6 male, mage: 26	elite soccer player	12-26m	not mentioned	20% of BW after pain elevation	3 x 15 rep twice a day (KS+KB)	12w	same EL	VAS  Collagen synthesis  Collagen degradation	SG: increased, CG: unchanged SG: unchanged, CG: unchanged
(Mahieu et al., 2008)	RCS	recreational athletes 18 male, mage: 23 17 female, mage: 23	recreational athletes 14 male, mage: 21 15 female, mage: 21		EL phase in 6s		3 x 15 rep twice a day (KS+KB)	6w	no EL	DROM  PRT  stiffness	increased in SG  before 16 after 12  unchanged
(Stergioulas et al., 2008)	RCS	recreational athletes 12 male, mage: 30.1 8 female, mage: 30.1	recreational athletes 13 male, mage: 28 7 female, mage: 28	SG:10m CG:9m	not mentioned	No	gradual increase in reps over w1-w3 12 x12 rep-w4-w12 4days/week (KB+KS)	8w	SG:EL+ placebo LLLT  CG:EL+LLLT	VAS	SG:37  CG:62
(Chester et al., 2008)	RCS	sedentary  4 male, mage:  4 female, mage:	sedentary  7 male, mage:  1 female, mage:	SG:23 m CG:14 m	slow	patients capacity	10 s holding in plantarflexion and dorsiflexion rep depending on patient's capacity once a day (KS+KB) depending on patient's capacity	12w	US	VAS	SG: before; 70 after 62  CG: before; 76 after 55

T: tendinopathy stage; P: exercise period; CG: control group; SI: Single intervention; CS: control study; RCS: randomised control study; mage: mean age; w: week; m: month; KS: knee straight; KB: Knee bend; PRP: platelet rich plasma; LLLT: low level laser therapy; BW: body weight; R: reduction; SG: study group; RLSWT: repetitive low-energy shock wave therapy; US : ultrasound;

Authors	Study Type	Study group	Control group	T	Speed	Load	Intensity	P	CG Intervention	Output measures	Results
(Maffulli et al., 2008b)	SI	athletes		6.4 m	Slow: w 1,4-6	x 5kg-week 4-12	1 x 10 rep twice a day - 1st w(KS+KB)	12w		VISA-A	16% increase
		29 male, mage: 26 16 female, mage: 28			Fast: w2,3, 7-12		3 x15 rep twice a day - 11 w(KS+KB)				60% responded
(Rompe et al., 2009)	RCS	non-athletes	non-athletes	13 m	Slow: w 1,4-6	x 5kg-week 4-12	1 x 10 rep twice a day - 1st w(KS+KB)	12w	CG: Eccentric loading +RLSWT	VISA-A	SG: before 50; after 73
		14 male, mage: 46 20 female, mage: 46	16 male, mage:53 18 female, mage:53		Fast: w 2,3, 7-12		3 x15 rep twice a day - 11 w(KS+KB)			Pain level	CG: before 51; after 87 SG: before 7; after 4
(de Vos et al., 2010)	RCS	mix	mix				walking -w1	2w + 12w	SG:EL + PRP injection CG: EL+ Saline injection	VISA-A	SG: increased by 9.6 points CG: increased by 10.1 points
		13 male, mage:49 14 female, mage:49	13male, mage50 14 female, mage 50	SG:36 m CG:26 m			Stretch -w2 3 x15 rep twice a day - W3-W14(KS+KB)				
(Gardin et al., 2010)	SI	Active in sports									CS: before 7 after 2
		20, mage:49	N/A	12 m	slow speed	with pain	3 x15 rep twice a day (KS+KB)	12w		tendon volume interatendinous signal	before:6.7 after 6.4cm <sup>3</sup> decreased signal

T: tendinopathy stage; P: exercise period; CG: control group; SI: Single intervention; CS: control study; RCS: randomised control study; mage: mean age; w: week; m: month; KS: knee straight; KB: Knee bend; PRP: platelet rich plasma; LLLT: low level laser therapy; BW: body weight; R: reduction; SG: study group; RLSWT: repetitive low-energy shock wave therapy; US : ultrasound;

Summarising the various protocols detailed in *Table 1.2*, three main variations for each of the three variables can be established (*Table 1.3*).

**Table 1.3:** Summary of the differences between the EL protocol employed, derived from *Table 1.2*.

Speed	Load	Dose
<b>Fast pace (sudden heel drop, as quickly as possible)</b>	Pain dependent	2(3x15) KS & KB – 6week
<b>Slow pace (dropping slowly going through the pain)</b>	Progressive from week 1	2(3x15) KS & KB – 12week
<b>Slow pace for early weeks of training and then fast afterwards</b>	No load for early weeks of training and then progressive afterwards	180 reps daily – 11-14 weeks Variable reps

*KS: knee straight; KB: Knee bend*

Speed, load and intensity of loading are important variables of any resistance training protocol, because they can be manipulated to produce an optimal stimulus for strength development.

### 1.11.1 Speed

Muscle force production is dependent on two main factors; firstly muscle activation level, as produced by a voluntary command, and secondly the speed at which the muscle changes its length. The typical force-velocity relationships for muscles are well known, based on the early work by AV Hill (Hill, 1970). During CL, the faster the contraction, the less force a muscle can exert. Conversely, the maximum force an isolated muscle can achieve during EL is largely independent of the changes in the lengthening speed *Figure 1.12*.



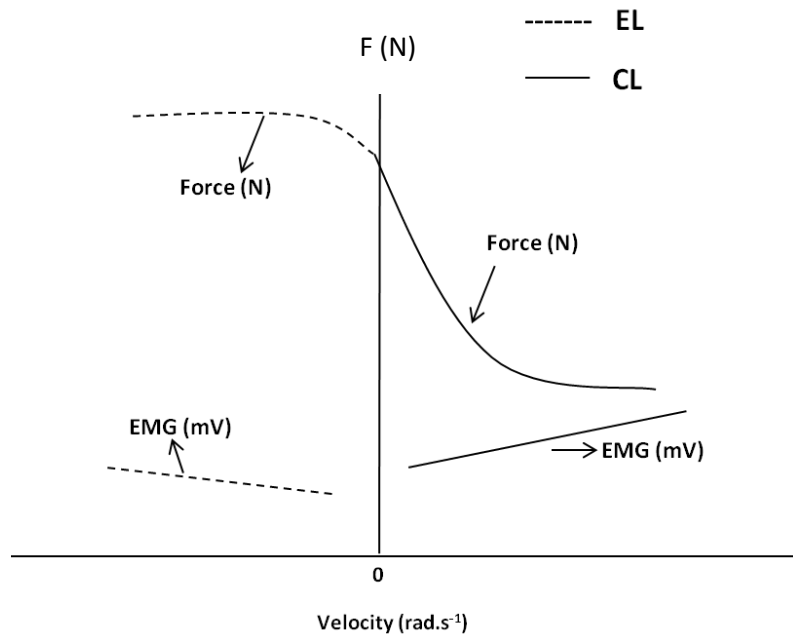


**Figure 1.12:** The amplitude of muscle force is higher during eccentric loading (EL) but unchanged with load velocity. By contrast, the amplitude of EMG is higher during concentric loading (CL) and increases with increasing velocity (Bigland and Lippold, 1954, Westing et al., 1988).

During an isometric contraction there is no movement, so technically the muscle does no external work as there is no displacement, however significantly higher force can be either generated or resisted than in the concentric mode. Heat will also be produced, as it is during shortening, in addition to the work done by muscle (Jones et al., 2004).

Furthermore, muscle activation increases with speed during CL, whereas for EL it largely remains independent of speed. These observations were made in isolated muscles and it should be noted that there are some studies which suggest that moment-velocity curves differ in isolated muscles (Kellis and Baltzopoulos, 1995, Stauber, 1989, Westing et al., 1991). Indeed, the relationship between muscle activation and loading speed is less evident when the muscles are artificially activated (Dudley et al., 1990). It has been suggested that because of the inhibitory activity of several neurons, joint and muscle structures, the nervous system is unable to maximally activate the muscle during maximum voluntary tests performed at any particular angular velocity (Hortobagyi

and Katch, 1990). Research comparing the EMG-speed relationship in conjunction with the force/moment-speed relationship is limited (Taylor et al., 1991).

Data concerning the dependency of tendon EL peak force on speed remain controversial. A study investigating the effect of ankle joint rotation at two speeds on tendon force used isokinetic dynamometer measurement, and found no effect on tendon force (Wakahara et al., 2009). However, resistance exercise performed at fast speeds elicited increased forces within the tendon during exercise and thus led to an increase in subject power and strength over time compared to exercise at drastically reduced speed (Hatfield et al., 2006a). Consequently, the effect of speed during EL and CL training protocols should be investigated, to further establish changes in force production, muscle activation, tendon stiffness and perturbations.

Indeed, variation in loading speed will affect the muscle-tendon strain rate. As both muscle and tendon are viscoelastic materials, loading speed will impact the material properties they display, meaning that knowledge of the *in vivo* mechanical properties of the unit at different strain rates during EL and CL is of interest, as it provides a possible insight into the mechanism of healing. However, the effect of strain rate on tendon elastic properties is controversial and inconclusive and *in vivo* mechanical properties of the AT vary significantly from the *in vitro* properties. Some *in vitro* studies have reported that the elastic modulus of the tendinous tissue increases with increasing strain rate or speed of loading (Noyes et al., 1974, Yamamoto and Hayashi, 1998) while others have reported no effect (Blevins et al., 1994). It could be that training at different strain rates can result in different therapeutic effects. A recent *in vivo* study has shown that fast isokinetic EL resulted in the greatest increase in elbow flexor muscle strength when compared with slow and fast isokinetic EL and CL (Farthing and Chilibeck, 2003). However the effect of different loading velocities on tendon biomechanical properties was not investigated and thus the cause of this improved healing due to high speed loading remains unexplored. Understanding the biomechanical effect of speed during EL

and CL, can improve understanding of the phenomenon behind EL and subsequently treat the condition with greater efficacy and perhaps in a shorter time period.

### **1.11.2 Load**

A complete EL programme is normally 12 weeks in duration, during which time the use and amount of additional load incorporated into training varies from study to study, with some studies starting to use an incremental load of 5 kg from week 4 (Rompe et al., 2009, Rompe et al., 2007, Gardin et al., 2010, Sayana and Maffulli, 2007) while others will start incorporating as much load as the patient can tolerate as soon as they feel able (Alfredson et al., 1998, Mafi et al., 2001). It is notable that the selection of load dose tends to be based on clinical experience, rather than derived from any evidence based study. This may be appropriate, however the differential effects of loading need to be better understood in order that therapists can understand the effects of their clinical decisions.

Loading is important for tendon health with tendons known to be functionally and structurally mechano-responsive to altered loading stimuli (Wang, 2006, Wang et al., 2011). Mechanical loading is known to initiate tenocyte signalling mechanisms in a strain dependent manner (Scott et al., 2011). Furthermore, studies in other similar cell types, such as fibroblasts and osteocytes have shown a loading frequency dependence to cell metabolism (Rubin et al., 2001, Barkhausen et al., 2003, Bacabac et al., 2006), indicating that tenocyte mechano-transduction may well be frequency dependent also. Exploring the potential effects of force perturbations on tenocyte healing could enable optimization of therapeutic approaches to the treatment and prevention of conditions such as tendinopathy and rupture.

Load applied within the physiological range has been shown to be beneficial for ensuring tendon homeostasis or even enhancing its mechanical properties (Wang et al., 2011). Recent work shows

that without a certain amount of mechanical load, tendon stiffness and tensile strength reduce (Sun et al., 2010). However, rapid tendon overload is an acknowledged injury mechanism (Maffulli et al., 2011a). Even small changes in loading profile may alter the fluctuating strain environment of tenocytes and subsequently influence cell metabolism. It has been shown that tendon stiffness and modulus increase in a curvilinear manner with increased force (Maganaris and Paul, 2002). However, the biomechanical effects of additional load during EL, as it is typically applied clinically, have not been reported.

The amplitude and frequency of tendon perturbations may also change if the leg is loaded in different ways, and it is possible that the addition of load may further increase the magnitude of tendon perturbations and alter mechano-transduction responses in this manner. However, no such studies to date have investigated the effect of load on perturbation frequency and magnitude.

### **1.11.3 Dose**

The dose of an exercise, or number of repetitions carried out, can influence the mechanical stimuli seen by the muscle tendon unit. It has been reported that two maximal eccentric actions of the elbow flexors attenuated the muscle damage developed by 24 maximal eccentric muscle actions (Nosaka et al., 2001). Practically, in the early stages of rehabilitation, the use of submaximal eccentric loads rather than high dose eccentric training could benefit, by curtailing the negative consequences of exercise-induced muscle damage. It has also been shown that a high dose session of 12 sets of 10 maximal eccentric voluntary efforts, with 2 minutes between sets, effect muscle performance more compared to low dose session (Paschalis et al., 2005). However, no relationship has been reported between tendon force perturbations and repeated bouts of exercise. It is essential to understand how the muscle fatigues during one bout of a typical EL protocol as compared to CL.

*Table 1.4* demonstrates studies conducted so far to compare the effect of these parameters during EL or CL. The table highlights that appreciable work has been done to understand the mechanism behind EL. However, the protocols employed to measure mechanical or muscle parameters are predominantly not clinically relevant, and no study alone has investigated all the parameters. As is evident from the table, only one study has attempted to measure tendon mechanics during dynamic loading of tendon as done clinically. However, the study was unable to report tendon stiffness or strain, muscle activation or perturbations. Clinically relevant EL that has shown to be successful in the literature is consistently performed dynamically on a step and not on a dynamometer. Although devices like isokinetic dynamometers provide good control of movement, true understanding of EL mechanisms cannot be achieved unless tendon mechanics are studied during clinically relevant EL. In addition there is no data available to relate muscle-tendon mechanics and perturbations to the variation in exercise parameters. Indeed, there is a need for a series of studies that can relate triceps surae mechanics with the range of clinically employed exercise variables used in a clinical setting.

**Table 1.4:** Review of the notable studies conducted to investigate the effect of exercise variables during EL and CL. Note that most studies have measured isometric, only one study has investigated clinically relevant loading conditions.

	Testing condition	Relevant studies	Parameters				Effect
			ATF	MP	EMG	FP	
El/CL	Clinical set up EL/CL	Rees et al, 2008	√	×	×	√	No effect on ATF, ↑ EMG during CL, ↑FP during EL
	EL/CL- full plantarflexion dorsiflexion on one leg	Henriksen et al., 2009	√	×	√	√	No effect on ATF, ↑ EMG during CL, ↑FP during EL
Speed	Clinical set up EL/CL		×	×	×	×	
	Dynamometer - CL	Wakahara et al., 2007	√	×	√	×	↓ ATF with ↑ speed ↑ EMG with ↑ speed
	Dynamometer - EL	Wakahara et al., 2009	√	×	√	×	No effect on ATF ↑ EMG with ↑ speed
	Dynamometer - CL	Theis et al., 2012	√	√	×	×	↑ Stiffness with ↑ speed
Load and Dose	Clinical set up EL/CL		×	×	×	×	
	Dynamometer - CL	Sugisaki et al., 2011	√	√	×	×	↑ Stiffness with ↑ force
Mapping of the triceps surae muscle activation	Clinical set up EL/CL		×	×	×	×	
	Dynamometer Isometric and isotonic CL	Staudenmann et al, 2009	×	×	√	×	Substantial heterogeneity of the triceps surae muscle

ATF = Achilles tendon force, MP = Complete spectrum of tendon mechanical properties, EMG = electromyography, FP = force perturbations, CL = concentric loading, EL eccentric loading.

## **1.12 Conclusions**

It is concluded from the literature review that there is no consensus on the employment of exercise variables during EL. The mechanism behind the efficacy of EL is unknown. It has been shown recently that EL results in high frequency GrF perturbations. However, the effect of exercise variables is largely unknown on the tendon biomechanics, muscle activation and perturbations.

## **Chapter 2: Aims and Objectives**



## 2.1 Aims

The effects of eccentric rehabilitation regimes might be better explained with a more thorough clarification of the biomechanical characteristics of the exercise, exploring differences between eccentric and concentric loading, particularly exploring and quantifying the effect of speed, load and dose variation on the mechanical properties, muscle activation and force perturbations of the triceps surae complex.

The overall aim of this thesis was to biomechanically characterise and compare EL and CL. Specifically, this thesis aims to explore and quantify the effects of speed, load and dose variation on the mechanical properties, muscle activation and force perturbations of the triceps surae complex. Investigating these critical questions may improve our knowledge of EL and its efficacy, potentially facilitating the development of EL protocols, to make them more effective and efficient.

These aims were achieved through a series of objectives.

## 2.2 Objectives

The main objectives of the study were:

- 1) To develop methods to measure *in vivo* tendon force and extension (Chapter 3).
- 2) To compare the biomechanical properties of the Achilles tendon and muscle activation of the triceps surae during EL and CL (Chapter 4).
- 3) To determine how movement speed affects the biomechanical properties of Achilles tendon and muscle activation of triceps surae during EL and CL (Chapter 5).
- 4) To determine how load affects the biomechanical properties of Achilles tendon and muscle activation of triceps surae during EL and CL (Chapter 6).
- 5) To determine a) how the temporo-spatial muscle activation features vary during EL and CL and b) whether tendon perturbations have a muscular origin (Chapter 7).

## 2.3 Hypotheses

The following alternate hypotheses were tested in a series of studies:

- 1) A reliable method to measure *in vivo* mechanical properties will be developed (Chapter 3).

Using this method to compare EL and CL, it is hypothesised that:

- 2) On changing exercise movement (Chapter 4)
  - a. Muscle activation will be higher during CL than EL.
  - b. Tendon force will be higher during EL than CL.
  - c. Tendon stiffness and strain will be higher during EL than CL.
  - d. Perturbation magnitude and frequency will be higher during EL than CL.
- 3) On changing exercise speed (Chapter 5)
  - a. Muscle activation will be higher during fast EL and CL.
  - b. Tendon force, stiffness and strain will be higher during fast EL and CL.
  - c. Perturbation magnitude and frequency will be higher during fast EL and CL.
- 4) A) On changing exercise load (Chapter 6)
  - a. Muscle activation, tendon force, stiffness and strain would all be greater when the triceps surae was subjected to higher loads.
  - b. Tendon perturbation will be higher with higher loads

B) On changing load and speed

  - a. Tendon perturbations would be larger in magnitude under eccentric conditions, particularly at higher speed and loads.

C) On changing dose

  - a. Variable dose of exercise would result in altered mechanics in the fatigue state; specifically, the ATF will increase the triceps surae muscles will show more activity, and tendon perturbations will increase in magnitude and frequency

- 5) On triceps surae activity (chapter 7)
  - a. Different patterns of muscle activation will not be observed across different regions of the triceps surae during exercise.
  - b. Tendon perturbations will not be of muscular origin.

## **Chapter 3: Materials and Methods**

### **3.1 Introduction**

In this chapter the generic features of the utilised equipment are outlined, accompanied by detail of how the specific devices used in the study were employed during the subsequently performed studies. Further, stages in the development and testing of the experimental setup are described, accompanied by developmental results.

### **3.2 Experimental techniques and equipment**

To realise the aims of the study, monitoring of both tendon and muscle during dynamic testing was required. In order to measure muscle activation, surface electromyography was used. To measure the mechanical properties of the tendon, a method that combined real-time ultrasonography (US) with lower limb kinematics and force plate analysis was utilized. *Figure 3.1* illustrates the setup of the study and the equipment used for synchronized data collection.

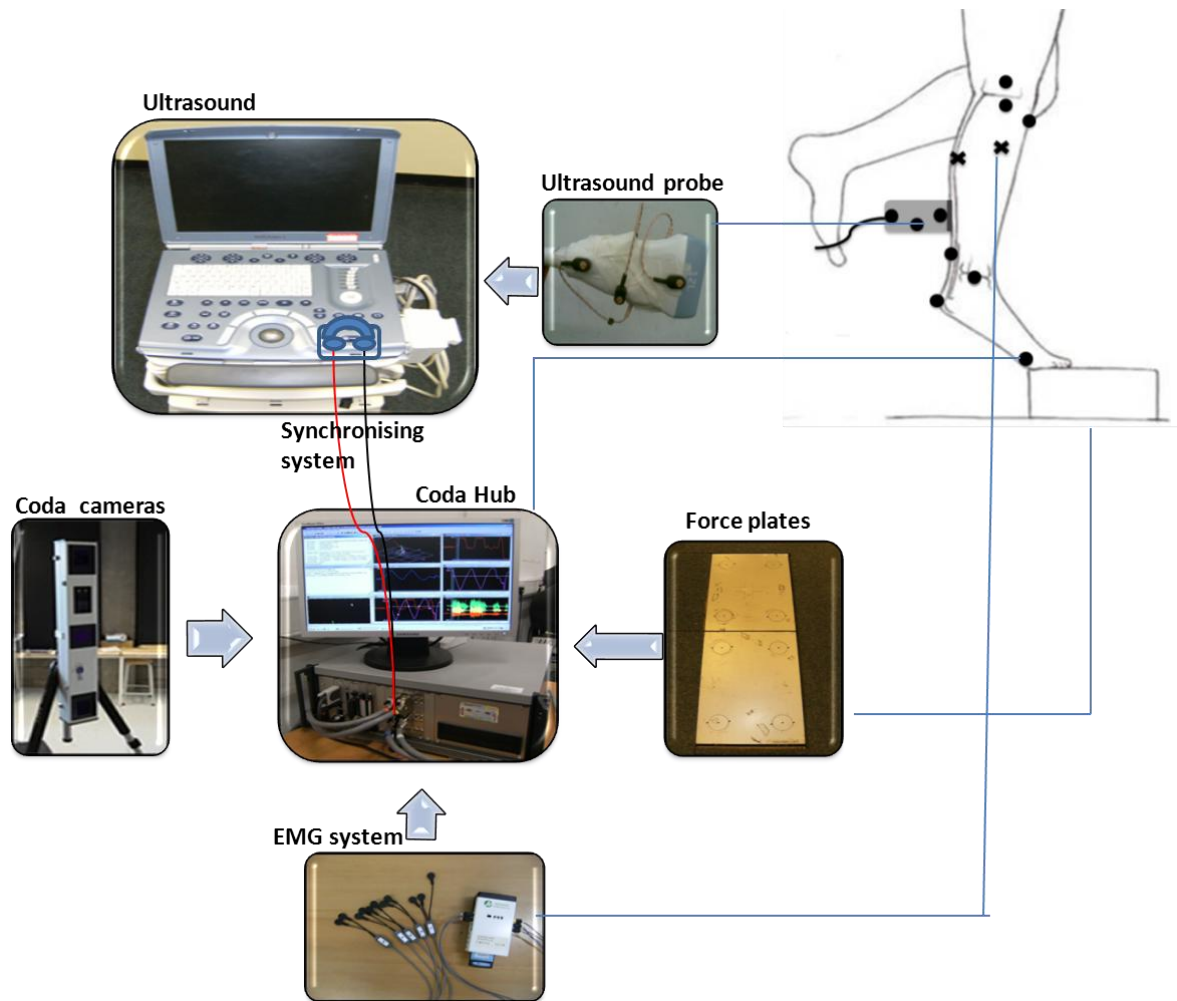


**Figure 3.1:** Diagram showing the experiment setup and the synchronization of the collection. An ultrasound probe was used to track the muscle-tendon junction (MTJ), motion analysis to track the lower limbs and ultrasound probe movements, force plates to measure the ground reaction force, and surface electromyography to measure muscle activation. To synchronise the force, EMG and motion data collected using CODA motion software with the ultrasound data, a synchronisation switch was developed. The placement of each piece of equipment on the leg is shown in the top right.

### 3.2.1 Electromyography

#### 3.2.1.1 General background

Electromyography (EMG) measures the electrical discharge of muscles (Basmajian and De Luca, 1985). These signals are typically recorded by electrodes, measuring differences in voltage between two points. Muscle contraction occurs in response to depolarisation of the motor endplate, in turn

due to arrival of a neuronal action potential. The action potential can be measured by placing the conducting material (electrodes) across the muscle fibre or muscle. The action potential across a single muscle fibre membrane is approximately - 90 mV at rest (Basmajian and De Luca, 1985). This potential rises to 30 - 40 mV on sufficient stimulation, representing a fibre action potential. In an intact muscle, all the fibres that make up any motor unit contribute towards this action potential, and make up the EMG signal. The EMG signal obtained from the depolarization of a motor unit is regarded as the motor unit action potential (MUAP). Generally the EMG signal obtained from voluntarily contraction is a result of many motor units firing at different rates. An increase in the firing rates or number of motor units is known to increase muscle force and the corresponding integrated EMG as well (Guimaraes et al., 1994).

As such it is important to carefully consider the positioning of electrodes for recording EMG signals (Hermens et al., 2000). To date, the widely adopted recommendations for electrode placement are from Surface Electromyography for the Non-Invasive Assessment of Muscles (SENIAM) guidelines, and these recommendations were followed during this project.

There are two main considerations when selecting EMG electrodes for a specific study. Firstly, the required positioning of the electrodes must be considered. If the specific action potential of a fibre is required, then invasive electrodes, commonly known as indwelling – or intramuscular – electrodes, are used, to target a specific location. By contrast, a compound action potential from a larger area of muscle can be recorded by positioning the electrodes on the skin over the muscle, using surface electrodes. In sports medicine, most studies rely on non-invasive measurements and subsequently surface EMG (sEMG) is preferred (Hermens et al., 1986). Surface electrodes are simpler to use and non-invasive, so safer to use during dynamic measurements as fine wire electrodes can break, and sEMG provides a general picture of the electrical activity of an entire muscle or muscle group. However, surface electrodes can only be used for recording from superficial, relatively large muscles.

The second consideration for electrode selection is electrode configuration, which can be either mono-polar or bipolar. Generally, a bipolar electrode configuration is employed for dynamic EMG recording in which the electrical potential between two electrical contacts is measured. Each individual measurement is relative to the common ground electrode, using a differential amplifier to amplify the difference across the electrodes and reduce the effects of extra-muscular electrical signal. In the mono-polar setting, there is only one electrical contact and the potential is measured with respect to a reference electrode. The signal obtained in this manner can contain other unwanted electrical signals (Nigg and Herzog, 2007), thus requiring sophisticated post-processing to filter the measured signal.

### **3.2.1.2 Current study**

A number of studies investigating the mechanical properties of the AT record the gastrocnemius and soleus muscle activity (Zwerver et al., 2007, Henriksen et al., 2009, Richards et al., 2008). In order to investigate the contribution of the triceps surae muscle in the effectiveness of EL, EMG of these muscles, as well as tibialis anterior, was analysed under different loading conditions.

In the current study a wireless system was used to allow free movement of the lower leg during movement (*Figure 3.2*). A telemetric EMG unit was used (Telemetry 2400T G2, Noraxon, USA, Input impedance > 100 MΩ, common mode rejection ratio > 100 dB, Base gain = 500,  $f_c = 10 - 500$  Hz) with 16-bit analogue-to-digital resolution and preamplifier leads, at a sampling rate of 1500 Hz. The output was up to 100 mW, transmission frequency DSSS 2412-2464 MHz, and the system could send real-time EMG up to 300 feet by wireless transmission of in line-of-sight recordings.



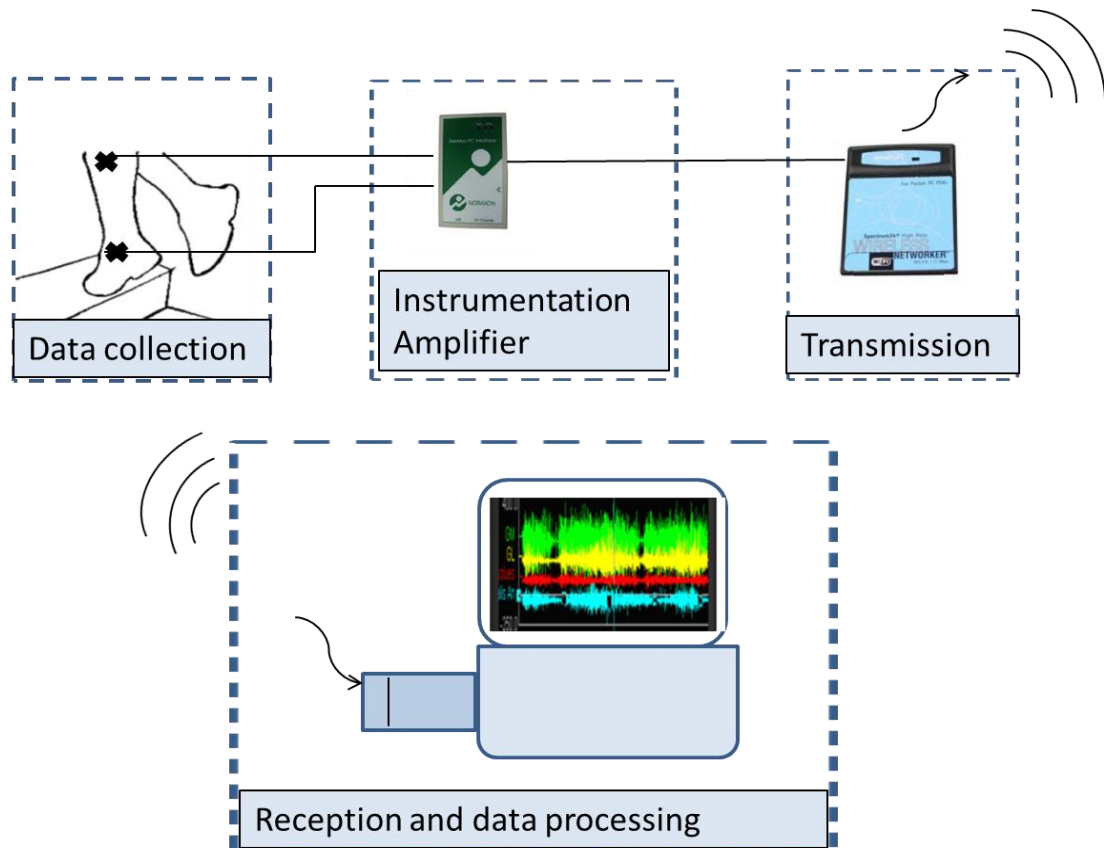


**Figure 3.2:** Block diagram of the EMG setup. Muscle activation is recorded for the lower leg muscles, with a reference electrode on the lateral malleolus, and then amplified within the on-body EMG device. A transmission card is used to transfer the data over a wireless network to a PC mounted receiver.

The electrodes were placed on the subject according to the SENIAM guidelines (Hermens et al., 2000). The skin was carefully prepared by shaving the area, abrasion with medical grade sand paper and cleaning with spirit. Bipolar electrodes (Noraxon dual electrodes; spacing 20mm; disposable, self-adhesive AG/AGCL snap electrodes for surface EMG applications) were placed over the:

a) Soleus Muscle

With the subject sitting with the knee approximately 90 degrees flexed and the heel of the investigated leg on the floor, electrodes were placed at 2/3 of the line between the medial condyle of the femur and the medial malleolus.

b) Tibialis anterior

With the subject in a supine position electrodes were placed at 1/3 of the line between the tip of the fibula and the tip of the medial malleolus.

c) Medial Gastrocnemius

Electrodes were placed on the most protuberant part of the muscle with the subject lying prone, the knee extended and the foot projecting freely over the end of the table.

d) Lateral Gastrocnemius

Electrodes were placed with the subject lying supine, the knee extended and the foot projecting over the end of the table. Electrodes were placed at 1/3 of the way along the line between the head of the fibula and the heel.

### **3.2.2 Force Plates**

#### **3.2.2.1 General background**

Force plates are commonly used in biomechanics for quantifying forces exerted on the supporting surface during human and animal locomotion. Current force plates use a construction in which a rectangular plate is supported at each of the four corners where force transducers are also mounted (*Figure 3.3*). The force components along each of the three main axes  $F_x$ ,  $F_y$  and  $F_z$  are typically used in biomechanical analysis. Force plates also provide a resultant force. The vertical component corresponds to the sum of the gravitational forces acting on the body and the product of the mass and acceleration of the centre of mass of the subject in the vertical direction.

### 3.2.2.2 Current study

In the current study two 600 x 400 mm<sup>2</sup> force plates (Kistler force platform, 9281 B, Kistler instruments, US) were used. The coordinate axes of a Kistler force plate are defined in *Figure 3.3*. The force plate output was sampled at 1000 Hz. The applied Force (F) and point-of-ground application (PoA) were calculated first in the force-plate coordinates, and then converted to ground reaction force (GRF) and centre of pressure (CoP) or PoA in Coda/Lab coordinates.

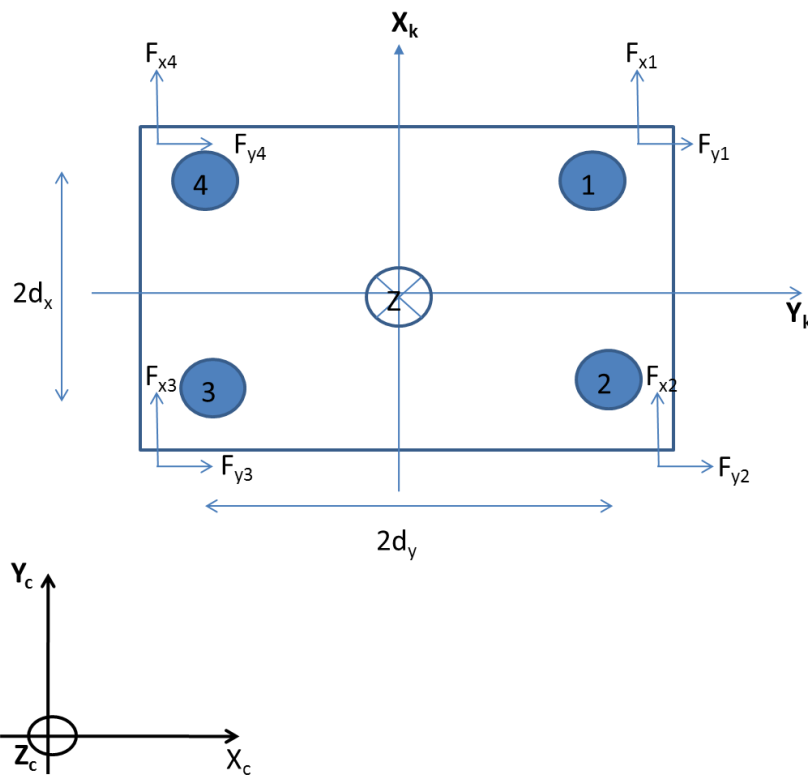


**Figure 3.3:** Kistler Force plate coordinate axes where  $dx = 120\text{mm}$ ,  $dy = 200\text{mm}$   $dz = 54\text{mm}$  for the 9281 Force plate (400 × 600). Four pressure sensors named as 1, 2, 3 and 4 are used to measure the force.

The components of the applied Force, F are given by:

$$F_{1x} = F_{x12} + F_{x34} \quad (F_{x12} = \text{Horizontal force on sensors 1 and 2}) \quad \text{Equation 3.1}$$

$$F_{1y} = F_{y14} + F_{y23} \quad \text{Equation 3.2}$$

$$F_{1z} = F_{z1} + F_{z2} + F_{z3} + F_{z4} \quad \text{Equation 3.3}$$

The point of application ( $a_x$ ,  $a_y$ ) of the force ( $F$ ) was calculated by equating moments about the horizontal axes:

Clockwise moments about the x-axis:

$$Fz \cdot a_y = -Fy \cdot dz + (Fz_1 + Fz_2) \cdot dy - (Fz_3 + Fz_4) \cdot dy \quad \text{Equation 3.4}$$

Clockwise moments about the y-axis:

$$-Fz \cdot a_x = Fx \cdot dz + (Fz_2 + Fz_3) \cdot dx - (Fz_1 + Fz_4) \cdot dx \quad \text{Equation 3.5}$$

( $dx$ ,  $dy$ ,  $dz$  are all positive values)

Thus,

$$a_x = (-Fx \cdot dz + (Fz_1 - Fz_2 - Fz_3 + Fz_4) \cdot dx) / Fz \quad \text{Equation 3.6}$$

$$a_y = (-Fy \cdot dz + (Fz_1 + Fz_2 - Fz_3 - Fz_4) \cdot dy) / Fz \quad \text{Equation 3.7}$$

In the current study, the force plate was oriented at 0 degrees. This orientation was set up so the force-plate y-axis was coincident with the Coda/Lab X-axis, hence the plate X-axis was coincident with the Coda/Lab Y axis, and the z-axis was coincident with the Coda/Lab Z-axis but with reversed polarity (the Coda/Lab Z-axis is positive upwards) as shown in *Figure 3.3*.

Thus point of reaction ( $p_x$ ,  $p_y$ ) is:

$$p_x = a_y = (-Fy \cdot dz + (Fz_1 + Fz_2 - Fz_3 - Fz_4) \cdot dy) / Fz \quad \text{Equation 3.8}$$

$$p_y = a_x = (-Fx \cdot dz + (Fz_1 - Fz_2 - Fz_3 + Fz_4) \cdot dx) / Fz \quad \text{Equation 3.9}$$

### **3.2.3 Motion tracking system**

#### **3.2.3.1 General background**

Kinematic measurement by motion capture is an important part of characterising segmental mechanics. By tracking the motion of bony landmarks, a close approximation of joint movement can be made and, in combination with kinetic data, the forces acting on these joints can be achieved. Motion can be tracked using cameras with sufficient resolution, accuracy and identification of object features.

Increasingly advanced imaging devices have been developed over the past decade to track and record the movement of skin-mounted markers to greater accuracy. Skin markers generally fall into 2 categories: passive (markers which are coated with a retro-reflective material to reflect light that is generated near the camera lens e.g., reflective tapes) or active (markers that emit light themselves e.g., electronic transmitters, LEDs). Cameras are also either passive or active in nature. Passive camera types includes film, video, Infra-red signal or source sensors. Active cameras send a beam of light to an object, using rotating mirrors or scanners that sequentially sweep a beam of light through the space of interest.

#### **3.2.3.2 Current study**

A four passive camera, active marker, motion analysis system (CODA CX1, Charnwood Dynamics, Rothley, UK) was used in the current study. It is a general-purpose 3-D active source sensor motion tracking system, with interfacing for synchronous analogue and digital data acquisition such as force-plate or EMG. The measurement unit contains four pre-aligned solid-state cameras which track the position of up to 28 active markers (infra-red LEDs) in real-time (*Figure 3.4*).

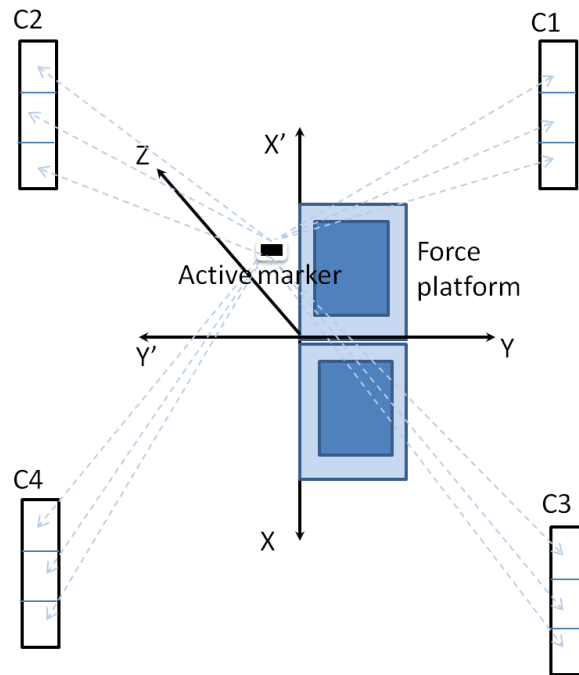


**Figure 3.4:** Schematic of the CODA motion analysis system with four cameras (C1-4) receiving signals from a single active marker placed arbitrarily, in this case, within the volume. Motion analysis is generally combined with force plate data to acquire forces during movement. In such a setup, cameras are aligned to an origin between the two force platforms. The motion analysis coordinate system (XYZ) is also shown.

The CODA system has the advantages of simple marker labelling and high sampling rates; however there are also a few disadvantages. The main problem with this system is the restricted light-emission angle from the markers, which can potentially reduce the field of view. However, this is regularly dealt with using more than two sensors to ensure accuracy of the recording, as adopted during the present study. Also, active marker systems require time-multiplexed lighting, limiting the number of markers that can be used on the subject and resulting in non-simultaneous sampling of the marker's coordinates (Nigg and Herzog, 2007). However, only 15 markers were required for the present study to quantify the lower single leg mechanics which will not lead to any significant time delay. Sampling rates for CODA motion analysis system are selectable from 1Hz to an upper limit, ranging from 100 - 800 Hz, depending on the number of markers used. When multiple measurement units (cameras) are used, all markers are tracked simultaneously by each unit. In the present study 4

cameras and 15 markers were used at a sampling rate of 200Hz. The angular resolution of each camera is approximately 0.03 rad (0.002 degrees), resulting in a lateral position resolution of approximately 0.05 mm at a distance of 3 metres (horizontally and vertically), and a range resolution of about 0.3 mm. For standard markers, the measurement volume extends from a distance 2.0 m to 6.0 m in front of the measurement unit, at a width and height approximately 1.6 times the distance (Codamotion, 2010).

In the present study, to measure the moments around the ankle and knee joint, active markers were placed on the lateral and medial malleoli, metatarsal 1 and 5, calcaneus, tendon, medial and lateral tibial condyle, tibial tuberosity, femoral epicondyle and hip joint according to ISB recommendations (*Figure 3.5*)(chapter 1, section 1.2.6).

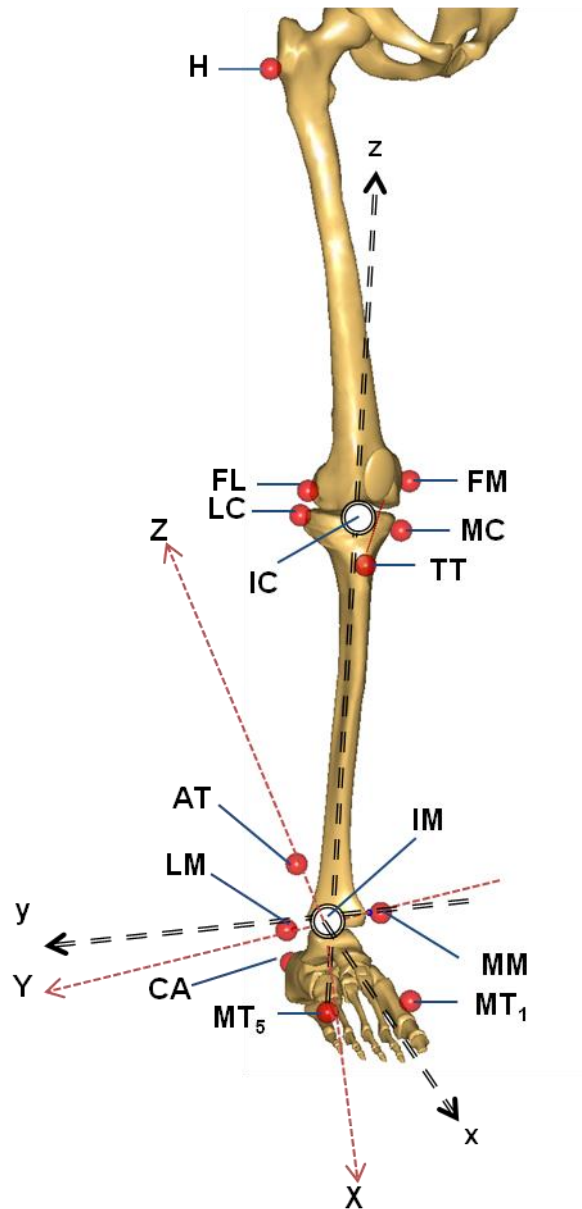


**Figure 3.5:** Marker placement: H = greater trochanter; FM = Femur Medial epicondyle; FL = Femur Lateral epicondyle; MC = Tibia Medial Condyle; LC = Tibia Lateral Condyle; IC = inter condyle point (virtual Marker shown in white); TT = Tibial tuberosity; LM = Lateral Malleolus; MM = Medial Malleolus; IM = inter Malleolus (virtual Marker shown in white); AT = Achilles tendon; CA = Calcaneus;  $MT_1$  = Metatarsal 1;  $MT_5$  = Metatarsal 5. The coordinate systems for tibia\fibula (XYZ) and calcaneus (xyz) are also shown.



### **3.2.3.3 Motion analysis software**

Data from the force plates, cameras and EMG were collated using Coda motion analysis software which controls the simultaneous input of the CODA channels. It provides the user-interface to the Coda hardware which also provides real-time display of marker position, analogue force and EMG. It also provides data processing functions for initial data analysis and display. Of importance in the current study, it can record the velocity/acceleration of a marker, and provides information on the centre of pressure data from force plates. While the software is designed for general-purpose motion analysis, most of the *analysis* tools are specific for clinical gait analysis. For this reason most of the analysis in this study was done by developing analysis tools and programmes in MatLab (Version 7.9.0.529 (R2009b), 32-bit, The MathWorks Inc, USA).

## **3.2.4 Ultrasound**

### **3.2.4.1 General background**

Ultrasound (US) is widely used in medicine, and its number of applications is continuing to grow. It is routinely used for imaging across a wide range of clinical areas, gaining popularity as a result of its portability, reliability, non-invasive use and real time display (Wells, 1987). Ultrasound imaging covers a variety of applications, such as B-mode imaging, colour flow imaging, spectral Doppler, three dimensional imaging and tissue motion measurements (Beach, 1992). US imaging is most commonly carried out in B-mode, describing a two dimensional brightness image of echo magnitude. However, developments in hardware have facilitated the development of 3D and 4D imaging also.

*Figure 3.6* illustrates the steps involved in acquiring an image of any tissue, such as the muscle-tendon junction required in the current study. Ultrasound is sound waves with a frequency above the bandwidth of human perception (20 - 20 kHz). Ultrasound waves are generated by piezoelectric transducers located in the Ultrasound probe. The Piezoelectric transducer converts electronic pulses to short ultrasound pulses with a determined pulse repetition rate (PRR). The pulses are then

transmitted and interact with the tissue. As the Ultrasound pulse travels down through the tissue, a portion of the pulse gets attenuated and absorbed. However, some of the pulse is reflected back, particularly from the interface between materials in the body that have different acoustic impedances. The reflected echoes are collected and converted to an electric signal by the transducer. The reflected ultrasound pulse is referred to as the Radio Frequency (RF) pulse. The received echoes are then amplified, including time gain compensation, to compensate for attenuation of the transmitted signal as it travels through the tissue. The signal is sampled and converted to a digital signal using an analogue to digital (A/D) converter. Demodulators are then used to recover the signal (echo) (York and Kim, 1999). The absolute magnitude of the signal is established, then the signal is processed to take its logarithm (LOG), before finally filtering (to enhance the edges) or speckle reduction is applied, to get better contrast. Finally the signal is display on an LCD in full display (York and Kim, 1999).

The Ultrasound device estimates the distance to tissue structures in an area of interest, according to the speed of sound of the ultrasound wave in the tissue and the time it takes for the ultrasound echoes to return to the transducer. The ultrasound unit then displays the data of the echo intensity and distance on the screen, in the form of a two-dimensional image.

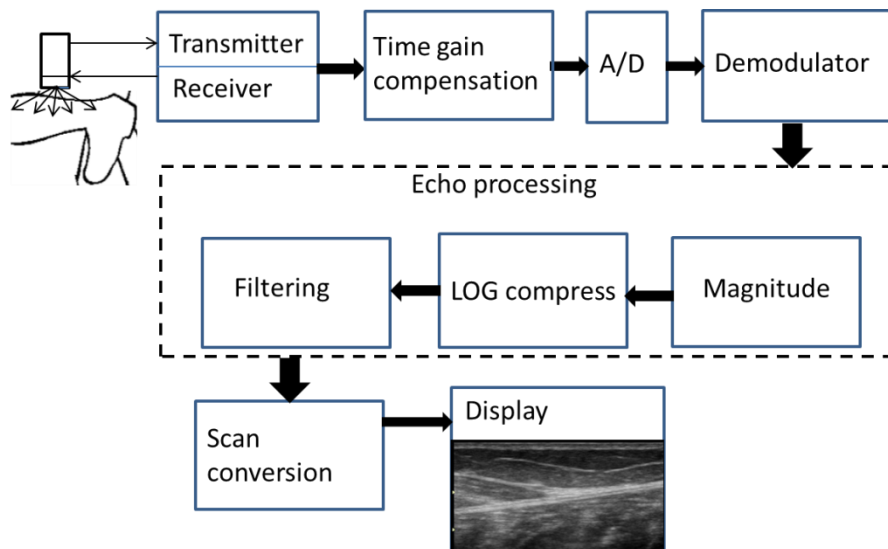


**Figure 3.6:** Block diagram of a standard ultrasound imaging system.

### 3.2.4.2 Current study

Ultrasound has become a popular device to examine tendons for research and clinical purposes (Magnusson et al., 2008, Lichtwark and Wilson, 2005b, Carroll et al., 2008, Mahieu et al., 2008) due to the high resolution and dynamic nature of scanning. Many tendons, particularly the Achilles, are superficial structures, and it is possible to use high frequency imaging, yielding high resolution images. The frequency range for imaging the Achilles tendon is usually between 5 MHz and 13 MHz. Ultrasound can be used to investigate tendon structure, rupture, degenerative changes, dislocation, inflammatory conditions and tendon tumour (Arya and Kulig, 2010, Boesen et al., 2006, de Vos et al., 2007a).

Although ultrasound has been used by a number of authors to track the muscle-tendon junction (MTJ) during movement it is difficult to track the complete junction with standard probes, as the movement is longer than the image width (Henriksen et al., 2009, Kulig et al., 2009). In the present study a 'Voluson e' (GE Healthcare, UK, wide band, frequency = 3.7 - 11.3 MHz, FOV = 37.4 mm, FR = 25 Hz) wide band, multi frequency linear transducer was used in B-mode. The field of view (FOV) of the probe was 37.4 mm which is sufficient for small movements but as the movements during this

study were larger, the probe was manually (hand held) placed such that the MTJ was on the edge of the field of view, so that the MTJ can be tracked for the whole movement.

### **3.2.4.3 Synchronising device**

It was crucial to synchronise the data collection from all the four systems (EMG, motion tracking, force plates and US) to ensure accurate data combination during subsequent analysis. The CODA software simultaneously collects sEMG and force data alongside marker positions. To ensure US data synchronisation, different possibilities were assessed. The most reliable and practical method was considered to be the use of a trigger-start to commence both the US and Coda acquisition. This was achieved by manual integration of a TTL switch with the acquisition button on the US unit. This gave an output signal defining the start of US data acquisition (*Figure 3.7*). This signal was fed to the digital input channel of the CODA active hub and used to trigger motion data acquisition. Coda motion analysis, EMG, force plates and US could therefore be synchronised as shown schematically in *Figure 3.7*. The accuracy of the synchronisation pulse was within 55ms according to the hardware specifications.

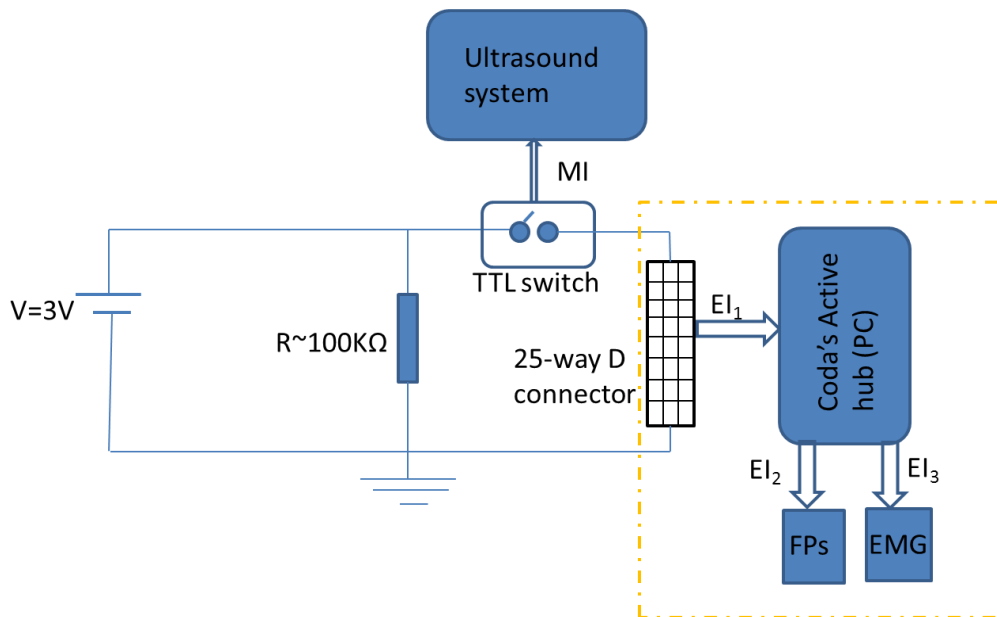


**Figure 3.7:** Schematic diagram of the synchronization system developed for synchronising the motion analysis, force plates (FPs), EMG and US data. Manual integration (MI) of US was achieved with a switch which triggered the CODA active hub through electrical integration ( $EI_1$ ). The hub (shown with a yellow dotted line) was further electronically integrated ( $EI_2$ ,  $EI_3$ ) with the Force plates and wireless electromyography (EMG) system.

### 3.3 Experimental procedure

This section describes the *in vivo* measurement methodology. It covers the generic study protocol, used as the basis for the bulk of the experimental work. All protocols were approved by Queen Mary, University of London Research ethics committee (Appendix I).

To biomechanically characterize the triceps surae response to varied movement types, measurements combined ultrasonography to track the muscle-tendon junction, motion analysis to track the lower limbs and ultrasound probe movements, force plates to measure the ground reaction force, and EMG recording to measure muscle activation (*Figure 3.8*).

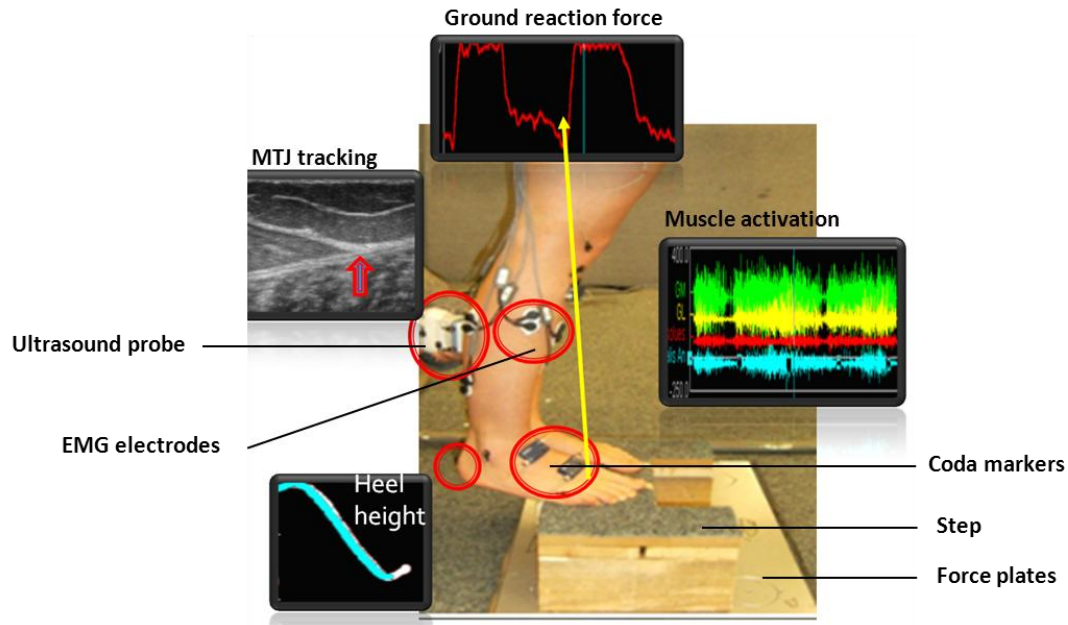


**Figure 3.8:** The exercise was performed on a wooden box placed on a recessed force plate. EMG was recorded by electrodes placed on the calf muscle and joint motion was tracked by placing CODA markers on the leg joints. An US probe tracked the MTJ, with motion tracking markers attached to monitor its position.

In addition, in order to investigate the MTJ movement and the motion of the body, the position of the ultrasound image relative to the probe coordinate system was required. For this purpose, motion tracking markers were placed on the probe. As shown in *Figure 3.1*, two markers were placed along the ultrasound axis while a third marker was placed approximately 60 mm from the midpoint of the line intersecting the initial markers, so its position could be tracked and spatially synchronised with the motion data.

### 3.3.1 Subjects

A total of 40 subjects participated in the four studies described in this thesis, recruited by advertisement and snowball recruiting, predominantly from the QMUL staff and student body. All subjects were informed about the testing and training procedures, understood the risk involved, and gave written consent for participation. Not all subjects performed all conditions so sample details are given alongside sub-study specifics in each results chapter.

### **3.3.2 Movement protocol**

For performing eccentric loading EL, each subject was asked to stand on the ball of the foot of the right leg with the heel raised (*Figure 3.9*). To perform the exercise, the heel was lowered in a controlled manner. The exercise was performed off the edge of a step to allow full dorsi-flexion to be reached. For concentric loading (CL), subjects started with the heel below the toes and raised the heel during the exercise in the same controlled manner. In order to keep the speed consistent, subjects were taught to complete the heel raise or heel drop at the required speed using guidance from a metronome set at 60 Hz. After completing either exercise, the subjects used the other leg to assist in returning to the starting position, by stepping on a separate step placed on a second force plate, before repeating the exercise. A single data collection consisted of 2 cycles of either CL or EL performed consecutively. Three sets of such data were recorded for each loading paradigm, for each subject, in a randomized order. Time was allowed to perform familiarisation exercises. These trials also provided pre-conditioning of the triceps surae muscle-tendon unit to ensure minimal variation in the load-deformation curves (Maganaris and Paul, 1999). It has been reported that warm up and stretching does not significantly affect the mechanical properties of Achilles tendon (Park et al., 2011), thus small variations in the time subjects spent on familiarisation was not felt likely to affect the results.

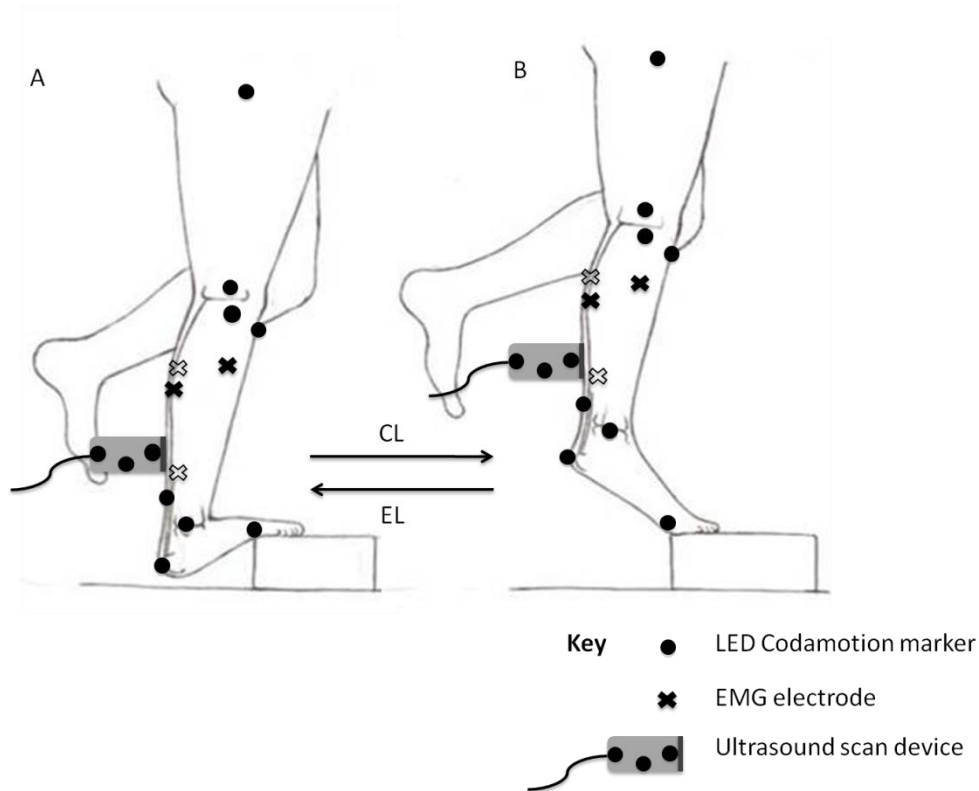
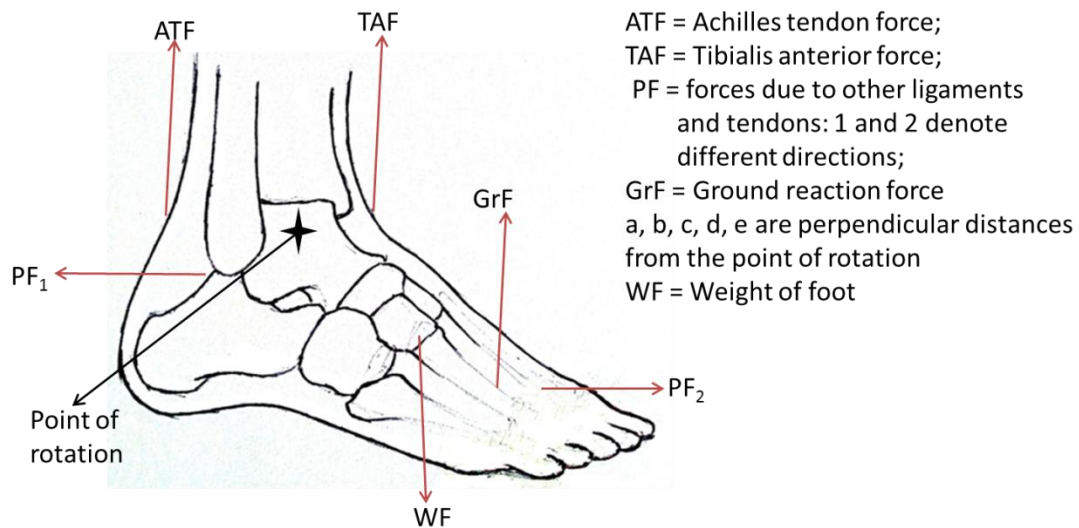


**Figure 3.9:** Eccentric and concentric loading of the Achilles tendon. (A) Image shows the starting position for concentric loading. Concentric loading involves shortening of the triceps surae muscle and lifting to the position in image B. (B) Image shows the starting position of EL, the triceps surae lengthens as the heel is lowered below the level of the forefoot to the position in image A during eccentric loading (open crosses show EMG electrode placed on the medial side of the leg).

### 3.3.3 Measurement of Achilles tendon Force

Achilles tendon force (ATF) has previously been estimated in biomechanics studies by inverse dynamics (Rees et al., 2008, Lichtwark and Wilson, 2005b, Henriksen et al., 2009). This technique assumes that forces due to other tendons and ligaments including the tibialis anterior are negligible. The spectrum of forces acting on the foot is shown in *Figure 3.10*. There are a number of forces acting in different directions on the foot that include, but are not limited to the force passing through the tendon, the force due to the contraction of the tibialis anterior, the GrF, and the forces due to other tendons and ligaments in the foot.





ATF = Achilles tendon force;  
 TAF = Tibialis anterior force;  
 PF = forces due to other ligaments  
 and tendons: 1 and 2 denote  
 different directions;  
 GrF = Ground reaction force  
 a, b, c, d, e are perpendicular distances  
 from the point of rotation  
 WF = Weight of foot

$$\Sigma \text{Torques} = 0 = \text{ATF} \cdot a - \text{TAF} \cdot b - \text{GrF} \cdot c - \text{PF}_1 \cdot d + \text{PF}_2 \cdot e$$

$$\text{ATF} \cdot a = -(\text{TAF} \cdot b + \text{GrF} \cdot c + \text{PF}_1 \cdot d - \text{PF}_2 \cdot e)$$

$$\text{PF}_1 \pm \text{PF}_2 \sim 0 \text{ N but TAF not } \sim 0 \text{ N}$$

Therefore

$$\text{ATF} \cdot a = -(\text{TAF} \cdot b + \text{GrF} \cdot c)$$

**Figure 3.10:** Illustration of some of the forces acting on the foot.

In order to estimate the ATF (following previously described methods), the 3D ground reaction force was captured using the Kistler force plates (section 3.2.2). The CODA motion system with four cameras (section 3.2.3.2) was used to measure the moments around the ankle and knee joint by placing markers on the lower leg (Figure 3.5). The motion analysis global coordinate system was aligned to the force plate so that the ground reaction vector could be transformed into it. The tibia/fibula coordinate system was defined as per ISB recommendations (Wu et al., 2002) (section 3.2.3.2).

The moment arm of a muscle-tendon unit is defined as the perpendicular distance between the line of muscle/tendon force action and the rotational centre of the corresponding joint (Spoor and van Leeuwen, 1992). The ankle joint centre was estimated by creating a virtual point corresponding to

an approximation of the centre of rotation of the ankle (Wu et al., 2002) (*Figure 3.5*). This point was half the distance between the lateral and medial malleoli. The perpendicular distance to the ankle joint centre from the line joining the calcaneus marker and the AT marker was calculated for each time point. The moment arm from the line of the AT to the ankle joint was taken to be the length of this perpendicular minus a correction for skin thickness (determine for each subject, by measurement of US images in transverse mode) and a constant value of 2.5 mm representing half the thickness of the AT. ATF was calculated by dividing the externally applied ankle joint moment by this moment arm (*Figure 3.11*).

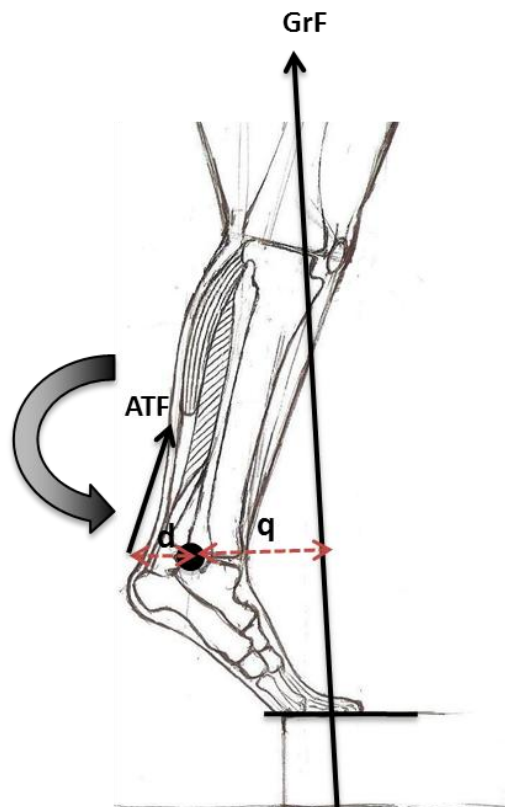


**Figure 3.11:** Schematic illustration of the ATF calculation. ATF was calculated by dividing the ankle joint external moment ( $GrF \times q$ ) by the moment arm between the AT and the ankle joint centre ( $d$ ).

### 3.3.4 Measurements of tendon cross sectional area

The cross sectional area (CSA) of the tendon was measured at the narrowest point by taking multiple ultrasound scans across the tendon in the transverse plane. Image J software (version 1.44o, NIH,

<http://rsbweb.nih.gov/ij/download.html>,) was used to analyse images and calculate CSA by tracing the outline (Figure 3.12).

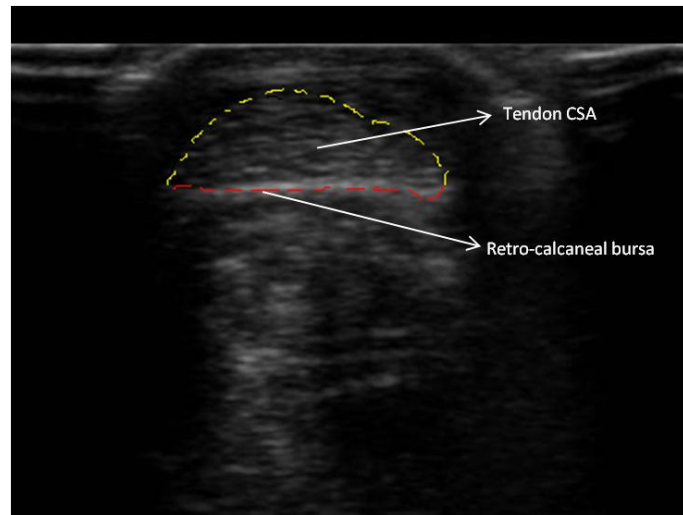


**Figure 3.12:** An example of the measurement of the Achilles tendon area. Image J software was used to analyse the area. The image in transverse mode was taken and the CSA is shown as area bounded between the red and yellow lines shown above.

### 3.3.5 Measurement of tendon elongation

Achilles tendon length (ATL) at any time was defined as the distance between the AT insertion, defined by a single marker placed on the calcaneum, and the distal muscle-tendon junction (MTJ) of the medial gastrocnemius (GM) (Figure 3.13). In order to establish this length, it was necessary to track the three dimensional position of these two locations throughout each exercise, so that the instantaneous tendon length and displacement could be established. The MTJ was visualised using the US probe, which was in turn tracked using three motion tracking markers (CODA) placed on the probe. As shown in Figure 3.13, two markers were placed along the ultrasound axis, while a third marker was placed approximately 60 mm from the midpoint of the line intersecting the initial markers.

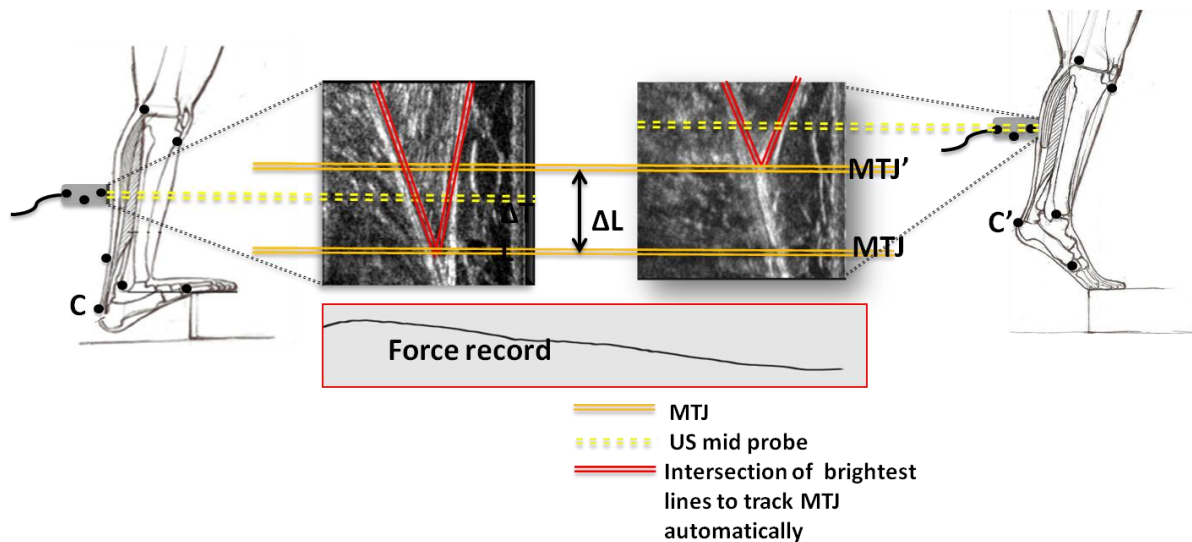


**Figure 3.13:** Set up used for MTJ tracking to establish Achilles tendon length. *C* and *C'* denote the calcaneus position at full plantarflexion and dorsiflexion respectively. *MTJ* and *MTJ'* is the location of the muscle-tendon junction at full dorsiflexion and plantarflexion. The distance between the two positions is defined as Achilles tendon length change. Tendon length at each time point was defined as the distance between *C* and the *MTJ*.

### 3.3.5.1 Ultrasound probe tracking accuracy

The accuracy of probe tracking using the combined ultrasound and CODA was assessed using a phantom. A metallic wand of known dimensions was immersed in a container full of ultrasound gel, such that the container of the gel represented the leg and the wand represented the tendon. Along the length of the wand, a metallic coil was placed to represent the MTJ (Figure 3.14). Moving the US gel bath thus simulated the muscle and MTJ moving within the leg. Movement of the wand and coil was tracked directly with the motion markers and compared with the movement measured with the US probe.

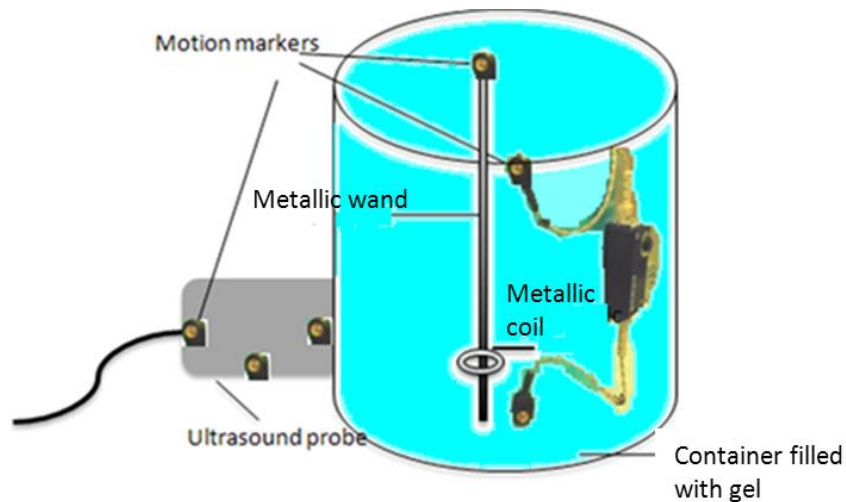


**Figure 3.14:** Illustration of a wand immersed in a gel container being imaged by an ultrasound probe with motion markers attached. The position of the coil relative to the laboratory coordinate system was tracked by the motion analysis markers and also with the ultrasound probe. The tracking results from the two were compared.

### 3.3.5.2 Tracking of the muscle-tendon junction

To obtain tendon length from the US images of the MTJ, it was necessary to define and track a consistent feature of the MTJ within each frame of the video and then combine these data with the known 3D location of the probe. Tracking the MTJ throughout the US video is a complicated task that requires locating the intersection of the muscle fascia in every frame of the video. This has previously (see *Table 3.1*) been carried out by methods such as manual marking of the MTJ using standard software (Maganaris, 2002, Maganaris and Paul, 2002). However, such a method is a labour intensive task, as one 15 s video at 17 Hz consists of 255 frames. In addition, while the human eye is very good at image correlation, the independence and reproducibility of this approach cannot be guaranteed, and a manual method will also fail if the movement is large and the junction moves off the screen. In the past there have been attempts to develop algorithms to analyse MTJ movement automatically (Korstanje et al., 2010, Loram et al., 2006, Magnusson et al., 2003). These techniques have been mainly based on the cross-correlation or Lukas-Kanade feature tracking, and

were tested on relatively small movements. However, such techniques have an inherent limitation in that the same feature of interest must be present in similar form in adjacent frames of interest. In addition the algorithm fails if the features of gastrocnemius and soleus changes with the movement and particularly when the movements are large. During dynamic movements, movements can be large enough to make the MTJ move off the screen and change its features. A method that tracked MTJ changes during large movements automatically was therefore required. *Table 3.1* summarises the main studies investigating *in vivo* biomechanics of the Achilles tendon, their measurement mode and the selected MTJ tracking method along with the stiffness and strain reported, in order to facilitate the comparison of the present and previous studies.

**Table 3.1:** Summary of the studies outlining a biomechanical analysis of the Achilles tendon/Gastrocnemius tendon.

	Study	Measurement Protocol	Mechanical Parameters studied	Reported stiffness and strain values (normal tendons)	MTJ tracking technique
<b>US Measurement</b>	(Kubo et al., 2002b)	isometric	Strain, modulus	8.1 %	Manual
	(Kubo et al., 2002a)	isometric	Stiffness	25.6 ± 9.0 N/mm	Manual
	(Kubo et al., 2003)	isometric	Stiffness, strain, modulus	Women:16.5 ± 3.4 N/mm, 9.5 ± 1.1% men : 25.9 ± 7.0 N/mm , 8.1 ± 1.6%	Manual
	(Mahieu et al., 2008)	Isometric	Stiffness	45.394 ± 3.792 N/mm	Manual
	(Morrissey et al., 2011)	Isometric	Stiffness, modulus	20.9 ± 7.26 N/mm	Image J
	(Magnusson et al., 2003)	Isometric	Stiffness, strain,	36.5 ± 4.6 N/mm, 8.0 ± 1.2%	Lukas-Kanade algorithm
	(Csapo et al., 2010)	Isometric	Stiffness, strain, modulus	111.3 ± 20.2 N/mm, 6.98 ± 1.00%	Image J
	(Reeves et al., 2003b)	Isometric	Stiffness, modulus	1376 ± 811 N/mm	Manual
	(Maganaris and Paul, 2002)	Isometric	Stiffness, strain	875 ± 85 N/mm, 4.9 ± 1 %	Manual
	(Reeves et al., 2005)	Isometric	Stiffness, modulus	136 ± 66 N/mm	NIH Image (digitize)
	(Maganaris, 2002)	Isometric	Strain	4.7- 6 %	Manual
	(Arya and Kulig, 2010)	Isometric	Stress, Stiffness, Strain,	375.25 ± 61.88 N/mm, 4.36 ± 0.31 %	Manual
	(Child et al., 2010)	Isometric	Strain	3.4 ± 61.8 %	Image J
<b>US + Motion System Measurement</b>	(Arampatzis et al., 2005)	Isometric	Strain	4.727 ± 1.85 %	Simi Motion for image digitization
	(Lichtwark and Wilson, 2005b)	hopping	Stress, Stiffness, Strain, Modulus	188 ± 43 N/mm 8.3 ± 2.3% (max=11.4%)	NR (manual)
	(Arampatzis et al., 2007b)	Isometric	Strain, Stiffness	186.7 ± 38.3 N/mm 4.6 ± 1.5%	Simi Motion for image digitization
	(Arampatzis et al., 2007a)	Isometric	Strain, Stiffness	21.9 ± 4.5 k N/strain 6.27 ± 1.3%	Simi Motion for image digitization
	(Rees et al., 2008)	EL and CL	NR	NR	NR
	(Peltonen et al., 2010)	isometric	Stiffness	430 ± 200 N/mm	Vicon Motus for image digitization
	(Farris et al., 2011)	Running, hopping	Stiffness, Strain	Running: 176 ± 41 N/mm, 3.57 ± 1.8 % Hopping:176 ± 41 N/mm ,8 ± 2 %	NR (manual)
(Farris et al., 2012)	running	Stiffness, Strain	163 ± 41 N/mm, 3.5 ± 1.8 %	NR (manual)	

NR=Not reported

### **3.3.5.3 Semi-Automatic tracking**

In order to prevent human discrepancies, an algorithm was developed and implemented in MatLab (Version 7.9.0.529 (R2009b), 32-bit) to track the MTJ (Appendix II). *Figure 3.15* illustrates the steps involved in the algorithm, tracking the MTJ as the crossing point of the two brightest lines. The size of the image was 800 x 600 pixels, which was immediately trimmed to a region of interest of 481 x 412 pixels (*Figure 3.15A*). To provide automatic MTJ recognition, the projection of both bright fascia lines was established along the radial line, and their angle of orientation relative to this determined using the Radon transform. Briefly the radon transform provides an intensity map of an image, from which the 2D location and angular orientation of the most intense image points can be determined (*Figure 3.15B*). Extracting data from the most intense points (*Figure 3.15C*) enabled the MTJ to be located from the intersection of these lines by finding the eight brightest lines on each side of the junction. From the 8x8 matrix of brightest lines, the 64 intersection points were located, and the junction taken as the median of these intersection points (*Figure 3.15D*). The reliability of this algorithm was checked by comparing results from three separate attempts to track each video and a comparison between manual and automatic tracking was also carried out.



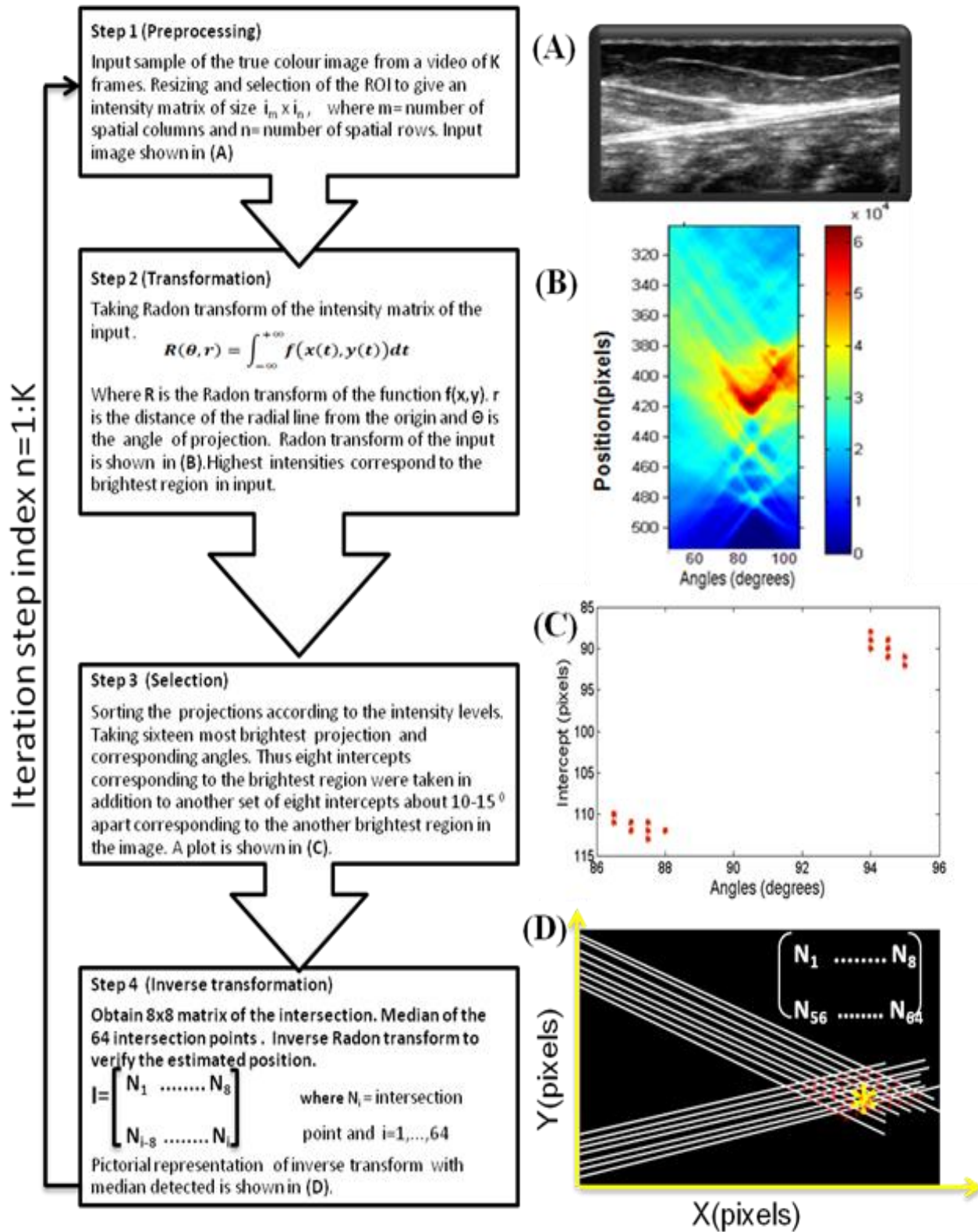


**Figure 3.15:** Algorithm steps for tracking MTJ displacement. The MTJ was found throughout the movement, by taking the median of the 64 intersection points as a result of 8 brightest lines on each side of the junction.

A schematic description of the Radon transform for a single frame is shown in *Figure 3.16*. A video frame is shown in (A) and the same frame in a blue rectangle (B) with dimensions  $X_f$  by  $Y_f$ ,  $X_m = X_f/2$  and  $Y_m = Y_f/2$ . An axis system (X & Y) is shown by the blue horizontal and vertical lines, with its origin at the centre. The line labelled  $X_r$  is a rotated X axis, rotated through an angle A which is greater than  $90^\circ$  in this example. The small red arcs show two angles which are equal to a, where  $a = A - 90^\circ$ . The line  $R_d$  is a line of a single element of the radon transform. It is perpendicular to  $X_r$ . It has an intercept on the  $X_r$  line at I. The designation of this line in the radon transform result is by the angle A and the intercept I. Its equation in the video system (shown by green lines) was required.

The intercept of  $R_d$  on the green Y axis is given as:

$$R_{dInt} = Y_m - d + q \quad \text{Equation 3.10}$$

where

$$d = I / \cos(a) \quad \text{Equation 3.11}$$

$$q = X_m * \tan(a) \quad \text{Equation 3.12}$$

and

The slope of  $R_d$  in the video axis system is:

$$S = -1 * \tan(a) \quad \text{Equation 3.13}$$

Equation of  $R_d$  in the video axis system is:

$$y = Y_m - I / \cos(a) + X_m * [\tan(a) - x * \tan(a)] \quad \text{Equation 3.14}$$

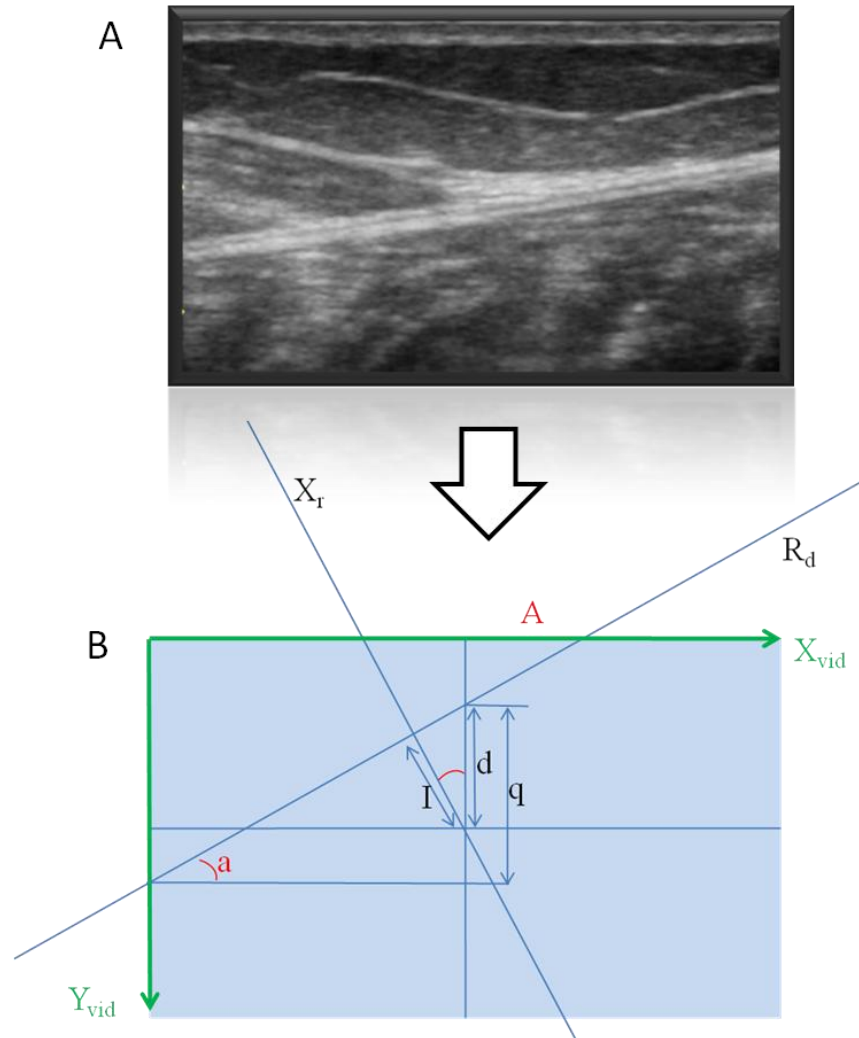


**Figure 3.16:** A) An MTJ image. B) A schematic description of the Radon transform, applied to calculate the MTJ in each frame of the US video.

#### 3.3.5.4 Total tendon length change

In order to find tendon length, it was necessary to embed the US images into the laboratory coordinates. To achieve this, a new origin was defined at the top left corner of the image as shown in (Figure 3.17). The MTJ displacement, as measured with the algorithm, was then subtracted from this distance to determine the Achilles tendon length.

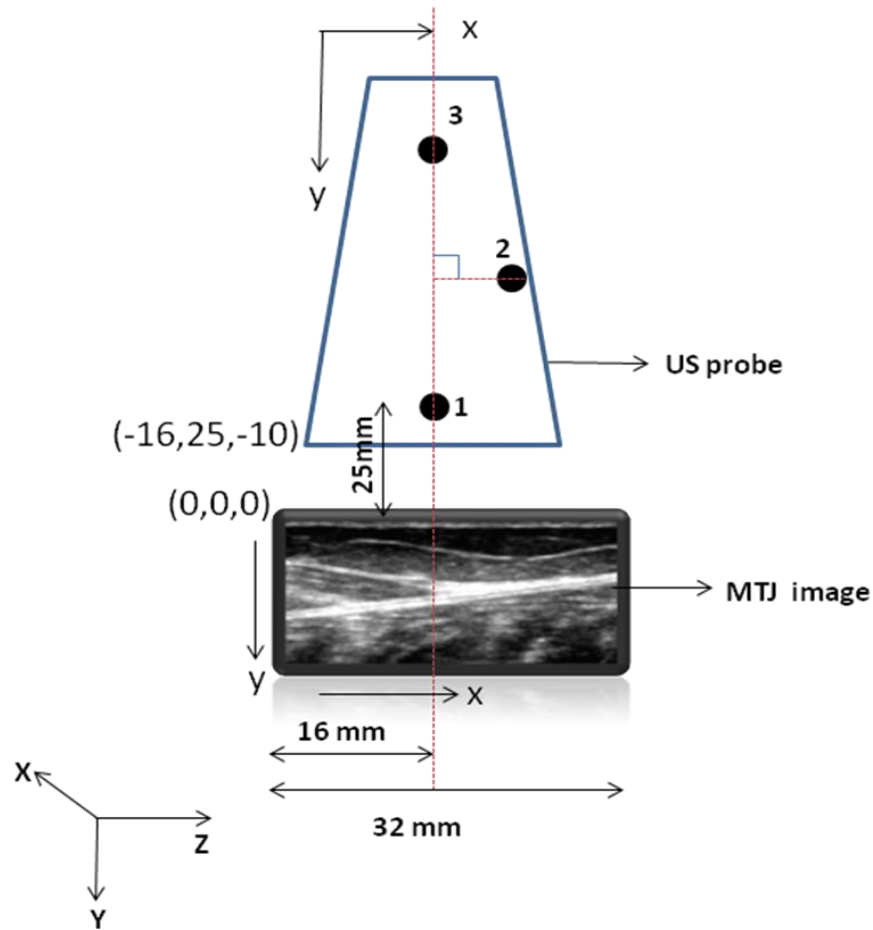


**Figure 3.17:** Schematic illustration of the tracking of MTJ. The junction was imaged by ultrasound whilst synchronously determining the position and orientation of the ultrasound image. The origin was initially defined at marker 1 which was then redefined at the top left corner of the image. The distance between middle of the US probe and the corner of probe was 16 mm in the negative x direction. The distance between the marker and the skin was found to be 25mm in the negative y direction, while the thickness of the probe was 10mm in the z direction. The image was embedded into the lab coordinates. The distance between the new origin and the calcaneus marker was measured. The MTJ displacement, as measured by the algorithm, was taken away from this length and the Euclidean distance defined as the AT length was measured.

### 3.3.5.5 Technique accuracy

In order to check the accuracy of the automatic tracking method against the current gold standard, MTJ tracking was carried out using Image J software (version 1.44o, NIH) (Figure 3.18) which has been employed in many previous studies (Child et al., 2010, Csapo et al., 2010). Two lines were drawn on each frame of video such that the lines were parallel to the inner boundary of the brightest region. The point of intersection of these two lines was considered to be the MTJ. The automatic tracking results were compared with those achieved using Image J software tracking.

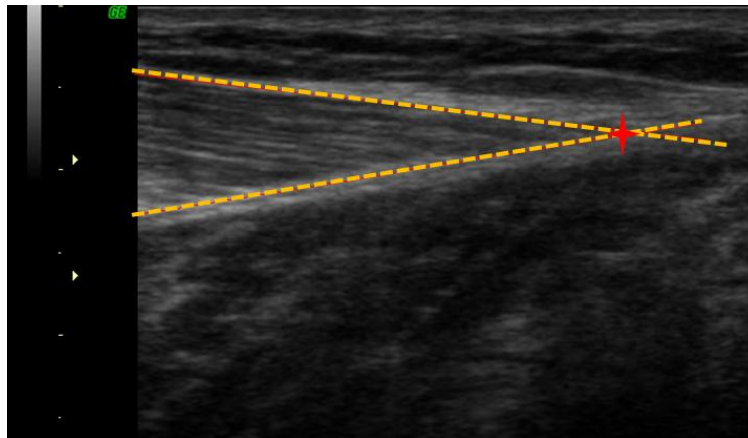


**Figure 3.18:** Manual tracking of the MTJ was carried out using Image J software. The intersection of the two lines (shown with a red star) was considered as the MTJ. The lines were drawn manually on each frame and the x, y pixel of their intersection was taken.

## 3.4 Data analysis

Data analysis was carried out in Matlab. For each exercise task, only the accurately paced cycles (within 10 % of the desired pace) were retained for further analysis. This was confirmed by observing the acceleration of the calcaneum marker using CODA software.

### 3.4.1 Registration

Points of minimum and maximum heel height (Hht) were identified as shown in *Figure 3.19*, and the portion of the record between them was re-sampled by interpolation to uniformly spaced points. This data registration isolated times of single leg support, as confirmed by the absence of a force reading from the plate under the contra-lateral foot (*Figure 3.20*). For descriptive purposes, ankle angles were extracted during each test. After registration, the mean data was obtained for the GrF and EMG for each individual subject. When required, the data from each individual were combined, to determine a group mean across all subjects.

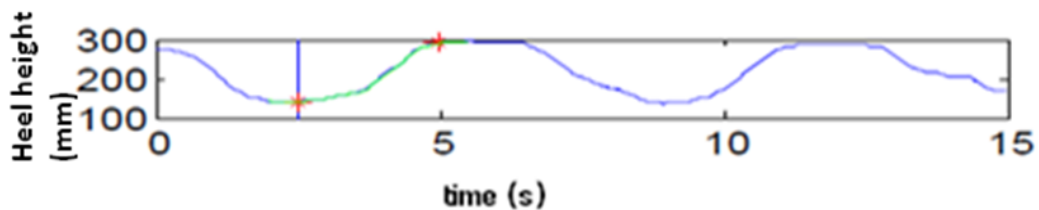


**Figure 3.19:** Data registration was carried out with respect to the heel height. Red stars represent the minimum and maximum heel height and the green line plotted between them shows the region of single leg support taken for further analysis.

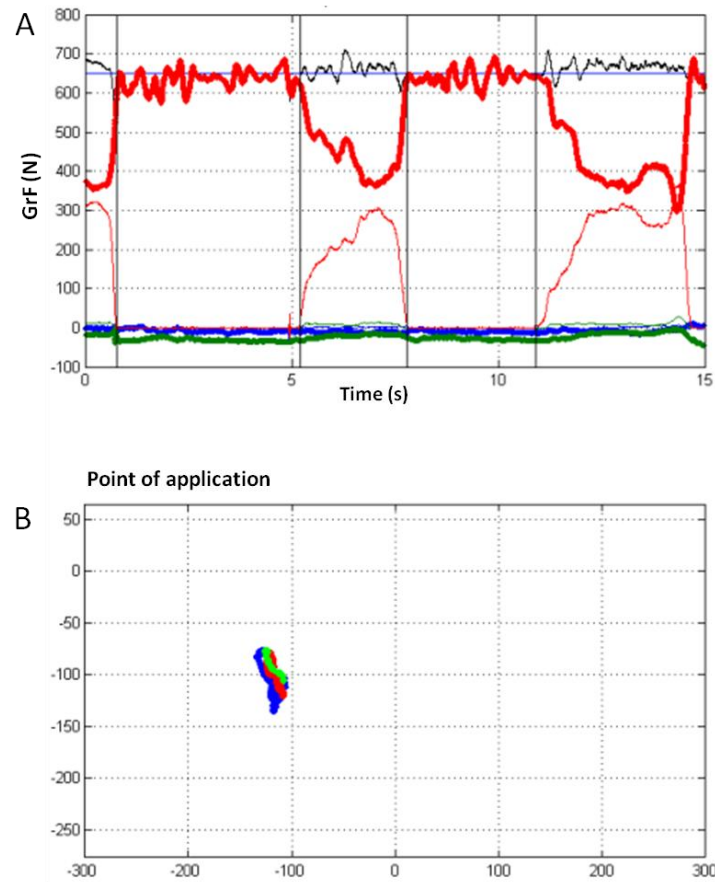


**Figure 3.20:** Description of the data registration. (A) Single leg phase data were isolated by checking the ground reaction force under the untested leg (thin red line). Z component of GrF under the test leg (bold red line) and x, y components (blue, green) are also shown. Body weight (black line) is also plotted. (B) The point of application of the force is shown including the x, y (blue, green) and z (red) components.

### 3.4.2 EMG analysis

The raw EMG signal was full-wave rectified and filtered. To better correlate the EMG signal with the contractile features of the muscle, the high frequency components were eliminated with a low pass filter (implemented in a custom MATLAB programme) in order to compare the activation patterns during EL and CL. *Figure 3.21* shows the steps involved in collecting the smoothed EMG signal from the raw data.

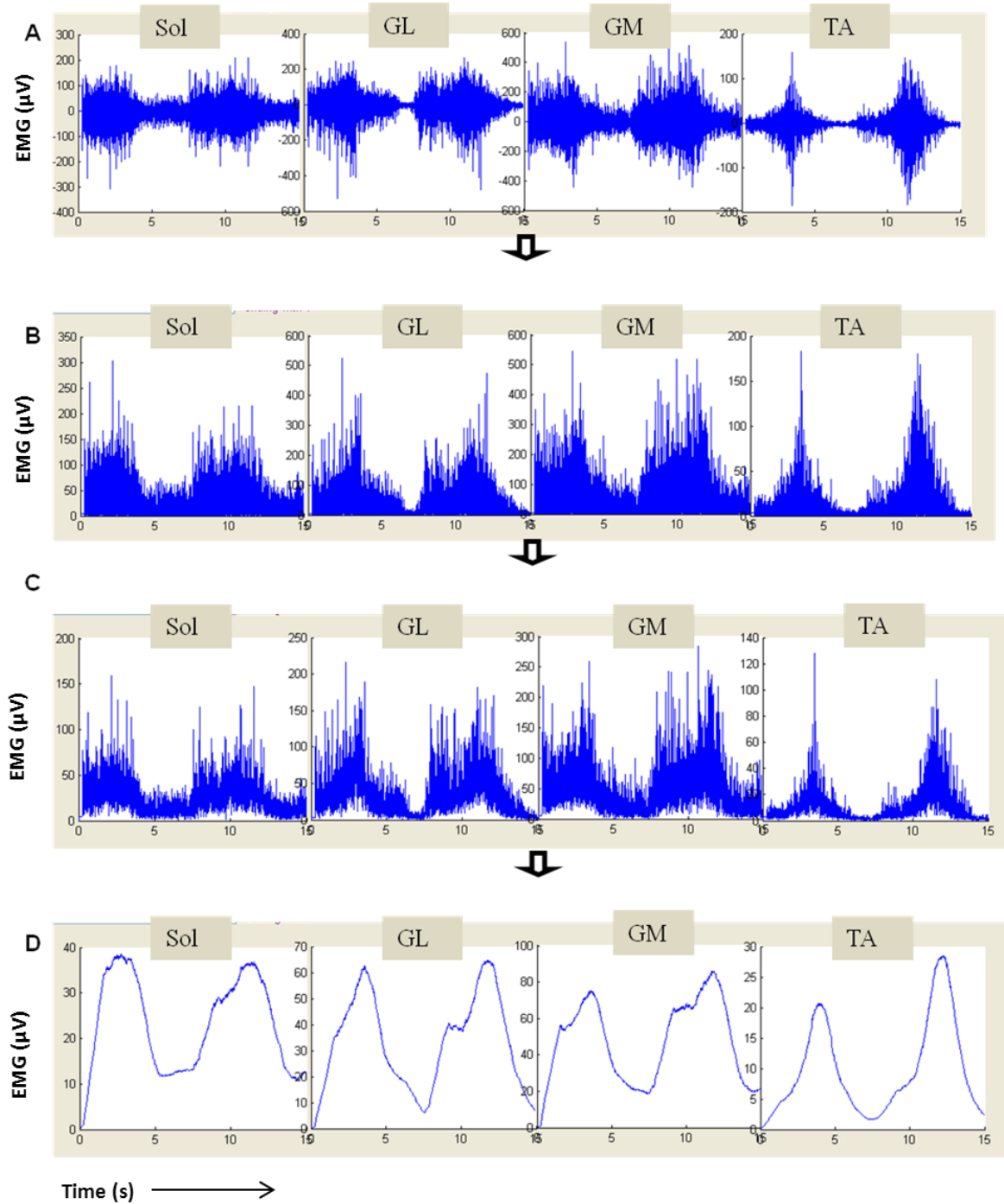


**Figure 3.21:** Graphs showing the sequence of analysis of EMG data for the soleus (Sol), lateral gastrocnemius (GL), medial gastrocnemius (GM) and tibialis anterior (TA) during concentric loading. (A) Raw EMG, (B) Rectified EMG, (C) Smooth EMG with a smoothing window size = 10, (D) Smoothed EMG with a smoothing window: size = 2000.



### **3.4.3 Stress and strain**

For each individual tendon, stress at any point in time was calculated by dividing the instantaneous force by the minimum CSA. Tendon strain ( $\epsilon$ ) at each point was calculated by finding the instantaneous length of the tendon at any point in time, and dividing the change in length ( $\Delta L_i$ ) by the length of the tendon at minimum tendon force (*Figure 3.9b*). As the aim of the study was to measure the strain changes during the exercise and the tendon is never unloaded during either of the loading regimes, the point at which the tendon length and tendon force were minimal was taken as the initial length ( $L_i$ ) to maintain consistency in length measurement. This assumption will result in an underestimate of tendon strain which is difficult to quantify, but previously studies have assumed a force of around 200N giving a strain of less than 1 % (Lichtwark and Wilson, 2005b). Considering this, our underestimate is likely to be less than 2.5 %, but most importantly, this assumption stays consistent for both loading environments. As the motivation behind the current study was to compare the strain between CL and EL, this methodology will not preclude data analysis.

### **3.4.4 Stiffness**

Individual subject data was used to create an average force-length plot for the three repeats carried out by that subject, and then a group mean was calculated from the subject mean data. Tendon stiffness, defined as the slope of the force-length curve, was measured by placing a linear regression line through the average data for each individual.

### **3.4.5 Measurement of perturbations**

After registration, the vertical component of the GrF vector was further analysed for force perturbations. Firstly, the mean value was subtracted to make GrF independent of the body mass.. To obtain the magnitude and frequency of the perturbations, power spectrum densities were calculated

using a fast Fourier transformation (FFT) method, after elimination of the dc component. The power was subsequently summed within 1 Hz windows across the frequency range of 0 to 16 Hz, and the resulting summed powers estimated as a mean and standard error of the mean (SEM).

### 3.4.5.1 FFT optimisation

The method used to take the FFT of the signal was developed by collecting information from MatLab help and literature. To test the methodology, a sinusoidal signal with Gaussian noise (*Figure 3.22*) was generated. The digital Fourier transform was computed using the `fft` command in MatLab and the Power of the output signal computed by taking the square of the amplitude of the FFT. An FFT command script was subsequently developed in MatLab.

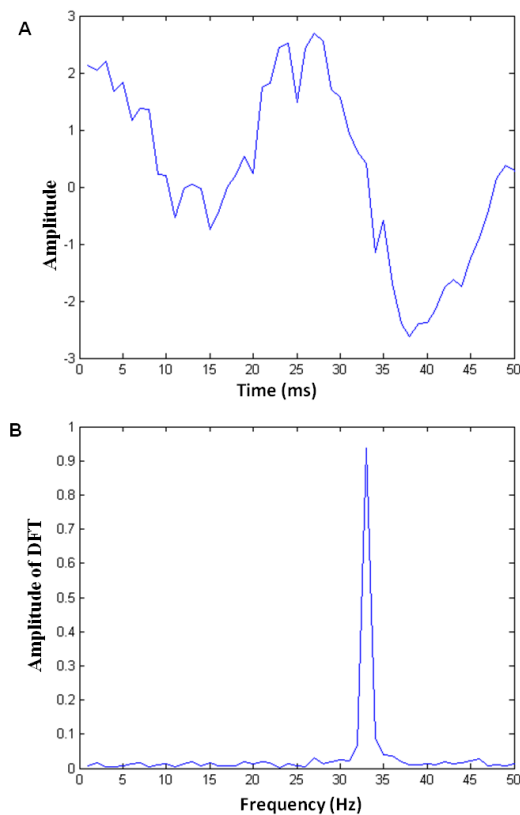


**Figure 3.22:** Description of FFT. (A) Test signal (B) Fourier transform of the signal.

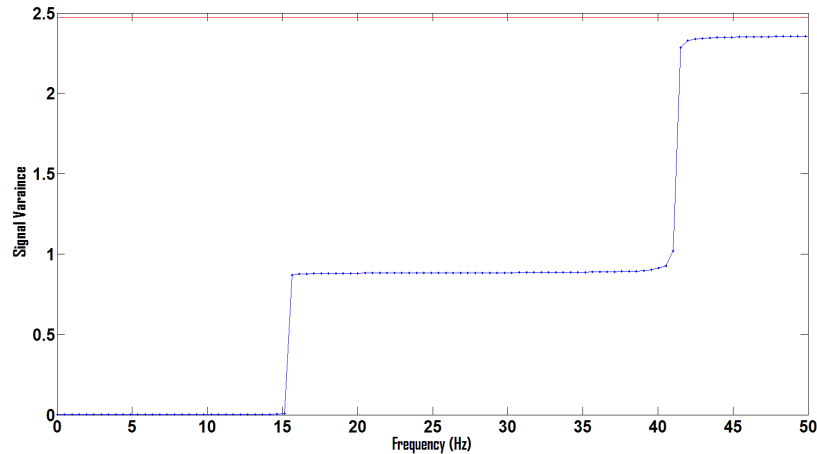


**Figure 3.23:** Description of the signal variance. Signal maximum variance should be equal to the cumulative summed power of that signal. Here cumulative sum power =  $\text{Var}X = 2.5359$  and maximum variance =  $\text{SV} = 2.5347$ .

The maximum variance of a signal is equal to the cumulative sum of power of the signal. In order to ensure this method is correct, the cumulative sum of the power of the signal was computed and compared with its maximum variance. As shown in *Figure 3.23* the two values are very close to each other, which ensure that this technique of completing FFT is correct. This method was used in all studies to compute FFT.

### 3.4.5.2 FFT of EMG

An FFT of the EMG was also calculated, in order to establish the frequency components present in the signal. The post processing of raw to refined EMG was discussed in section 3.4.2 and it was important to test at which stage of processing the signal should be used as an input to the FFT. In order to ensure that there were no artefacts as a result of smoothing, the effect of smoothing was observed on the FFT of the EMG signal. This was carried out by generating a test EMG signal (*Figure 3.24*) and taking its FFT with and without applying the smoothing filter pre-processing. Window size dictates the level of smoothing; the higher the number, the smoother the signal will be. Window size was adjusted from 121 for a highly

smoothed signal to 1 for an unsmoothed signal. It was observed that smoothing the EMG diminished the frequency components present in the original signal (*Figure 3.24*).

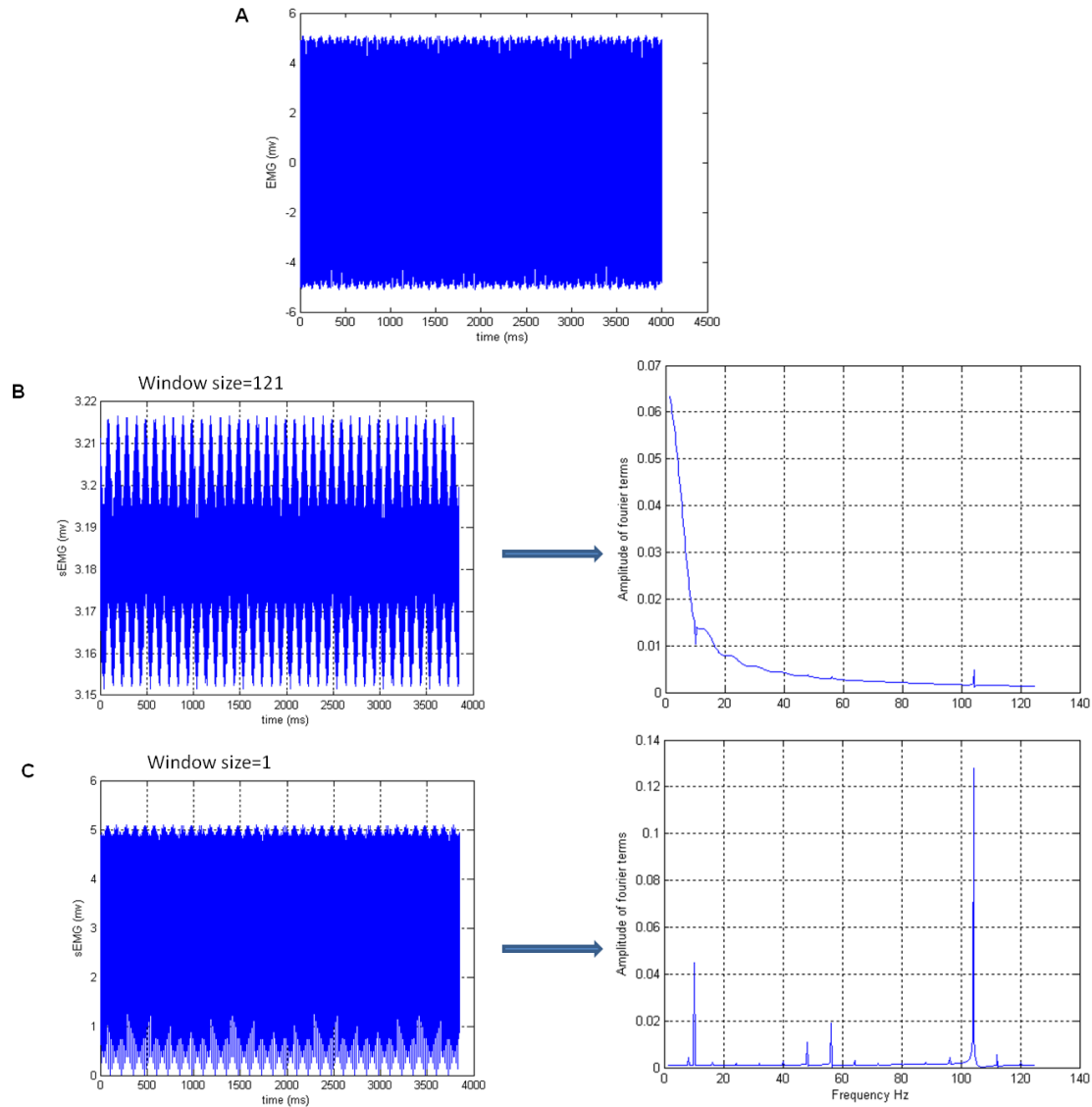


**Figure 3.24:** Graphical description of the effect of smoothing the EMG signal on the resulting signal FFT. (A) Test EMG signal (B) smoothed EMG signal with a window size of 121, and its resulting FFT. Frequency components of the original signal are heavily diminished. (C) Unsmoothed EMG signal with a window size of 1 and its resulting FFT. The frequency components present in original signal can be seen here.

### **3.4.6 Statistical analysis**

Normality tests were performed on the data using the Shapiro-Wilk method (OriginPro, version 8, OriginLab, USA) on original or logarithmic data. Once data was shown to be normally distributed, paired t-tests were used to find the significant differences in tendon force, muscle activation and material parameters between EL and CL movements for study I. A 4 or 3-way analysis of variance (ANOVA) was performed for the rest of the studies. For all statistical tests, significance was accepted if  $p \leq 0.05$ . Data are presented as mean  $\pm$  SD.

## **3.5 Results**

### **3.5.1 Marker position**

Marker positions were checked for visibility, with any sudden marker jumps due to light reflection or loss of balance being discarded by checking the visibility in CODA software. The ankle joint axis was taken as the centre of rotation, with moments being calculated around that axis as explained in section 3.3.3. *Figure 3.25* shows the markers in different colours and the point of application of force.

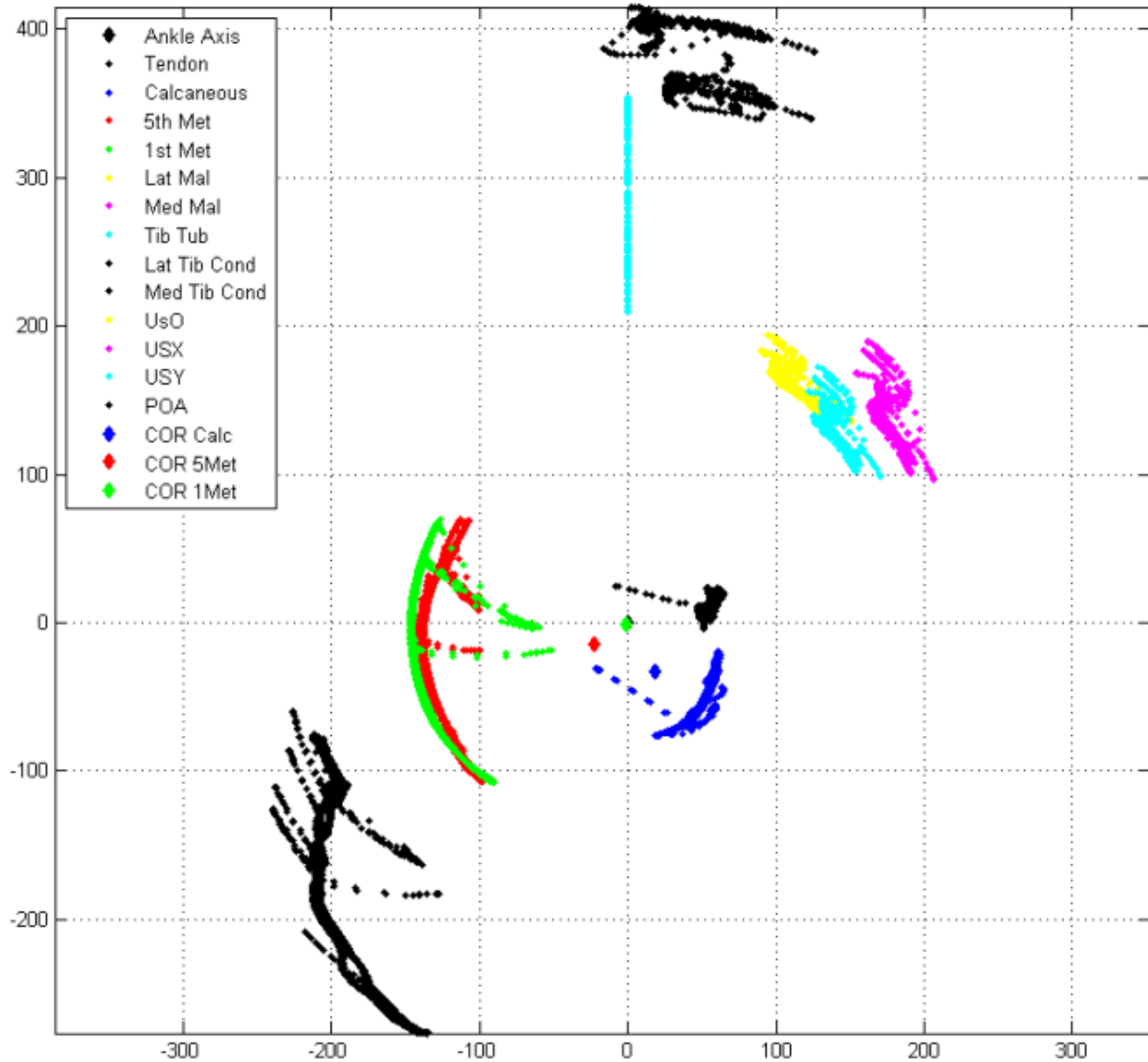


**Figure 3.25:** Representation of all the 15 markers used on the lower leg and US probe seen perpendicular to the plane of action. The large arcs in red and green indicate the movement of 1<sup>st</sup> and 5<sup>th</sup> metatarsal with a red or green dot showing the centroid of these circles. Small arcs in black and blue represent motion of the tendon and calcaneum, whereas the big black arc is the point of application of force. Black arcs at the top are the movements of the lateral and medial tibial condyle. The US markers are shown in cyan, yellow and pink and these markers indicate any movement of probe.

### 3.5.2 Achilles tendon force

Achilles tendon force was calculated using the method described in section 3.3.3. *Figure 3.26* shows a typical result during EL with the corresponding ankle angle and heel height. The raw Achilles tendon force is shown in figure A along with the GrF from the force-plate under the testing leg. The relationship between the ATF and both the ankle angle and HHT is shown in figure B, and as the heel moves from maximum to minimum height, force increases from minimum to maximum.

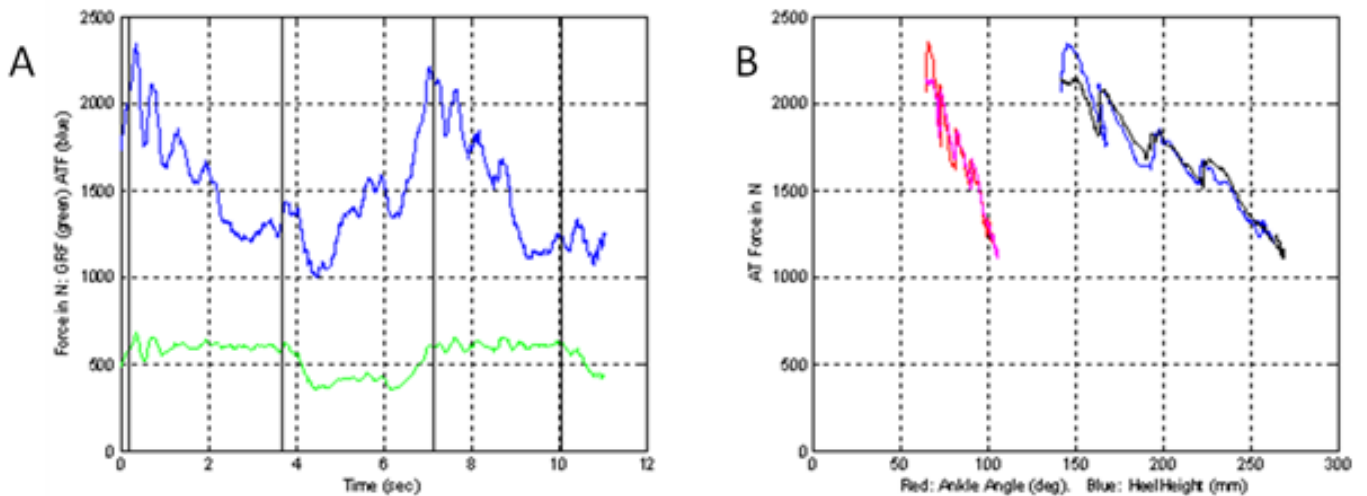


**Figure 3.26:** Description of AT force (ATF) calculation. (A) ATF for two cycles of EL (blue) and ground reaction force (green) with registration of single leg and double leg support (black lines). (B) ATF during two cycles (isolated for the time points of single leg support) drawn against ankle angle (red and pink) and against heel height (blue and black).

### 3.5.3 EMG

EMG data was extracted and analysed as detailed in section 3.4.2. *Figure 3.27* shows example data during EL with the corresponding ATF. Data from the single leg support section of two loading cycles is highlighted as blue. There is an increase in activity during the loading of the tendon.

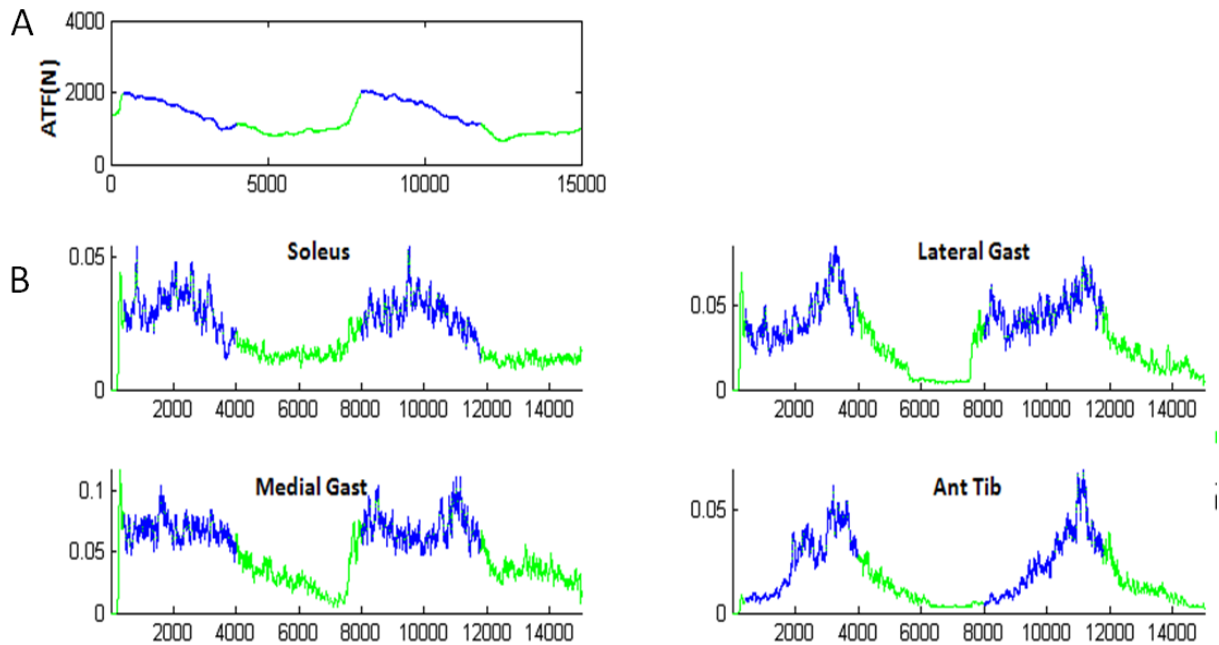


**Figure 3.27:** EMG data during EL. Single leg phase EMG data was isolated by aligning it with the single phase data (blue) and double leg (green) of GrF and AT force (ATF). (A) ATF plotted as data points. (B) EMG data from the four muscles.

### 3.5.4 Accuracy of US tracking

#### 3.5.4.1 US and motion analysis tracking comparison

The combined motion analysis and US capture technique to scan the movement of the phantom showed that the system was capable of determining the position of the coil with a maximum error of  $1.51 \pm 0.5$  mm. A typical test is shown in *Figure 3.28*, directly comparing US tracking of a phantom with automated motion analysis tracking, showing good agreement between the two measurements.



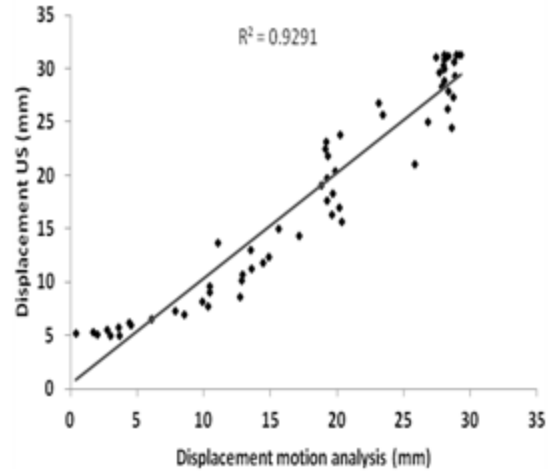


**Figure 3.28:** Relationship between the US and motion analysis tracking of the phantom.

#### 3.5.4.2 Image software and automatic tracking comparison

In order to ensure the accuracy of the automatic tracking algorithm, a comparison between the horizontal displacement from automatic and image J software tracking (explained in 3.3.5.5) was made. *Figure 3.29* shows the agreement between the two tracking techniques for an example video. Automatic tracking was 10 times more rapid than when carried out with image J software.

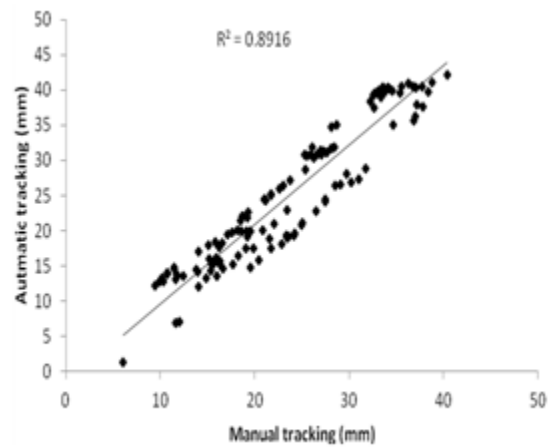


**Figure 3.29:** Relationship between Automatic tracking, and tracking done using Image software.

### 3.5.4.3 Reproducibility of the automatic tracking

Reproducibility of any tracking technique is paramount. A single video was tracked multiple times by different users to ensure that it was user independent. A correlation between the results obtained with two users tracking the same video is shown in *Figure 3.30*. The tracking from different users produced similar results with  $R^2 = 0.99$ .

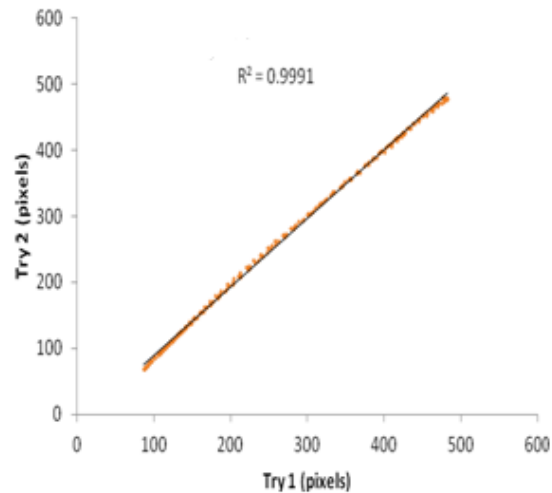


**Figure 3.30:** Relationship between tracking analyses of the same video by two different users (try 1 and try 2).

### 3.5.4.4 Calcaneus and MTJ displacement

An example calcaneus movement is shown in *Figure 3.31*. The data was resampled so the frequency matched the video sampling, and at each frame, the position of the calcaneus marker was plotted. MTJ displacement was also plotted for each frame as shown in *Figure 3.32*.

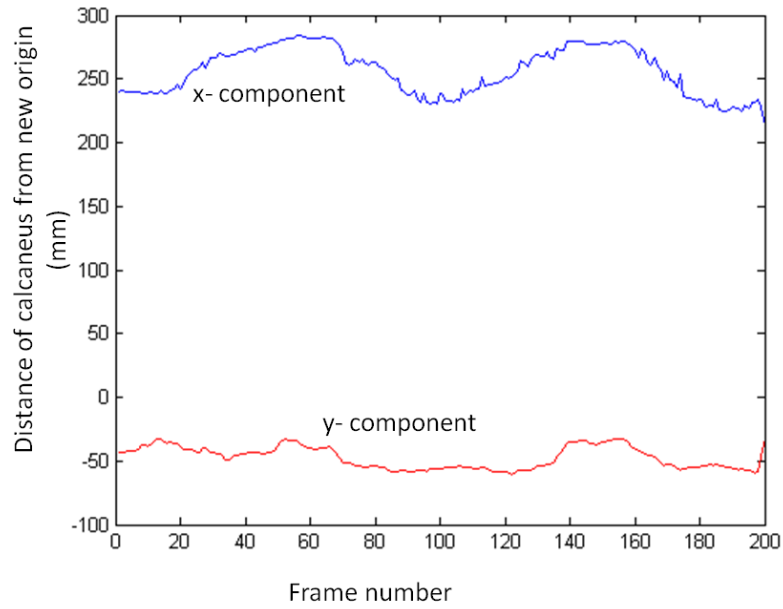


**Figure 3.31:** An example of the calcaneus movement data. Both  $x$  and  $y$  components are shown.

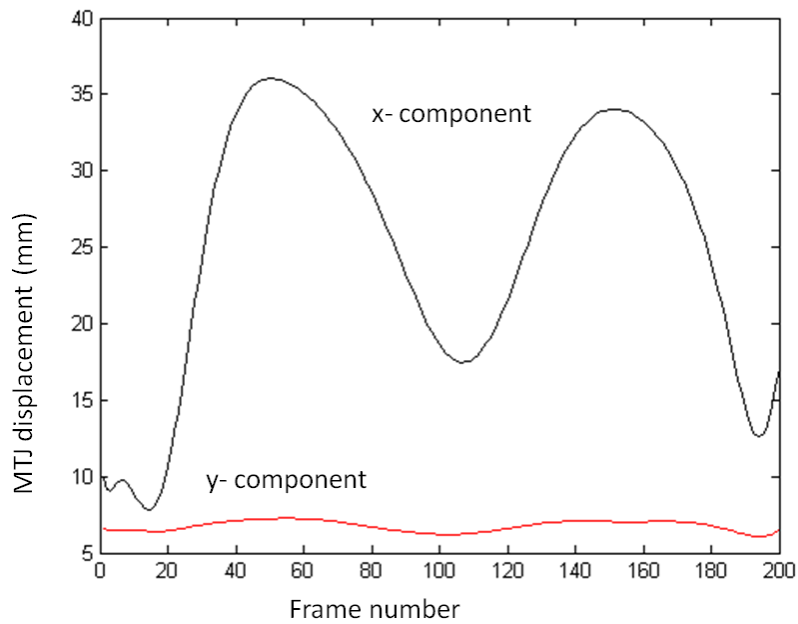


**Figure 3.32:** An example of the measurement of MTJ displacement using the algorithm developed. Both  $x$  and  $y$  components are shown.

In addition to calcaneal and MTJ movement, force measurement is required for recording AT properties. Force change with MTJ displacement during two leg and single leg weight bearing phases during both EL and CL is shown in *Figure 3.33*.

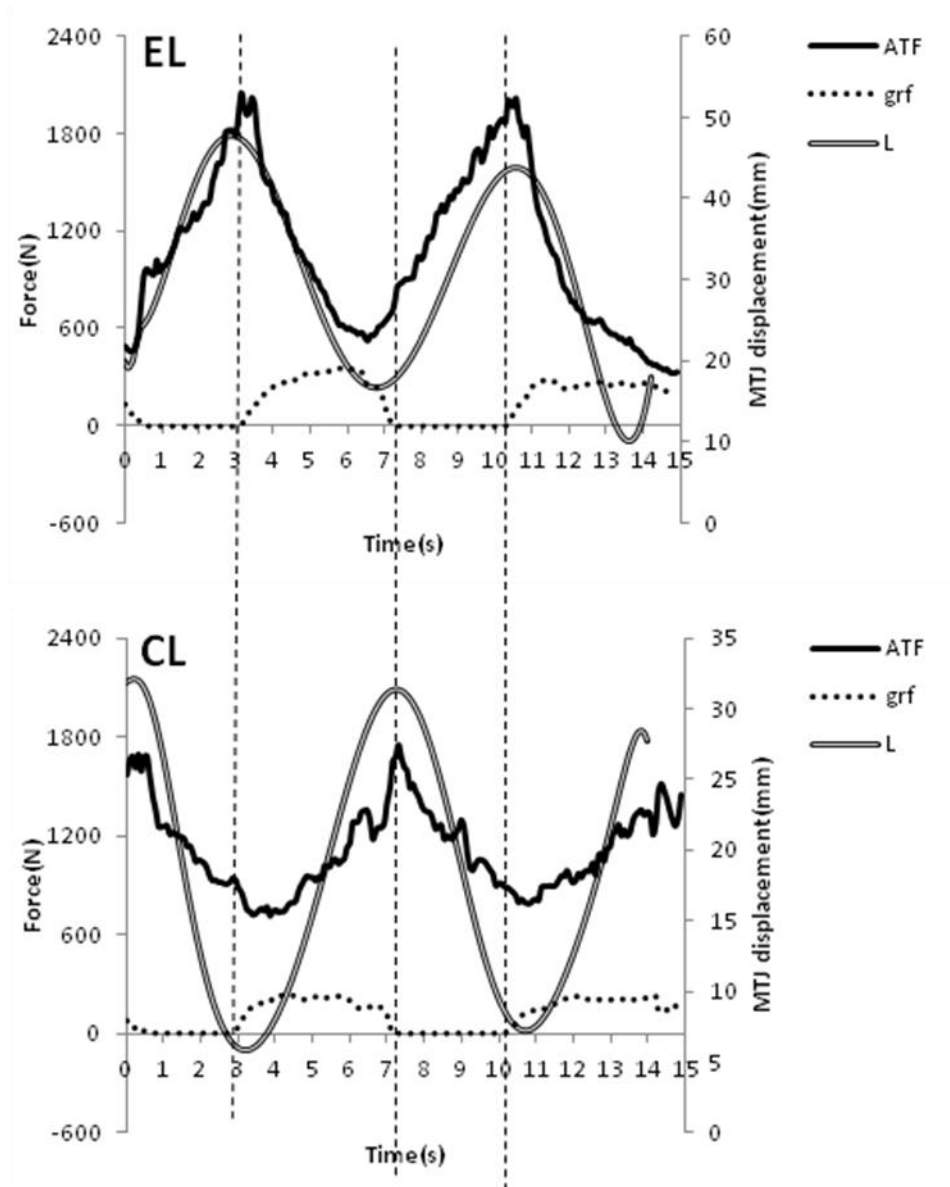


**Figure 3.33:** Raw MTJ displacement (*L*) and force measurement. Note that the period of single leg support and double leg support (highlighted by the vertical dividing lines) are separated by the zero ground reaction force under the untested leg to ensure only the single support data is further analysed.

#### **3.5.4.5 Error in ATL**

Overall error in measuring ATL was calculated by taking into account the accuracy from the phantom experiment which was 1.51 mm, coda error at both sides of AT attachment (0.4mm on each side), and dispersion in the reproducibility of the force-extension from repetitive measures was found to be 3.00 mm at a single time point, so the overall error in estimating ATL was judged to be 3.42 mm over an average tendon length of 230 mm for a typical subject.

### **3.6 Conclusions**

This chapter details the techniques developed for the measurement of *in vivo* biomechanics of the triceps surae. An *in vivo* system was successfully developed and tested for further studies. In addition, a semi-automatic MTJ tracking algorithm was developed and tested.

**Chapter 4: Eccentric and concentric loading of the triceps surae:  
an *in vivo* study of biomechanical parameters**

## **4.1 Introduction**

The mechanisms by which EL treats tendinopathy remain unknown. It is also unclear why EL should be reported to be notably more successful than CL in treating patients. Initially it was believed that the tendon experienced higher forces during EL than CL, resulting in more tendon remodelling in response to the higher strains (Stanish et al., 1986). However, recent *in vivo* human studies have reported no difference in Achilles tendon force (ATF) during EL and CL (Rees et al., 2008). Rather, larger magnitudes of tendon perturbations around 10Hz (~8-12Hz range) have been observed to occur during EL alone (Henriksen et al., 2009), and could be hypothesised to provide the mechanism through which EL successfully initiates tendon repair. The frequency of these perturbations and their effect at a cell level will vary depending on the mechanical properties of the tissue (Stiles and Randall, 1967, McAuley and Marsden, 2000). However, studies comparing EL and CL have yet to report the mechanical parameters of the tendon such as stress, stiffness and strain during matched EL and CL exercises (details in Chapter 1), making it difficult to establish if high frequency perturbations are indeed the key difference between EL and CL. Understanding and comparing these parameters during EL and CL is an essential aspect of interpreting the mechanical effects of loading within the tendon. Such data will help identify the key differences in loading parameters and may subsequently provide insight into the loading conditions that best promote healing.

The aim of this chapter was to compare eccentric and concentric loading performed at the same speed, load, intensity and range of motion, to investigate any differences in muscle activity levels and tendon stiffness occurring in response to the different loading modalities. Secondly this study explores the correlation between tendon and muscle tremor, in order to determine if muscle activity is the origin of the observed tendon perturbations.

### **4.1.1 Hypotheses**

Alternative hypotheses for this study were that:

- Muscle activation will be higher during CL than EL.
- Tendon force will be higher during EL than CL.
- Tendon stiffness and strain will be higher during EL than CL.
- Perturbation magnitude and frequency will be higher during EL than CL.

## 4.2 **Methods**

### 4.2.1 **Overview**

In the present study, the biomechanical characteristics of the lower leg were assessed during EL and CL as previously described (Chapter 3). Twelve normal subjects had three series of measurement made on their right leg on the same day by the same examiner.

Each series of measurements yielded two complete cycles of loading (*Figure 4.1*). Three subjects had a fourth series of measurement taken by the same examiner and of the same leg, but on the next day, in order to establish the intra-test reliability. *Table 4.1* outlines the range of parameters calculated from each data set.

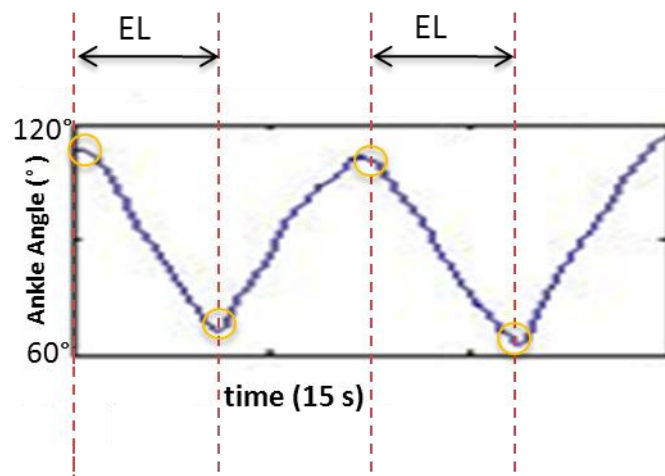




**Figure 4.1:** The total range of movement is shown for a typical subject during set of 2 cycles of EL. The data is shown in the laboratory coordinates system. The first and second cycle of loading selected for analysis are marked.

**Table 4.1:** Parameters extracted and calculated from the data.,

Parameters extracted from kinetic and kinematic data	Parameters extracted from US	Parameters extracted from EMG
ROM during EL and CL	MTJ displacement	Muscle activation
Joint angles	Tendon length and cross-sectional area	Fourier transform of EMG
Measurement of ATF using inverse dynamics		
Calcaneus displacement		
Fourier transform of GrF and ATF		

*ROM: range of motion*

#### 4.2.2 Subjects

A sample of 12 subjects was recruited (*Table 4.2*). Subjects were moderately physically active but had not taken part in any organised program of regular exercise over the last year and had no history of tendon injury or any systemic disease.

**Table 4.2:** Subject characteristics

Sample	N	Age (years)			Body mass (kg)			Height (m)		
		Mean	Range	SD	Mean	Range	SD	Mean	Range	SD
<b>All</b>	12	26.5	24-30	1.8	67.6	55-85	9.5	1.73	1.62-1.84	0.08
<b>Male</b>	6	26.3	24-29	1.8	73.2	60-85	10.8	1.74	1.62-1.84	0.05
<b>Female</b>	6	27.2	25-30	1.7	62.1	55-75	8.1	1.70	1.64-1.74	0.07

Anyone with current or previous Achilles tendon pain, pathology or surgery was excluded. Written informed consent was obtained from all subjects. Subject's occupation and sports participation were recorded. Nine of the subjects were students and three were working. None of the subjects

participated in any sports beyond a recreational level, nor did their employment require significant lower leg activity. Subjects were measured for height and body mass. Tendon cross-sectional area was measured before the exercise set up using US in transverse mode, and the resting tendon length was also established (Chapter 3 (section 3.3.4)).

### **4.2.3 Data collection**

A summary flow chart for the data collection process is shown in *Figure 4.2*, detailing the range of parameters being extracted for each subject.

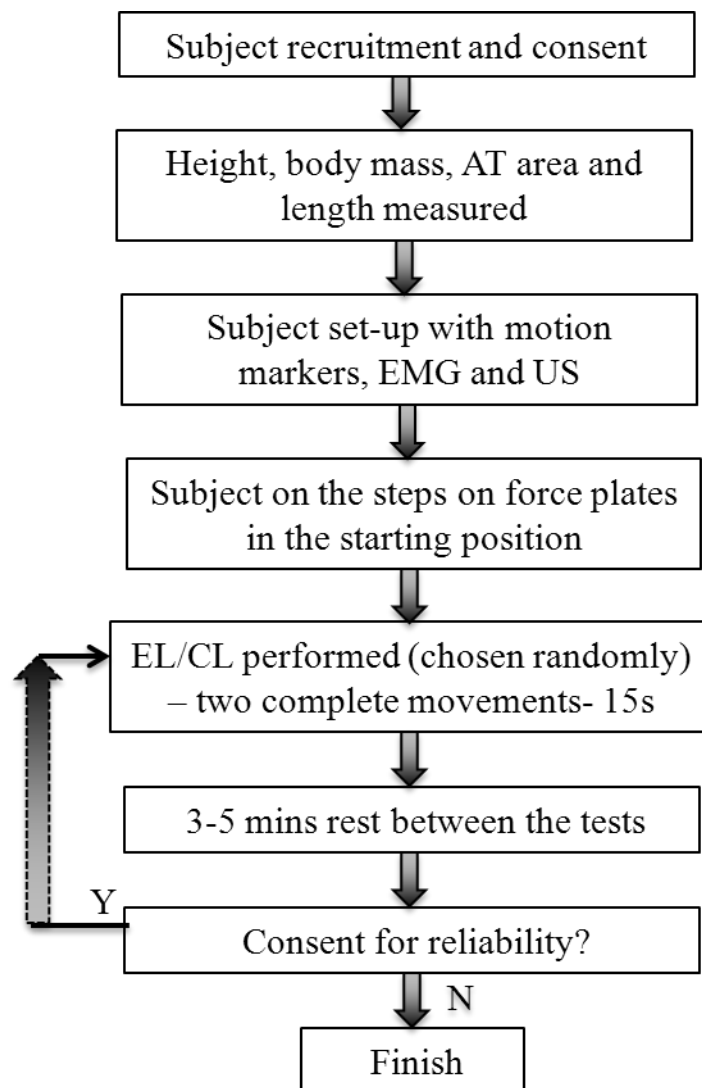


**Figure 4.2:** Flowchart for methods describing the data collection process for each subject.

EL and CL exercises were performed at an average speed of  $0.5 \text{ rad}\cdot\text{s}^{-1}$  (3s descent or ascent phase). A sufficient familiarisation period was given to enable subjects to familiarise themselves with the exercise. Foot position was marked on the step with tape, to assist them in completing reproducible trials. After completing either exercise, the subjects used the other leg to assist in returning to the starting position, before repeating the exercise. A single data collection consisted of 2 cycles of either CL or EL performed consecutively. Three sets of such data were recorded for each loading paradigm, for each subject. The order of exercise was randomized, by each subject making a blind selection of cards (*Table 4.3*).

**Table 4.3:** Order of exercise as determined by each subject making a blind selection from an envelope.

Subject no	1	2	3	4	5	6	7	8	9	10	11	12
Order of	EL	CL	CL	EL	EL	EL	EL	CL	CL	EL	EL	EL
exercise	CL	EL	EL	CL	CL	CL	CL	EL	EL	CL	CL	CL

#### **4.2.3.1 Measurement of muscle activation**

Electromyography (EMG) recordings were made using dual electrodes with a 20mm inter-electrode distance placed on the belly of the soleus, lateral gastrocnemius, medial gastrocnemius and tibialis anterior muscles following the SENIAM guidelines (Hermens et al., 2000). A single, self-adhesive Ag/AgCl snap reference electrode was placed on the shinbone, as previously described in Chapter 3 (section 3.2.1.2).

#### **4.2.3.2 Measurement of tendon force**

In order to measure the ATF, the 3D ground reaction force was captured and the data from the motion tracking markers collected. The ATF vector was found using inverse dynamics as detailed in Chapter 3 (section 3.3.3).

#### **4.2.3.3 Measurement of tendon elongation**

Achilles tendon length (ATL) at any time was defined as the distance between the AT insertion and the distal muscle-tendon junction (MTJ) of the medial gastrocnemius (GM). The position of these two locations was tracked throughout each exercise, from which the relative tendon length and displacement could be established. The details of the tracking technique are provided in chapter 3 (section 3.3.5).

#### **4.2.3.4 Measurement of perturbations**

Tendon and muscle perturbations during exercise were determined by taking the fast Fourier transform of the GrF, ATF and the EMG. The 3D GrF and muscle activity were recorded and processed for this purpose, as detailed in chapter 3 (section 3.4.5).

#### **4.2.4 Repeated measures**

All subjects consented to three repeat series of measurements taken by the same examiner with a 3 - 5 minute break between each repeat, without removal of the apparatus from the subject. Three subjects consented to participate in a reliability testing session, arranged the following day at a time convenient for the subjects. Reliability testing involved repositioning all apparatus, before asking the subject to repeat the EL and CL procedures. Data was assessed by the same examiner.

#### **4.2.5 Data analysis**

Data analysis was carried out with a Matlab script (Version 7.9.0.529, R2009b, USA), the details of which are in Appendix II. Briefly, for each exercise task only the accurately paced cycles (done within  $3 \pm 0.2$  s of time with metronome pace, without loss of balance and with consistency in ROM), were retained for further analysis. Points of minimum and maximum heel height were identified and the record was then re-sampled by interpolation to 111 uniformly spaced points. This data registration

isolated times of single leg support, as confirmed by the zero force measured under the contralateral foot. For descriptive purposes ankle angles were extracted during the two loading modes.

After registration, the data was obtained for the ground reaction force and EMG for each individual subject. The ATF was then found throughout each loading cycle completed by each subject. The tendon force was normalised to the body weight to highlight any differences between subjects that might otherwise be obscured by sample variation in body mass. For each individual, tendon stress throughout the cycle was calculated by dividing the instantaneous ATF by the minimum CSA. Tendon strain ( $\epsilon$ ) at each point was calculated by finding the instantaneous length of the tendon at any point in time, and dividing the change in length ( $\Delta L_t$ ) by the length of the tendon at minimum tendon force. From these an average force-length graph for each subject during EL and CL was drawn from the three repeats of each exercise. Tendon stiffness was measured from the slope of the force-length curve, by placing a linear regression line through the average data for each individual.

In order to determine the tendon perturbations, the vertical component of the GrF vector was further analysed. The mean value was subtracted from the GrF to make it independent of the body mass and power spectrum densities were calculated using the fast Fourier transformation (FFT) method, after elimination of the dc component in order to de-trend the data. The power was subsequently summed within 1 Hz windows across the 0 to 16 Hz frequency range, and the mean and standard error of the mean (SEM) of the summed powers calculated. Muscle perturbations were measured in the same manner, and the FFT of the rectified EMG signal was taken, as described in chapter 3 (section 3.4.5).

The raw EMG signal was full-wave rectified and filtered. To better correlate the EMG signal to contractile features of the muscle, high frequency components of the EMG data were eliminated and smoothed. Muscle activation patterns were then compared during EL and CL. In order to

compare posterior and anterior compartment activation, the posterior compartment (triceps surae) percentage activation, the contribution of the gastrocnemius and soleus were summed to establish posterior activation, taking activation values of 25 % each from the lateral gastrocnemius and soleus and 50 % from the medial gastrocnemius; values were taken based on the correlation between ATF measures and muscle activation. Anterior data was taken directly from the tibialis anterior.

#### **4.2.6 Statistical analysis**

Normality tests were performed on the data using the Shapiro-Wilk test. Summary statistics were reported for each parameter. Once data was shown to be normally distributed, paired t-tests were used to find the significance of EL and CL on tendon force, muscle activation and material parameters for each subject.

Repeated measures were analysed by performing an analysis of variance between the measurements to find the same day and different day, same tester reliability to quantify the measurement accuracy, and investigate if subjects moved in a repeatable fashion. All results were calculated using MatLab and Origin (OriginPro, version 8, OriginLab, USA). For all statistical tests, significance was established at  $p \leq 0.05$ .

### **4.3 Results**

#### **4.3.1 Achilles tendon force**

While some inter-subject variability was apparent, CL and EL resulted in similar loading patterns across all subjects (*Figure 4.3*). Summary data is shown in *Figure 4.4*.

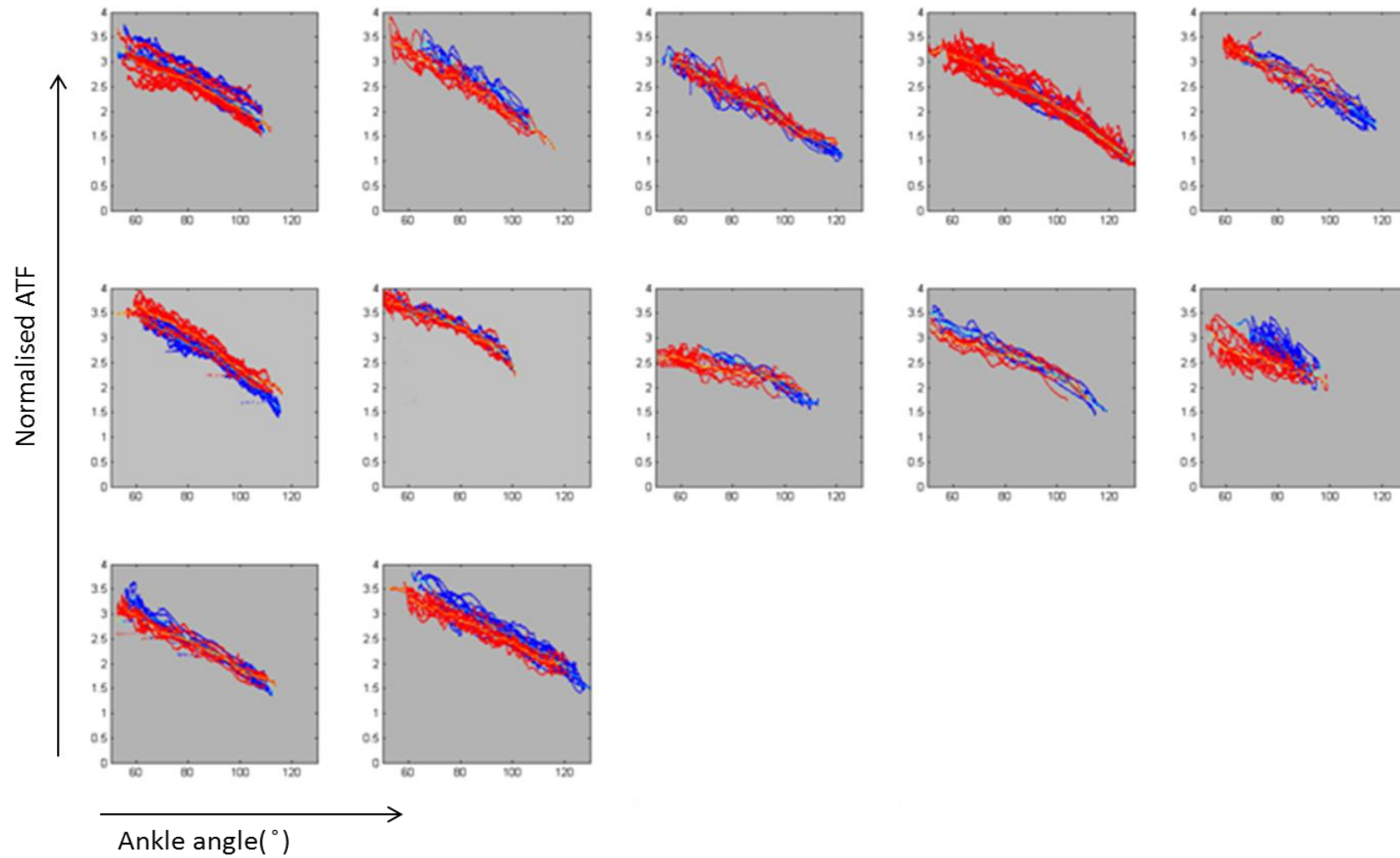


**Figure 4.3:** Normalised AT force (ATF) plotted against ankle angle showing all repeats of each subject. A separate plot is shown for each subject. CL data is in blue and EL in red.

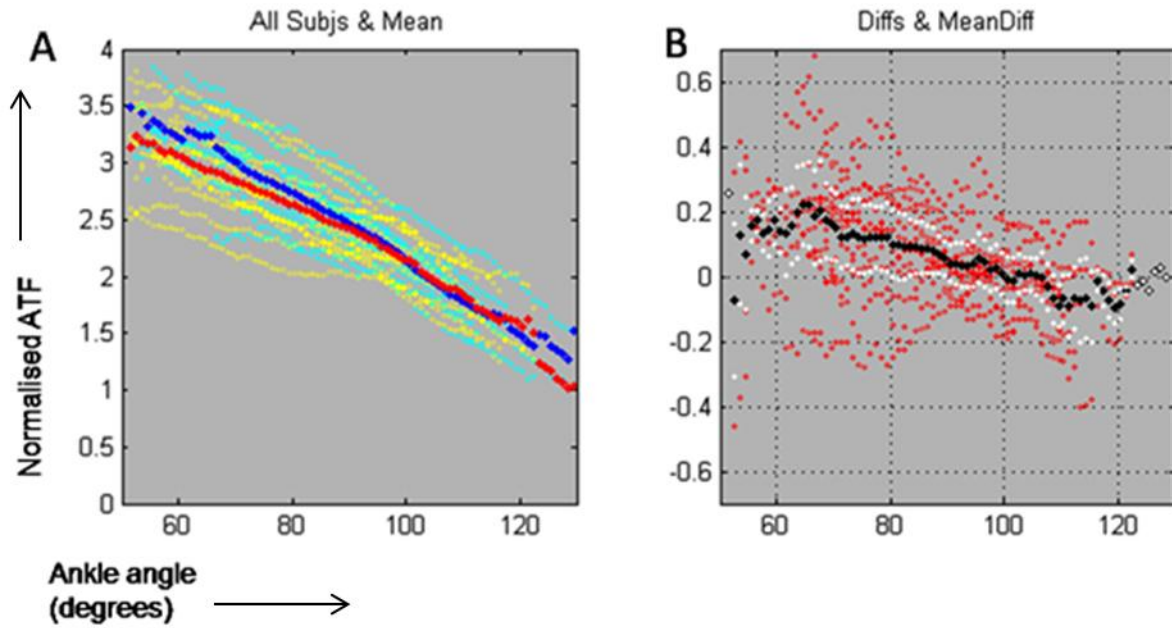


**Figure 4.4:** (A) Mean change in AT force(ATF) (normalised to body weight) for each subject, showing EL data in yellow and CL in cyan. The overall mean AT force is shown in red for EL and blue for CL. (B) For each subjects, the AT force during CL and EL are compared giving a difference value (CL - EL). The mean difference across all points is calculated (black line) and plotted with the 95% confidence intervals (white lines).

Whilst no overall significant differences were found in the ATF (normalised to body weight) between the two types of loading ( $t = 1.23$ ,  $p = 0.24$ ), significant differences ( $p < 0.05$ ) were evident during the first 20° of the movement (ankle angles of 60° - 80°, when the forces passing through the tendon are near maximum), and higher for CL (Figure 4.4 B).

### 4.3.2 Achilles tendon length

#### 4.3.2.1 MTJ tracking

Measurement of Achilles tendon length is heavily dependent on accurately tracking MTJ displacement. Figure 4.5 shows the automatic tracking results for 80 complete videos of 2 cycles of loading. Results indicate that the tracking worked very well, consistent with the reliability testing previously carried out (explained in Chapter 3 (section 3.3.5)). In the present study, 8 out of 88 videos were found to be below the standard required (blurred) for tracking and were therefore



discarded. Thus the data from 10 subjects were further analysed for biomechanical parameter evaluation. *Figure 4.6* shows the raw ATF and corresponding ATL changes during both EL and CL for a typical subject. From these data, subject mean data was calculated, as shown in *Figure 4.7*.

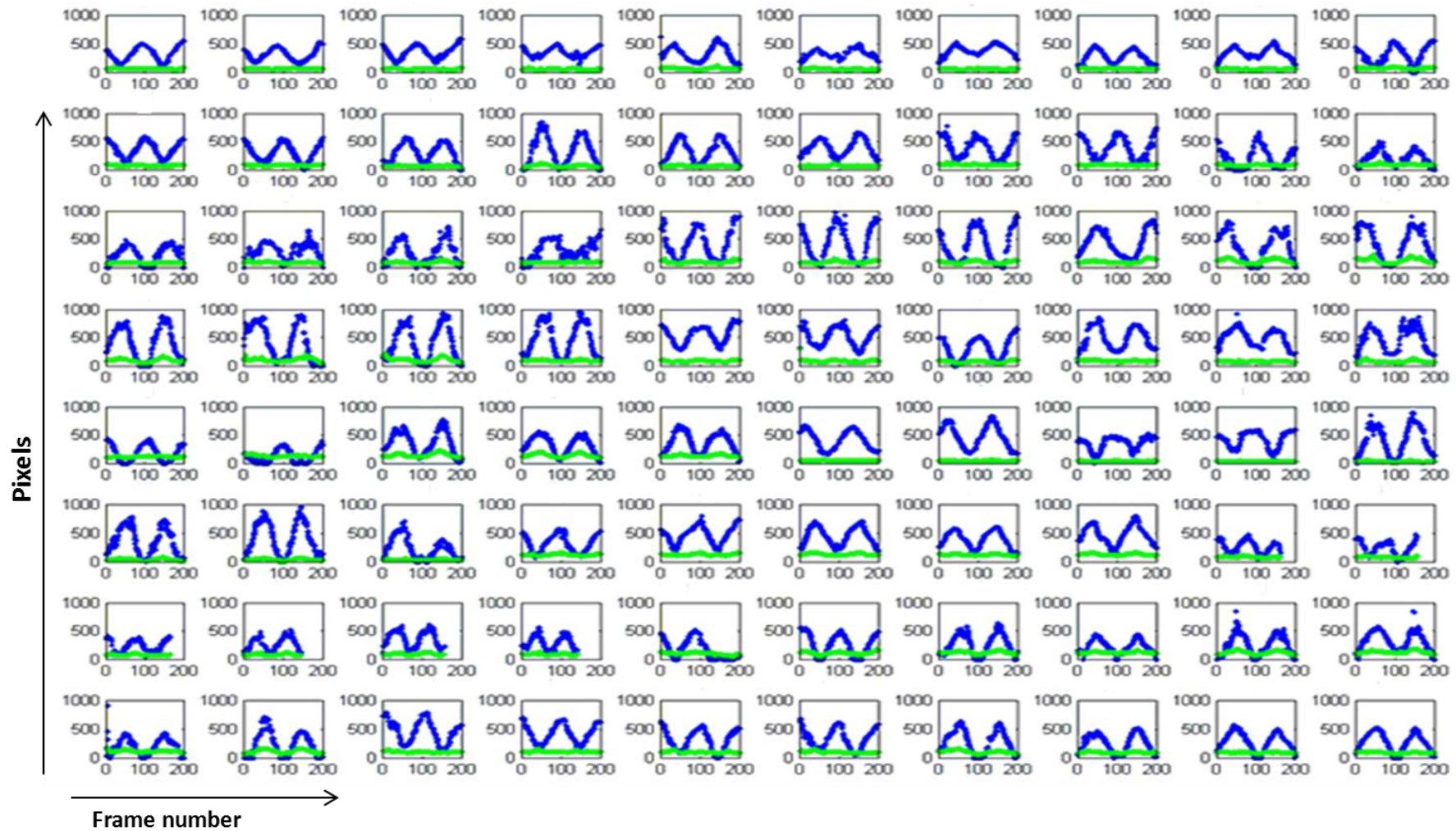


**Figure 4.5:**MTJ tracking results for 80 videos. The X component of the movement is shown in blue whereas the y component is shown in green. Frame number is on the x axis and pixels are on y axis.

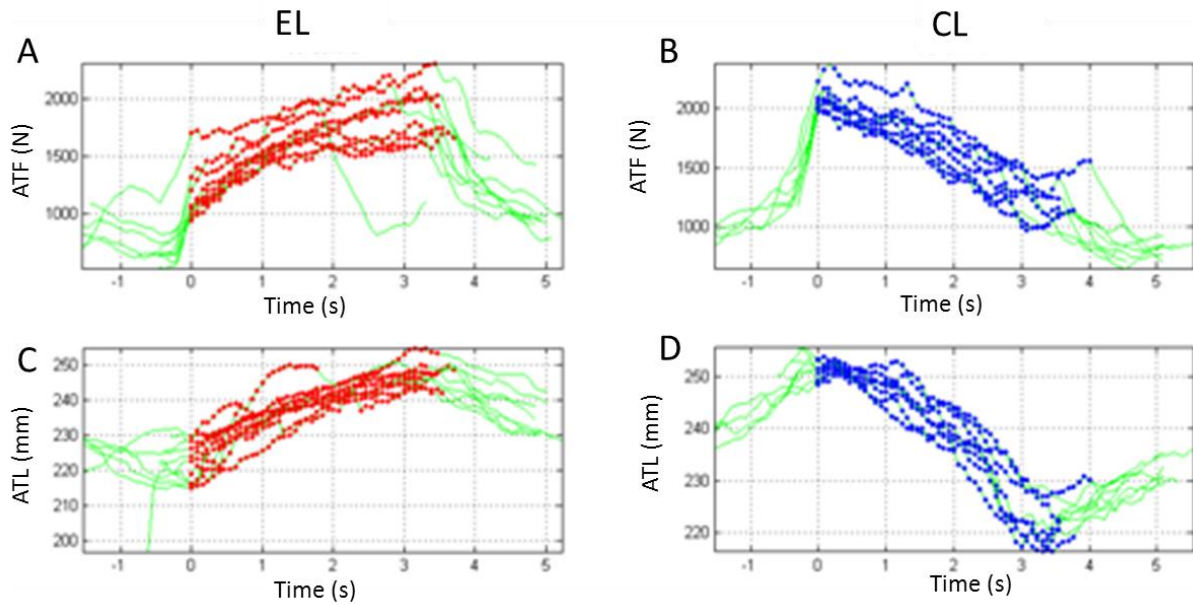


**Figure 4.6:** Achilles tendon length (ATL) and Achilles tendon force (ATF) data for all the repetitions by a single subject, plotted against time. The single leg support phase is shown in red for EL (A) and (C) and in blue for CL (B) and (D). A and B report the change in ATF with time and C and D report the change in ATL with time.

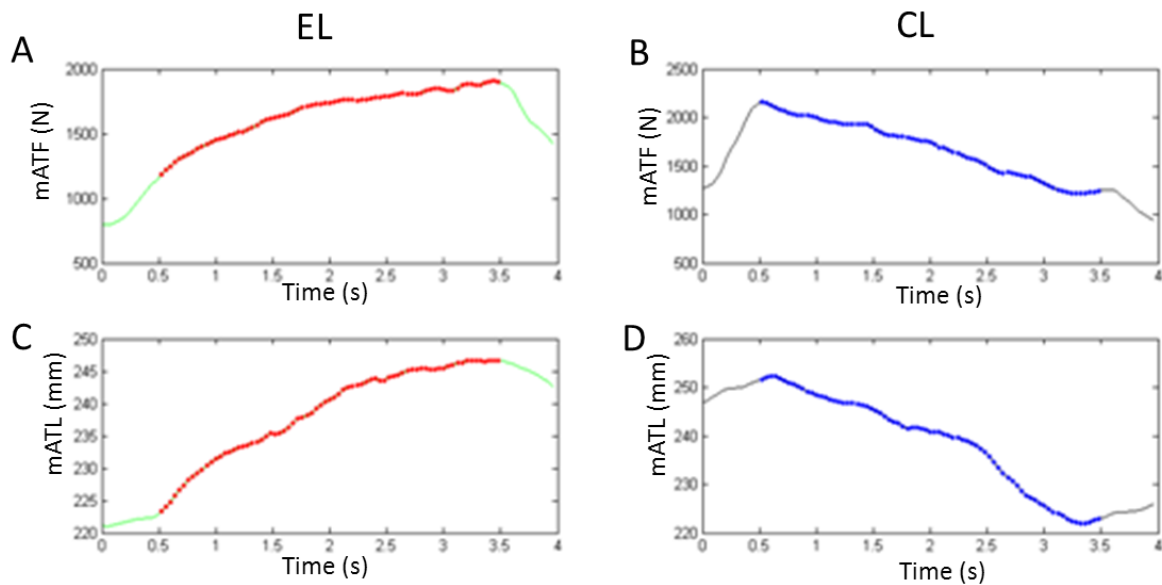


**Figure 4.7:** Mean Achilles tendon length (mATL) and mean Achilles tendon force (mATF) data for all the repetitions of the single subject in Figure 4.6, plotted against time. The single leg support phase is shown in red for EL (A) and (C) and in blue for CL (B) and (D). A and B report the change in mean ATF with time. C and D report the change in ATL. Double leg support phase is shown in green.

### 4.3.3 Achilles tendon force-length relationship

The mean force-length relationship during EL and CL for one individual is shown in *Figure 4.8*. No significant difference was observed between the two patterns. As such the stiffness of the tendon did not vary significantly between EL and CL; however there was a marked variation in stiffness across the population. Plots of tendon force-length relationship during EL and CL for each individual subject are shown in *Figure 4.9*. Most of the subjects show similar force-length relationships for both EL and CL. However, there were a few subjects, such as subject number 4 and 8, for which there was a significant difference between the two movements.

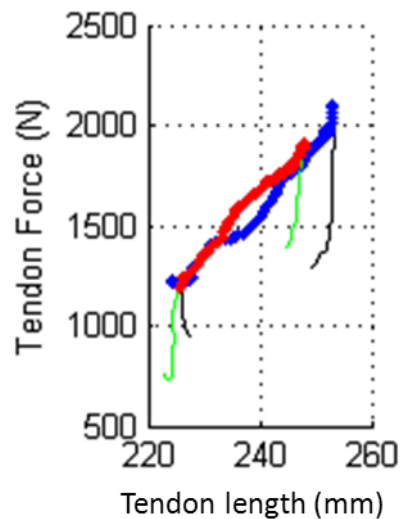


**Figure 4.8:** Mean plot of Achilles tendon force (ATF) against Achilles tendon length (ATL) for one subject, comparing EL (red) and CL (blue). The periods of double leg support are shown in green (EL) and black (CL).

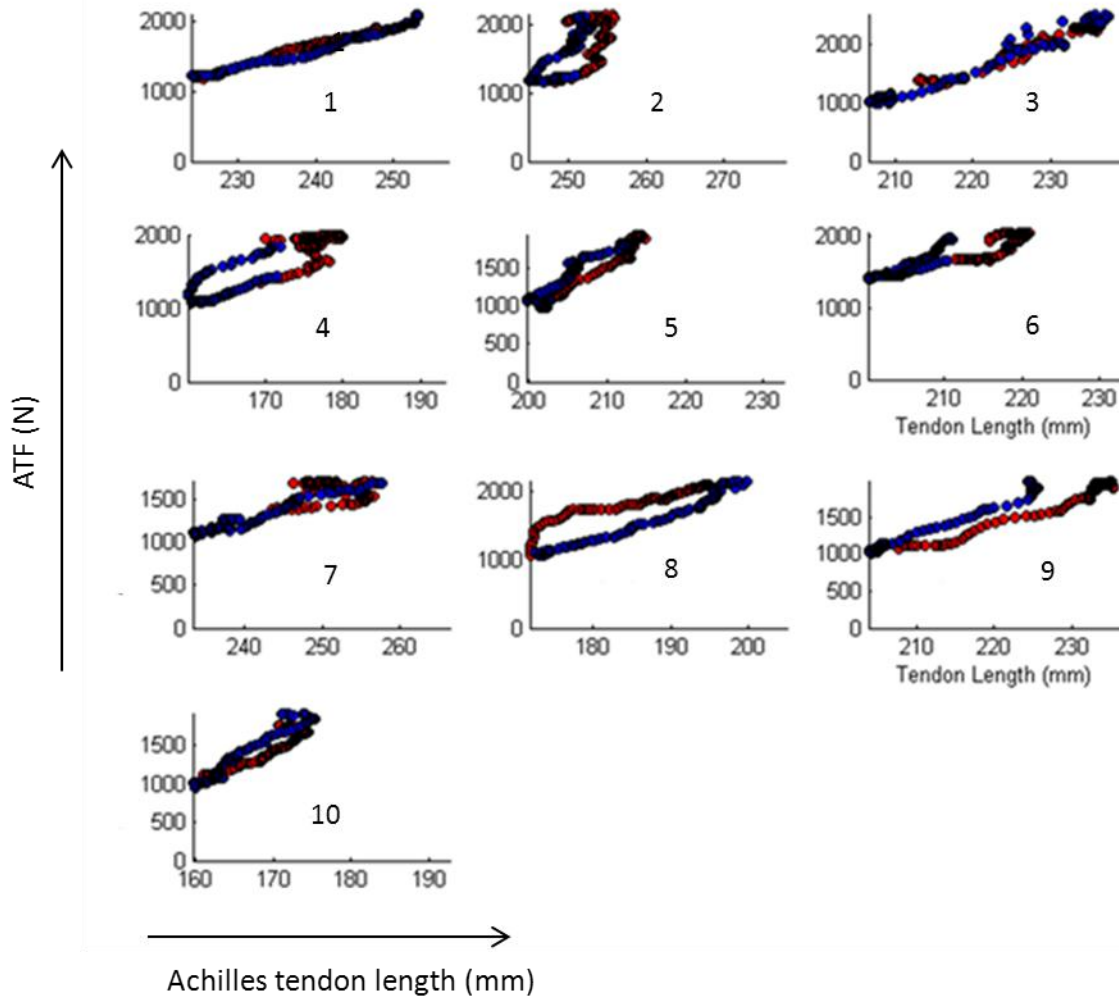


**Figure 4.9:** Mean AT force-length graphs for each subject comparing EL data (filled red circles) and CL data (filled blue circles).

Summary results for normalised ATL (to mean tendon length) and ATF (to mean Achilles tendon force) plotted against both heel height and ankle angle are shown in *Figure 4.10*. A maximum stress of 37 MPa was also reported with no significant difference between EL and CL ( $t = 0.55$ ,  $p = 0.59$ ). No significant difference was observed between tendon length ( $t = -0.77$ ,  $p = 0.45$ ) or force ( $t = 1.23$ ,  $p = 0.24$ ) during the two movements. On average, maximum tendon strain was 9% during both EL and CL, and no significance was observed ( $t = -0.82$ ,  $p = 0.43$ ). The tendon apparent stiffness varied across the population of subjects, but not between loading types ( $t = 0.82$ ,  $p = 0.43$ ), with mean ( $\pm$  SE) values of  $62.79 \text{ Nmm}^{-1}$  ( $9.37$ ) during CL and  $58.89 \text{ Nmm}^{-1}$  ( $9.21$ ) during EL.

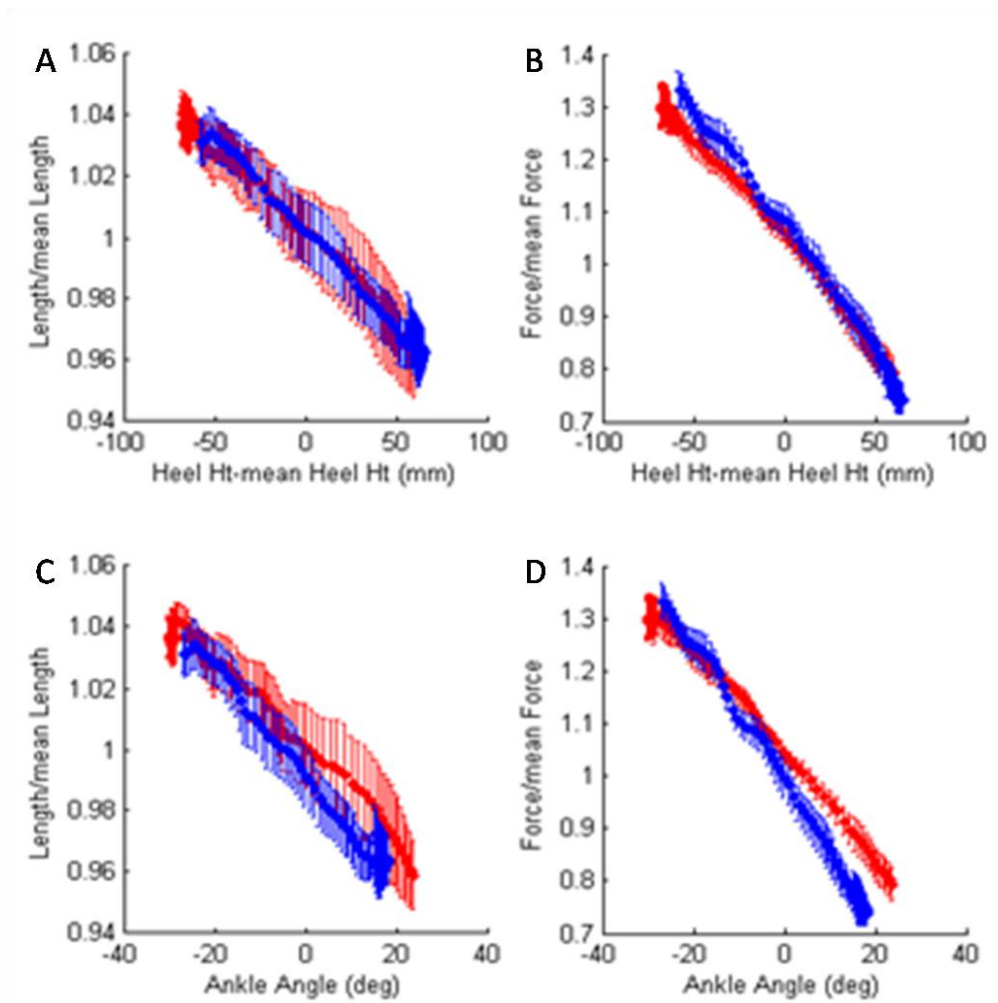


**Figure 4.10:** Summary results for mean Achilles tendon length (ATL  $\pm$  SE) and Achilles tendon force (ATF  $\pm$  SE) against heel height (A, B) and against ankle angle (C, D).

**Table 4.4:** Summary of the mechanical properties of the AT during CL and EL.

		Achilles tendon peak force (N)	Achilles Tendon length change (mm)	AT Stiffness (Nmm <sup>-1</sup> )	AT Stress (MPa)	AT Strain (%)
<b>Concentric loading</b>	CL	2278 $\pm$ 225.1	18.56 $\pm$ 2.22	62.79 $\pm$ 9.21	37.96 $\pm$ 3.88	9.24 $\pm$ 1.03
<b>(Mean <math>\pm</math> SE)</b>						
<b>Eccentric loading</b>	EL	2116 $\pm$ 220.2	19.82 $\pm$ 1.82	58.89 $\pm$ 9.54	35.26 $\pm$ 3.21	9.91 $\pm$ 0.87
<b>(Mean <math>\pm</math> SE)</b>						

#### 4.3.4 Muscle activation

When looking at muscle activity from EMG data, the maximal activation values were significantly higher ( $p < 0.01$ ) in CL than EL. *Figure 4.11* shows the raw data for muscle activation during EL and CL for a selection of subjects.

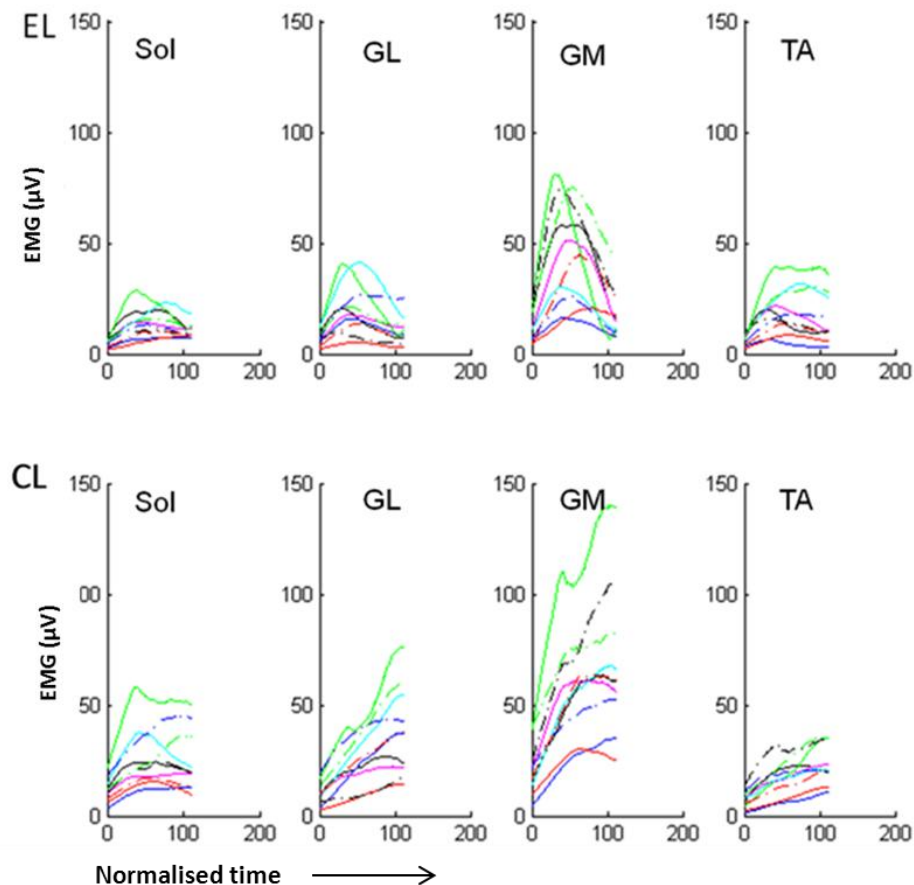


**Figure 4.11:** EMG is plotted against normalised time for a group of 10 subjects (each shown in a different colour). The top four panels show activity during EL and bottom four show CL data. Four muscles are shown: Sol = Soleus, GL = Lateral Gastrocnemius, GM = Medial gastrocnemius, TA = tibialis anterior. Muscle activation was higher for all calf muscles during CL as compared to during EL.

Pairing eccentric and concentric EMG data for each subject highlighted that, whilst the mean CL muscle activity levels were higher, the ratio of mean concentric to mean eccentric activity for each

subject varied between muscles, with values of 1.08 - 2 for soleus, 1.25 - 3.03 for lateral gastrocnemius, 1.08 - 1.48 for medial gastrocnemius and 0.9 - 1.83 for tibialis anterior (*Figure 4.12*).

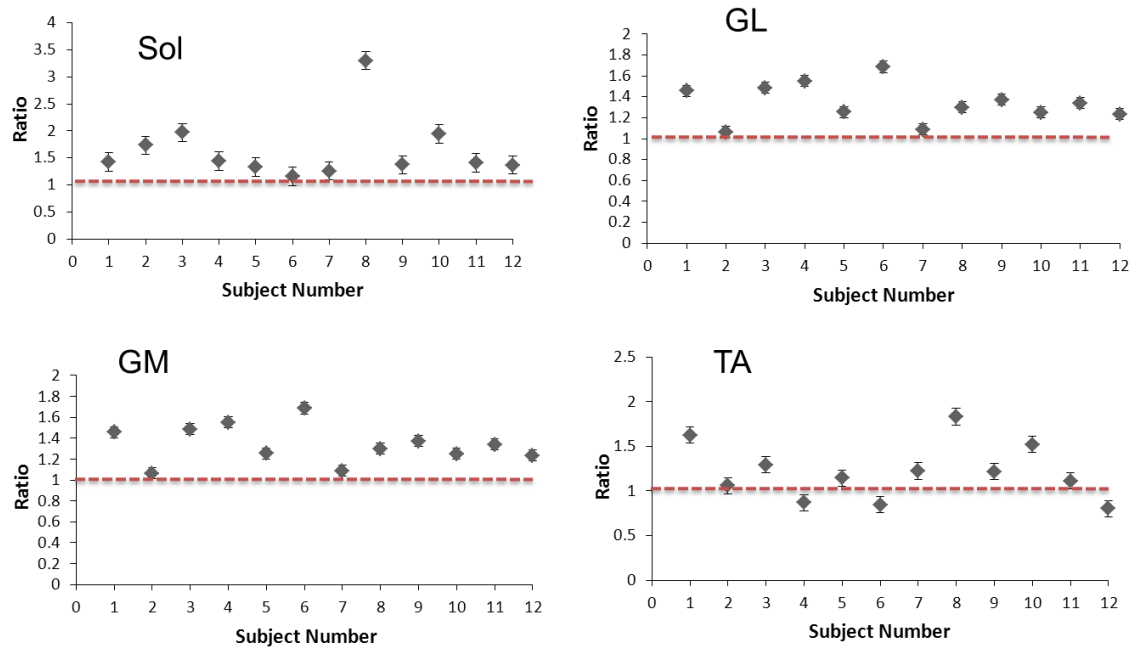


**Figure 4.12:** Ratios of mean EMG during EL to mean EMG during CL for each subject. (A) Soleus muscle (Sol). (B) Lateral Gastrocnemius (GL). (C) Medial Gastrocnemius (GM). (D) Tibialis anterior (TA). The red dotted line is drawn at a ratio of 1 as a reference line.

#### 4.3.5 Summary results for ATF and EMG

Summary results, showing all subjects mean tendon force and length, as well as the EMG; all at different percentages of the complete exercise cycle are shown in *Figure 4.13*. Temporal differences can be seen in ATF and ATL. EMG is summed to compare the contribution from the anterior and posterior compartments.

No notable differences were observed between the apparent stiffness of the tendon during EL and CL. However, the corresponding EMG was always higher during CL as compared to EL.



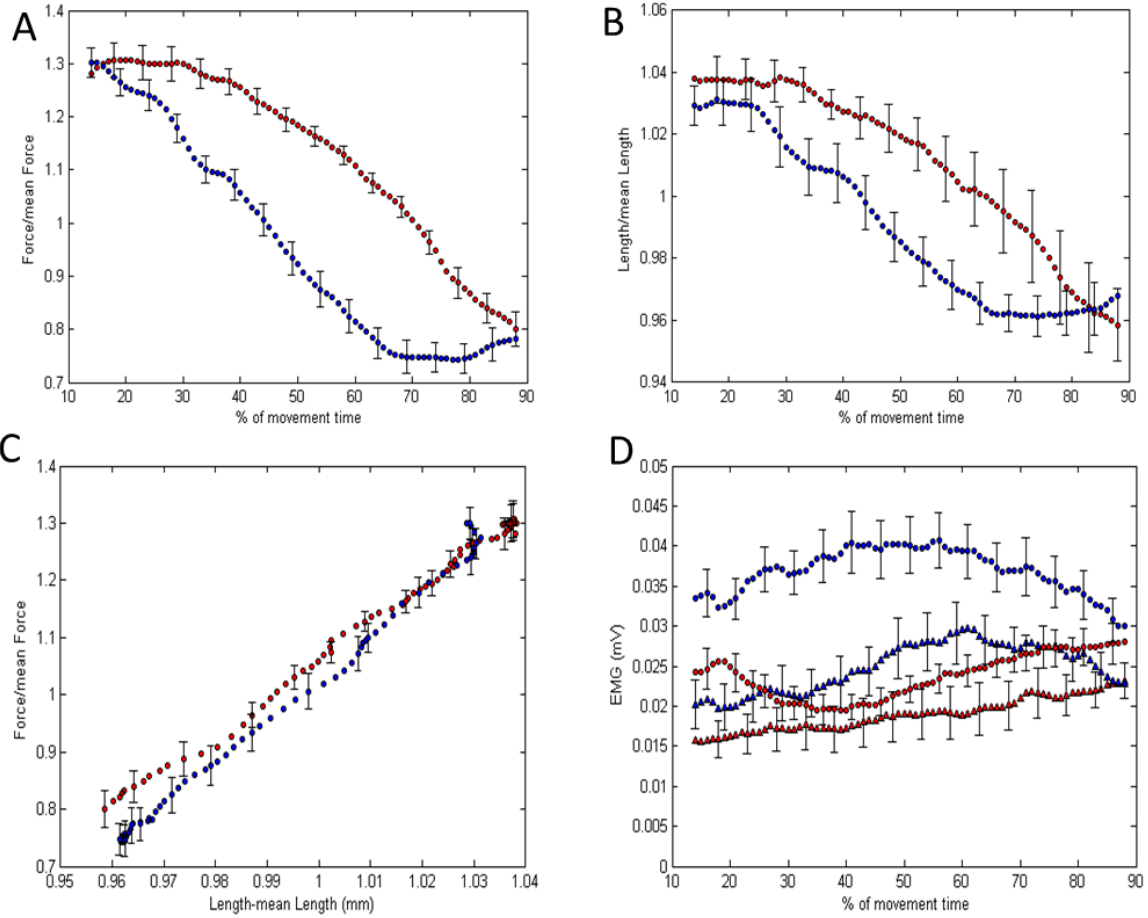


**Figure 4.13:** (A) Mean Achilles tendon force ( $ATF \pm SE$ ) and (B) Achilles tendon length ( $ATL \pm SE$ ) across all subjects and (C) resulting Force-length curve for EL (red circles) and CL (blue circles). Parallel to that, EMG data ( $\pm SE$ ) is also shown (D) for the anterior compartment during EL (red triangles) and CL (blue triangle) and the posterior compartment during EL (red circles) and CL (blue circles).

### 4.3.6 Force perturbations

Perturbations, defined by the fast FFT of either the GrF or the ATF were calculated for each exercise for all subjects. *Figure 4.14* shows the processing of the FFT for a single subject during EL. The normalised (to body weight (BWt)) data was de-trending by fitting the first order polynomial to the data and taking it away from the original data.

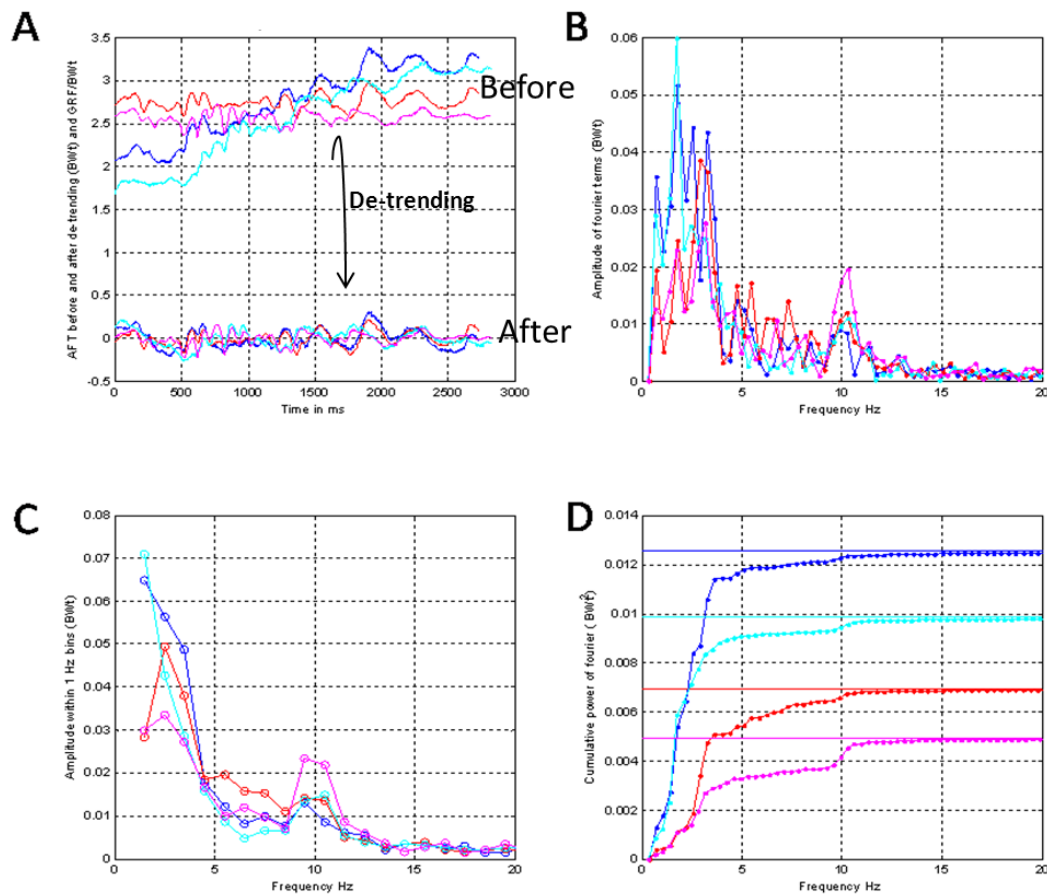


**Figure 4.14:** (A) Raw data for the normalised ATF (red and pink) and GrF/Body weight (blue and cyan) before (higher traces) and after de-trending (lower traces) during EL. (B) The corresponding amplitude of the FFT for each de-trended signal. (C) The corresponding amplitude within 1Hz bins. (D) Fourier cumulative power, from which a straight line is drawn at the maximum variance for each record, to show that the cumulative sum is equal to the variance.

The Fast Fourier transform (FFT) of the GrF, shown for each subject in *Figure 4.15*, demonstrated that the main amplitude of the power component was typically seen at vibration frequencies below 5 Hz, with a peak around 2 - 3 Hz representative of low frequency movements. However a range of vibration frequencies of up to 15 Hz were present in all subjects, with a greater amplitude of higher frequency force perturbations occurring during EL ( $t = -2.81$ ,  $p = 0.02$ ) at 10 Hz. As expected, ATF perturbations were found to be very similar to GrF perturbations, as ATF is directly derived from the GrF. However, it was notable that the magnitude of these perturbations was twice as high in the ATF than the GrF. It must be noted that not every subject showed a higher power of perturbations at around 10 Hz during EL.

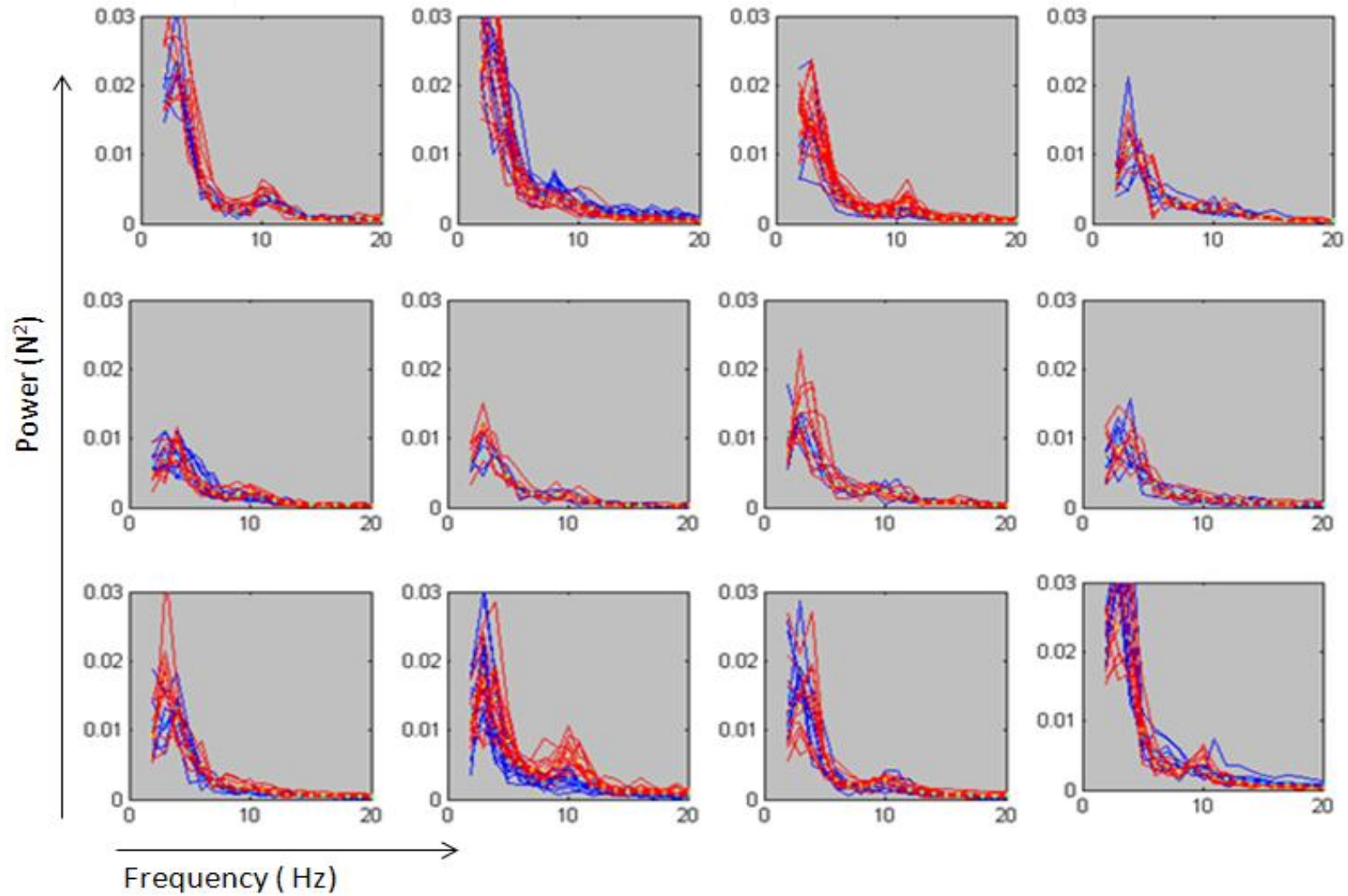


**Figure 4.15:** FFT amplitude of the GrF (in  $N^2$  on y axis) within 1Hz bin for all the subjects. All repeats for each subject are shown on separate graphs. EL data is in red and CL in blue.

Summary data showing the FFTs of GrF and ATF are shown in *Figure 4.16* and *Figure 4.17*. Statistical significance between EL and CL was observed at around 5 Hz and 10 Hz, where tremor during EL was observed to be higher than during CL.

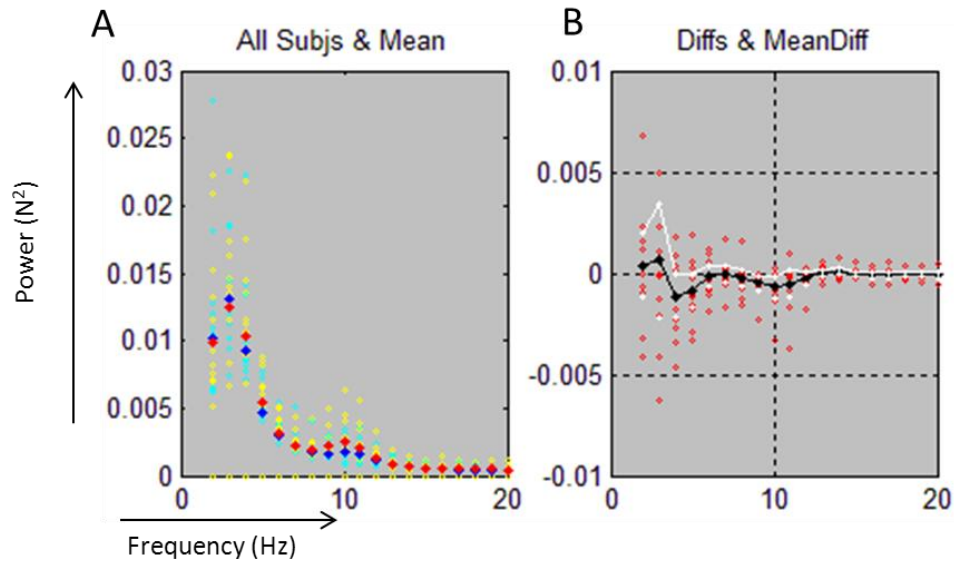


**Figure 4.16:** (A) All subject FFT mean data for the GrF for EL (red) and CL (blue) ( $\pm$  SE yellow for EL, cyan for CL) and (B) mean difference between the power of EL and CL for each subject (CL- EL). The mean difference across all points is calculated (black line) and plotted with the 95% confidence intervals (in white).

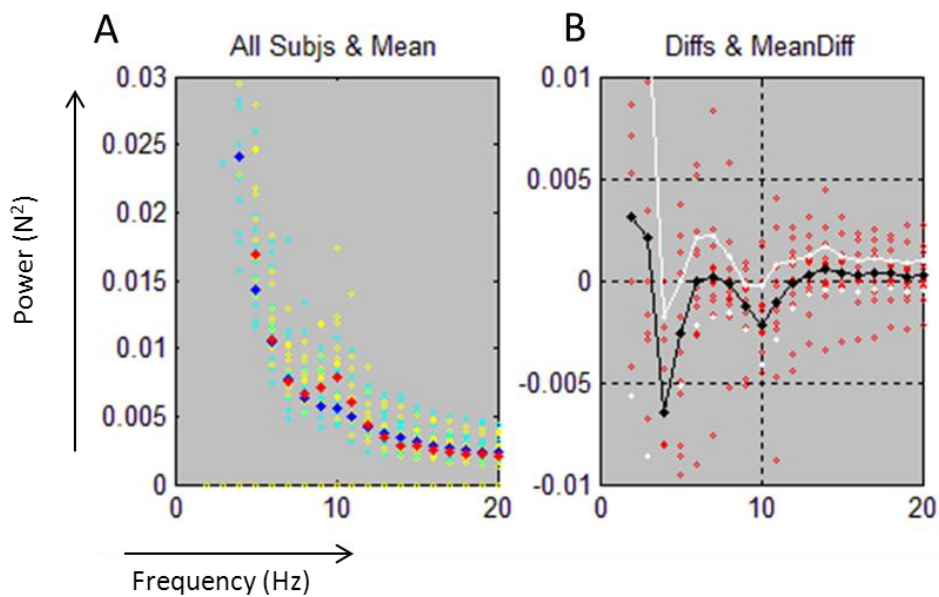


**Figure 4.17:** (A) All subject FFT mean data for the ATF for EL (red) and CL (blue) ( $\pm$  SE yellow for EL, cyan for CL) and (B) mean difference between the power of EL and CL (CL- EL). The mean difference across all points is calculated (black line) and plotted with the 95% confidence intervals (in white).

### 4.3.7 EMG perturbations

The FFT of the raw EMG data was also calculated for all four of the study muscles. Difference and mean difference plots for all four muscles are shown in *Figure 4.18*.

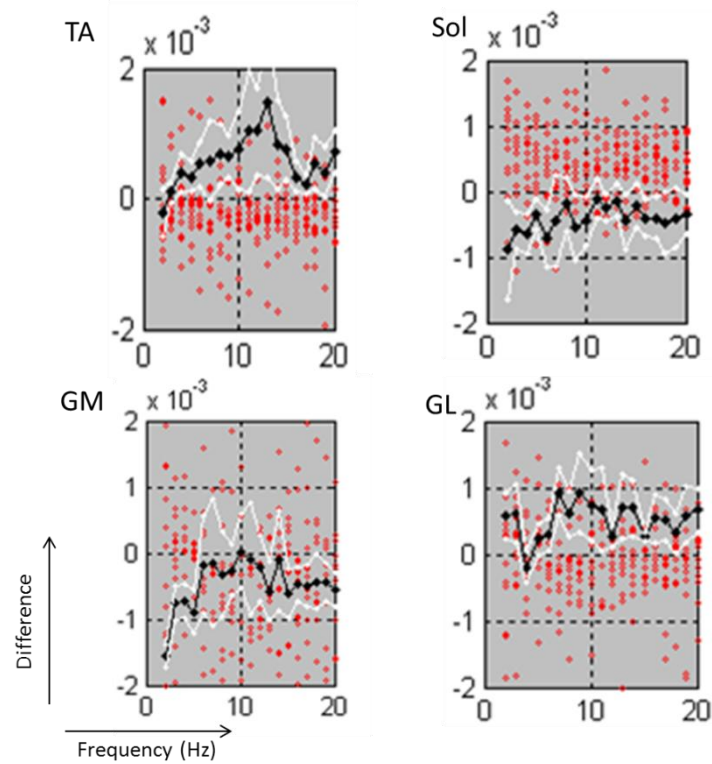


**Figure 4.18:** The differences between EMG FFT data for EL and CL, showing  $CL - EL$  for each subject, with the mean difference in black with 95 % confidence intervals in white, for the TA = tibialis anterior, Sol = Soleus, GM = medial gastrocnemius and GL = lateral gastrocnemius.

A notable difference between EL and CL was observed at lower frequencies for all muscles except the tibialis anterior. However, the lateral gastrocnemius and the tibialis anterior both showed a notable higher magnitude of tremor at around 10 Hz during EL than during CL. No significant differences between EL and CL were observed for the medial gastrocnemius muscle at this frequency. For the soleus, CL perturbations remained higher than EL perturbations for nearly the whole range of frequencies.

### 4.3.8 Correlation between force and EMG perturbations

The correlation between the GrF FFT and EMG FFT was calculated for each of the triceps surae muscles investigated. It was observed that the tremor in all the muscles was strongly correlated to the GrF fluctuations during EL. However, for CL this significance and correlation was only seen at 6 Hz, 13 Hz -15 Hz for the tibialis anterior and between 7 - 9 Hz for the medial gastrocnemius (Figure 4.19).

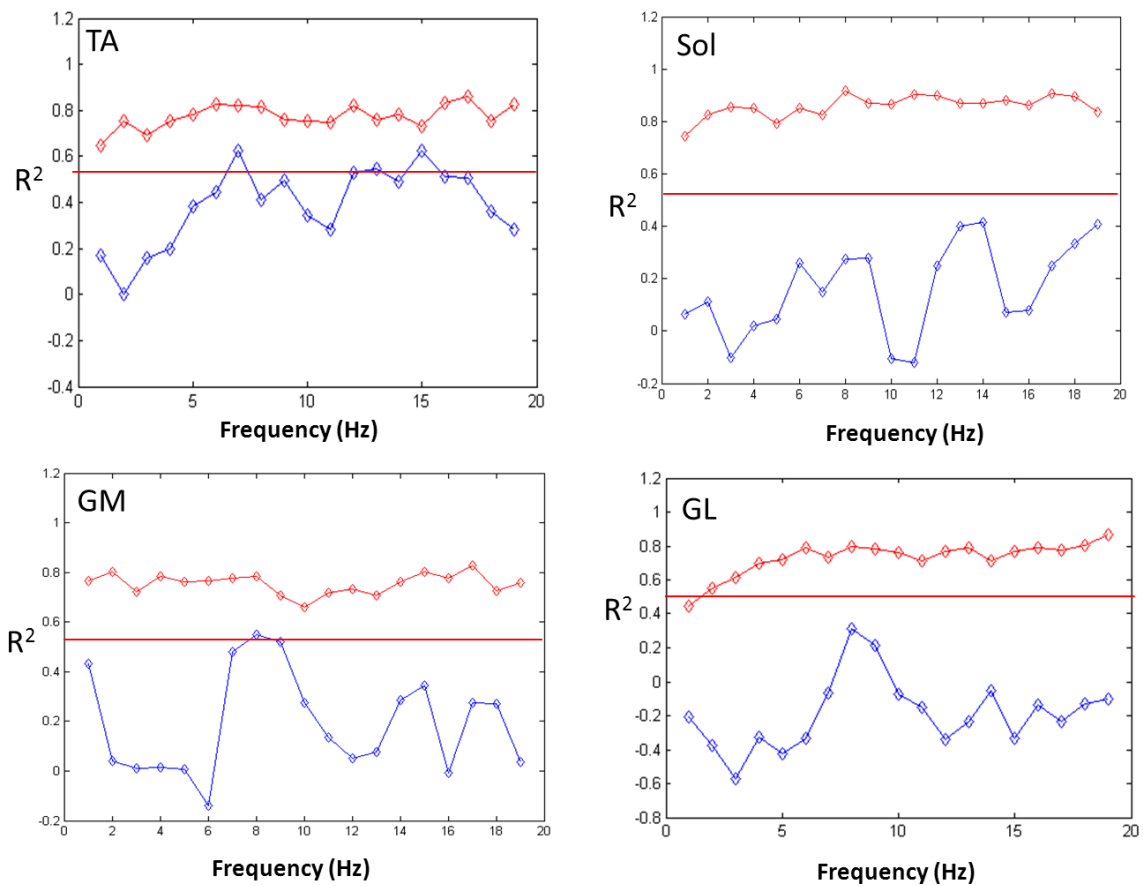


**Figure 4.19:** The correlation between the FFT of the GrF and that of the TA = tibialis anterior, Sol = Soleus, GM = medial gastrocnemius and GL = lateral gastrocnemius during EL (red) and CL (blue). The red line is drawn at 5% to indicate significance level.



### **4.3.9 Reliability**

The same day inter-test reliability of subject kinematics was found to have an  $R^2$  value of 0.81, indicating good reliability. Consistency between the measurements was checked for the speed of loading, ROM and force before other calculations were made. The different day intra-tester reliability between the strain measurements was found to be good ( $R^2 = 0.63$ ) for both EL and CL. Analysis of variance for the measurements performed on different days showed no significant differences in force ( $F = 0.64, p = 0.59$ ) or strain ( $F = 0.77, p = 0.53$ ).

## **4.4 Discussion**

This study demonstrates that the biomechanical behaviour of the Achilles tendon does not differ when performing EL and CL. The muscle tendon junction was successfully tracked with a semi-automated algorithm and a linear tendon force-length relationship observed during both loading protocols. The tendon stiffness varied across the population of subjects, but not between loading types. A mean maximum strain of 9% was also reported during EL and CL. No significance differences were observed between the force-extension characteristics of the tendon during EL and CL. However the EMG stayed significantly higher during CL when compared to EL for both the anterior and posterior compartments of the triceps surae. Furthermore higher perturbations at ~5 and 10 Hz were observed during EL than CL, and EMG perturbations were found to be significantly correlated to tendon perturbations during EL but not so consistently during CL.

A novel technique to measure tendon strain and stiffness during high strain movement is presented. Systematic error is always to be considered with any such measurement technique. However, a series of validation procedures were carried out, to ensure confidence in the resulting data. Using US to measure *in vivo* strains means that skin and probe rotation can be a potential source of error, estimated to result in roughly a 1 % strain deviation in a similar setting (Lichtwark and Wilson, 2005b). Error is minimised by placing markers on the probe to account for probe rotation, such that

US tracking is considered to be a reliable method (Lichtwark and Wilson, 2005b). However, the US image tracking technique developed and tested during this study can still be sensitive to image quality and both skill and practice are therefore required to track the MTJ accurately. It was observed that any blurred or low intensity images prevented accurate tracking. However any videos that did not meet the quality standards were not included in the analysis. For the 88 videos collected, only 8 were below the required standard. In addition, while the technique was shown to be reproducible for one participant, there is still some chance of individual to individual variability, owing to factors such as individual muscle architecture, the shape of the MTJ and changes in tissue shape during movement. These may alter the apparent location of the MTJ which would in turn influence strain and stiffness measures. However, using identical test procedures and a single tester in the current study minimised error and enabled EL and CL to be successfully compared. Indeed, no significant differences in tendon or muscle data were observed as long as the ROM, subject foot placement and US probe position were consistent between the measures. This was ensured by carefully marking the positions for the second day of measures.

Results from the study show that at the start of a concentric movement, the calf muscles are activated, increasing the activation level as they accelerate the subject upwards. The ATF is at its peak at the start of the CL movement, possibly as the moment arm of the triceps surae is furthest from the ankle joint axis for sagittal plane movement at this point. As the subject rises to dorsiflexion, the ATF reduces. In contrast, the subjects start an EL movement with heel at its highest point, and drops 'under control'. The movement is controlled (resisted) by lengthening of the activated calf muscle, and subsequently stretching of the AT. The maximal derived ATF occurs at the end of the eccentric movement when maximum force is required to decelerate the subject against gravity. Normalising ATF curves to heel height enables the change in force during each movement to be readily compared. From these data, significantly higher forces in the tendon were observed during CL for a small range of ankle angles when the foot was fully flexed, and the forces passing

through the tendon are maximum. However, no overall significant differences in force or stress during the loading cycle were observed between EL and CL. Such a finding is consistent with a previous study by (Rees et al., 2008), comparing similar EL and CL loading approaches. However, Rees et al were unable to report the range of forces, only reporting the maximum forces during EL and CL.

Also in agreement with previous studies (Enoka, 1996, Henriksen et al., 2009), data highlighted a comparatively lower EMG activity during eccentric than concentric loading. The muscle activation within the medial gastrocnemius, lateral gastrocnemius and soleus were all significantly lower during eccentric than concentric loading ( $p < 0.01$ ). By contrast, considering the antagonistic muscles (the tibialis anterior) there was no significant difference in muscle activation between EL and CL. Such a response from the tibialis anterior also follows previously reported findings, in which no significant effect of contraction type on EMG activity within the tibialis anterior has been reported (Reeves et al., 2003a). However, there is variability considering data from a range of different studies, as a result of different test methodologies (Kellis and Baltzopoulos, 1998, Reeves and Narici, 2003).

Considering EMG and force data together, indicated that eccentric contractions required lower levels of voluntary muscle activation by the nervous system to achieve a given muscle force, applied to the tendon (Enoka, 1996). It might be that the associated energy preservation during EL, via ATP sparing, allows a greater volume of exercise to be carried out under eccentric conditions than concentric.

The current study has additionally investigated tendon stiffness during EL and CL. Achilles tendon stiffness has previously been measured during EL or CL using a dynamometer, with variable results. A period of 6 weeks of EL has been shown to both decrease tendon stiffness (Morrissey et al., 2011) and have no effect (Mahieu et al., 2008). However, the current study is the first to assess how the

tendon stiffness varies during dynamic EL and CL exercises, and provides the rationale for a training study to track repeated dynamic stiffness changes over time.

Individual variations in the tendon properties, particularly stiffness, were evident across the group of participants. However, no significant differences in tendon stiffness between EL and CL were reported. Repeats by an individual were similar, and tendon properties reported (stiffness  $\sim 60$  N/mm, strain  $\sim 9\%$ ) were within the range of previously published data (*Table 3.1*). The variation in AT stiffness between individuals could be partly dependent on previous training (Reeves et al., 2003a); although all subjects in the study performed only moderate activity, the effect of specific training cannot be ruled out. In addition measurements were done in a clinical setting, where no control for the muscle activation was considered, a factor previously shown to affect stiffness measurements (Hof, 1998, Hof, 2003). However, to get a true understanding of the differences between EL and CL, it was necessary to carry out measurements during the typical protocol and not under isometric conditions. Recent studies have shown strains of around 5–10 % during isometric contractions (Finni et al., 2003, Maganaris and Paul, 2002, Muramatsu et al., 2001) thus the strains of around 9 % found in this study are within the previously described physiological range.

Strain is an important stimulus towards tendon repair. A number of studies have indicated that mechanical loading is an essential stimulus for tendon repair at the cellular level (Takai et al., 1991, Wang et al., 1993). Mechanical loading is known to initiate tenocyte signalling mechanisms in a strain dependent manner, with strain thus considered as an important stimulus for tendon repair (Scott et al., 2011). The results from the present study indicate that EL and CL, performed under equal load and at the same speed, result in different temporal strains within the tendon. However, if the data is plotted for normalised position, this difference disappears. Consequently, differences in strain alone are unlikely to be the differentiating trigger for EL repair during such exercise, although the situation may differ in patients with tendinopathy.

By contrast, tendon perturbations have been shown to differ between EL and CL, and were higher during EL, particularly around the 10 and 5 Hz ranges ( $p < 0.05$ ). Significantly higher perturbations during EL, in a range of 8-12Hz, has been reported previously by Henriksen et al, during a full dorsiflexion followed by plantar flexion movement protocol. However, the present study additionally demonstrates that tendon perturbations are independent of tendon mechanical properties. It is important to note that in the present study, not every subject showed 10 Hz perturbations. This would imply that not every patient performing EL would receive this stimulus; hence if it is the factor treating – or even causing - tendinopathy, this may partly explain why not all subjects respond to EL. It has been reported previously that if these perturbations are due to mechanical resonance, then the frequency of these tremors will depend on the tissue stiffness, hence it seems likely that the current perturbations are from a different origin than mechanical resonance. Their origin could be multifactorial in nature, as detailed in chapter 1 (section 1.10.3), however, tremors at around 10 Hz are often considered to be primarily associated with muscle activity.

It was shown in the present study that EL is characterized by lower EMG than CL, reflecting a lower level of motoneuron activation, (Moritani et al., 1987, Nardone et al., 1989). It is possible that the observed force perturbations result from this preferential recruitment of large motor units. The present study has also shown that the perturbations during EL were strongly correlated to the activation perturbations in all muscles and especially in the tibialis anterior and gastrocnemius. However, this study could not investigate the exact origin of these perturbations. These findings suggested that further research was necessary to investigate muscle perturbations in detail and establish their role in tendon perturbations.

There is a lack of consensus concerning the management of tendinopathy, which has limited the possibility of developing new and more effective treatments. This study has given the most complete

contemporary biomechanical characterisation of EL and CL performed during a single session. There is a revealed need to carry out controlled training studies, where EL and CL must be performed at same load and speed to investigate the training effects on healing.

#### **4.5 Conclusions**

This study demonstrates that the biomechanical behaviour of the Achilles tendon does not differ when performing EL and CL. However, measured EMG was significantly higher during CL when compared to EL for both the anterior and posterior compartments of the triceps surae. Furthermore higher perturbations at ~5 and 10 Hz were observed during EL than CL, and EMG perturbations were found to be significantly correlated to tendon perturbations during EL alone.

**Chapter 5: The effect of eccentric and concentric loading speed  
on the biomechanical parameters of the triceps surae**

## **5.1 Introduction**

While EL is often promoted for treating Achilles tendinopathy, the specific training parameters employed during this therapeutic exercise have not been fully evaluated, to determine those with optimal efficacy, as described in chapter 1 (section 1.11.1). In particular, there is a lack of consensus on loading speed with some groups adopting a slow and steady exercise speed, as initially outlined (Alfredson et al., 1998, Mafi et al., 2001, Gardin et al., 2010), while others have utilized progressively higher speeds (Stanish et al., 1986, Maffulli et al., 2008b, Sayana and Maffulli, 2007). Unfortunately, precise data concerning the speed adopted for exercise is rarely reported (Fahlstrom et al., 2003, Silbernagel et al., 2001), perhaps reflecting our limited understanding of the importance of this parameter, and certainly limiting our understanding of the effect of speed variation on treatment efficacy.

Exercise speed during rehabilitation is important for many reasons. The concept of specific adaptation to imposed demand is now well established, and clearly outlines that strength changes due to exercise are speed specific, as they are to other factors such as type of contraction (Bird et al., 2005). For example, a recent study has shown that the gain in muscle strength during EL is speed dependent (Farthing and Chilibeck, 2003). The mechanism behind this elevated effect has not been explored, and it remains unclear if speed of loading during EL may also influence tendon repair. Further, a number of studies have investigated the effect of walking, running and hopping speed on human muscle and tendon mechanics (Cavagna and Kaneko, 1977, Sasaki and Neptune, 2006, Farris and Sawicki, 2012). It has been shown that the mechanical work done in moving the body during walking and running is gait and speed dependent. This indicates that the muscle-tendon unit may adjust its mechanical behaviour in relation to exercise speed, in order to deliver variable contributions to total mechanical work.



Indeed, the different tendon strain rates, resulting from different exercise speeds, may influence tendon *in vivo* mechanical properties and subsequently the mechanism of healing. However the effect of strain rate on tendon elastic properties is controversial and inconclusive. Some *in vitro* studies have reported that the elastic modulus of tendon tissue increases with increasing strain rate or speed of loading (Cui et al., 2009, Wu, 2006) while others have reported no effect (Ng et al., 2004) at comparable strain rates. By contrast *in vivo* studies generally suggest that the stiffness of connective tissues increases with an increase in strain rate (Pearson et al., 2007). It could be that training at different strain rates can result in different therapeutic effects. An *in vivo* study has shown that fast isokinetic EL resulted in greater muscle hypertrophy compared to slow EL (Shepstone et al., 2005), while other work has reported a greater increase in elbow flexor muscle strength with fast EL exercise when comparing slow and fast isokinetic EL and CL (Farthing and Chilibeck, 2003). However, the effect of different loading velocities on tendon biomechanical properties was not investigated and thus the cause of this improvement in response to faster loading remained unexplored.

Furthermore, the effect of exercise speed on tendon perturbations is unknown. Henriksen and co-workers demonstrated that high frequency perturbations occur during EL at a moderate speed (Henriksen et al., 2009). With similar findings in the current study (chapter 4), it has been hypothesized that the high frequency vibrations occurring in the AT during EL may underpin the therapeutic mechanism of EL. However, the differential effect of speed on tendon perturbations has not been addressed. As a secondary outcome, this study also examined if exercise speeds may influence the magnitude and frequency of tendon force perturbations in EL and CL.

### **5.1.1 Hypotheses**

The aim of this chapter was to compare eccentric and concentric loading, performed at different speeds, to investigate any differences in muscle activity levels, and tendon properties or force perturbations during the exercises. This study hypothesized that on changing exercise speed:

- Muscle activation will be higher during fast EL and CL.
- Tendon force, stiffness and strain will be higher during fast EL and CL.
- Perturbation magnitude and frequency will be higher during fast EL and CL.

To explore these hypotheses, a biomechanical characterization of one-legged weight bearing EL and CL was performed in a group of normal subjects.

## **5.2 Methods**

### **5.2.1 Subjects**

Thirteen healthy volunteers (7 male and 6 female) were recruited with mean age 22.1 years (SD = 1.7), mean body mass 69.1 kg (SD = 11.6) and mean height 1.75 m (SD = 0.06). The study was approved by the Queen Mary, University of London Research Ethics committee and all participants gave written informed consent. All the subjects had engaged in moderate physical activity over at least the previous year, amounting to around 2 - 3 hours of exercise per week over the last year. Inclusion and exclusion criteria remained the same as detailed in chapter 4 (section 4.2.2).

Subjects were measured for height and body mass. Occupation and sports activities were recorded. Eleven of the subjects were sports and exercise medicine students, engaged in recreational sports. None of the participants were involved in sports activities above recreational level or in any occupation requiring significant lower limb activities.

## **5.2.2 Exercise protocol**

The experimental setup and data collection protocols followed those outlined in chapter 4 (section 4.2). EL and CL exercises were performed at two speeds, designated fast ( $\sim 1 \text{ rad}\cdot\text{s}^{-1}$ ) and slow ( $\sim 0.2 \text{ rad}\cdot\text{s}^{-1}$ ), yielding 4 test groups when combined with exercise type: fast eccentric (EF), slow eccentric (ES), and fast concentric (CF) and slow concentric (CS) with exercise times of 1s (fast) and 6s (slow), as guided by common clinical practice. To keep speed and range of motion consistent, up to 5 familiarization exercises were completed before the actual tests started, in which subjects were taught to complete the heel raise or heel drop at the required speed, guided by a metronome set at 60 beats per minute. Their foot position was marked on the step with tape, to assist them in completing reproducible trials. Subjects then carried out the EL or CL exercise at the desired speed and consistent ROM, checking for consistency in ROM, by monitoring the calcaneum marker movement by the examiner. After completing either exercise, the subjects used the other leg to return to the starting position, before repeating the exercise. Five sets of data were recorded for each loading paradigm for each subject, in a randomized order.

Electromyography (EMG) recordings were made using dual electrodes with a 20 mm inter-electrode distance placed on the belly of the soleus, lateral gastrocnemius, medial gastrocnemius and tibialis anterior muscles following the SENIAM guidelines (Hermens et al., 2000). A single, self-adhesive Ag/AgCl snap electrode was placed on the shinbone as a reference as previously described in chapter 3 (section 3.2.1.2).

## **5.2.3 Data collection**

### **5.2.3.1 Measurement of muscle activation**

Electromyography (EMG) recordings were made using dual electrodes with a 20mm inter-electrode distance placed on the belly of the soleus, lateral gastrocnemius, medial gastrocnemius and tibialis

anterior muscles following the SENIAM guidelines (Hermens et al., 2000). A single, self-adhesive Ag/AgCl snap electrode was placed on the shinbone as a reference as previously described in chapter 3 (section 3.2.1.2).

### **5.2.3.2 Measurement of tendon force**

In order to measure the ATF, the 3D ground reaction force was captured and the data from the motion tracking markers collected. As outlined in chapter 3 (section 3.3.3), the ATF vector was found using inverse dynamics.

### **5.2.3.3 Measurement of tendon elongation**

Tendon length (ATL) at any time was defined as the distance between the AT insertion and the distal muscle-tendon junction (MTJ) of the medial gastrocnemius (GM). In order to establish this length, both locations were tracked throughout each exercise as outlined in chapter 3 (section 3.3.5).

### **5.2.3.4 Measurement of perturbations**

The perturbations were established from the fast Fourier transform of the GrF. The 3D GrF was recorded and processed for this purpose, as detailed in chapter 3 (section 3.4.5).

## **5.2.4 Repeated measures**

Three sets of measurements were taken for every subject, all collected by the same examiner, with a 3 - 5 minute break between tests. Apparatus was not removed between tests. For intra-test reliability, the complete protocol was repeated after a 10 minute break for 3 of the subjects. For inter-tester reliability, one subject was recruited for a second series of measurements, made by a second examiner, but with the same set-up and without removal of the apparatus.

### **5.2.5 Data analysis**

Data analysis was carried out with custom developed Matlab scripts (chapters 3 and 4). For each exercise task only the three most accurately paced cycles, were retained for further analysis. These were defined as  $\pm 0.3s$ , without loss of balance and maintaining consistency in ROM. Points of minimum and maximum heel height were identified and the record was then re-sampled by interpolation to 111 uniformly spaced points as detailed in chapter 3 and 4.

After registration, ground reaction force and EMG data were obtained for each individual subject. The ATF was then found throughout each loading cycle completed by each subject. The tendon force was normalised to body weight to help highlight any differences between subjects. For each individual tendon, stress at any point in time was calculated by dividing the instantaneous ATF by the minimum CSA. Tendon strain ( $\epsilon$ ) at each point was calculated by finding the instantaneous length of the tendon at any point in time, and dividing the change in length ( $\Delta L_i$ ) by the length of the tendon at minimum tendon force.

An average force-length graph for each subject during EL and CL was drawn, over the three repeats of each exercise. Tendon stiffness was measured from the slope of the force-length curve by placing a linear regression line through the average data for each individual.

To study the force perturbations, the vertical component of the GrF vector was further analysed, firstly subtracting the mean value to make it independent of the body mass. To obtain the magnitude and frequency of the perturbations, power spectrum densities were calculated using fast Fourier transformations (FFTs - 111 points) after elimination of the dc component. The power was subsequently summed within 1 Hz windows across the frequency range of 0 to 16 Hz, and the resulting summed powers estimated as a mean and standard error of the mean (SEM).

The raw EMG signal was full-wave rectified and normalised with the heel height. To better correlate the EMG signal to contractile features of the muscle, high frequency components of the EMG data were filtered and smoothed by finding the running average of the signal to give the linear envelope. From the envelope, the average EMG was calculated. Muscle activation patterns and magnitudes were then compared between speed conditions.

### **5.2.6 Statistical analysis**

Normality tests were performed using the Shapiro-Wilk method (OriginPro, version 8, OriginLab, USA). Pearson's product moment correlation coefficient was used to describe the correlation between parameters. Three or four way ANOVAs, were performed to investigate significant differences with force, stiffness, strain or EMG as the dependent variable and eccentric or concentric; fast or slow; different subjects; and time points as the main factors. A four way ANOVA was also performed inputting subjects, contraction type, movement speed and frequency as factors, and summed power from individual tests as the dependent variable. Interactions between the main effects were included. Frequency was analysed for the average power in intervals of 1Hz width between 0 and 16Hz. Statistical significance was accepted at  $p \leq 0.05$ .

In order to quantify the stability of repeated measures, analysis of variance between individual movements was performed, to establish that subjects moved in a repeatable fashion. Tukey's tests were chosen to make post hoc comparisons, where the ANOVA showed there to be a significant difference between the data sets. Tukey's tests were preferred over other commonly employed methods, for example, least significant differences and Bonferroni, to avoid potential type I error. Type I error occurs when we reject a null hypothesis when it is true, biasing the decision by concluding that a real difference exists when, in fact, the differences were due to chance (Portney and Watkins, 2009). Least significant difference methods were not used as they are generally considered to be lenient and prone to type I errors, whereas Bonferroni wasn't adopted owing to

the inflexibility in the judgement, minimising the type I error but being particularly prone to type II errors (Portney and Watkins, 2009).

## **5.3 Results**

### **5.3.1 Normality**

The data for height and body weight were found to be normally distributed ( $p = 0.43$  and  $p = 0.47$  respectively) with a significance correlation ( $r = 0.90$ ,  $p < 0.01$ ) showing that the population was not skewed with particularly small, tall, heavy or light subjects.

### **5.3.2 Raw data - marker position**

In order to ensure there were no discrepancies in marker data (including any random jumps), the position of all the markers was plotted for each exercise for all subjects, for all speeds and compared. An illustrative example is shown in *Figure 5.1*.

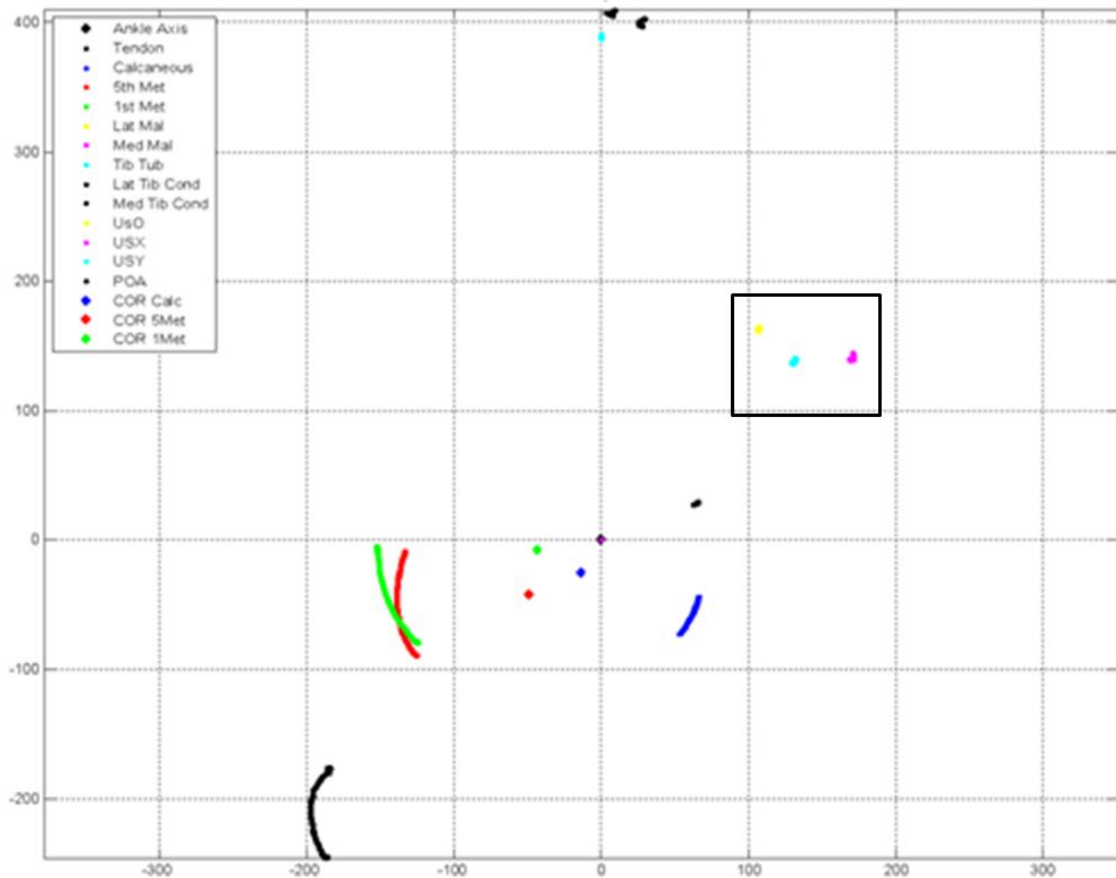


**Figure 5.1:**Representation of all 15 markers used on the lower leg and US probe seen perpendicular to the plane of action during fast CL. The big arcs in red and green indicate the movement (centre of rotation) of 1<sup>st</sup> and 5<sup>th</sup> metatarsal with red and green dots denoting the centre of the projected circles. Small arcs in black and blue represents motion (Centre of rotation) of the tendon and calcaneum, whereas the large black arc is the point of application of force. Black arcs at the top are the movements from the lateral and medial tibia condyle. The US markers are shown (black box) in cyan, yellow and pink, monitoring any movement of probe.

### 5.3.3 Range of motion and speed

Figure 5.2 illustrates a single data set for a typical subject by way of example, showing the range of motion and the vertical component of the GrF data during EL and CL for both loading speeds. As a result of the opposing direction of EL and CL movements, during EL the ankle angle decreases from maximum to minimum while it increases during CL. Fluctuations in the GrF during EL appears higher than during CL. Unsurprisingly, there was considerable variation in the GrF between subjects, as a



result of varying body weight. An initial comparison of the raw data collected during CL and EL showed no significant differences in the range of motion or GrF at any speed (Table 5.1).

**Table 5.1:** Summary of the GrF and range of motion for CL and EL at each speed.

Measurement	Group	Concentric loading	Eccentric loading	p
		Mean ± SE	Mean ± SE	
GRF(N)	Slow	706.2 ± 67.8	705.7 ± 65.9	0.83
	Fast	709.1 ± 71.8	708.35 ± 80.2	0.85
ROM(°)	Slow	51 ± 3.1	52 ± 4.15	0.56
	Fast	51 ± 3.8	52 ± 3.6	0.43

Values are means ± SE, GRF= ground reaction force, ROM= range of motion, SE= standard error

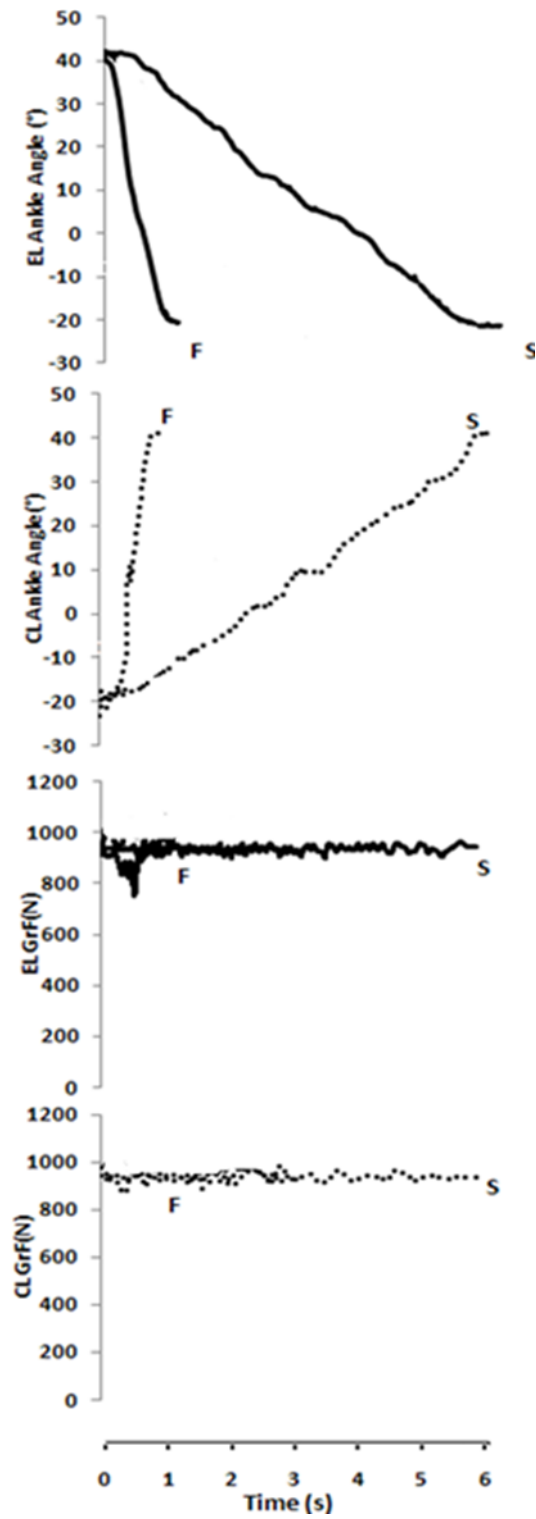


**Figure 5.2:** Illustrative example of ROM (ankle angle) and GrF for a typical subject comparing EL and CL at fast (F) and slow (S) speeds.

#### **5.3.4 Achilles tendon force**

Tendon force plots for all subjects were plotted in *Figure 5.3*. Forces during EL/CL fast appear to be higher at the fast loading speed but no statistical significant differences in ATF between any conditions were observed. Mean ATF data from all the subjects is shown in *Figure 5.4*. Data from two subjects did not satisfy the analysis criteria, as the ROM was not consistent between the trials, so these data were not considered for further analysis. As is evident from *Figure 5.4*, no significant differences in ATF were observed between the eccentric and concentric protocols ( $F = 0.23$ ,  $p = 0.53$ ). An effect of speed that trended towards significance was observed ( $F = 3.63$ ,  $p = 0.056$ ), however consideration of the interaction of type of loading and speed shows no difference ( $F = 0.91$ ,  $p = 0.34$ ). There were also no significant interactions between the main factors.

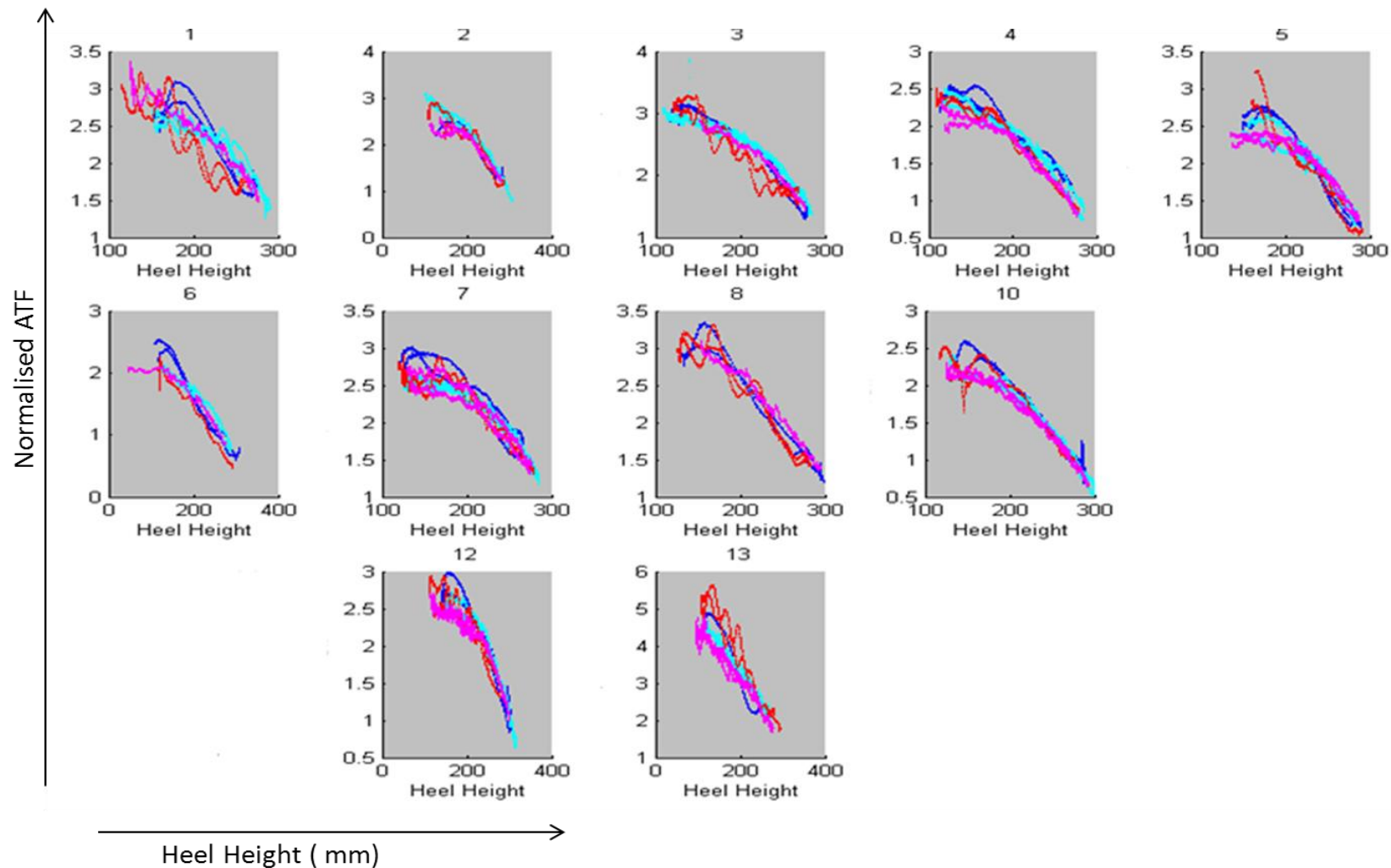


**Figure 5.3:** Normalised Achilles tendon force (ATF) data for all subjects, comparing fast eccentric (red), slow eccentric (pink), fast concentric (blue) and slow concentric (cyan).

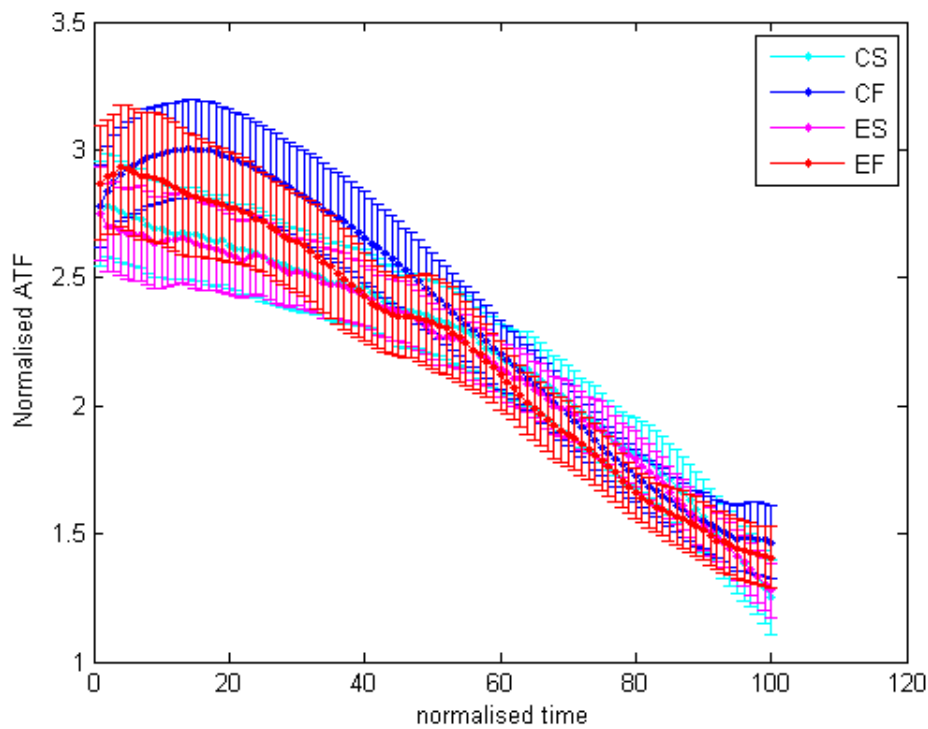


**Figure 5.4:** A comparison of the mean normalised Achilles tendon force (ATF) across all subjects during EL and CL at two loading speeds (CS = slow concentric, CF = fast concentric, ES = slow eccentric, EF = fast eccentric).

The ANOVA showed that the force data varied significantly among the subjects ( $F = 21.1$ ,  $p = 0.01$ ), however no significant effect of speed was observed on the tendon force.

### 5.3.5 Achilles tendon force-length relationship

Typical raw force-length graphs for each of the loading conditions are shown for two different subjects in *Figure 5.5* and *Figure 5.6*. Individual variations in tendon behaviour were evident and the tendon tended towards stiffer behaviour during concentric fast, than concentric slow, however no significant effect was observed ( $t = 1.51$ ,  $p = 0.16$ ). No overall significant differences were observed between EL and CL at either loading speed ( $F = 0.77$ ,  $p = 0.51$ ).

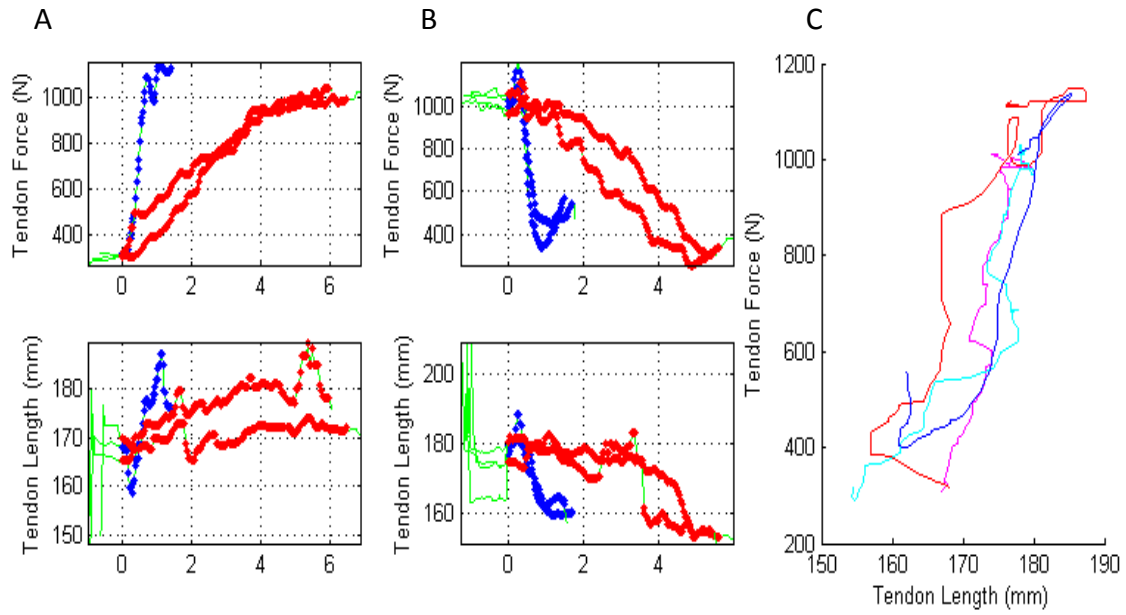


**Figure 5.5:** Typical graphs for one subject, showing raw Achilles tendon force and Achilles tendon length with time (s) for (A) eccentric loading: fast in blue and slow in red and green is the double-leg support phase (B) concentric loading: fast in blue and slow in red and green shows double leg support (C) raw mean AT force-length curve for a single subject, during EL and CL at two loading speeds, EF (red), ES (pink), CF (blue) and CS (cyan).

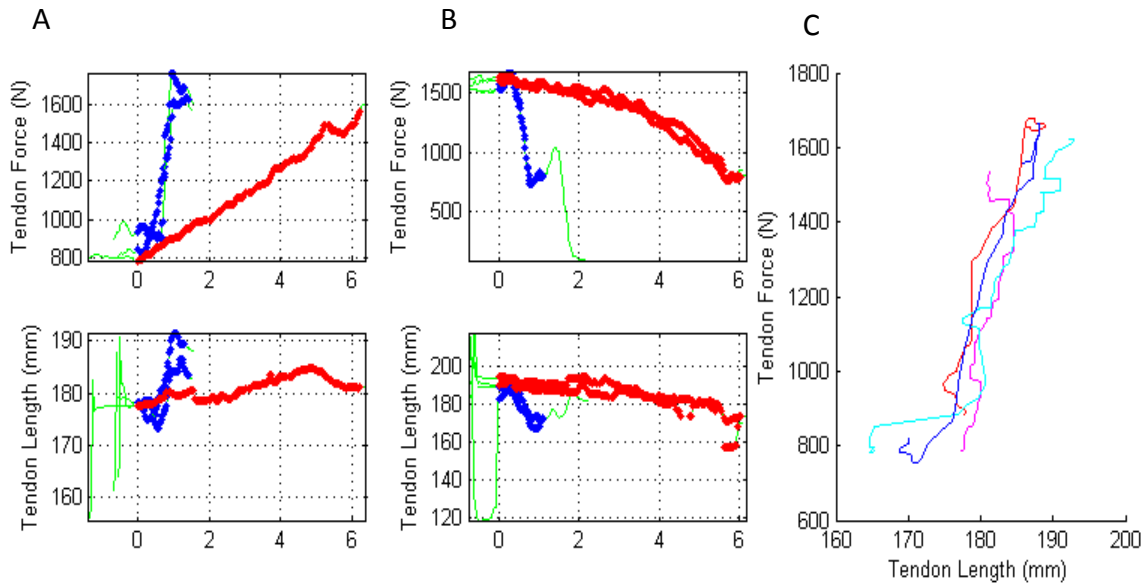


**Figure 5.6:** Typical graphs for one subject, showing raw Achilles tendon force and Achilles tendon length with time (s) for (A) eccentric loading: fast in blue and slow in red and green shows double leg support (B) concentric loading: fast in blue and slow in red and green shows double leg support (C) raw mean AT force-length curve for a single subject, during EL and CL at two loading speeds, EF (red), ES (pink), CF (blue) and CS (cyan).

**Table 5.2.** Summary of the mechanical properties of the AT during CL and EL at the two loading speeds.

		Achilles tendon force (N)	Achilles Tendon length change (mm)	Stiffness (Nmm <sup>-1</sup> )	Stress (MPa)	Strain (%)
<b>Concentric loading (Mean ± SE)</b>	Fast	1942 ± 187	15.92 ± 1.84	61.26 ± 5.92	38.84 ± 3.68	7.83 ± 0.89
	Slow	1789 ± 192	17.09 ± 1.79	51.92 ± 3.32	35.78 ± 3.27	8.23 ± 0.85
<b>Eccentric loading (Mean ± SE)</b>	Fast	1887 ± 224	16.01 ± 1.77	57.86 ± 5.58	37.74 ± 4.37	7.61 ± 0.92
	Slow	1781 ± 180	16.74 ± 1.56	56.69 ± 3.32	35.71 ± 3.62	7.93 ± 0.81

Values are means ± SE, SE = standard error

Mean maximum tendon stress was in the range of 35 - 38 MPa for all test groups, whilst mean maximum strains ranged from 6 - 9%. The strain values were found to be unaffected by the speed of loading.

### **5.3.6 Force perturbations**

The Fast Fourier transform (FFT) of the GrF for all subjects demonstrated that the main amplitude of the power component was typically seen at vibration frequencies below 5 Hz with a peak around 2 - 3 Hz, representative of low frequency movements (*Figure 5.7*). However a range of vibration frequencies of up to 15 Hz were present in all groups, with the greatest amplitude of higher force perturbations occurring at the fast test speed ( $p = 0.01$ ). ANOVA results indicated a significant effect of the type of loading ( $F = 97.87$ ,  $p = 0.01$ ) and speed ( $F = 172.64$ ,  $p = 0.01$ ). When speed and loading type were combined, results indicated a significantly higher power component in the 5 - 12 Hz range during EL when compared to CL at fast speeds ( $F = 82.74$ ,  $p = 0.01$ ) (*Figure 5.8*). By contrast, at the slow exercise speed, no significant differences between EL and CL were observed for the entire frequency spectrum ( $p > 0.05$ ). The highest power overall was in the eccentric group moving at the fast speed. Considering the discovery of 10 Hz vibrations during EL only (chapter 4), a comparison of these frequency perturbations with the current data highlights that the magnitude of perturbations at the slow speed is less than at the medium speed (chapter 4; 3 s), while at the fast speed, the perturbations are largest. However, the perturbation magnitude as well as the range of frequencies present varies among subjects.



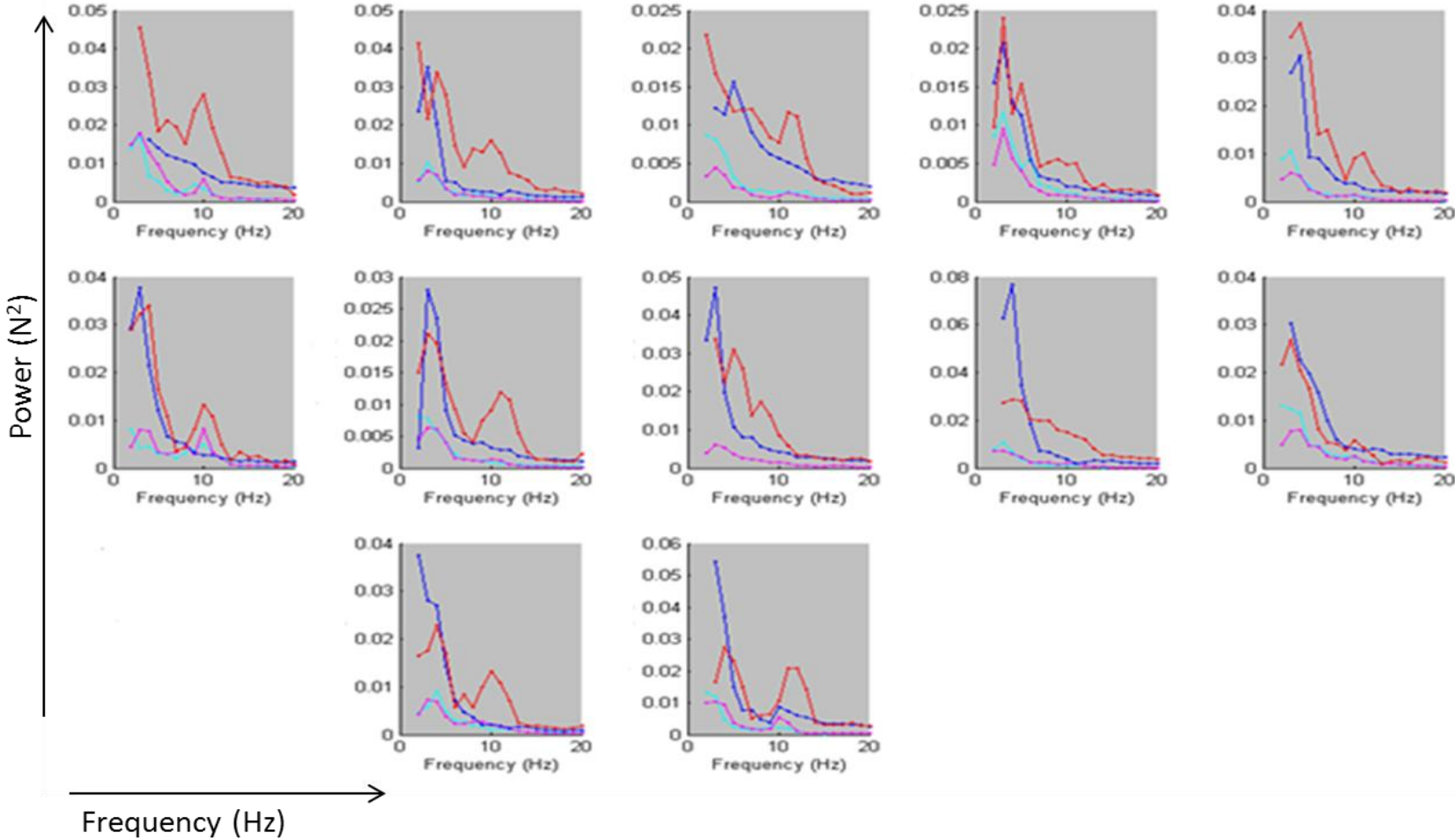


**Figure 5.7:** Mean power densities comparison for all subjects, during fast eccentric (red) and concentric (blue) movements, and slow eccentric (pink) and concentric (cyan) movements.

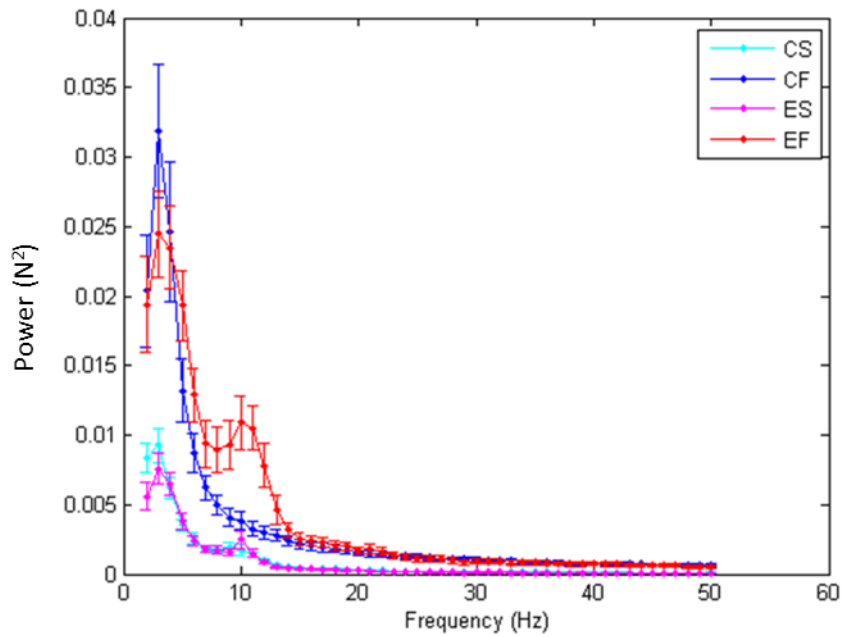


**Figure 5.8:** Mean Power density spectrums, comparing the relative magnitudes of perturbations for eccentric loading at fast (EF) and slow speeds (ES), and concentric loading at fast (CF) and slow (CS). Error bars represent the standard error of the mean.

### 5.3.7 Muscle activation

Figure 5.9 reports example EMG data for all analysed muscles, from five different subjects. A marked variation in EMG activity among individuals was observed but there was also a significant interaction between the main factors eccentric/concentric and fast/slow in all four muscles.

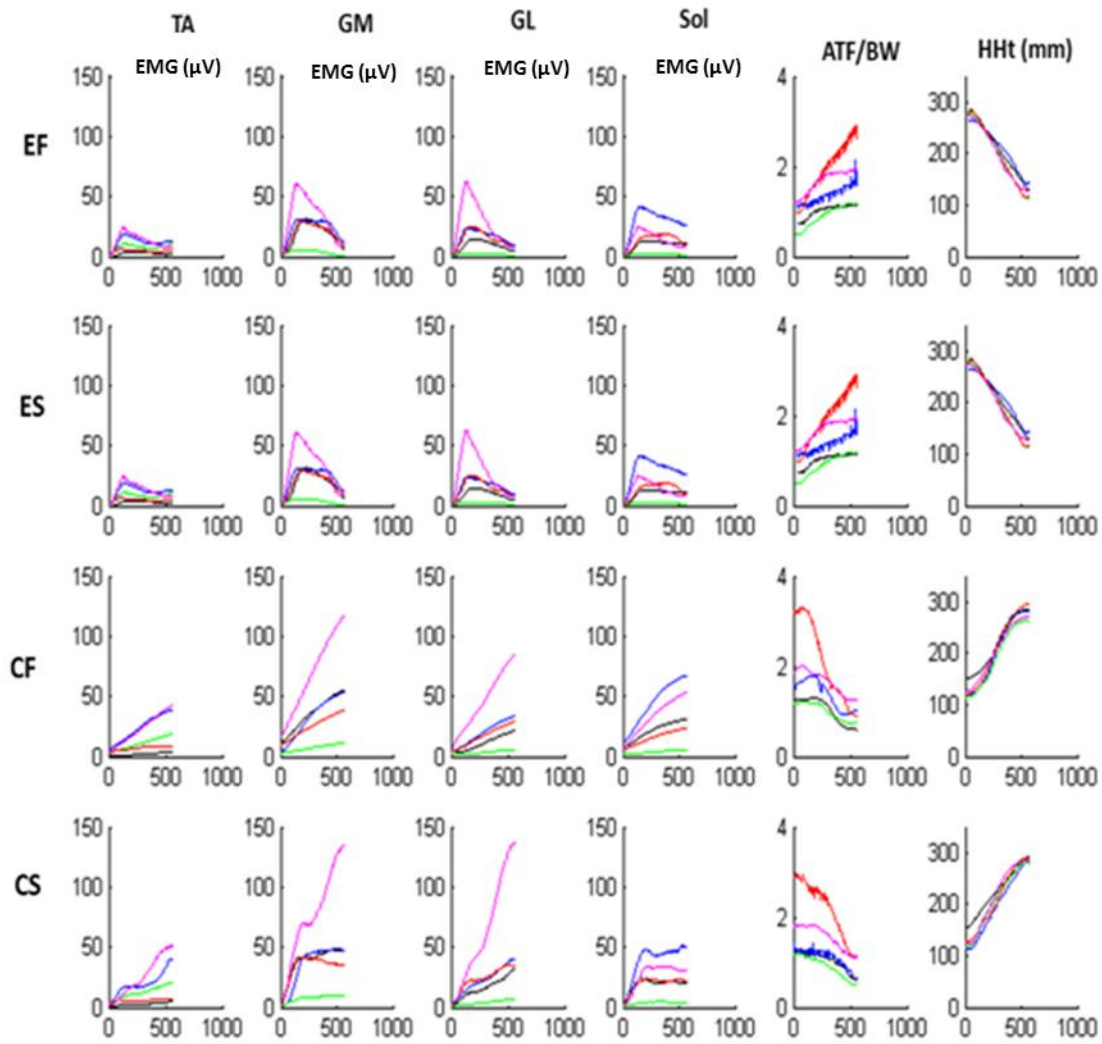


**Figure 5.9:** Graphs of the mean EMG data for the TA= tibialis anterior, GM = medial gastrocnemius, GL = lateral gastrocnemius, Sol = Soleus for five different subjects (each shown in a different colour) during each exercise regime. The 2 panels on the far right show mean Achilles tendon force (ATF) and heel height (HHT) for the same subjects during exercise.

Figure 5.10 compares the mean EMG data for fast and slow EL and CL in the tibialis anterior, medial gastrocnemius, lateral gastrocnemius and soleus. Distinct patterns of activation were observed when comparing EL and CL. However, the ANOVA's for the soleus ( $F = 313.77$ ,  $p = 0.01$ ), medial gastrocnemius ( $F = 96.59$ ,  $p = 0.01$ ) and the lateral gastrocnemius ( $F = 26.66$ ,  $p = 0.01$ ) show a significant difference between eccentric and concentric loading in terms of EMG activation. No

significant difference was observed for tibialis anterior ( $F = 0.71$ ,  $p = 0.058$ ). Furthermore, EMG activation within all the muscles appear to be significantly affected by speed during CL. Speed significantly increased the muscle activity in all muscles except the tibialis anterior during CL. However, during EL, muscle activity in all the muscles was observed to be unaffected by speed. The ANOVA results for the tibialis anterior show no significant differences in muscle activation at any speed. Furthermore no significant interaction between type of loading and speed was observed ( $F = 3.11$ ,  $p = 0.07$ ).

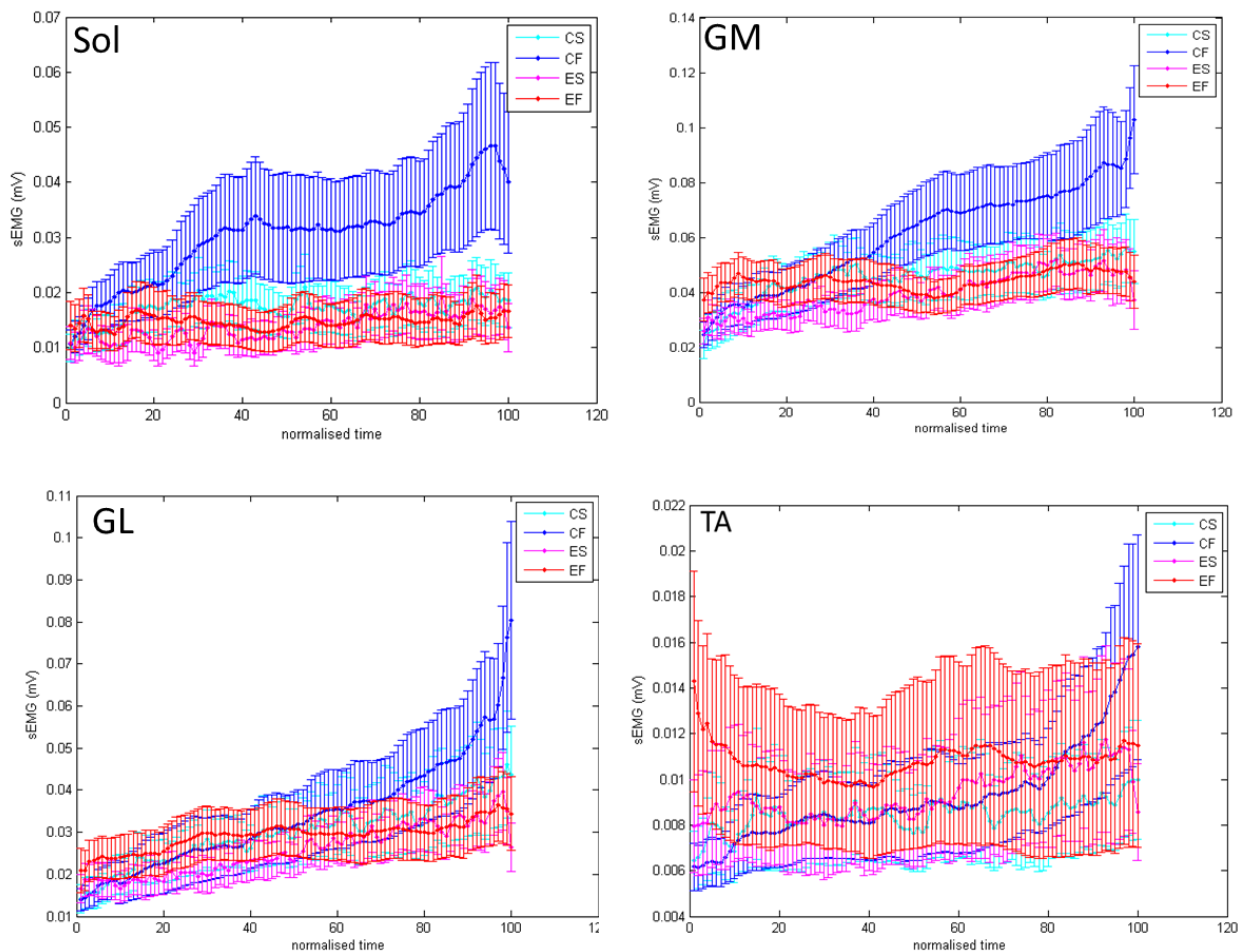


**Figure 5.10:** Mean EMG data for the posterior compartment consisting of the soleus (Sol), medial gastrocnemius (GM) and lateral gastrocnemius (GM) and anterior compartment consisting of tibialis anterior (TA) comparing EL and CL at fast and slow loading speeds. (CS = slow concentric, CF = fast concentric, ES = slow eccentric, EF = fast eccentric).

### 5.3.8 Reliability

#### 5.3.8.1 Intra-tester reliability

A very strong agreement between sequential measurements of three repeat sets of exercises was observed ( $R^2 = 0.87$ ). Speed consistency was also checked between the trials to develop confidence in the results and found not to be different between trials ( $p = 0.67$ ).

#### 5.3.8.2 Inter-tester Reliability

Good correlation ( $R^2 = 0.61$ ) was found between the two testers for two measurements of MTJ displacement, demonstrating the reliability of the technique.

## 5.4 Discussion

This study demonstrates that speed - in the range employed clinically - has no significant effect on the Achilles tendon force, length, stiffness, stress or strain. By contrast, a significant effect of speed was observed on triceps surae muscle activation during CL. Furthermore, the magnitude of perturbations during fast eccentric exercise was significantly higher, as compared to slow eccentric and fast or slow concentric loading.

This study highlighted a similar peak force in the tendon during eccentric and concentric loading at both fast and slow exercise speeds. While *Figure 5.4* suggest that peak forces may be higher during eccentric loading than during concentric loading, the ANOVA shows that this is not significant ( $p = 0.53$ ) and there was no main effect for speed in the ANOVA analysis for force ( $p = 0.056$ ), nor were there any significant interactions. *In vitro* derived force - velocity curves for the muscle (Hill, 1970, Westing et al., 1990) indicated that EL has no speed dependency, while force increased with speed in CL. By contrast, some *in vivo* studies have indicated a force-velocity or torque-velocity relationship during EL also, with an initial increase in muscle force with velocity (Griffin, 1987, Rodgers and Berger, 1974) whilst others show no effect of velocity on either muscle torque (Westing et al., 1988,

Kues et al., 1994) or behaviour of the muscle fascicle (Reeves and Narici, 2003), however tendon force - velocity relationship of the lower calf during eccentric and concentric loading using a dynamometer has been reported in two separate studies showing that tendon force increases with speed during CL (Wakahara et al., 2007) but speed has no effect on tendon force during EL (Wakahara et al., 2009). The results from the present study show that tendon force is not velocity specific during either dynamic eccentric or concentric loading. The current data may differ from previous studies as a result of differences in protocols. In particular, previous *in vivo* studies have all examined force - velocity relationships during maximum voluntary contraction using isokinetic devices, not under clinical EL and CL conditions. It is possible that employing a wider range of speeds, as employed in previous isometric/isokinetic studies (0.5 - 4  $\text{rads}^{-1}$ ), would have shown effects. However, the speeds used in this study (0.2 - 1  $\text{rads}^{-1}$ ), are comparable to what can realistically be achieved, and has been reportedly employed, in the clinical setting.

With no velocity related changes in tendon force or extension, tendon stiffness is also unsurprisingly seen to be independent of exercise speed. Therefore, in agreement with the hypothesis of the present study, tendon mechanical properties are not affected by exercise speed during either eccentric or concentric loading in normal healthy tendons, suggesting that force differences are not responsible for the superior efficacy of EL in tendinopathy management.

One of the aims of this study was to observe calf muscle activity during the two loading protocols at different speeds. The relatively low EMG activity seen during eccentric action reproduced the findings reported in chapter 4 (*Figure 5.10*). The current data additionally highlights that muscle activation levels during CL are significantly increased by speed for the soleus, medial gastrocnemius and lateral gastrocnemius, whereas for EL, no effect of speed on EMG was observed for any of the muscles. These results are largely in accordance with a very early study, in which EMG activity was shown to increase with an increase in angular velocity for CL (Bigland and Lippold, 1954), and the

results of an *in vivo* study carried out during eccentric plantarflexion loading using a dynamometer, in which no significant effect of speed was observed for the three triceps surae muscles or the tibialis anterior (Wakahara et al., 2009). Reeves and Narici also reported no effect of speed on the tibialis anterior during isokinetic eccentric and concentric contractions (Reeves and Narici, 2003). Indeed, previous studies have highlighted that speed related effects on EMG are muscle specific (Cramer et al., 2004). However, of particular relevance to the current study, speed has been shown to have a significant effect on EMG activity in the three main muscles of triceps surae, but not the antagonistic tibialis anterior muscle.

This study investigated if EL and CL resulted in different force fluctuations and to what extent these were influenced by exercise speed. There were clear differences between the two loading modes, with an increased power frequency spectrum for EL, particularly in the frequency range of 8 - 12 Hz. Further, the data demonstrates that speed does have a significant effect on the magnitude and frequency range of tendon perturbations, with higher perturbation frequencies consistently occurring at faster loading speeds (*Figure 5.8*). It is well established that muscles are activated to control the frequency and damping of these perturbations by means of a process known as *muscle tuning* (Wakeling et al., 2001, Nigg, 1997) and that the body responds to the impact forces during, for example, heel strike and running by muscle activation to reduce these perturbations (Friesenbichler et al., 2011, Wakeling et al., 2002a, Wakeling et al., 2002b). This might suggest the perturbations are generated by the EL exercise and that the efficiency of the muscle in shielding the triceps surae from vibrations is reduced with increasing muscle contraction speed. This may be a result of muscle damping mechanisms becoming less effective at higher speeds or these may simply be reduced damping.

Considering specifically the 8 - 12 Hz range, relevant to physiological tremors, the combination of speed and loading type revealed that the highest perturbations were associated with fast EL and the

lowest with slow CL. It must be noted that these perturbations were present at 8 - 12 Hz in the present study and at 10 Hz in the previous study (Chapter 4 (section 4.3.6)). In addition, not every subject shows these perturbations. Such findings emphasise that either the range of frequencies is speed specific or this mechanical parameter is subject dependent. Results so far (chapters 4 and 5) indicate that tendon perturbations are speed as well as subject specific. Indeed, specific studies need to be run in order to explore this phenomenon.

It is also well known that EL is characterized by lower motoneuron activation than CL hence the reduced sEMG signal overall. However, previous studies have indicated that there is selective activation of high – threshold motor units occurring during EL without the phased tuning between variably sized motor units (Moritani et al., 1987, Nardone et al., 1989), which may be responsible for generating the observed force perturbations during EL. With minimal impact during EL to generate perturbations, it seems likely the muscle may be the source of vibrations - although alternative mechanisms need to be explored such as possible inter-segmental oscillation and agonist-antagonist interactions.

Care was taken to give subjects proper training, with speed guided by the metronome, to enable them to carry out the exercises at a consistent pace. However, using a metronome to control exercise speed relied on all subjects reacting to the beat in the same way as each other, as well as each subject reacting the same way each time they performed an exercise. The metronome only signalled specific points within the eccentric or concentric movement, and did not guarantee consistent motion throughout the movement. However, every effort was made to ensure speed consistency by providing training and performing trial exercises before the actual test was carried out. In addition, any faulty acquisitions, defined as trials in which the subjects lost balance or varied from the set pace by more than 10 % off target, were discarded.



It should also be noted that this study was a 'snapshot' study and we have not measured the effect of multiple repetitions of exercise or training on tendon force, stiffness or perturbations. It has previously been shown that vibration intensity increases as muscles fatigue during prolonged running (Friesenbichler et al., 2011). As such, there is a need to explore the effects of fatigue during a typical EL protocol (one day), to determine how this may influence the frequency and amplitude of tendon perturbations.

## **5.5 Conclusions**

In conclusion, it has been shown that tendon stiffness, stress, and strain during EL and CL are independent of the speed of exercise as clinically employed. However, tendon perturbations varied with both the type and speed of loading, showing the highest perturbations in a range of 8 - 12 Hz during EL performed at a fast speed.

**Chapter 6: The biomechanical effects of varying applied load and  
exercise dose during eccentric and concentric triceps surae  
exercises**

## **6.1 Introduction**

A typical clinical EL rehabilitation approach for Achilles tendinopathy lasts for at least 12 weeks during which the amount of added load varies from study to study. Some studies have used a 5kg incremental load from the 4<sup>th</sup> week (Rompe et al., 2009, Rompe et al., 2007, Gardin et al., 2010, Sayana and Maffulli, 2007) while others have incorporated as much load as the patient could tolerate as soon as they felt able (Alfredson et al., 1998, Mafi et al., 2001). It is notable that the selection of load dose tends to be based on clinical experience, rather than derived from any evidence based study. This may be appropriate, however the differential effects of loading need to be better understood in order that therapists can understand the effects of their clinical decisions.

It is necessary to devise and understand the loading condition during rehabilitation protocols in order to better understand the biomechanics behind tendon healing. Varying exercise load has been shown to alter the forces perceived by tendon which in turn affects mechanical properties (Wang et al., 2011). It has been shown that tendon stiffness and modulus increase in a curvilinear manner with increased force (Maganaris and Paul, 2002). However the biomechanical effects of additional load during EL, as it is typically applied clinically, have not been reported.

The purpose of this study was to measure load - dependent differences in the biomechanical characteristics of the triceps surae during typical EL and CL exercises, to better understand the differential effects of EL and CL on tendon biomechanics. Furthermore, chapter 5 highlighted that exercise speed affected tendon perturbations so the effects of additional load on perturbations were also examined, including an analysis of how load interacts with exercise speed. In addition, the difference between the biomechanics of CL and EL were also compared between the start and end of a bout of EL or CL was investigated, to determine whether ATF, EMG or tendon perturbations were influenced by fatigue.

### **6.1.1 Hypotheses**

Alternative hypotheses for this study were that:

- Muscle activation, tendon force, stiffness and strain would all be greater when the triceps surae was subjected to higher loads.
- Tendon perturbations would be larger in magnitude under eccentric conditions, particularly at higher speed and loads.
- Variable dose of exercise would result in altered mechanics in the fatigue state; specifically, the ATF will increase the triceps surae muscles will show more activity, and tendon perturbations will increase in magnitude and frequency.

## **6.2 Methods**

### **6.2.1 Subjects**

Seven healthy volunteers (4 male and 3 female) were recruited with mean age 27.8 years (SD = 2.9), mean body mass 68.4 kg (SD = 5.1) and mean height 1.74 m (SD = 0.05). The study was approved by the Queen Mary, University of London Ethics committee and all participants gave written informed consent. Inclusion criteria included regular, moderate exercise (defined as 2 - 3 hours of exercise per week maximum over the last year), age between 18 and 40 years, no current or previous Achilles tendon pain, pathology or surgery, and no history of systemic disease.

### **6.2.2 Exercise protocol- Effect of load**

Subjects were asked to complete the eccentric and concentric loading exercises (as explained in chapter 4) with and without load on their back in a rucksack. The test group with the additional load were described as heavy eccentric or concentric loading (HEL or HCL). Tests were performed at medium (3 s,  $\sim 0.5 \text{ rad}\cdot\text{s}^{-1}$ ) speed. Three sets of data were recorded for each loading paradigm for

each subject, in a randomized order. Up to five familiarization exercises were completed before the actual tests started and a metronome used to guide loading speed during the tests. There was a 3 - 5 min rest allowed between each set of exercises. Data was analysed for tendon force-extension behaviour.

### **6.2.3 Exercise protocol- Effect of load and speed**

Subjects were asked to complete the eccentric and concentric loading exercises (as explained in chapter 4) with and without load on their back in a rucksack. The test group with the additional load were described as heavy eccentric or concentric loading (HEL or HCL). Tests were performed at 3 different speeds, defined as slow (6 s,  $\sim 0.2 \text{ rad}\cdot\text{s}^{-1}$ ), medium (3 s,  $\sim 0.5 \text{ rad}\cdot\text{s}^{-1}$ ) and fast (1 s,  $\sim 1 \text{ rad}\cdot\text{s}^{-1}$ ). Three sets of data were recorded for each loading paradigm for each subject, in a randomized order. Up to five familiarization exercises were completed before the actual tests started and a metronome used to guide loading speed during the tests. There was a 3 - 5 min rest allowed between each set of exercises. All 12 possible exercise orders were written on separate pieces of paper and the order of loading was chosen by the subject at random, drawing a piece of paper from a box. With previous data sets indicating that no differences could be expected in tendon force-extension behaviour, all data was analysed simply for tendon perturbations.

### **6.2.4 Exercise protocol - Effect of varying dose**

Of the seven participants in the current study, three were also asked to perform 11 continuous repetitions of EL or CL with and without additional load at the fast exercise speed. During these repetitions, EMG, ATF and tendon perturbations were measured to observe changes with fatigue. ATL was not investigated, as the accurate collection and appropriate analysis of US images over the time period could not be guaranteed.

### **6.2.5 Data collection**

Measurements of tendon mechanical properties, EMG and GrF perturbations were taken as outlined in chapter 3 (section 3.3). The methods for measuring ATF, tendon perturbations and EMG activity during the longer bouts of EL and CL were identical to those previously described.

### **6.2.6 Data analysis**

Data analysis was carried out with Matlab scripts (Version 7.9.0.529 (R2009b), 32-bit). Data was analysed as detailed before (Chapter 3, section 3.3).

### **6.2.7 Statistical analysis**

Normality tests were performed on the data using the Shapiro-Wilk method (OriginPro, version 8, OriginLab, USA). Having established a normal distribution, a three way ANOVA was performed inputting subjects (to enable a paired contraction), contraction type, and load as factors, then with force, EMG and stiffness as the dependent variables. Interactions between the main effects were included. An ANOVA was also performed inputting subjects, contraction type, load and frequency as factors, with summed power from individual tests as the dependent variable. Frequency was analysed for the average power in intervals of 1Hz width between 0 and 15 Hz. Statistical significance was accepted at  $p \leq 0.05$ . Tukey's post hoc test (Origin software, OriginPro8) was used to determine which groups were significantly different.

## 6.3 Results

### 6.3.1 Effect of load

#### 6.3.1.1 Achilles tendon force

No significant differences in the range of motion were observed between any of the loading conditions ( $p > 0.05$ ). This finding, alongside the careful control of speed during exercise, enables comparison of heavy and normal EL and CL without potential confounding factors. ATF was observed to increase with additional load under both EL and CL conditions ( $F = 4.36$ ,  $p = 0.02$ ). However, a direct comparison of HEL and HCL showed no significant differences between the loads produced during EL and CL. The mean normalised force for all subjects is shown in Figure 6.1.

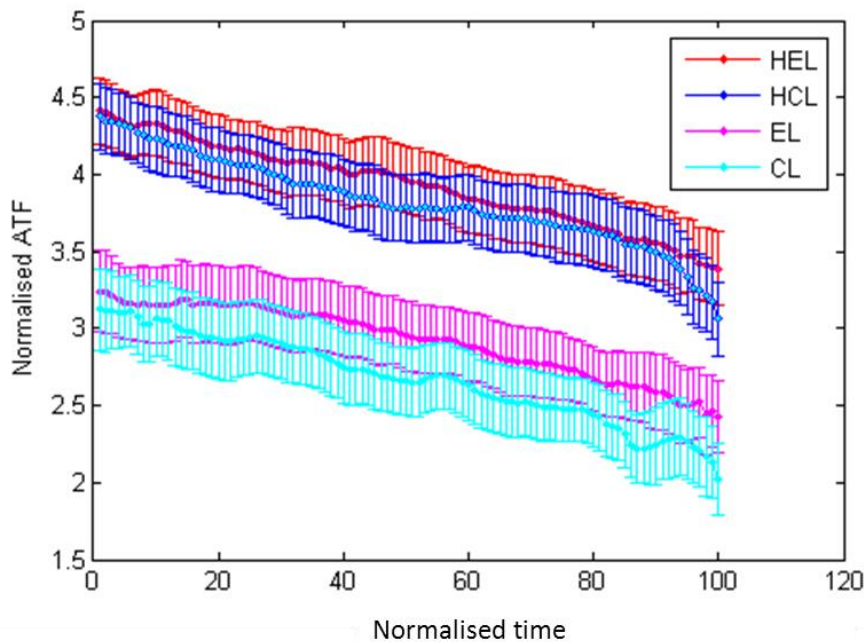


**Figure 6.1:** A comparison of the normalised mean AT force (ATF) ( $\pm$  SE) during EL and CL at the two loads at medium speed (The test group with the additional load were described as heavy eccentric or concentric loading (HEL or HCL)).

On average, the Achilles tendon length changed by  $12.42 \pm 1.03$  mm during EL,  $12.58 \pm 1.60$  mm during CL,  $15.07 \pm 1.87$  mm during HEL,  $14.01 \pm 1.01$  mm during HCL. *Figure 6.2* compares example force - length graphs for the tendon under each loading condition. Change in tendon length was not significantly different between EL and CL under either body weight or heavy weight conditions, but the tendon stiffness was found to be significantly higher under heavy load conditions in both EL and CL ( $F = 6.70, p = 0.003$ ) (*Table 6.1*).

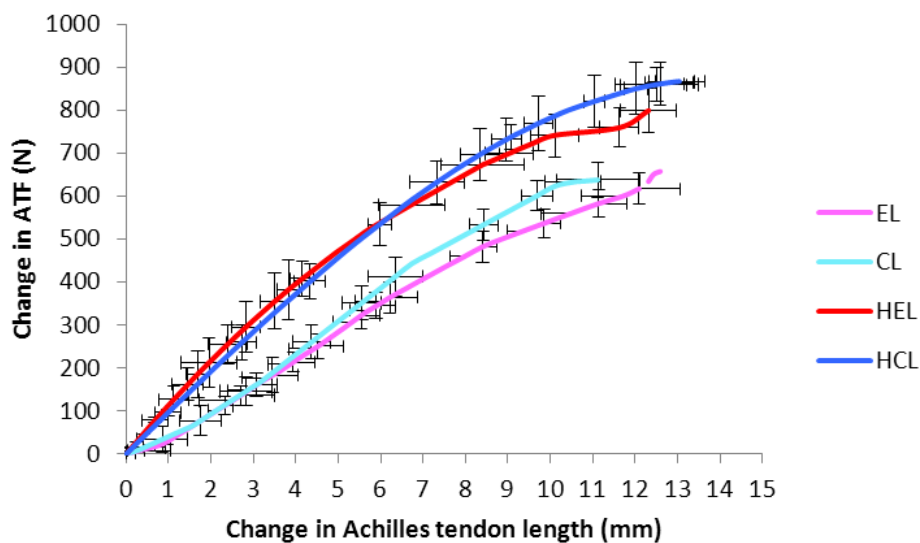


**Figure 6.2:** Typical graph showing mean change in AT force (ATF) against change in AT length (ATL) for repeats by a single subject, during EL and CL with and without load ( $\pm$  SD) (The test group with the additional load were described as heavy eccentric or concentric loading (HEL or HCL)).

The increase in ATF led to a significant increase in tendon stiffness during HEL and HCL. However, the small increase in ATL with load was not significant during EL and CL, so no significant differences in strain between EL and CL at either load were reported ( $F = 0.75, p = 0.53$ ).

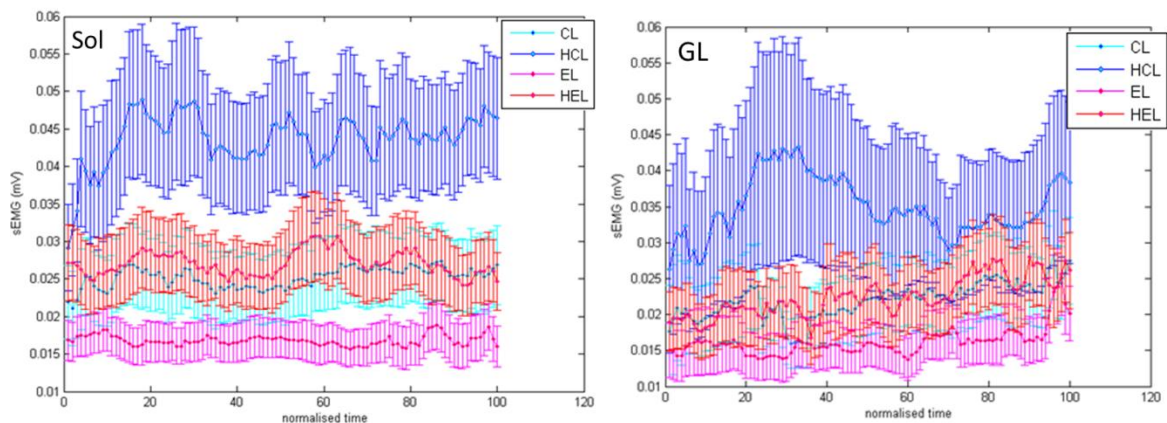


**Table 6.1:** Summary of the results comparing eccentric and concentric loading at two loads.

		Achilles tendon peak force (N)	Achilles Tendon length change (mm)	AT Stiffness (Nmm <sup>-1</sup> )	AT Stress (MPa)	AT Strain (%)
<b>Concentric loading</b> (Mean ± SE)	CL	2188 ± 190	12.58 ± 1.60	54.95 ± 5.67	33.78 ± 2.92	6.11 ± 0.76
	HCL	3120 ± 210	14.01 ± 1.01	79.19 ± 3.11	47.89 ± 3.23	6.70 ± 0.50
<b>Eccentric loading</b> (Mean ± SE)	EL	2163 ± 204	12.42 ± 1.03	57.06 ± 6.13	33.21 ± 3.14	6.03 ± 0.50
	HEL	3188 ± 224	15.07 ± 1.87	85.89 ± 3.55	48.93 ± 3.43	7.32 ± 0.91

### 6.3.1.2 Muscle activation

The addition of load resulted in greater EMG activation levels than bodyweight alone during both EL and CL in the soleus ( $F = 3218.52$ ,  $p < 0.01$ ), medial gastrocnemius ( $F = 551.30$ ,  $p = 0.01$ ) and lateral gastrocnemius ( $F = 572.86$ ,  $p < 0.01$ ) (*Figure 6.3*), but not in the tibialis anterior. However, the relationship between EL and CL, first reported in chapter 4, was maintained, and muscle activation was consistently lower during EL than CL even with the addition of load ( $p < 0.01$ ). Indeed, the contrast between EL and CL with load was significantly greater than that seen under body weight conditions alone in each of the triceps surae muscles.



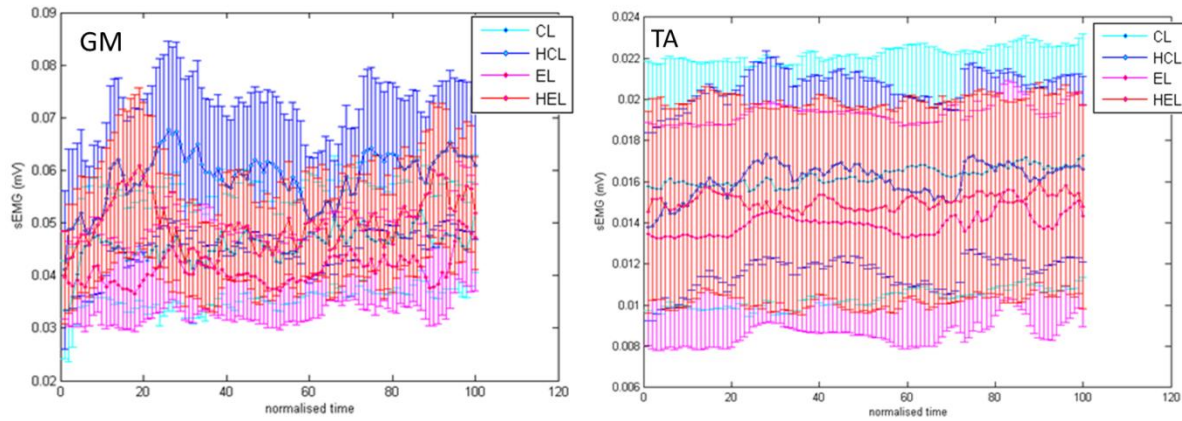


**Figure 6.3:** Mean EMG ( $\pm$  SE) data from the Soleus (Sol), lateral gastrocnemius (GL), medial gastrocnemius (GM) and tibialis anterior (TA) during eccentric and concentric loading, with and without additional load. The test groups with the additional load were described as heavy eccentric or concentric loading (HEL or HCL).

### 6.3.2 Effect of speed and load

While perturbations varied between subjects, a significant difference in the force fluctuation spectrum between EL and CL was consistently seen (Figure 6.4). As reported in previous chapters, the largest power outputs were seen at frequencies below 5 Hz, with the peak occurring around at 2 - 3 Hz during EL and CL under both heavy load and body weight conditions, with no significant differences between groups. However, whilst the magnitude of perturbations was smaller at higher frequencies, significant differences were observed between the spectra around 10 Hz, while a higher magnitude of perturbations was evident in EL compared to CL at both a medium ( $F = 95.85$ ,  $p < 0.01$ ) and fast ( $F = 31.78$ ,  $p < 0.01$ ) exercise speeds. Data confirmed that, as described in chapter 5, faster exercise speeds particularly increased tendon perturbations and this occurred with and without additional load ( $F = 31.78$ ,  $p < 0.01$ ). However, the current data set additionally enables an assessment of how load interacts with speed. Data showed that the addition of load did not influence perturbation spectra at slow ( $F = 0.04$ ,  $p = 0.89$ ) or medium ( $F = 0.4$ ,  $p = 0.53$ ) exercise speeds for either EL or CL, but at the fast speed it led to a significant increase in the magnitude of

the 10 - 12 Hz frequency component during EL ( $F = 4.87$ ,  $p = 0.035$ ). Figure 6.4 shows this effect at the three speeds of loading.

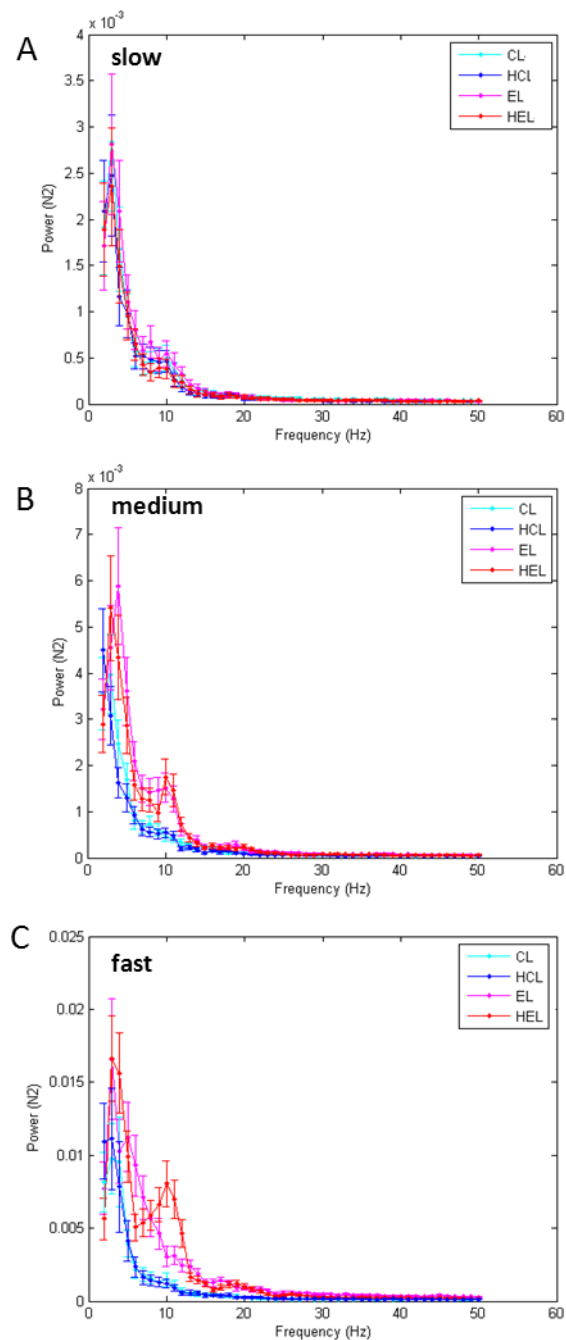


**Figure 6.4:** Mean ( $\pm$  SE) power of the ground reaction force summed over 1Hz windows, comparing eccentric and concentric loading at heavy load and body weight during (A) slow, (B) medium and (C) fast speeds exercise. The test groups with the additional load are described as heavy eccentric or concentric loading (HEL or HCL). Note the increasing scale of the y axes, as the magnitude of perturbations increases with exercise speed.

### 6.3.3 Effect of dose

The data for a bout of 11 repetitions of EL and CL was analysed for each subject. Firstly, the marker placement throughout the exercise bout was plotted (Figure 6.5), to ensure the accuracy of the range of motion and consistency within the repeats. Evidence of repeatability in movement is shown in Figure 6.5 and Figure 6.6.

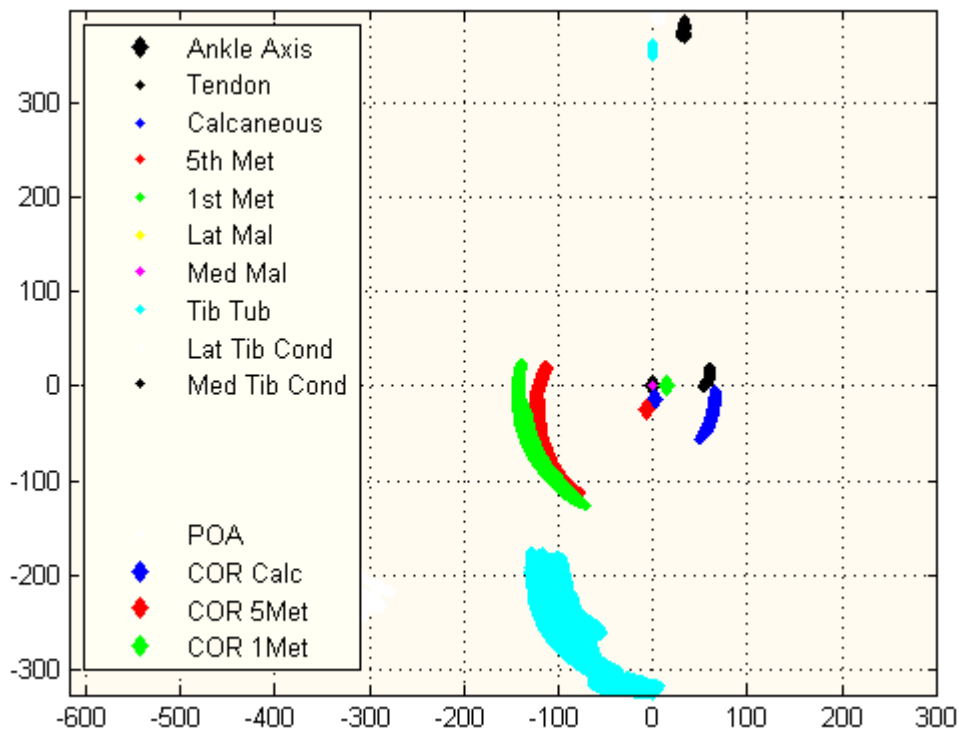


**Figure 6.5:** Representation of all 15 markers used on the lower leg, and the US probe (seen perpendicular to the plane of action) during 11 repeats of CL. The big arcs in red and green indicate the movement (centre of rotation) of the 1<sup>st</sup> and 5<sup>th</sup> metatarsal, with red and green dots at the centre of these circles. Small arcs in black and blue represent motion in the tendon and calcaneum, whereas the big cyan arc is the point of application of force. The black arcs at the top are the movements from the lateral and medial tibia condyle.

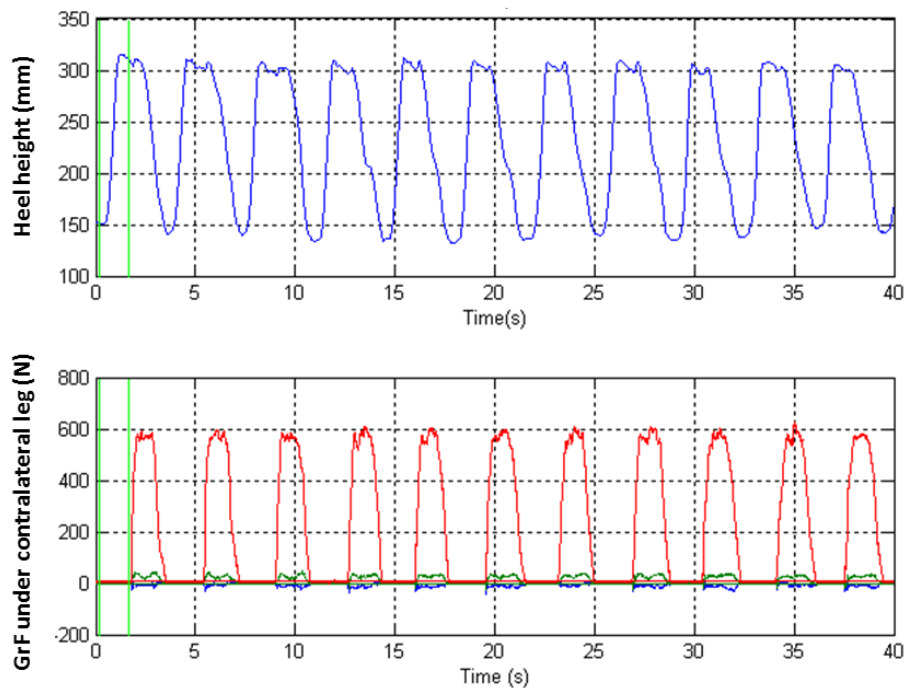


**Figure 6.6:** Description of the consistency in heel height and speed of loading between the 11 repetitions during CL. A plot of the GrF under the contralateral leg (z in red, x in green and y in blue) is also shown to ensure that only the data during one leg support was analysed. The single leg loading data is marked with green lines for first cycle.

### 6.3.3.1 Achilles tendon force

The ATF over 11 repeats of HEL or HCL is plotted in *Figure 6.7*. Force values are comparable with previous data, but it is notable that the force appears to decrease towards the end of the bout. However, no significance was observed for this effect, when comparing the 1<sup>st</sup> and 11<sup>th</sup> cycles ( $p > 0.05$ ). A similar trend was observed for HCL and HEL (*Figure 6.8*).

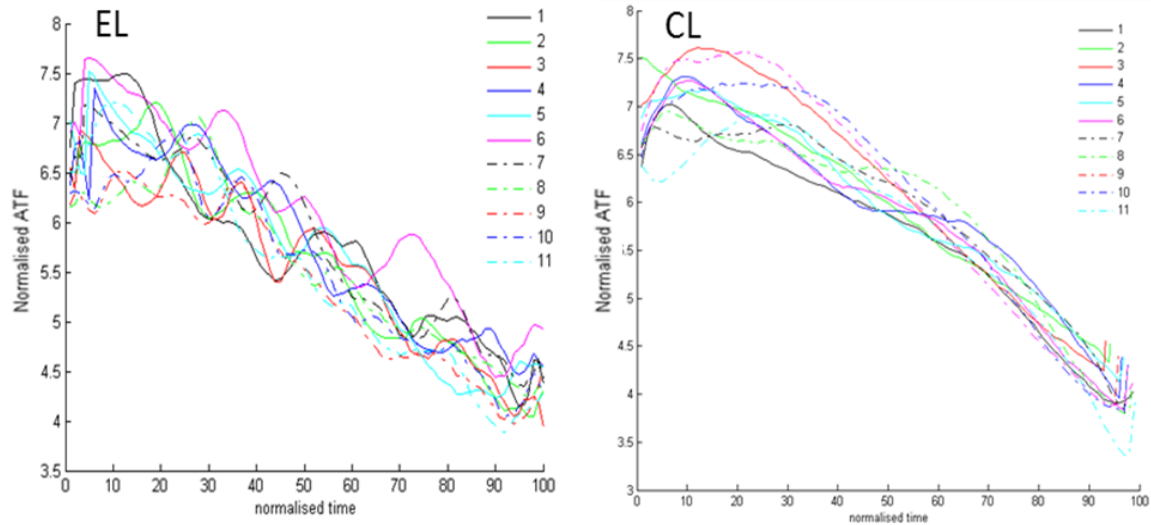


Figure 6.7: An example data set, showing the ATF for each repeat of EL or CL by a single subject.

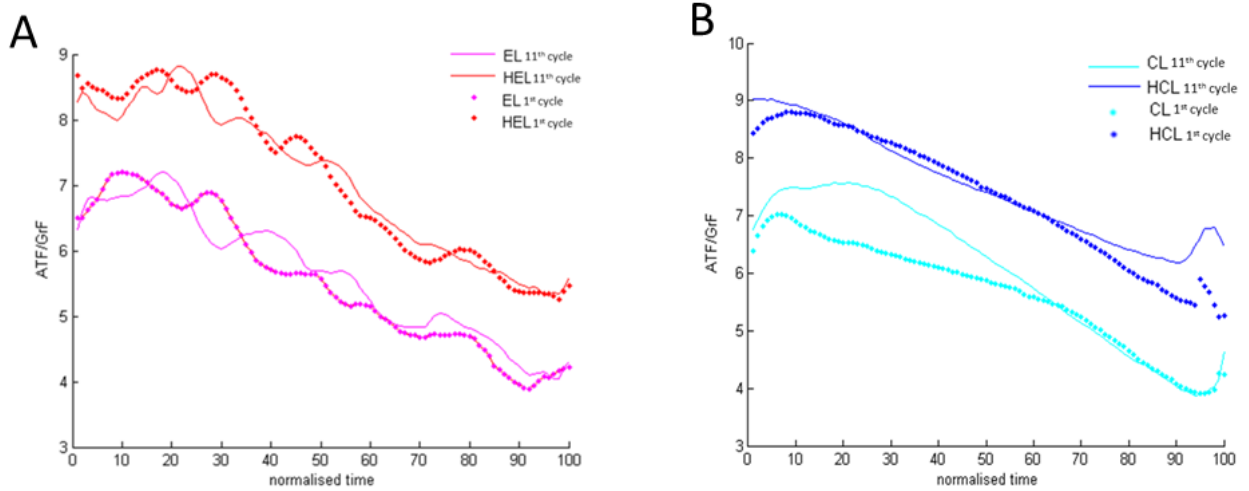
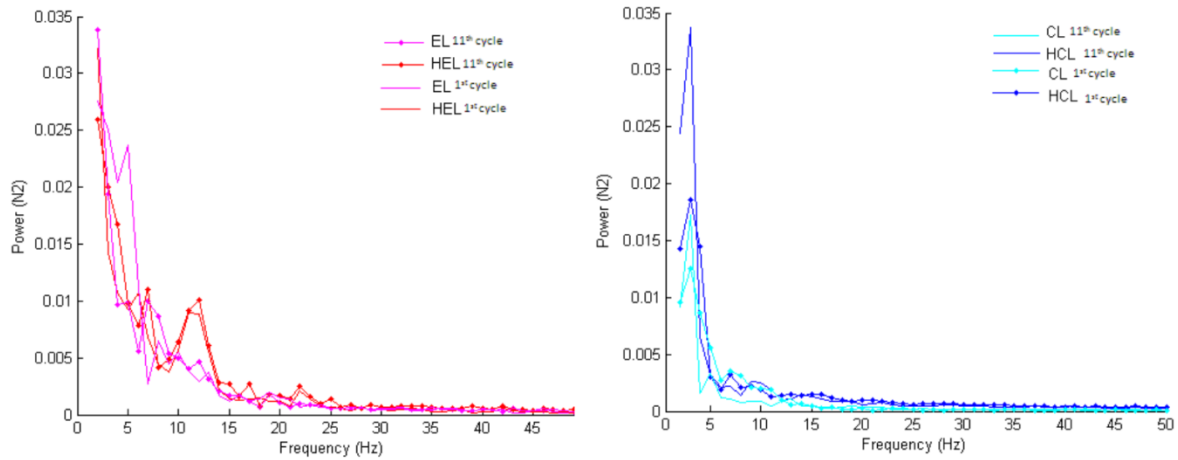


Figure 6.8: Data for the first and last cycle of exercise are isolated to show more clearly the change in ATF over 11 repeats of exercise for (A) EL and HEL and (B) CL and HCL. The test groups with the additional load were described as heavy eccentric or concentric loading (HEL or HCL).

### 6.3.3.2 Force perturbations

Data from a typical subject, comparing tendon perturbations for EL and CL under the two loading conditions are shown in *Figure 6.9*. Similar patterns were seen for EL and CL as reported before. However, a closer observation shows that the numbers of inflexions during HEL are higher than during EL, leading to the greater 10 - 12 Hz perturbations seen in HEL. However, no significant differences in perturbations between the first and eleventh cycle of loading were observed. Perturbations followed the same trend as shown earlier; significantly higher perturbations were observed around 5 - 12 Hz during EL as compared to CL and during HEL as compared to HCL, CL or EL ( $F = 5.02$ ,  $p = 0.02$ ). However, no trend was observed between increasing numbers of repetitions and perturbation amplitude or frequency ( $p > 0.05$ ).



**Figure 6.9:** A typical record of GrF perturbations over the 1<sup>st</sup> and 11<sup>th</sup> cycles of exercise for a subject completing EL and CL with and without additional load. High magnitude perturbations are evident at 10 - 12 Hz during HEL at both cycle 1 and 11.

### **6.3.3.3 Muscle activation**

Muscle activation followed the same patterns as outlined in chapters 4 and 5, with significantly higher EMG output during CL than EL and further elevated muscle activity with additional load. Looking more specifically at the effects of increasing cycle numbers on EMG, the output during the last two cycles of the 11 repetitions tended to be higher. However, no significance differences were observed ( $p > 0.05$ ), perhaps as a result of the smaller number of subjects.

## **6.4 Discussion**

This study has demonstrated that the addition of load during eccentric and concentric triceps surae loading alters many of the resulting biomechanical parameters in the triceps surae. Only a relatively small number of healthy subjects were investigated in this study. However, an initial study in healthy subject is mandatory in order to understand what is normal and abnormal, and such studies provide a platform for future patient studies. While some of the changes seen in triceps surae properties are intuitive and to be expected, other are less obvious. An increase in muscle activation to support the addition of load is a necessary biomechanical response and has previously been reported (McGowan et al., 2006). While increased EMG activity during heavy load exercises is thus to be expected, EMG was also seen to remain significantly higher during CL than EL, irrespective of the amount of load. Greater muscle activation during CL has been reported previously and, as outlined in chapter 4 is probably a result of an incomplete activation of the motorneurons that innervate the muscle (Moritani et al., 1987). However, the increase in EMG activity with load was not a defined amount, but differed for EL and CL.

Also following biomechanical principles, the ATF increased with additional load, in both EL and CL. However, it was also seen that there were no significant differences in ATF between EL and CL at either



high or low loads. These data confirms our early findings that ATF does not vary between EL and CL irrespective of the addition of load. However, the addition of load did result in higher tendon stiffness, highlighting that the AT cannot simply be considered as an elastic spring in series with muscle fibres. One possible reason for the increase in stiffness could be the co-activation of muscles. However, data from the present study do not support that fact, as the increase in muscle activation under load was seen for posterior (triceps surae) muscles but not for the anterior muscle (the tibialis anterior) and the increase was also EL or CL dependent. Nevertheless, as a result of mutli-directional nature of muscle attachments, the posterior muscles alone could stiffen the tendon, via their varied attachment sites. Recent data has shown that the stiffness of the Achilles tendon is shifted as a function of the level of muscle activation, resulting in higher tendon stiffness values in response to higher muscle contraction levels, for a given AT strain (Sugisaki et al., 2011). The increase in stress and not in strain indicates that the modulus of the tendon may also be higher under load. It is not clear which musculo-tendon parameters may have generated this shift, but it has been shown previously that tendon stress and modulus increase in a curvilinear manner relative to measured force using an isokinetic dynamometer (Maganaris and Paul, 2002). In addition, it has recently been reported that the longitudinal stiffness of the aponeurosis increases as a function of its transverse strain (Azizi and Roberts, 2009). As such it is possible that the transverse deformation applied to the aponeurosis or tendon at higher muscle activation levels (during HCL and HEL) may have resulted in this increase in stiffness. However, if such mechanisms exist, further studies and different methods are needed to ascertain this from three-dimensional tendon deformation.

Considering the high frequency tendon perturbations (above 5 Hz) seen during exercise, the perturbation amplitude was higher during EL as compared to CL, both when completing exercises under body weight and with load (**Error! Reference source not found.**). It was noted that the addition of load

has no effect on tendon perturbations during medium and slow speed exercise. However, at the fast exercise speed, a frequency specific elevation in perturbation magnitude was observed when comparing HEL with EL. The particular increase in perturbation amplitude in HEL compared to all other exercises may depend upon a combination of mechanical, geometric and reflex factors (Stiles and Randall, 1967). Stress and fatigue have been hypothesised to increase perturbation amplitude (McAuley and Marsden, 2000), and it is possible that HEL is particularly demanding compared to other exercise types.

The mechanical properties of a tissue will also influence these perturbations (McAuley and Marsden, 2000); However, while the current data shows that tendon is stiffer at higher loads, no difference in perturbations was found. It has been reported previously, during the spontaneous flexion-extension tremor of the elbow, that there is an increase in tremor amplitude with force, but that the amplitude decreases again when the tendon is exposed to very large forces (Joyce and Rack, 1974). It would be of interest to use higher percentages of body weight to see how these tremors may also vary under high load conditions. This emphasises that other factors, like central nervous system 10Hz oscillatory activity, motor unit firing properties, mechanical resonance and reflex loop resonance may be the dominant factor influencing perturbations in these loading conditions.

Most of the clinical studies to date have utilised additional load during exercise, with the specific aim of increasing the tendon force (Alfredson et al., 1998, Fahlstrom et al., 2003). While the increase in tendon force is inevitable in these conditions, at the same time, elevated vibration intensity has been reported in this study, when a fast exercise speed is adopted. If tendon repair is the result of higher forces during exercise, then there is no clear rationale why equally loaded concentric training cannot produce the same effect as an eccentric training regime. However, various studies have reported an increase in

strength and endurance following eccentric training programmes, which are not seen in response to concentric training regimes (Roig et al., 2009).

The present study illustrates that perturbation intensity (calculated as power densities) does not increase with the addition of load at medium or slow speeds, suggesting that an interaction between speed and load is required to increase perturbation magnitude. Exposure to perturbations has been shown to produce a mixed effect, with some studies reporting a decrease in motor unit firing rates and muscle contraction force when exposed to prolonged perturbations (Bongiovanni et al., 1990) while others have shown an increase in muscle strength and bone density (Rubin et al., 2001, Verschueren et al., 2004). However, if such mechanisms exist in tendon, these were beyond the scope of this study.

Interestingly it was observed that tendon force, EMG and tendon perturbations all remained consistent during a bout of 11 repetitions of EL or CL loading for three of the subjects. Data indicates a possible reduction in tendon force, and increase in EMG amplitude (during the last 2-3 repeats), however no significant effects were observed. It can be speculated that 11 reps is not sufficient to fatigue the muscle-tendon unit in such setting, and that changes in the triceps surae response may become more pronounced with further cycles. However, 10 - 15 reps are usually employed in a single set of EL or CL loading, which is thought to be enough to generate some fatigue in the muscle-tendon unit. It has been shown that ten 6-s maximal cycling sprints, separated by 30 s rest, can cause muscular fatigue (Billaut et al., 2006). However, it has been reported that subjects with a higher percentage of fast twitch fibres responded more sensitively to fatigue than those with more slow twitch fibres (Colliander et al., 1988), and it is quite possible the small number of subjects in the current study may be more fatigue resistant. It must be noted that the subjects in the present study were healthy young and relatively more active

than the subjects from previous studies (chapter 4 - 5), and a bout of 11 repetitions of exercise did not produce a significant fatigue. However, it is possible that in patients where the muscle tendon unit is already damaged, fatigue during the repetitive loading may occur in early repetitions. It would be of interest to carry out such investigations in patients. Furthermore, it should be noted that this is a snapshot study and does not examine the effects of carrying out exercises over a 12 week period, as is applied clinically. Such studies would be useful in both normal and pathological subjects, to establish the correlations, over time, between tendon properties and symptomatic change.

## **6.5 Conclusions**

Based on the results from the present study, the dependence of tendon stiffness and perturbations stimuli on the load applied during EL/CL is a significant finding, which can pave the path for more controlled training programmes and *in vitro* experiments to further investigate this phenomena. No effect of fatigue on perturbation frequency or amplitude was observed with increasing the numbers of repetition in an exercise bout.

**Chapter 7: Low density high surface area electromyography of the calf during eccentric and concentric loading**

## 7.1 Introduction

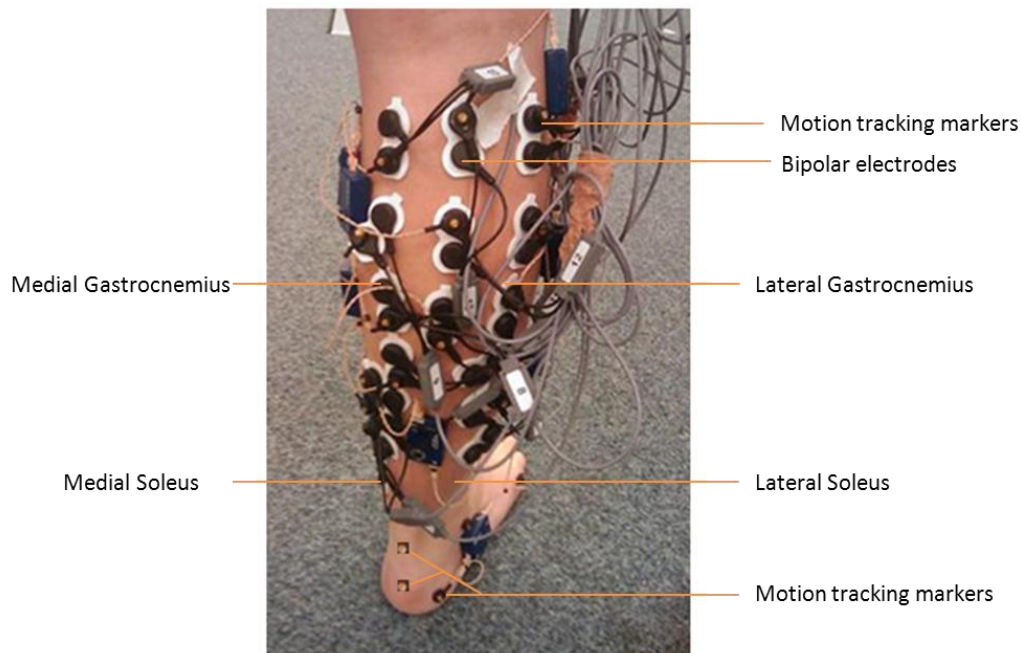


**Figure 7.1:** EMG electrode and motion marker arrangement, set up on the lower leg. Motion markers are attached to each of 16 pairs of sEMG electrodes to enable tracking of position as well as muscle activation. In addition the usual lower limb maker protocol is applied.

The magnitude of muscle activity observed in the triceps surae was consistently lower during EL than CL when measured with conventional single channel per muscle surface electromyography. Furthermore, the perturbations measured using GrF were consistently of greater magnitude in the 10 - 12 Hz range during EL. Chapters 4-6 concluded that the GrF perturbations probably originated from the muscle, on the basis of a process of exclusion. To establish from where within the muscle they may originate, it was judged important to characterise muscle activity levels and pattern across the entire surface of the triceps surae during EL and CL exercise (*Figure 7.1*). From this, it was hoped that one could then investigate the anatomical origin of the 10 - 12 Hz perturbations observed during EL, to establish if these perturbations were region specific in the muscle. The technical limitations of conventional high density,

low surface area, multiple channel or intramuscular methods were not suitable to investigate this question and other methods were needed.

MRI has been used to study muscle activation across the entire triceps surae. In a recent study, transverse relaxation time T2 - weighted spin echo images were acquired with MRI before and immediately after five sets of 10 repetitions of a single calf raise exercise (Kinugasa et al., 2005). It was reported that 46 % of the medial gastrocnemius muscle (GM), 35 % of the lateral gastrocnemius (GL) and 35 % of the soleus muscle (Sol) were activated, suggesting that the distribution of muscle activation levels varies among the triceps surae muscles. The study utilized a technique that relies on an exercise induced increase in the proton transverse spin-spin relaxation time (T2) in magnetic resonance images of muscle (Kinugasa et al., 2005). More recently, using a similar technique to investigate submaximal muscle contraction intensity, it has been shown that an increase in contraction intensity does not always correlate with an increase in muscle activation (Kinugasa et al., 2011). However, it is known that resting T2 values are affected by the magnetic field and scan parameters, as well as varying with muscle fibre type, and this technique cannot be used during exercise to investigate dynamic muscle behaviour.

Another technique to study local muscular activation patterns is fine wire EMG (needle or wire electrodes) in which electrodes are inserted into particular muscle fibres to investigate their behaviour, at resolutions down to single muscle fibre (Westgaard and de Luca, 1999). However, such techniques are not commonly employed because of the invasive nature of the technique, and the lack of suitability for studying movement. Surface EMG is more popular, but can only give the muscular activation pattern from the area under the electrode. To overcome this limitation, high density surface EMG recording has been developed, which can provide detailed activation patterns between distinct parts of a muscle

(Holtermann et al., 2005). However, such a technique is useful to study the motor unit behaviour and can only acquire data from a very small area of muscle and is typically employed during small isometric muscle activities.

Multi-channel surface EMG involves covering a large portion of the muscle with surface electrodes, allowing activity across the whole muscle to be examined in a spatial manner. Many studies have utilized this technique to provide an insight into the heterogeneity of muscle activation (Scholle et al., 2001, Chanaud et al., 1987). Changes in EMG amplitude, measured using multi-channel EMG, have revealed that during the course of an isometric contraction, the active parts of the muscle vary (Grassme et al., 2003, Kleine et al., 2000, Scholle et al., 1992). This heterogeneity can be due to the fact that muscle fibre types are not randomly distributed through a muscle, but are organised into regions, depending on the different muscle fibre composition (Chanaud et al., 1991). In a recent study, cluster analysis of multichannel EMG signals has shown substantial heterogeneity in triceps surae activation during isometric and isotonic plantarflexion (Staudenmann et al., 2009). However, to date, there has been no measurement of regional activation during clinically relevant EL and CL exercise protocols.

The technique used in the present study was similar to the multi-channel surface EMG technique described above, but utilised 16 channels of EMG spread over the entire surface in contrast to the typical 64 channels in an area of 8 - 10 cm<sup>2</sup> in high density multi-channel EMG. The technique termed LDHA (low density high area) was adopted, as the focus of the current study was to investigate muscle activity over specific regions of triceps surae during dynamic movements (*Figure 7.2*), making the less dense LDHA method most appropriate. Region specific variations can be obtained in this manner and has recently been used in few studies showing that surface EMG mapping of the quadriceps and showed



site-dependent delay onset muscle soreness after EL (Hedayatpour et al., 2008, Hedayatpour et al., 2010).

The triceps surae consists of three distinct muscles, the bi-articular medial and lateral gastrocnemius medial, and the mono-articular soleus muscle as detailed in chapter 1. Within these muscles, distinct compartments have also been identified (Wolf and Kim, 1997, Loh et al., 2003, Segal et al., 1991). Results from chapters 4-6 indicate that the perturbations in GrF and ATF could be the result of muscle tremor. The aims of this chapter were to investigate which parts of the triceps surae are particularly active during EL and CL and whether there were corresponding activation patterns across the triceps surae during EL and CL. As a secondary aim, this chapter focused on characterising the spatial origin of the 10 - 12 Hz perturbations.

### **7.1.1 Hypotheses**

Alternative hypotheses for this study were that:

- Distinct pattern of muscle activation will be observed during EL and CL, with higher activity from soleus and medial gastrocnemius.
- Tendon perturbation will be of muscular origin, mainly originating from the gastrocnemius muscle.

## **7.2 Methods**

### **7.2.1 Subjects**

Nine healthy subjects (5 males and 4 females, age =  $24 \pm 3.84$  yrs, mass =  $77 \pm 14.16$  kg, height =  $1.76 \pm 0.05$  m) participated in the study. They were recruited from the student cohort at Barts and The London

School of Medicine and Dentistry. General demographic data for each subject are in *Table 7.1*, along with information concerning the order in which the subjects performed the EL and CL exercises. The study was ethically approved by the Queen Mary Research and Ethics Committee. All the participants were young healthy individuals. Inclusion criteria included; age between 18 and 40 years, subject engaged in regular moderate exercise (but no more than 2 - 3 hours of exercise per week over the last year), no current or previous Achilles tendon pain, pathology or surgery and no history of systemic disease. They had no muscular disorders or disease and no chronic illness such as diabetes.

**Table 7.1:** Demographic data for each participant and detail of the order in which they completed the testing exercises

No.	Age (years)	Gender (M/F)	Mass (kg)	Height (m)	BMI	Order
1	23	M	74.6	1.75	24.4	CL\EL
2	24	F	60	1.78	18.9	EL\CL
3	24	F	65	1.74	21.5	CL\EL
4	25	M	92	1.82	27.8	EL\CL
5	22	M	80	1.8	24.7	CL\EL
6	23	F	62	1.63	23.3	CL\EL
7	19	F	74.5	1.78	23.5	EL\CL
8	23	M	78	1.78	24.6	CL\EL
9	34	M	107	1.75	34.9	CL\EL

*EL = eccentric loading, CL = concentric loading*

### 7.2.2 Exercise protocol

Subjects performed EL or CL as detailed in chapter 3, the order of which was randomised (*Table 7.1*). For each exercise, the subject performed 3 exercise cycles on their right leg. Each cycle was completed in  $3 \pm 0.2$ s ( $\sim 0.5 \text{ rad}\cdot\text{s}^{-1}$ ). Three separate acquisitions were acquired.

### **7.2.3 Data collection**

Standard surface anatomy was used as a reference for electrode placement on the calf (Lumley, 2008). Before placing the EMG electrodes, the skin was prepared according to standard surface EMG techniques as detailed in chapter 3 (3.2.1). For mapping the calf muscle, 32 (16 pairs of) disposable, self-adhesive Kendall ARBO 24 mm EMG electrodes were used on the right leg only. The three compartments of the triceps surae muscle, the medial gastrocnemius, lateral gastrocnemius and soleus were further divided into proximal, middle and distal sub regions in order to facilitate the electrode placement (*Figure 7.2*). The calf muscle was surface marked using an ink marker to identify the required location for the electrode placement.

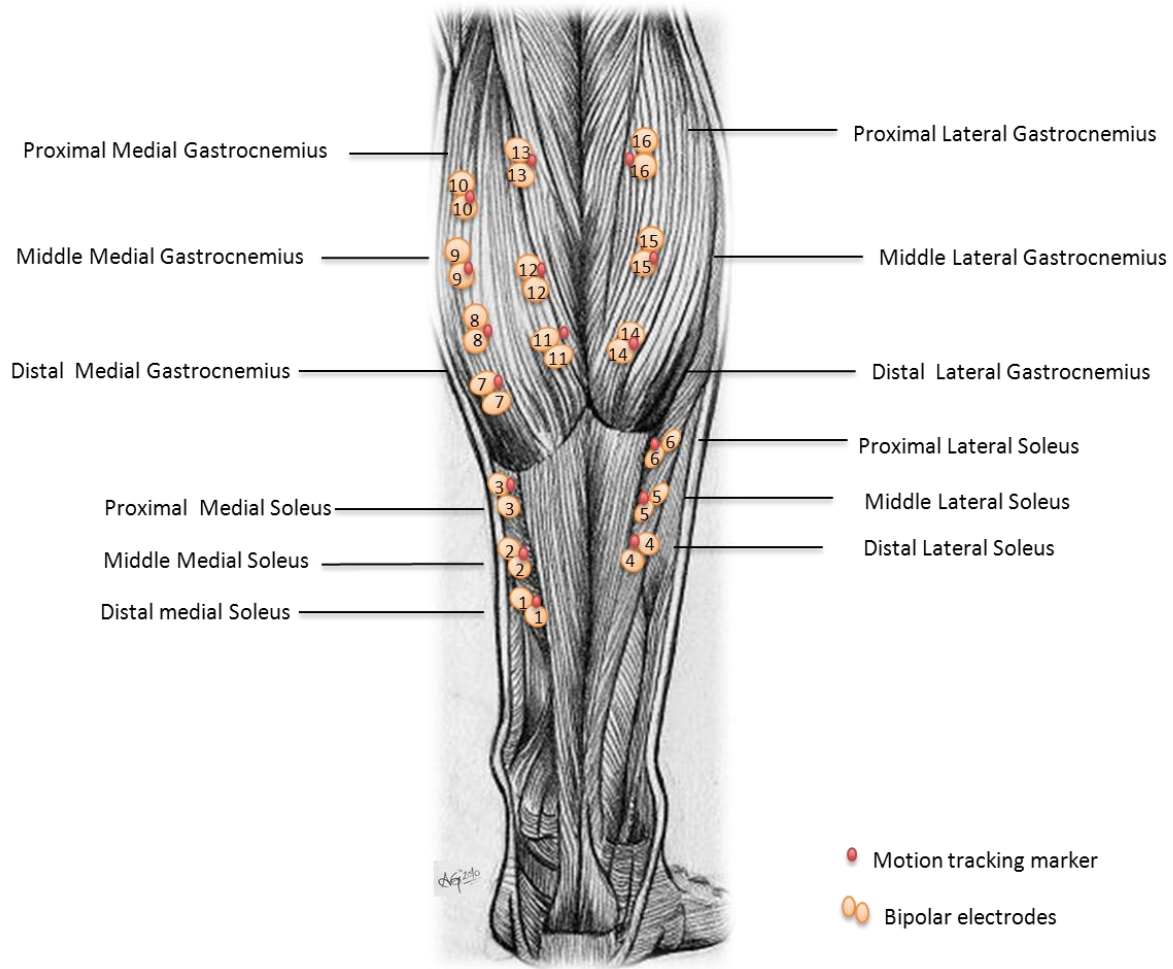


**Figure 7.2:** Schematic drawing of the calf muscle showing the positioning and orientation of the 16 channel dual EMG set up. A motion tracking marker was placed on each electrode pair to track the position in space.

EMG data was recorded in synchrony with motion analysis data, to characterise muscle activation with movement as detailed in chapter 3 (section 3.2.3). In addition to the CODA marker on each pair of electrodes, markers were also placed on the bony landmarks of the lower leg, as demonstrated in chapter 3 (section 3.2.3.2). The step for completing EL and CL exercises was mounted on the force plates sampling at 1000 Hz, all following the previously outlined methods (chapter 3).

### 7.2.4 Data analysis

Data analysis utilised colour maps of EMG activity levels across the triceps surae, to compare spatial muscle activity during the two exercises. *Figure 7.3* shows raw EMG in blue and rectified EMG in red for all sixteen channels of data for three CL cycles. The burst of activation can be seen for three consecutive cycles.

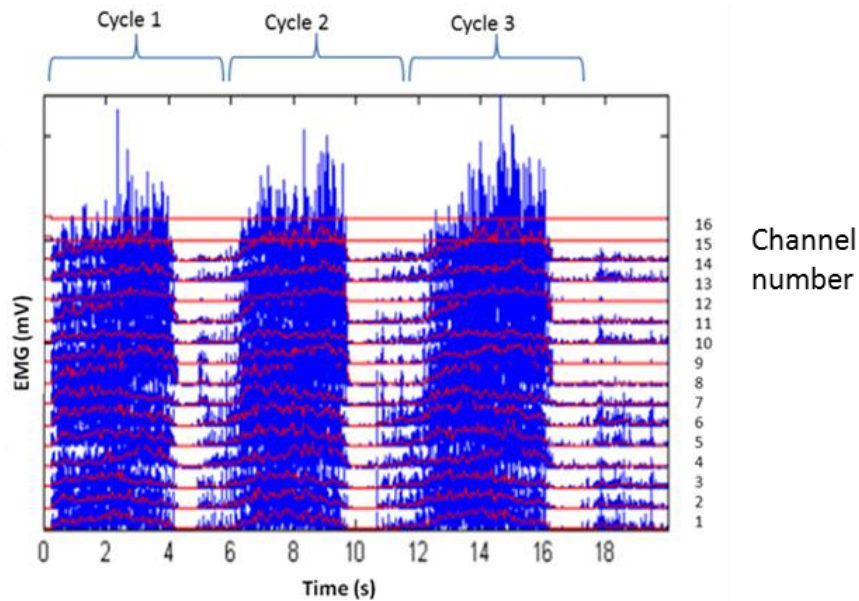


**Figure 7.3:** The raw EMG signal (blue), alongside the rectified and smoothed data (red) from all 16 channels across the triceps surae during three cycles of CL.

To generate colour maps of the muscle activity, the raw EMG signal from each channel was rectified by full wave rectification and converted to logarithmic values. Around the edges of the test area, EMG was assumed to be zero, and EMG data interpolated between each analysis point using Matlab. A colour scale was used to present EMG activity levels pictorially, value ranging from 0 - 1 (low - high), normalised for any individual to be 1 at the highest activity presented throughout the EL and CL exercise repeats (*Figure 7.4*). Colour maps were generated over the entire movement, creating a virtual movie of

changing muscle activity (frame rate ~ 25Hz). From these, colour maps at ten ankle angles during each cycle were chosen to investigate any pattern differences between EL and CL.

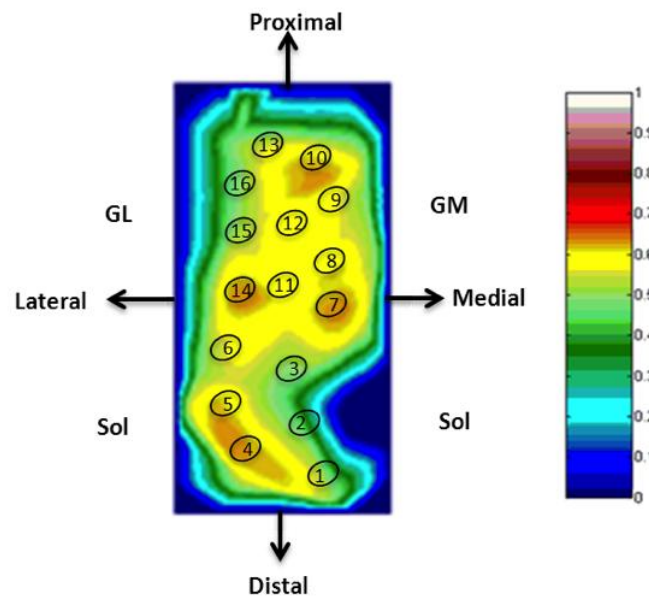


**Figure 7.4:** Colour representation of each channel of EMG activity across the calf muscle, with an intensity indicator.

A representative colour map, oriented relative to the stick diagram in the lab coordinates, is shown in *Figure 7.5*.

In order to measure the cross-talk between channels, cross-correlations between the data from different channels were carried out.

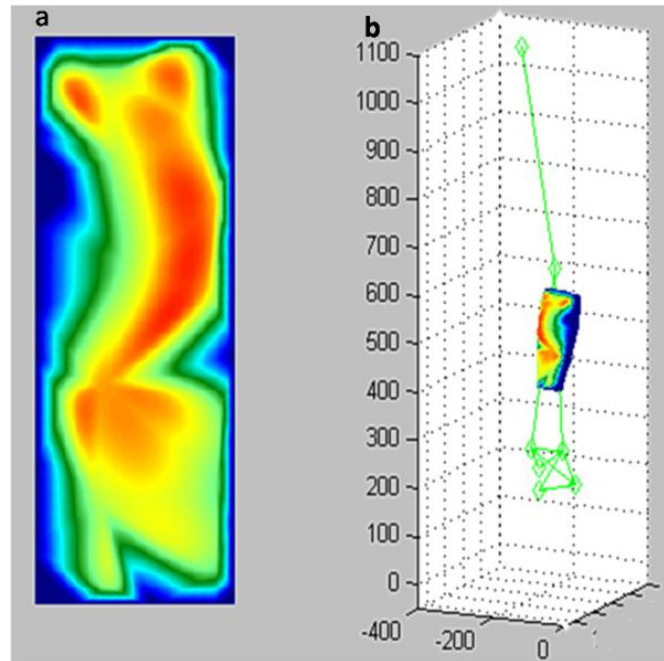


**Figure 7.5:** (a) Calf colour map during CL and (b) stick figure with the colour map representing calf muscle activation shown in the correct location. All in the laboratory coordinates.

A fast Fourier transform of the EMG data from each electrode pair was carried out over a complete EL or CL cycle, enabling the magnitude of each frequency component of the EMG signal to be determined across the triceps surae muscles. FFT power was also converted to a colour scale and normalised for each individual as previously described, enabling spatial maps of the magnitude of each frequency present in the triceps surae to be constructed.

ATF and tendon perturbations were also calculated, following procedures detailed in chapter 3.

### **7.2.5 Statistical analysis**

To quantitatively analyse the data, normalised EMG signals were obtained. Quantitative analysis of the EMG was performed using 3 way ANOVAs for both CL and EL, taking subject, each point in the cycle and channel number (location on the triceps surae) as the factors; interactions between these factors were also reported. The beginning and end of each cycle was found from the heel height data.

## **7.3 Results**

### **7.3.1 Muscle activation maps**

Normalised ATF was found to be in the same range as reported in previous chapters (4 - 6), with no significant differences between EL and CL. Also in line with previous data, GrF perturbations were significantly higher during EL than CL with a characteristic peak at around 10 - 12 Hz ( $p < 0.05$ ).

Colour mapping of EMG activity, directly at the sites of the electrodes, shows a clear spatial variation of muscle activity with movement. Looking holistically at calf muscle activity, CL resulted in significantly higher levels of activation throughout the calf muscle than EL, follow the previously reported findings (chapters 4 - 6).

Example data sets from a single subject, outlining EMG activity during 3 cycles of EL and CL, are plotted in *Figure 7.6* and *Figure 7.7* respectively. Clear and distinct activation patterns were observed during the course of exercise. As the heel goes into full dorsiflexion, where the force passing through the muscle-tendon unit is maximum, the muscle activation is highest for EL, but lowest for CL. Considering EL, there was little muscle activation at the very start of the movement (*Figure 7.6*), but activation increases



during the exercise, with the most activation in the distal soleus and medial gastrocnemius at the end of the movement. However, this pattern of increasing activity does not hold across the muscle and activity levels fluctuate during the cycle, particularly in the proximal medial gastrocnemius. *Figure 7.7* reports activity during CL, showing consistently higher activity than during EL across most of the muscle. There is increased activation in the gastrocnemius at the end of contraction (at peak heel height), while the distal soleus is most active mid-cycle.

Cross-talk assessment showed that cross-correlation values ranged from 0 - 0.6 across the different EMG channels. A cross-correlation value of 1 would indicate identical signals from two channels and a value of 0 two completely unrelated signals. The highest levels of cross-talk (values of 0.6) were observed for channels measuring the soleus muscle. This is likely due to the comparatively smaller area under investigation in the soleus.

### **7.3.1.1 Mean Group Data**

*Figure 7.8* shows the mean activity across 3 repeats for all subjects. These data indicate that overall the medial gastrocnemius and medial soleus are more active during CL as compared to EL. When variability in data is considered, repeat cycles by an individual subject showed more consistency than when comparing subjects. However, it was also notable that there was greater consistency in activation patterns between subjects during CL than EL. EMG data for selected ankle angles is tabulated in tables *Table 7.2* and *Table 7.3* for further understanding.

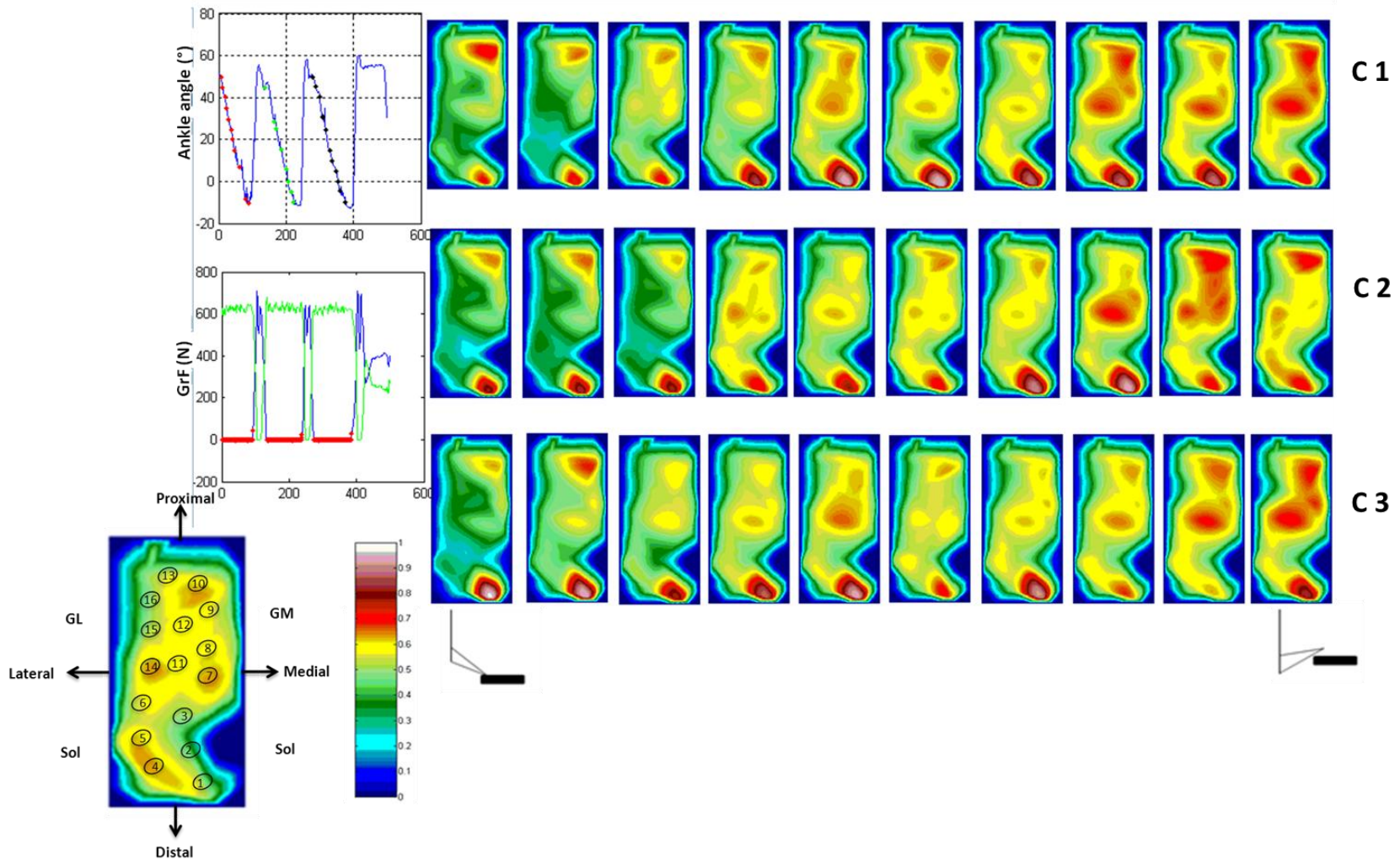


**Figure 7.6:** Colour maps depicting EMG activity across the triceps surae muscle during 3 cycles (C1-3) of EL for a single subject. Only the loading phase is depicted, as indicated by the coloured dots in the top left schematic. The guide to relative colour map intensities is also shown on the bottom left, where 1 is high and 0 is low.

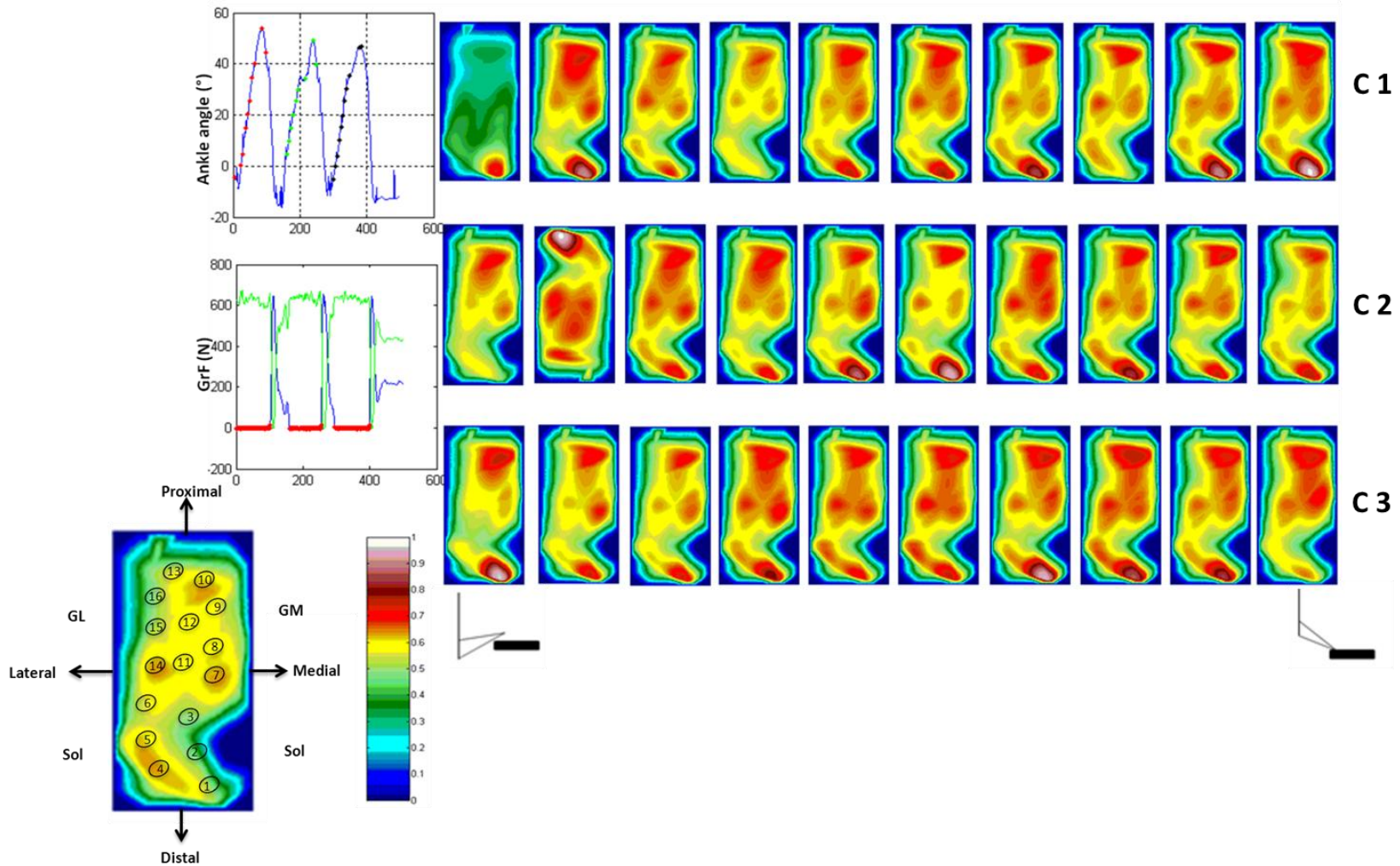


**Figure 7.7:** Colour maps depicting EMG activity across the triceps surae muscle during 3 cycles (C1-3) of CL for a single subject. Only the loading phase is depicted, as indicated by the coloured dots in the top left schematic. The guide to the relative colour map intensities is also shown on the bottom left, where 1 is high and 0 is low.

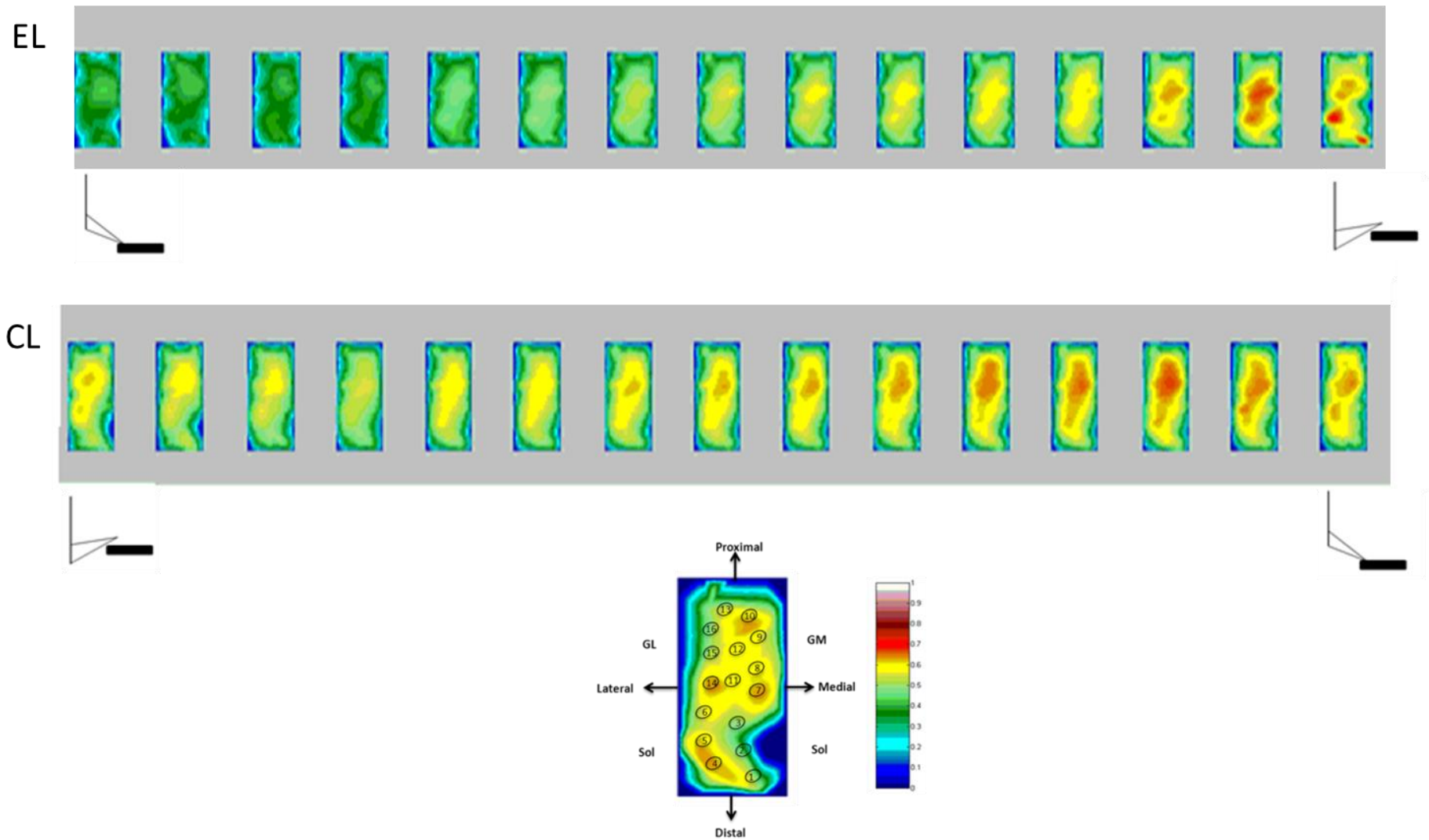


**Figure 7.8:** Mean EMG map data during EL and CL for all subjects. The guide to relative colour map intensities is also shown at the bottom, where 1 is high and 0 is low.

**Table 7.2: Group mean EMG data at selected ankle angle**

Type of Loading		CL									
Ankle Angle (°)		-20		-10		0		10		-20	
EMG (mV)		Mean	SE	Mean	SE	Mean	SE	Mean	SE	Mean	SE
<b>Channel number</b>	1	16.92	1.37	20.32	1.51	20.52	1.94	22.13	1.92	20.31	1.75
	2	13.93	1.98	13.57	1.2	22.05	1.78	23.99	1.71	14.88	1.54
	3	12.81	1.6	15.64	1.6	25.69	2	28.23	1.69	18.17	1.72
	4	14.34	1.81	13.95	1.83	19.47	2.13	20.48	2.37	14.7	2.06
	5	16.42	1.6	14.32	1.46	23.42	2.16	26.4	1.67	18.34	1.67
	6	17.07	1.05	17.04	1.81	30.74	2.04	30.39	1.55	21.98	1.67
	7	24.053	1.53	22.56	1.26	46.63	3.1	52.19	2.41	30.68	2.09
	8	31.16	1.44	25.42	1.54	35.25	2.07	40.78	1.61	26.21	1.68
	9	14.93	2.14	13.59	1.97	27.54	1.87	25.09	1.98	20.6	1.59
	10	1.78	43.62	6.11	8.91	7.42	12.52	8.76	9.05	4.7	14.42
	11	20.97	1.71	26.27	1.78	35.05	1.75	34.18	1.63	27.65	1.59
	12	20.48	1.11	20.37	1.198	27.59	1.67	22.57	1.27	22.18	1.33
	13	18	1.49	16.88	1.48	28.32	1.6	24.15	1.52	21.93	1.62
	14	39.8	1.74	44.17	1.68	50.49	1.7	43.97	1.48	44.12	1.68
	15	12.15	3.77	6.41	2.7	9.66	2.87	8.96	1.98	12.13	2.83
	16	7.58	1.42	14.39	2.25	13.12	6.05	12.88	5.46	10.38	5.36

**Table 7.3: Group mean EMG data at selected ankle angle**

Type of Loading		EL									
Ankle Angle (°)		-20		-10		0		10		20	
EMG (mV)		Mean	SE	Mean	SE	Mean	SE	Mean	SE	Mean	SE
<b>Channel number</b>	1	19.25	1.48	19.73	2.06	17.72	2.33	16.66	1.87	16.69	2.05
	2	22.05	1.76	16.25	2.61	11.92	2.39	12.4	2.36	12.24	2.78
	3	27.98	1.81	23.33	2.32	19.72	1.88	19.16	1.94	16.36	2.08
	4	28.29	1.17	25.95	1.66	24.49	2.74	21.11	3.17	18.04	3.01
	5	24.92	1.8	21.76	1.75	19.36	2.53	18.79	2.64	16.1	2.28
	6	28.45	2.039	27.72	1.77	22.75	2.28	21.03	2.96	16.94	1.92
	7	62.69	1.51	50.36	1.81	35.07	2.05	32.9	1.93	22.23	1.75
	8	55.62	2.59	48.45	2.87	42.22	2.25	34.37	2.67	24.64	1.85
	9	37.76	2.34	24.6	1.94	23.12	2.17	24.77	2.05	19.27	1.75
	10	44.09	2.53	8.36	7.63	10.48	7.61	8.52	9.53	10.24	4.19
	11	34.3	1.87	28.38	1.62	31.7	2.14	26.69	2.41	23.02	1.95
	12	29.96	1.88	22.01	1.92	19.56	1.74	20.11	2	18.29	1.51
	13	23.27	1.96	24.46	1.93	22.72	2.07	22.49	2.21	20.19	1.96
	14	81.86	1.98	50.11	1.87	37.48	2.07	36.3	1.9	28.57	1.45

15	18.35	1.54	16.33	1.12	8.04	1.66	7.77	1.73	6.49	2.18
16	19.88	18.42	13.13	12	14.15	10.82	14.19	11.64	14.97	6.99

ANOVA results showed that the ‘point in the cycle’ showed significant p values for both CL ( $F = 384.34$ ,  $p < 0.01$ ) and EL ( $F = 353.52$ ,  $p < 0.01$ ), meaning that muscle activation levels varied significantly during both the EL and CL movements. Channel number (location of the measure across the triceps surae) also showed a significant effect for both CL ( $F = 160.11$ ,  $p < 0.01$ ) and EL ( $F = 75.23$ ,  $p < 0.01$ ) and the interaction between channel number and point in cycle was also significant for CL ( $F = 5.3$ ,  $p < 0.01$ ) and EL ( $F = 4.62$ ,  $p < 0.01$ ), meaning that different parts of the muscle vary significantly in activation. In addition to the ANOVA, the mean standard deviation of muscle activation between set of pictures was calculated both ‘between subjects’ and ‘within subjects’ for both EL and CL. It was found that the between subject variation in muscle activation is significantly higher during EL as compared to CL (*Figure 7.9*). However, no significant differences between EL and CL were observed for within subject analysis.

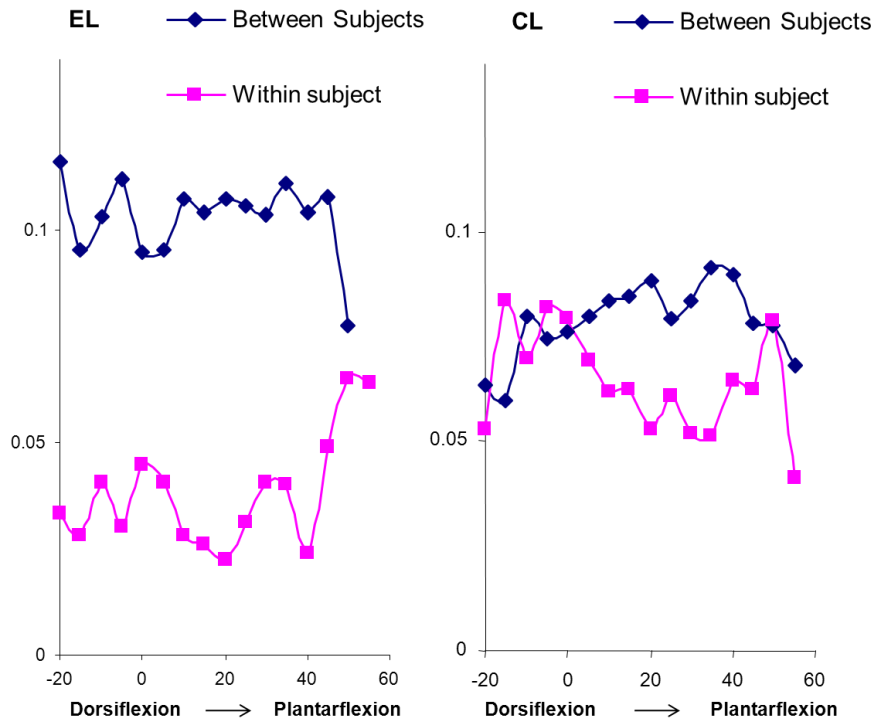


**Figure 7.9:** Mean standard deviation of muscle activity data between either a single subject repeats (within subjects) or across subject mean data (between subjects) shown with respect to range of movement.

### 7.3.2 Muscle perturbations maps

The FFT of the normalised EMG, was compared for all EMG channels for each subject. A typical series of FFT output graphs for each electrode pair are shown in *Figure 7.11* for EL and *Figure 7.12* for CL. These spectrums are markedly different from the perturbations recorded in the GrF and Achilles tendon, an example of which are shown in *Figure 7.10*; EMG FFTs shows no peak in the 1 - 5Hz range, but steadily increasing power with increasing frequency component. During EL, a peak in the signal at around 10 - 12 Hz is seen in all the three channels (1 - 3) from the medial side of soleus. Similar peaks were observed from distal medial gastrocnemius (channels 7 and 11), and the proximal medial gastrocnemius (channel 13). Interestingly, a clear peak at around 15 Hz can also be seen from the proximal lateral gastrocnemius. By contrast, CL showed a range of peaks at higher frequencies. However, the 15 Hz peak

from the proximal lateral gastrocnemius muscle, as reported in EL, was once again observed. Spatial maps of the FFT data, showing the magnitude of each separate signal frequency were calculated and are shown in *Figure 7.13* for EL and *Figure 7.14* for CL. Overall, perturbation magnitudes are higher in CL (particularly at very high frequencies). However, considering 10 - 12 Hz perturbations, the highest perturbations can be seen during EL in the lower leg, mainly the distal middle and proximal medial soleus and distal medial gastrocnemius and proximal medial gastrocnemius. The colour maps also highlight the lower magnitude of signals at lower frequencies (1 - 7 Hz).

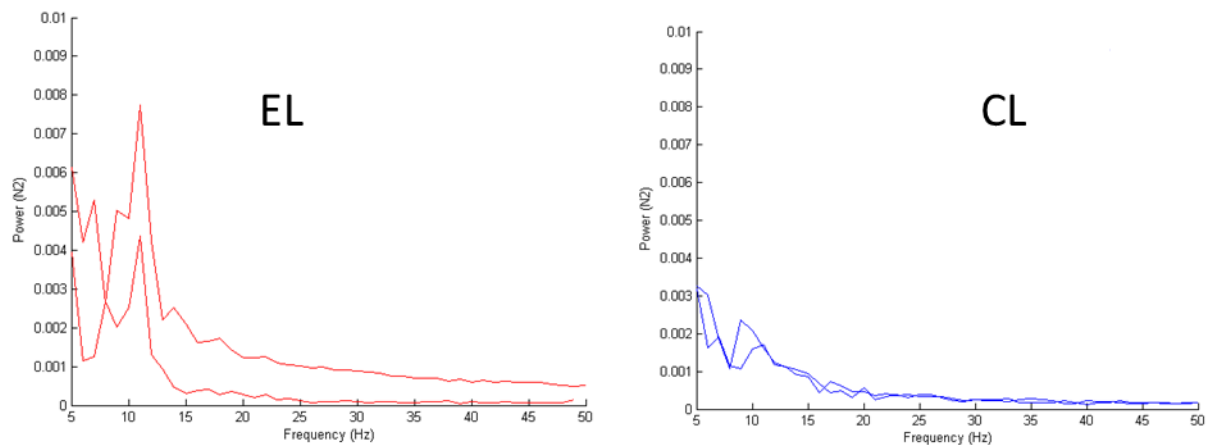


**Figure 7.10:** Two typical records of GrF perturbations for a subject completing EL and CL. High magnitude perturbations are evident at around 10 - 12 Hz during EL.



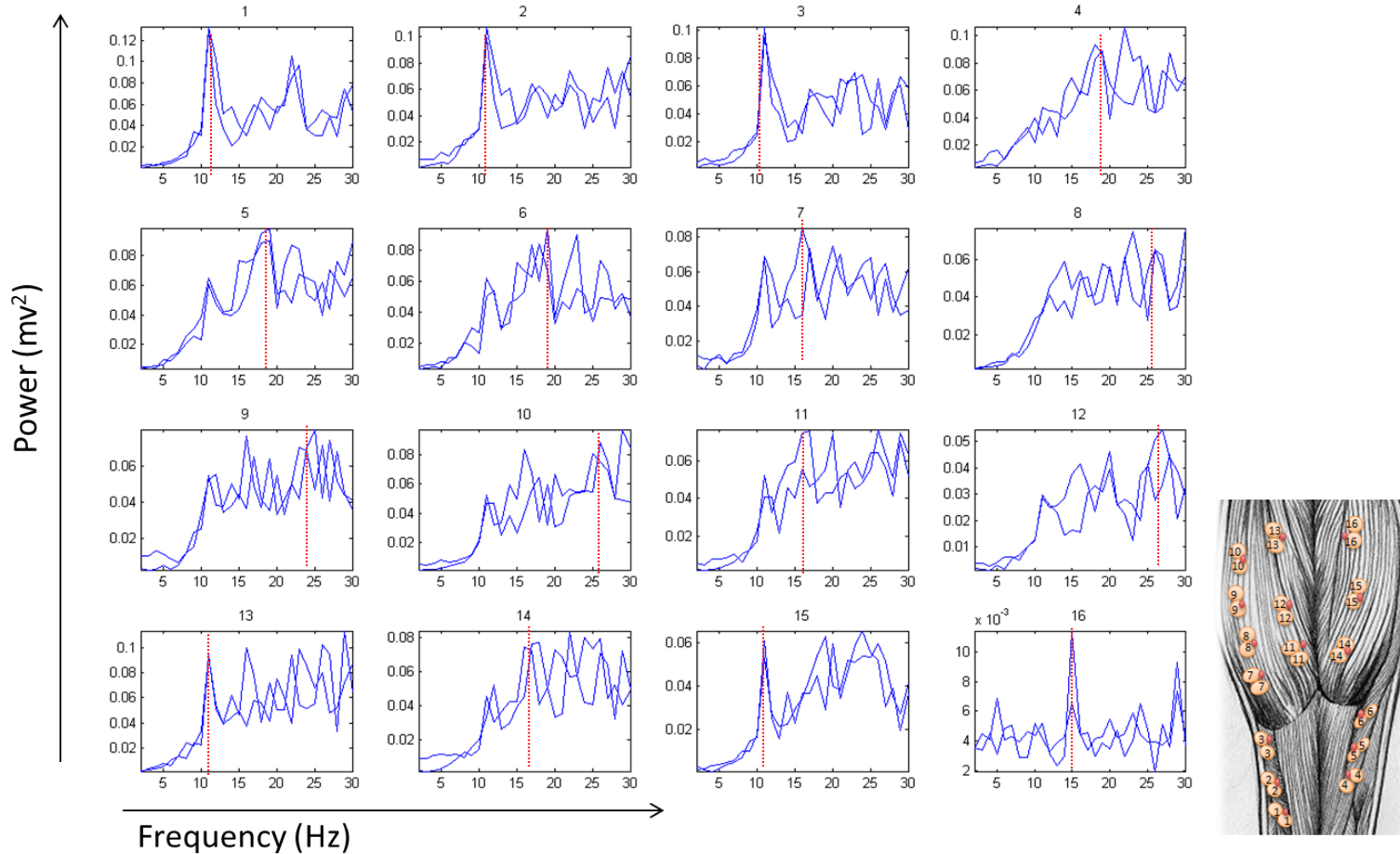


**Figure 7.11:** A series of typical FFT outputs, from the EMG signal in each of the 16 channels attached on the triceps surae during EL. The Y axis indicates the Power of the signal ( $mv^2$ ) and the X-axis indicated the frequency in Hz. Channel numbers are shown above each graph. The point of peak power, taken as a mean of both cycles from each channel, is marked with red lines.

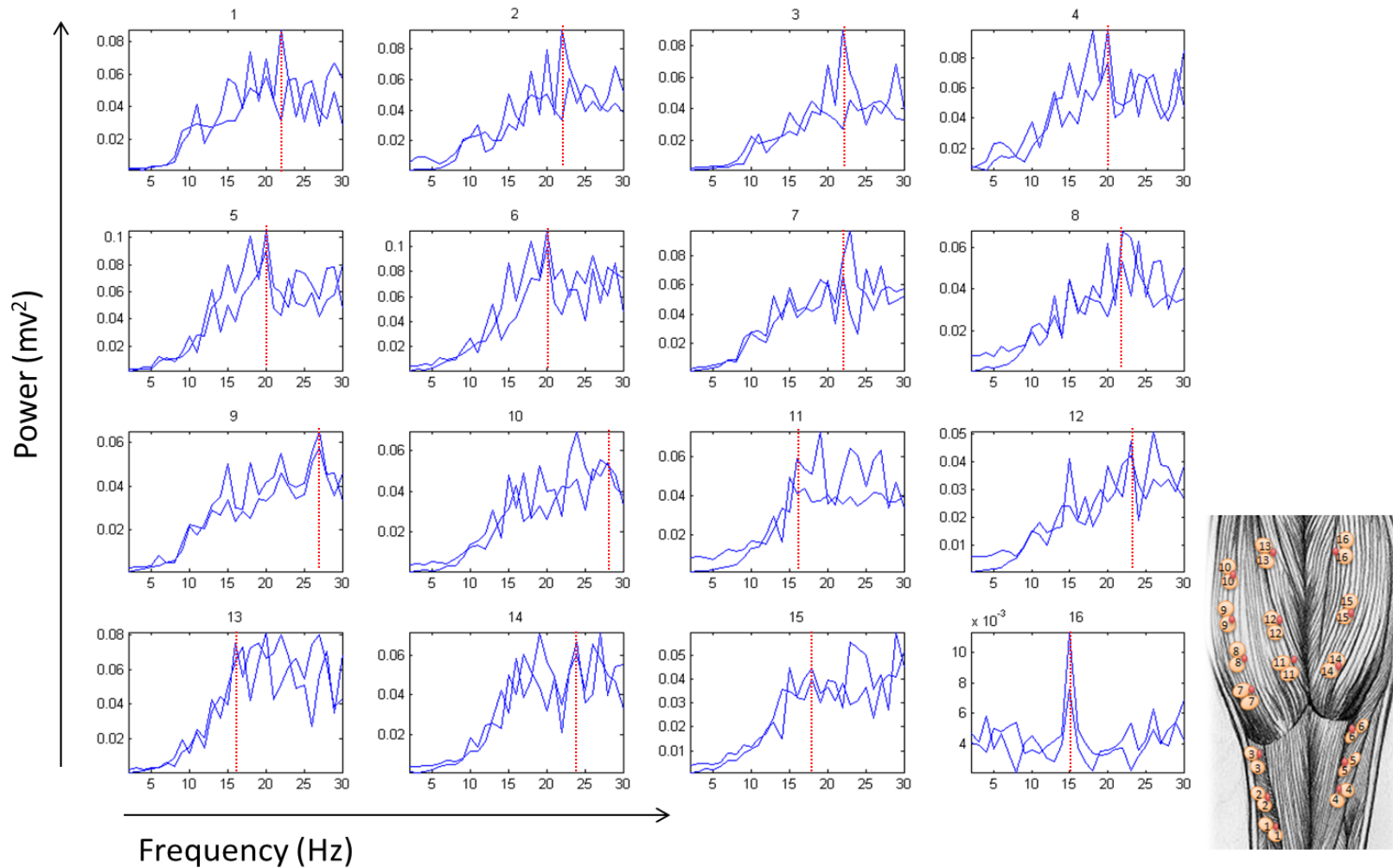


**Figure 7.12:** A series of typical FFT outputs, from the EMG signal in each of the 16 channels attached on the triceps surae during CL. The Y axis indicates the Power of the signal ( $mV^2$ ) and the X-axis indicated the frequency in Hz. Channel numbers are shown above each graph. The point of peak power, taken as a mean of both cycles, from each channel is marked with red lines.

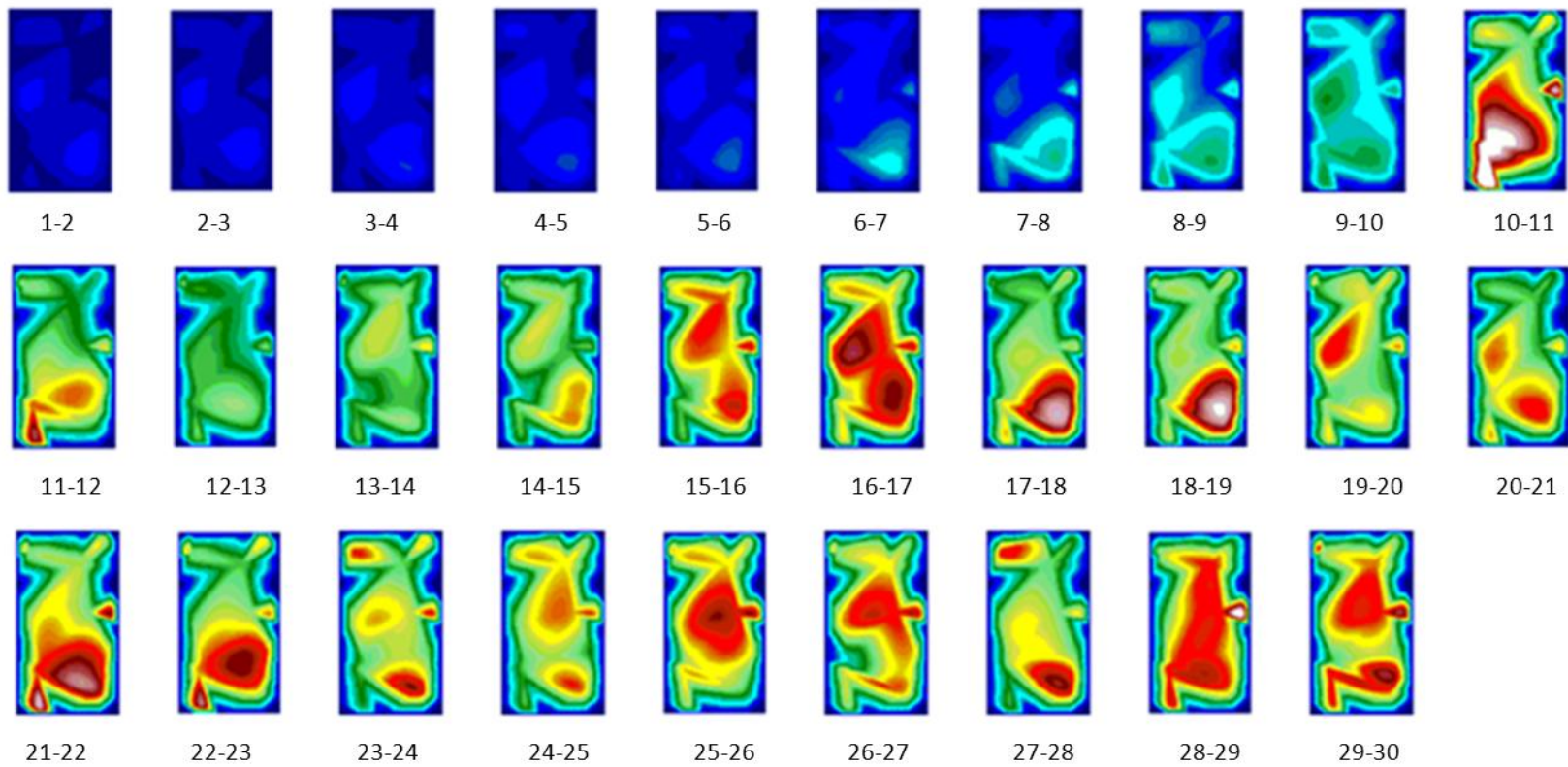


**Figure 7.13:** The FFT of the EMG from each channel across the triceps surae was taken, and the magnitude of each signal frequency (shown below each map: 2 - 30Hz) shown pictorially during EL.

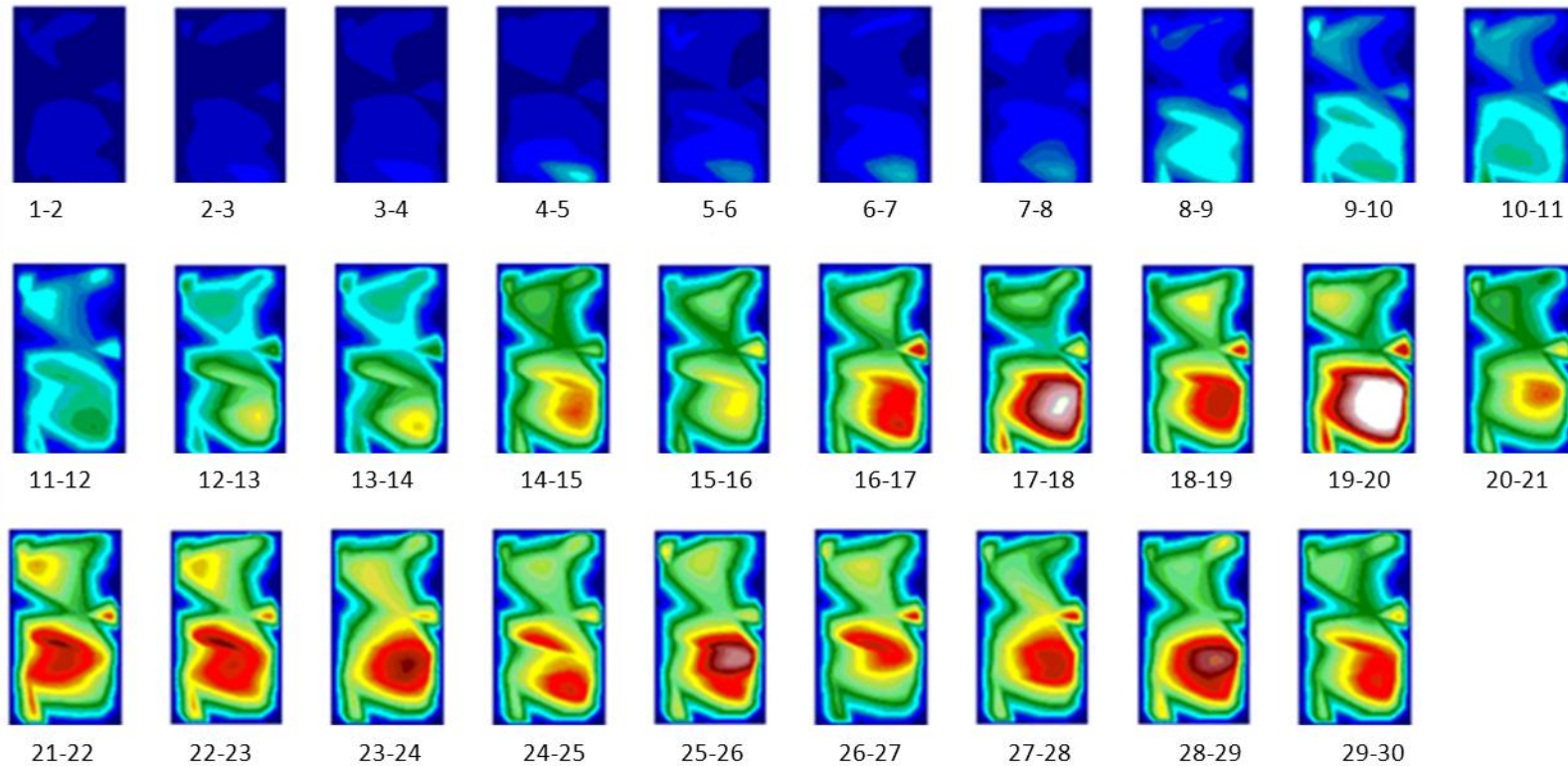


**Figure 7.14:** The FFT of the EMG from each channel across the triceps surae was taken, and the magnitude of each signal frequency (shown below each map: 2 - 30Hz) shown pictorially during CL.

## **7.4 Discussion**

The first aim of this chapter was to investigate whether high surface, low density EMG techniques can detect distinguishable muscle activation patterns within the triceps surae muscle regions. With appropriate data, the chapter then aimed to investigate whether EL and CL influenced activation of the different regions of triceps surae in specific ways. This study has confirmed that different parts of the triceps surae do behave differently at a given time point in the cycle during EL and CL ( $p < 0.01$ ). Indeed the results are consistent with a previous study, conducted with 128 channels of EMG, and measuring triceps surae activity during voluntary contraction (Staudenmann et al., 2009); similar spatial variations in triceps surae activity were observed in the present study, indicating that different regions of triceps surae have specific biomechanical functions to perform during various activities.

A common assumption in sEMG is that the measured potential originates solely from the muscle directly under the electrode. However, it is known that potential differences can reach the electrode site from further away, through volume conduction. Such affects can change the EMG signal; a phenomenon commonly known as 'cross talk'. In our experimental set up, cross talk from neighbouring muscles might have contributed to the spatially derived EMG signals. However, because of the large cross-sectional area of triceps surae, the contribution of the deeper muscles in cross talk would be minimal, and electrodes were also placed at least 1 cm away from the border of the muscle, to minimise crosstalk from neighbouring muscles. Another limitation of sEMG is the quality of the skin-electrode contact (Merletti et al., 2009). Every effort was made to reduce this effect by preparing the skin and placing the electrodes consistently in the same place, however muscle architecture varies between individuals, which might have contributed towards the differences seen between subjects. In multi- channel surface EMG, the signal is recorded at a depth 1 - 2 cm into the muscle, which is quite superficial and may bias the investigated unit samples. In

addition, recordings were made when the leg was fully extended, so that the whole of the triceps surae, including the medial gastrocnemius and lateral gastrocnemius, are activated and contributing towards the force generation (Cresswell et al., 1995).

A consistent pattern has been shown for EL and CL exercises across subjects. Generally, lower EMG was observed during EL as compared to CL (*Figure 7.6* and *Figure 7.7*). Furthermore, as the ankle angle increases, muscle activation also increases throughout the triceps surae during CL; however the EMG intensity stays consistently higher during CL. CL showed reasonably even activation of all muscles in triceps surae, however, high activity are really evident in soleus at start of the exercise and then gastrocnemius at the end. While previous studies have attempted to investigate the origin of increased muscle activation during CL (Enoka, 1996, Ono et al., 2010, Westing et al., 1991, Vaczi et al., 2011), the current study is the first to identify the response of individual triceps surae regions during clinically relevant EL and CL. According to the cross-bridge theory of the muscle contraction, force is generated by muscle as a result of the interaction of actin and myosin. In a concentric cross-bridge cycle, adenosine triphosphate molecules bond and detach in an orderly manner, whereas during EL, lengthening of the muscle-tendon unit occurs due to the stretching of sarcomeres in response to an external load, resulting in mechanical disruption of the actin-myosin bond. Such a phenomenon, along with the results from the present study, emphasises that it is not just the tendon that undergoes changes during EL, but remodelling of the complete triceps surae complex may be vital for EL effectiveness.

This chapter additionally aimed to investigate which parts of the muscle are dominant in generating the muscle-tendon unit perturbations seen in Fourier transforms of the GrF and ATF. The 10 - 12 Hz frequency peaks reported during EL in previous chapters were seen in the soleus and the proximal

medial gastrocnemius regions of the triceps surae, indicating that these areas of the muscle are likely to be responsible for generating the vibrations.

The final objective of this study was to investigate whether colour maps showing the FFT of muscle activation across the triceps surae are distinguishable, and if so, if there were any consistent patterns in the different EMG frequencies present during EL and CL, which can be related back to the perturbation origin. Data shows that the FFT of the EMG data also shows variation within the regions and clear and distinct patterns of muscle perturbations were observed during EL and CL. For CL, higher intensities of vibrations were present from 10 Hz upwards, focused in the distal gastrocnemius. By contrast, there was a less uniform spectra of frequencies present across the triceps surae during EL, but it is evident that certain triceps surae regions, for example the middle, proximal and distal soleus as well as medial gastrocnemius clearly shows a 10 - 12 Hz peak in EL data only. These findings signify the importance of these regions in the triceps surae; if 10 - 12 Hz stimulation is important in treating tendinopathy, these are the source. However, with no clear understanding if perturbations do have a beneficial effect on tendon healing, it currently remains unclear how best to manage training.

Training programmes including EL have been shown to result in structural changes in the muscle tendon unit (Grigg et al., 2009, Friden and Lieber, 1995, Malm et al., 2000). It is evident that the morphological and architectural structure of skeletal muscle fibres alters as an effect of training, which may in turn influence how the training affects the muscle. Such variation may result in regional muscle weakness which can cause muscle strength imbalances and eventually altered load distribution on the joints involved and may result in an injury (Hedayatpour and Falla, 2012). EL has been shown to be a beneficial treatment in tendinopathy and increases the muscle mass (Roig et al.,

2009). However, the non-uniform effect of EL, as seen in the present study, needs further investigation.

Future work needs to be carried out in order to investigate these questions further. Similar studies based on similar protocols and with similar analysis tools must be carried out in order to measure short and long term EL or CL training effects. The techniques developed here give a complete spectrum of frequencies present in each sub- compartment of the triceps surae. Future studies in patients with tendinopathy would be of real interest in order to answer many of the above stated questions. For example, it would be interesting to measure the force spectrum and EMG frequency spectrum of the sub-regions of the muscles attached to tendinopathic tendons, as it has been shown recently that muscle activation is higher in patients with Achilles tendinopathy as compared to health subjects (Reid et al., 2012).

## **7.5 Conclusions**

This study has confirmed that different parts of the triceps surae do behave differently at different time points in the cycle during EL and CL. A FFT of the EMG data also shows variation in the perturbation frequencies present within the regions of the triceps surae and clear and distinct patterns of muscle perturbations were observed during EL and CL. Certain triceps surae regions, for example the medial, proximal and distal soleus as well as medial gastrocnemius clearly shows a 10 - 12 Hz peak in EL data only.



## **Chapter 8: Discussion**

## 8.1 Introduction

Eccentric loading (EL) involves the lengthening of the muscle-tendon unit during the application of load, and has been employed as a treatment for Achilles tendinopathy since the 1980s. Since this time, a number of studies have confirmed superior outcomes with EL when compared to concentric loading (CL) or other interventions, with EL reporting treatment success rates ranging from 60-82 % for mid-portion Achilles tendinopathy (Rowe et al., 2012). The mechanisms through which EL treats tendinopathy remain unknown and it is unclear why EL should be reported to be notably more successful than CL in treating patients. Initially it was believed that the tendon experienced higher forces during EL than CL, resulting in more tendon remodelling in response to the resulting higher strains (Stanish et al., 1986). However, more recent *in vivo* human studies have reported no difference in the peak Achilles tendon force (ATF) during EL and CL (Rees et al., 2008); rather, the focus has switched somewhat to the higher 8-12 Hz perturbations in GrF reported during EL (Henriksen et al., 2009). However, no previous work has investigated the dynamic properties of the AT and triceps surae unit during typical EL and CL protocols, as performed clinically; key data for understanding the biomechanical effects of tendon loading protocols.

Accordingly, the global aim of the present study was to compare clinically relevant EL and CL loading protocols, in order to specifically investigate differences in tendon mechanical properties, perturbations and muscle activity levels. To achieve the aim, four studies were carried out. In the first study (chapter 4), tendon stiffness throughout the EL and CL protocol was examined. For this purpose, a suitable real time measurement system was developed and tested (chapter 3). Key to the work throughout the thesis, chapter 3 also describes the development and testing of a semi-automated analysis procedure for tracking movement of the muscle-tendon junction (MTJ) as measured by 2-D ultrasound and 3-D motion capture. The next two studies (chapters 5 and 6) were carried out to establish the effects of loading speed and applied external load on tendon

biomechanical parameters, muscle activation and tendon perturbations respectively. A final study (chapter 7) was carried out to characterise the spatial distribution of muscle activity during EL and CL and investigate the origins of tendon perturbations. The Achilles tendon was selected for this work, as a result of its high incidence of tendinopathy and also because most studies reporting a positive clinical outcome for tendinopathy in response to EL have focused on mid-portion Achilles tendinopathy. Healthy normal subjects were studied in order to fully characterise EL / CL in normal conditions, so that the results of future studies in patients can be compared with a normal reference.

A summary table of results from all these studies is presented in *Table 8.1*.

## **8.2 Study Limitations**

The addition of ultrasound to the study of muscle-tendon biomechanics has been an invaluable tool for assessing tendon extension during *in vivo* studies. However, there were some limitations associated with its use, when studying real time dynamic movements. Variations in probe orientation can notably influence measures of MTJ displacement; with studies suggesting that tendon elongation can be subsequently underestimated (Loram et al., 2006). However, this error was reduced in the current study, not just as a result of extensive imaging practice during the pilot study, but by placing motion markers on the probe to ensure the real time orientation of the probe with respect to the leg was known and accounted for.

Nevertheless, systematic errors can occur during any measurement technique. It was noted that the tracking technique developed and tested during this study can be sensitive to image quality. However, a series of validation process were carried out, to ensure confidence in the resulting data. Further, any blurred image or any trial not completed at an accurate pace or over the appropriate range of motion was discarded.

A potential criticism to the method could be that ATF was calculated using inverse dynamics rather than directly, using something such as implanted transducers (Fukashiro et al., 1995). However, this does not invalidate the conclusions of the thesis; this technique is non-invasive and has been employed in many previous studies (Lichtwark and Wilson, 2005a, Rees et al., 2008, Henriksen et al., 2009). Further, whilst the co-activation of tibialis anterior is not included in inverse dynamics, its contribution in the present study has been shown to be very small when compared to the large muscles of calf. In addition, it was also equally activated during EL and CL in the present studies, which would suggest that its effect in part would cancel out.

The mechanical properties were measured for Achilles tendon (defined as the attachment between medial gastrocnemius and calcaneum). This includes the free tendon and the aponeurosis section of the medial gastrocnemius and soleus muscle, meaning the mechanical behaviour of the individual elements of the complex are not clear. It is possible that each of the effects observed in the current study may differ from those specifically seen at the free tendon site, as tendon is not a uniform structure, and the current findings may thus not necessarily reflect conditions at the site of tendon which is prone to tendinopathy. However, the medial gastrocnemius tendon was chosen, as most studies measuring the mechanical parameters of tendinopathic tendons have used this measure (Child et al., 2010, Arya and Kulig, 2010, Morrissey et al., 2011) and the MTJ is also clearly accessible here. Adopting this method ensures that current data can be compared with that from previous studies. In addition, a recent study that has shown that Achilles tendinopathy alters the mechanical properties of the medial gastrocnemius Achilles tendon (Arya and Kulig, 2010), indicating that changes in free tendon mechanics should be observable with this technique.

### 8.3 Hypotheses 1 and 2

#### 8.3.1 Method development and the Differences between EL and CL

The purpose of the first study was to develop the currently available methodologies for measuring AT stiffness to enable monitoring of tendon mechanics during exercise. Whilst current techniques utilise motion capture and US imaging to track the calcaneus and MTJ for tendon length, typically tendon properties are only reported at the maximum extension point, as the location of the MTJ is tracked manually in individual video frames. Chapter 3 developed a tracking algorithm, for semi-automated tracking of the muscle-tendon junction throughout loading, enabling tendon force-extension curves to be derived for the complete EL and CL exercises.

For the first study it was hypothesised that there would be no biomechanical differences between EL and CL. In accordance with the hypothesis, it was found that EL and CL, performed at the same moderate speed and over the same range of motion, did not differ in terms of Achilles tendon force, stiffness and strain. However, in line with previous data, EMG activity in the calf muscles was significantly lower during EL than CL. Perturbations within the GrF were also investigated, showing an elevated magnitude around 10 Hz vibrations during EL only.

The GrF tremors at around 10 Hz are often considered to be primarily associated with muscle activity. A linear relationship between GrF perturbations and ATF perturbations was observed, suggesting that these perturbations may be of greater magnitude in the tendon. However, it must be noted that Achilles tendon force is measured from the GrF using inverse dynamics, so this may simply result from the scaling. While the use of inverse dynamics is considered to give a good estimate of ATF and has previously been outlined in a number of studies (Rees et al., 2008, Henriksen et al., 2009, Lichtwark and Wilson, 2005a), it cannot be ruled out that the GrF only

accounts for one component of the forces passing through the tendon, and the tendon might see additional elements of force or tremor to those present in the GrF and these may differ between EL and CL.

As 10 Hz tremors provide the only observed difference between EL and CL protocols in this study, it is reasonable to hypothesise that tendon perturbations may be involved in the therapeutic effects of EL. There are a number of potential theoretical mechanisms. Indeed, recent studies reporting the existence of perturbations have presented such a hypothesis (Henriksen et al., 2009, Grigg et al., 2012). However, our study has additionally reported that not all subjects showed these perturbations (25% do not tremor at 10 Hz). This is an interesting finding and may partially explain why some subjects benefit from EL, whilst others do not. Furthermore, GrF perturbations during EL were significantly correlated to the EMG perturbations at all frequencies, whilst no such correlation was observed for CL, emphasising the likely role of muscle in the development of these perturbations. It has been shown in previous studies that EL requires unique muscle activation strategies from the nervous system, with reduced spinal level excitability but enhanced motor cortical excitability as compared to other mode of contractions (Enoka, 1996, Gruber et al., 2009). The current data, showing significant correlation between the GrF and muscle perturbations during EL only, supports the possibility that these muscle perturbations are a feature of neural control of muscle and represent synchrony of firing of large motor units.

## 8.4 Hypothesis 3

### **8.4.1 Changing exercise speed will not influence the pattern of tendon mechanics, EMG activity or tendon perturbations.**

One of the primary aims of the present study was to study the effect of loading speed during typical EL and CL on the biomechanics and perturbations of the triceps surae. This is of particular importance as there is no current data addressing how speed may influence tendon mechanics, and no consensus on an appropriate exercise speed. Indeed, the majority of studies investigating EL fail to report exercise speed at all (review *Table 1.3* and chapter 1 section 1.11). However, exercise speed could have a notable effect on the tendon mechanical environment, as both tendon and muscle are viscoelastic materials. A recent study has shown that resistance training performed at very slow speeds (10 s concentric action and 10 s eccentric action) cannot elicit the same level of force or power as that which can be achieved with a voluntarily selected velocity (Hatfield et al., 2006b). However, no data on tendon biomechanics was reported. Numerous *in vitro* studies have reported that tendon stiffness increases with speed (Wren et al., 2001) and while this has also been seen *in vivo* (Pearson et al., 2007), the effect of clinically relevant exercise speeds on AT stiffness remains unknown. Understanding the influence of loading speed on mechanical properties is important in any viscoelastic material. Furthermore, there is no current data concerning the effect of loading speed on tendon perturbations. To investigate the effects of exercise speed on tendon behaviour, EL and CL were performed and compared at slow (6 s) and fast (1 s) speeds.

Results from the present study indicated that clinically relevant variations in speed affected muscle activation and perturbations but not the mechanical properties of tendon. No differences in tendon force, length or stiffness were seen. However, muscle activation levels increased with speed, particularly in CL, while speed increased the magnitude of perturbations in EL. The non-significant change in stiffness with speed is in contrast to other studies, which have shown that AT stiffness

does vary with the speed of task; for example, leg spring stiffness has shown to be velocity dependent during running (McMahon and Cheng, 1990), whilst another study, in which stiffness was calculated using a spring-mass model, suggests that running at different speeds should result in different spring stiffnesses at the knee but not around the ankle joint (Arampatzis et al., 1999). In a recent study, a linear relationship is reported between the Achilles tendon stiffness and strain rate during ramped maximum isometric plantarflexions (Theis et al., 2012). However the tasks, the range of speeds adopted and the methods employed in these studies are all different from those in the present study. To compare the current data with typical *in vitro* data, the loading speeds can be considered as strain rates of 1% / sec (slow) and 6% / sec (fast), which is not a huge range when compared with *in vitro* tests. Ng et al did not observe any effect on the tendon modulus below strain rates of 15% *in vitro* (Ng et al., 2004), so it seems reasonable that stiffness changes were not evident. Indeed, the AT stiffness was slightly higher in fast EL and CL, and it is possible that if the speed could be varied across a wider range, then it might result in differences in stiffness. However, the range of speeds (0.2 - 1  $\text{rads}^{-1}$ ) employed in the present study is comparable to what can realistically be achieved in a clinical setting.

Increasing exercise speed increased muscle activation levels in CL, probably related to the increased acceleratory demand on the limb. Increasing muscle activation when working at faster speeds allows the muscle to generate sufficient power to carry out the task, a strategy found in walking and running activities as well (Franz and Kram, 2012, Wu and Ren, 2009). Very often, the emphasis of a clinical EL protocol is to carry out the exercises as slowly as possible with some studies suggesting this is a more effective treatment. This is commonly difficult for a beginner, as it requires balance on one foot for longer periods of times, but clinical evidence also indicates that it causes tendinopathic patients some pain (Alfredson et al., 1998). Clearly, when the exercise speed is slow, the leg muscles are activated for longer and this prolonged and precise control of muscle activation may promote



appropriate remodelling of the muscle-tendon unit. However, no differences in perturbations were found between EL and CL when both were performed at a slow speed. Indeed, this study has shown no difference of any description between EL and CL performed at a low speed, so provides no clear data to support slow EL. Further investigations are required to study the effect of matched EL and CL, slow or fast, training regimes on tendinopathic patients, to look for differences in this subject group.

When considering perturbations, a significant effect of speed was observed on the magnitude of perturbations during EL only. At a slow speed there were no significant differences between perturbations during EL and CL, but when the exercise speed was increased from 6s to 1s for a repetition, significantly higher perturbations in the 5 – 12 Hz range were observed during EL with peak perturbations in the 8 – 12 Hz range. No equivalent elevation in perturbation magnitude was observed for CL. It is known that motor unit firing rates change with the strength of muscle contraction (McAuley and Marsden, 2000), so the lower amplitude tendon tremors seen during slow speed may be ascribed to the fact that contraction are better controlled when performed slowly.

## **8.5 Hypothesis 4**

### ***8.5.1 Changing the applied load during exercise will not influence the pattern of tendon mechanics, EMG activity or tendon perturbations***

The typically described therapeutic EL regime consists of 12 weeks of exercise, during which the EL is carried out with progressively more weight in a back-pack or equivalent. However, the rationale behind the use of extra load is not clear. For example, is this load applied to train muscle or stimulate tendon healing? The primary aim of the study was to establish the effect of additional load during typical EL and CL on the biomechanics and perturbations of the triceps surae. EL and CL

were carried out at three speeds (completing loading phase in 1s, 3s and 6s) with and without additional load (up to ~26 % of bodyweight). The effects of additional load on tendon perturbations were investigated at all three speeds, whereas the effect of load on tendon biomechanical parameters was investigated at medium speed only. In addition effect of a dose of 11 fast EL or CL repetitions on ATF, tendon perturbations and muscle activation was also investigated.

Adding load led to no change in the maximum tendon strain, but greater tendon force and subsequently stiffness during both EL and CL loading. Previous studies have demonstrated that peak muscular force capacity and tendon stiffness are related (Muraoka et al., 2005, Scott and Loeb, 1995). The increase in tendon stiffness, observed in these and the present study, suggest that the unit may be operating to ensure excessive tendon strain is avoided during loading. This would protect against rupture (Muraoka et al, 2005), whilst ensuring the optimum length of muscle fibres is maintained, for the efficient generation and transfer of force (Zajac, 1989, Reeves et al., 2004).

Both the magnitude and frequency of tendon perturbations were found to be independent of load at medium and slow speeds. However, perturbation magnitude significantly increased with the addition of load at the fast speed, and a shift in the peak perturbations frequencies from 5 – 12 Hz to 10 – 12 Hz was observed. Elevated perturbations were also observed at the fast exercise speed in the previous study (Chapter 5). However, the addition of load significantly increased perturbation magnitude yet again. The change in frequency spectrum seen in fast heavy EL is also of particular interest, as a recent study has shown that the 10 Hz perturbations observed during EL in healthy subjects shifted towards a lower 9Hz frequency in patients with Achilles tendinopathy (Grigg et al., 2012). It remains unclear if there is any really difference between these frequencies, nor which of these frequency ranges may be most beneficial, but data suggests that the range of perturbation frequencies is both possible to manipulate and variable between healthy and tendinopathic tendon.

It is interesting to note that it has recently been shown that tendinopathic tendons are less stiff (Arya and Kulig, 2010), hence the drop in perturbation frequency in tendinopathic tendons could be related to the stiffness of tendon. It can be speculated from the results of present study that training tendinopathic tendon with higher loads and at fast EL speeds, where they will exhibit greater stiffness, will shift the frequency spectrum of perturbations towards higher frequencies.

Dose testing of the tendon showed no significant effects of a bout of EL or CL on the ATF, muscle activation or tendon perturbations. Observing no changes in these parameters could simply be due to the fact that a bout consisting of 11 repetitions of EL might not be sufficient to induce sufficient fatigue in the tendon. However, it has been shown recently that a 30min run at 12kmph on a treadmill does not affect the stiffness of the Achilles tendon (Farris et al., 2012), whereas two leg hopping exercise consisting of 1150 – 2600 impacts significantly reduces the maximum ATF during MVC but no change in stiffness (Peltonen et al., 2010). Data from the present study may well indicate no changes in tendon load parameters with repeat exercise, suggesting that recommendations for the number of repeats in an exercise bout should not be solely based on inducing fatigue.

From the results of chapters 4 - 6, it can be speculated that perturbations may be dependent on tendon stiffness. A positive relationship was observed between tendon perturbation magnitude and tendon stiffness during EL, demonstrating that more compliant tendons exhibit lower magnitude perturbations. However, this relationship does not appear to be linear; perturbations were significantly larger in magnitude with the speed during EL but the change in tendon stiffness was not significant. It is also interesting to consider the change in peak frequency range with load and speed, where a shift in the peak perturbation frequency from 5 - 12 to 10 - 12 Hz was observed with the addition of load during fast EL. This tuning or tightening of the frequency band was not evident with

speed, where EL reported significantly higher perturbations than CL between 10 and 12 Hz at a medium speed, while at a fast speed the significant difference was evident between 5 and 12 Hz. At a slow speed there were no differences between EL and CL. The current thesis suggests that there may be an important relationship between tendon stiffness and perturbation, which can be controlled by modulating applied load or speed (*Figure 8.1*). However, this concept needs further investigation and there is a need to carry out longitudinal studies in healthy and tendinopathic tendons, with varying exercise variables, to test this proposed hypothesis.

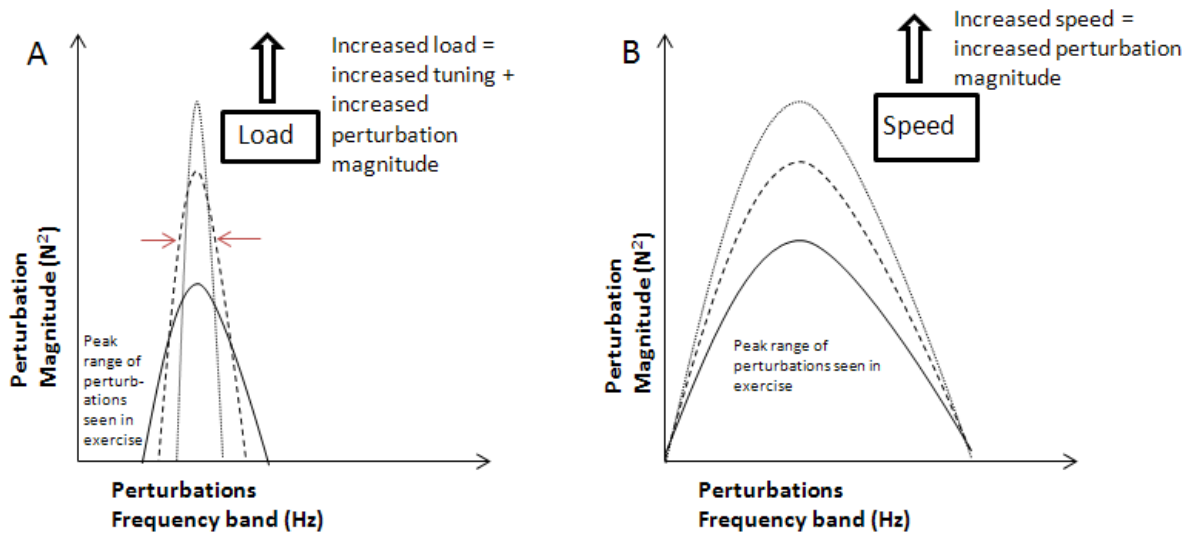


**Figure 8.1:** Schematic showing how perturbation magnitude and frequencies may vary during EL with tendon (A) load and (B) speed. Tendon stiffness can be increased by either increasing exercise speed, or exercise load, leading to higher magnitude, more tuned perturbations in the tendon during fast, heavy eccentric loading.

## 8.6 Hypothesis 5

### **8.6.1 Different patterns of muscle activation will be observed across different regions of the triceps surae during exercise**

Having hypothesised the importance of high frequency perturbations to promote tendon healing, the aims of the final chapter of this thesis were to investigate temporo-spatial muscle activation during EL and CL, with a secondary aim to investigate the origin of the perturbations. Characterising the origin of perturbations may be key to optimising their use in the treatment of tendinopathy. With tendon perturbations only recently receiving attention, there is no data to date concerning their origin during EL and CL. It has been hypothesized that tendon tremors are mechanical in nature, and that the calf muscle is the primary source of tendon tremors. However, the triceps surae is composed of a number of large muscles and it seems likely that the spread of these perturbations will be different throughout the muscle sub-regions.

Multi-channel EMG was used to investigate the temporospatial activation of the muscle. Such a technique has been shown to be reliable, with a strong correlation between spatial EMG and MRI results (Kinugasa et al., 2011). Data demonstrated that while muscle activation was consistently significantly higher during CL than EL, in accordance with the previous studies, a more consistent pattern of activation was also observed and the regions of the triceps surae muscles each became progressively more active during the movement cycle. The progressive activation of the whole triceps surae muscle highlights that modelling of muscle is likely to occur. Muscle remodelling has been shown to occur with repeat of EL exercise regimes (Dimitrov et al., 2012) but no change in tendon structure was seen, even after 16 weeks of home based EL (de Vos et al., 2012). However, the regional variations in muscle strength and perturbations that occur with training across the triceps surae are likely to influence how the Achilles tendon is loaded and thus may be responsible for alleviating tendon pain.

When the muscle activity data was processed to investigate perturbations, the same 10 - 12 Hz perturbations seen in the tendon were apparent in the muscle during EL, confirming that muscle activity contributed to tendon perturbations. However, closer examination of perturbations across the triceps surae indicated that the distal and proximal medial soleus and distal and proximal medial gastrocnemius were the predominant contributors to 10 – 12 Hz perturbations, while the gastrocnemius lateral contributed a 15 Hz perturbation.

It was observed that the activation level of the gastrocnemius was higher than the soleus during both EL and CL, so the posterior aspects of the tendon may see greater strains, but it was the soleus that was responsible for generating 10 Hz perturbations, during EL. With the soleus attaching close to the site of most mid-portion Achilles tendinopathies, this might be critical for repair (*Figure 8.2*). These findings signify the importance of these regions in the triceps surae; and the need for further investigation in to their behaviour. The involvements of these muscles over an EL training period may have important implication for managing tendinopathy.

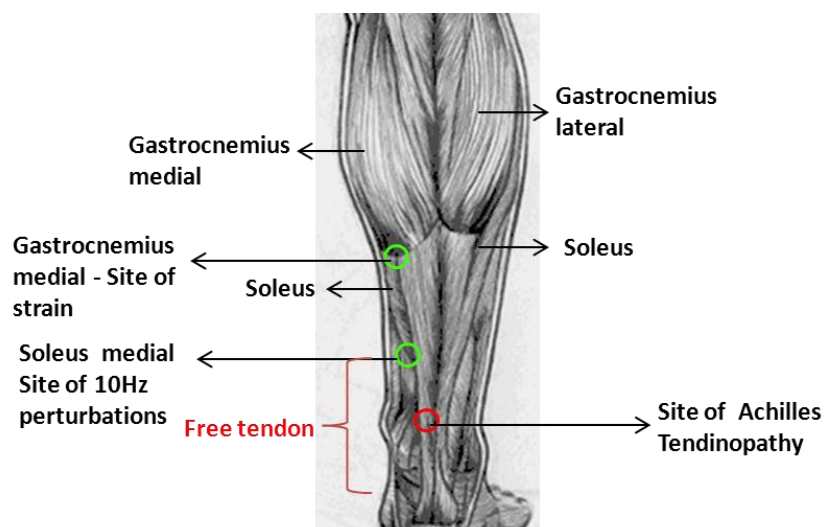


**Figure 8.2:** Schematic of the triceps surae muscle, in which the site of mid-portion Achilles tendinopathy is highlighted in red, whereas the location of the ~ 10 - 12 Hz perturbations are highlighted in green. It is speculated that EL may facilitate tendon repair in response to a combination of two biomechanical phenomenon, applied strain originating predominantly from the connection of medial gastrocnemius, and perturbations mainly originating at the site of medial soleus. Current findings indicate that perturbations may be focused on the free tendon and site of tendinopathy; a possible mechanism behind EL effectiveness as compared to CL.

Hypothesising that higher perturbations may provide the mechanism behind EL effectiveness, the current data may even indicate that faster exercise rates should be explored. Data on whole body perturbations applied *in vivo* is conflicting, suggesting they can have both negative and positive effects. In muscles, negative effects have been reported, including a decrease in maximal contraction force, and reduced motor unit firing rate (Bongiovanni et al., 1990). However, perturbations have also been shown to increase muscle strength (Verschuere et al., 2004), and have other positive effects such as increased bone density (Bacabac et al., 2006). Indeed, whole body perturbations have been shown to improve functional mobility to a greater extent than exercise alone in frail older fallers (Pollock et al., 2012), with a dependency between the frequency and amplitude of whole body vibration and the resulting muscle activity and acceleration (Pollock et al., 2010). The findings of this study emphasize the need to investigate the effects of perturbations at a tissue level, to see how the magnitude of perturbation might affect tenocyte responses. It is shown in *in vitro* studies that both matrix turnover and mechanical properties of cultured tendon fascicles are loading frequency sensitive (Lavagnino et al., 2003). Indeed, it is quite possible that the increased collagen I synthesis rate in tendinopathic over healthy Achilles tendon (Langberg et al., 2007) is a result of a modified high frequency stimulus.

The effects of a training program on the nature of perturbations remain unclear. Data from this thesis suggests that perturbation magnitude increases with exercise intensity, indicating that

perturbations may result from a lack of ability to control EL movement, and subsequently may reduce with training. Indeed, with most injuries known to occur as a result of eccentric loading conditions (LaStayo et al., 2003), it seems quite likely that EL is more demanding than CL and subsequently creates greater perturbations. Such a relationship may also explain why some subjects showed no perturbations at all in response to EL, if they already have strong muscles with excellent control of movement.

Training regimes, as outlined in chapter 1, tend to start with EL performed at slow speeds under body weight alone, and progress towards faster speeds with the addition of load, as the patient is able to manage these conditions. This progression in difficulty of training stimuli might train subjects to better control difficult movements in a progressive manner, with perturbations diminishing at each exercise stage as patients develop strength and control. This capacity to diminish perturbations with a controlled training programme may be the key to the success of an eccentric training programme. By contrast, if the high frequency stimulus from perturbations is essential for tendon repair, the progressive nature of an eccentric training programme, in which the tendon muscle complex is repeatedly and increasingly challenged, may be critical to ensure a continual supply of perturbations to the injured tendon.

## **8.7 Future work**

To draw more certain conclusions about the influence of loading parameters on muscle - tendon mechanics and subsequently on tendinopathy management, future studies should characterise tendon mechanics in patients, carrying out longitudinal studies, in which different groups are trained at different speeds, to see the effect of varying speed on tendinopathic tendon.

EL has shown to be effective for mid-portion Achilles tendinopathy and less so for insertional tendinopathy (Fahlstrom et al., 2003) unless modified to stop at plantar-heel (Jonsson et al., 2008).



It would be of interest to measure the propagation of tremors from the site of origin to the distal Achilles tendon and also to investigate if EL with a bent knee, during which the soleus muscle is more specifically targeted, generated more pronounced perturbations.

Motor unit recruitment strategy is known to differ between isometric ramp and step muscle contractions (Qi et al., 2011b), so future studies are required to compare the recruitment patterns of motor unit during EL and CL to investigate the 10 - 12 Hz perturbations. Furthermore, the results of present studies emphasize the need to investigate temporo-spatial muscle activation in patients with Achilles tendinopathy. It has been shown recently that EMG activity from the calf muscle is higher in patients with Achilles tendinopathy (Reid et al., 2012) and that tendinopathy alters the offset time of gastrocnemius and soleus muscle activation in the male runner during an over-ground running task (Wyndow et al., 2012). However, the regional differences in muscle function during EL or CL are unknown. Future studies will help to investigate any possible triceps surae remodelling during EL or CL in Achilles tendinopathy patients. Resistance exercise of the elbow extensor has shown to result in regional differences in muscle hypertrophy when applied over time course, and has been attributed to the regional muscle activation differences (Wakahara et al., 2012). To investigate this phenomenon further, future studies are warranted to investigate triceps adaptational differences between EL and CL during a course of 12 week training.

Indeed training studies are required to understand the meaning of high frequency perturbations as these are the source or the cure of the pathology. To understand this better, longitudinal training studies, in which the progression of perturbations is monitored, are needed. The response of tendinopathic patients may also differ substantially from normal subjects and should be investigated. Not only may they take longer to learn to control perturbations, but the current

hypotheses suggest that the perturbations may be more extensive in magnitude to begin with, in this cohort.

## 8.8 **Conclusions**

The optimal methods of applying tendon loading to maximize recovery from tendinopathy are unclear (Meyer et al., 2009), and there is no consensus in the literature concerning the correct exercise speed, load or dose. Indeed, the mechanisms by which EL may be effective in treating tendinopathy remain unclear. The current study is the first to investigate how speed, load and dose of loading influence tendon mechanical behaviour during EL and CL. EL and CL loading parameters have been correlated to tendon mechanics and perturbations, showing that tendon perturbations at  $\sim 10\text{Hz}$  are consistently greater during EL than CL. Following the developing hypothesis, that those perturbations are at least in part responsible for tendon healing; data indicates that increasing the speed of exercise and adding additional load will increase the magnitude of peri-10Hz perturbations. Along with considerations of exercise specific strengthening, clinicians can expect that changing exercise variables during a progressive programme may differentially challenge the recovering tendon. Longitudinal studies in injured subjects are warranted to explore the full clinical meaning of these findings.

Table 8.1: Summary of thesis findings

	Study Purpose	Methodology	Results	Conclusion
<b>Chapter 3 (Method development)</b>	Method to measure <i>in vivo</i> tendon mechanics specifically: includes the development of an automatic MTJ tracking algorithm.	US + EMG + motion tracking to draw tendon force extension curves resulting from dynamic movements. All techniques were assessed for accuracy and reproducibility.	Accuracy of the Achilles tendon length measurement system was within 3.42mm. The tracking algorithm was fast and able to monitor complete loading cycles.	Techniques were suitable for <i>in vivo</i> biomechanics measurements of tendons during dynamic EL and CL exercises.
<b>Chapter 4 (Study 1)</b>	Differences between EL and CL in terms of tendon force, stiffness, strain, and perturbations, as well as muscle activation and muscle perturbations.	12 healthy subjects. Motion tracking markers were placed on bony landmarks and the MTJ tracked using US during dynamic EL/CL loading. Activation of the calf muscles and tibialis anterior were recorded using an EMG system.	No difference in tendon force, stiffness and strain was observed. However, elevated perturbations in the GrF were observed at around 10Hz during EL only. EL was characterised by reduced calf muscle activation.	Tendon stiffness is independent of the type of loading (EL/CL). There is a linear relationship between GrF and ATF perturbations, indicating the perturbations are seen by the tendon itself. EL and CL differ in tendon and EMG perturbation: both amplitude and frequency.
<b>Chapter 5 (Study 2)</b>	Effect of loading speed on the mechanical properties of the Achilles tendon and the perturbations within both the tendon and muscle during EL and CL.	12 healthy subjects. Measurements taken during EL and CL performed at two commonly adopted speeds. As fast as possible (1 s) and as slow as possible (6 s).	No difference in tendon force or strain with speed. Muscle activation were significantly higher during fast loading speeds. In addition perturbation magnitude was significantly higher with speed during EL only.	Speed of loading can affect the viscoelastic behaviour of the muscle tendon unit. Stiffer tendon, seen under fast loading may impact tendon remodelling. Tendon perturbation magnitude but not frequency is speed sensitive in EL only.
<b>Chapter 6 (Study 3)</b>	The influence of external load on the mechanical properties of the Achilles tendon and the perturbations within both the tendon and muscle during EL and CL.	7 healthy subjects closely matched in weight and height. Measurements taken during EL and CL with or without external load carriage of 18 kg in back pack and at three speeds (fast (1s), moderate (3s) and slow (6s)). Moderate speed was used for further biomechanical analysis.	Significantly higher tendon force and stiffness under load was reported, irrespective of the loading type. Load didn't affect the magnitude or frequency of perturbations at moderate or slow speeds. Perturbation magnitude increased and frequency band narrows down with load, at a fast exercise speed only.	External load carriage can affect the tendon mechanical properties. However, external load doesn't affect either the magnitude or frequency of perturbations unless exercise is EL fast. The interaction of speed and load appears to have an effect on perturbation magnitude.
<b>Chapter 7 (Study 4)</b>	Temporo-spatial analysis of calf muscle activation and perturbation during EL and CL.	9 healthy subjects. Calf muscle mapping was carried out by placing the electrodes on six sub-regions of the GL, GM and Sol. Colour maps depicting muscle activity during the movements were developed. FFTs of these plots were carried out to study perturbations origin.	Colour maps highlighted significant differences in muscle activation intensity throughout the muscle. The standard deviation in muscle activation between subjects was found to be significantly higher during EL as compared to CL. 10 – 12 Hz perturbations were seen in the medial Sol, distal and proximal GM, and the proximal GL.	More variation in muscle activation among subjects was found during EL. The medial soleus and gastrocnemius was the main muscle compartment to show ~ 10Hz perturbations suggesting that perturbations may be particularly dominant in the free tendon on the medial side of the soleus.
<b>Chapter 8</b>	The current thesis has investigated a series of hypotheses in order to explore the mechanisms underpinning EL effectiveness as compared to CL. Biomechanical investigation of AT stiffness, stress, strain, perturbations was carried out along with the measure of muscle activation of the triceps surae. No significant differences were observed in tendon mechanical parameters between EL and CL. By contrast EL was characterised by lower levels of muscle activation and ~ 10 Hz perturbations. Carrying out the EL at faster speeds further elevated the perturbations, whereas the addition of load increased tendon stiffness, perturbation magnitude and the frequency range of higher perturbations magnitude significantly. The thesis also reported the muscular origin of these perturbations and specifically the role of medial soleus and medial gastrocnemius as the source of these perturbations			

## References

- ABRAHAMS, M. 1967. Mechanical behaviour of tendon in vitro. A preliminary report. *Medical & biological engineering*, 5, 433-43.
- ALEXANDER, R. M. & BENNET-CLARK, H. C. 1977. Storage of elastic strain energy in muscle and other tissues. *Nature*, 265, 114-7.
- ALFREDSON, H. 2003. Chronic midportion Achilles tendinopathy: an update on research and treatment. *Clinics in Sports Medicine*, 22, 727-41.
- ALFREDSON, H. & COOK, J. 2007. A treatment algorithm for managing Achilles tendinopathy: new treatment options. *British Journal of Sports Medicine*, 41, 211-6.
- ALFREDSON, H. & LORENTZON, R. 2000. Chronic Achilles tendinosis - Recommendations for treatment and prevention. *Sports Medicine*, 29, 135-146.
- ALFREDSON, H. & LORENTZON, R. 2003. Intratendinous glutamate levels and eccentric training in chronic Achilles tendinosis: a prospective study using microdialysis technique. *Knee surgery, sports traumatology, arthroscopy : official journal of the ESSKA*, 11, 196-9.
- ALFREDSON, H. & OHBERG, L. 2005. Sclerosing injections to areas of neo-vascularisation reduce pain in chronic Achilles tendinopathy: a double-blind randomised controlled trial. *Knee surgery, sports traumatology, arthroscopy : official journal of the ESSKA*, 13, 338-44.
- ALFREDSON, H., PIETILA, T., JONSSON, P. & LORENTZON, R. 1998. Heavy-load eccentric calf muscle training for the treatment of chronic Achilles tendinosis. *Am J Sports Med*, 26, 360-6.
- ALFREDSON, H., THORSEN, K. & LORENTZON, R. 1999. In situ microdialysis in tendon tissue: high levels of glutamate, but not prostaglandin E2 in chronic Achilles tendon pain. *Knee surgery, sports traumatology, arthroscopy : official journal of the ESSKA*, 7, 378-81.
- ANDRES, B. M. & MURRELL, G. A. 2008. Treatment of tendinopathy: what works, what does not, and what is on the horizon. *Clinical Orthopaedics and Related Research*, 466, 1539-54.
- ARAMPATZIS, A., BRUGGEMANN, G. P. & METZLER, V. 1999. The effect of speed on leg stiffness and joint kinetics in human running. *Journal of biomechanics*, 32, 1349-53.
- ARAMPATZIS, A., KARAMANIDIS, K. & ALBRACHT, K. 2007a. Adaptational responses of the human Achilles tendon by modulation of the applied cyclic strain magnitude. *The Journal of experimental biology*, 210, 2743-53.
- ARAMPATZIS, A., KARAMANIDIS, K., MOREY-KLAPSING, G., DE MONTE, G. & STAFILIDIS, S. 2007b. Mechanical properties of the triceps surae tendon and aponeurosis in relation to intensity of sport activity. *Journal of biomechanics*, 40, 1946-52.
- ARAMPATZIS, A., PEPPER, A., BIERBAUM, S. & ALBRACHT, K. 2010. Plasticity of human Achilles tendon mechanical and morphological properties in response to cyclic strain. *Journal of biomechanics*, 43, 3073-9.
- ARAMPATZIS, A., STAFILIDIS, S., DEMONTE, G., KARAMANIDIS, K., MOREY-KLAPSING, G. & BRUGGEMANN, G. P. 2005. Strain and elongation of the human gastrocnemius tendon and aponeurosis during maximal plantarflexion effort. *Journal of biomechanics*, 38, 833-41.
- ARNER, O., LINDHOLM, A. & ORELL, S. R. 1959. Histologic changes in subcutaneous rupture of the Achilles tendon; a study of 74 cases. *Acta chirurgica Scandinavica*, 116, 484-90.
- ARYA, S. & KULIG, K. 2010. Tendinopathy alters mechanical and material properties of the Achilles tendon. *Journal of applied physiology*, 108, 670-5.
- AZIZI, E. & ROBERTS, T. J. 2009. Biaxial strain and variable stiffness in aponeuroses. *J Physiol*, 587, 4309-18.
- BACABAC, R. G., SMIT, T. H., VAN LOON, J. J., DOULABI, B. Z., HELDER, M. & KLEIN-NULEND, J. 2006. Bone cell responses to high-frequency vibration stress: does the nucleus oscillate within the cytoplasm? *FASEB J*, 20, 858-64.
- BARKHAUSEN, T., VAN GRIENSVEN, M., ZEICHEN, J. & BOSCH, U. 2003. Modulation of cell functions of human tendon fibroblasts by different repetitive cyclic mechanical stress patterns. *Exp Toxicol Pathol*, 55, 153-8.
- BASMAJIAN, J. V. & DE LUCA, C. J. 1985. Muscle alive. Their functions revealed by electromyography *Willaims & Wilkins, Baltimore*, (5ed).

- BATTERY, L. & MAFFULLI, N. 2011. Inflammation in overuse tendon injuries. *Sports medicine and arthroscopy review*, 19, 213-7.
- BEACH, K. W. 1992. 1975-2000: a quarter century of ultrasound technology. *Ultrasound in medicine & biology*, 18, 377-88.
- BENAZZO, F. & MAFFULLI, N. 2000. An operative approach to Achilles tendinopathy. *Sports Med Arthrosc Rev*, 8, 96-1001.
- BENJAMIN, M., EVANS, E. J. & COPP, L. 1986. The histology of tendon attachments to bone in man. *Journal of anatomy*, 149, 89-100.
- BENJAMIN, M. & RALPHS, J. R. 1997. Tendons and ligaments--an overview. *Histol Histopathol*, 12, 1135-44.
- BIGLAND, B. & LIPPOLD, O. C. 1954. The relation between force, velocity and integrated electrical activity in human muscles. *The Journal of physiology*, 123, 214-24.
- BILLAUT, F., BASSET, F. A., GIACOMONI, M., LEMAITRE, F., TRICOT, V. & FALGAIRETTE, G. 2006. Effect of high-intensity intermittent cycling sprints on neuromuscular activity. *International journal of sports medicine*, 27, 25-30.
- BIRD, S. P., TARPENNING, K. M. & MARINO, F. E. 2005. Designing resistance training programmes to enhance muscular fitness: a review of the acute programme variables. *Sports medicine*, 35, 841-51.
- BLEVINS, F. T., HECKER, A. T., BIGLER, G. T., BOLAND, A. L. & HAYES, W. C. 1994. The effects of donor age and strain rate on the biomechanical properties of bone-patellar tendon-bone allografts. *The American journal of sports medicine*, 22, 328-33.
- BOESEN, M. I., KOENIG, M. J., TORP-PEDERSEN, S., BLIDDAL, H. & LANGBERG, H. 2006. Tendinopathy and Doppler activity: the vascular response of the achilles tendon to exercise. *Scandinavian Journal of Medicine & Science in Sports*, 16, 463-469.
- BONGIOVANNI, L. G., HAGBARTH, K. E. & STJERNBERG, L. 1990. Prolonged muscle vibration reducing motor output in maximal voluntary contractions in man. *J Physiol*, 423, 15-26.
- BROSSEAU, L., CASIMIRO, L., MILNE, S., ROBINSON, V., SHEA, B., TUGWELL, P. & WELLS, G. 2002. Deep transverse friction massage for treating tendinitis. *Cochrane database of systematic reviews*, CD003528.
- BROWN, R., ORCHARD, J., KINCHINGTON, M., HOOPER, A. & NALDER, G. 2006. Aprotinin in the management of Achilles tendinopathy: a randomised controlled trial. *British Journal of Sports Medicine*, 40, 275-279.
- BUTLER, D. L., GROOD, E. S., NOYES, F. R. & ZERNICKE, R. F. 1978. Biomechanics of ligaments and tendons. *Exerc Sport Sci, Rev* 6, 125-181.
- CACCHIO, A., ROMPE, J. D., FURIA, J. P., SUSI, P., SANTILLI, V. & DE PAULIS, F. 2011. Shockwave therapy for the treatment of chronic proximal hamstring tendinopathy in professional athletes. *The American journal of sports medicine*, 39, 146-53.
- CARROLL, C. C., DICKINSON, J. M., HAUS, J. M., LEE, G. A., HOLLON, C. J., AAGAARD, P., MAGNUSSON, S. P. & TRAPPE, T. A. 2008. Influence of aging on the in vivo properties of human patellar tendon. *Journal of Applied Physiology*, 105, 1907-1915.
- CAVAGNA, G. A. & KANEKO, M. 1977. Mechanical work and efficiency in level walking and running. *The Journal of physiology*, 268, 467-81.
- CETTI, R., CHRISTENSEN, S. E., EJSTED, R., JENSEN, N. M. & JORGENSEN, U. 1993. Operative versus nonoperative treatment of Achilles tendon rupture. A prospective randomized study and review of the literature. *The American journal of sports medicine*, 21, 791-9.
- CHANAUD, C. M., PRATT, C. A. & LOEB, G. E. 1987. A multiple-contact EMG recording array for mapping single muscle unit territories. *Journal of neuroscience methods*, 21, 105-12.
- CHANAUD, C. M., PRATT, C. A. & LOEB, G. E. 1991. Functionally complex muscles of the cat hindlimb. V. The roles of histochemical fiber-type regionalization and mechanical heterogeneity in differential muscle activation. *Experimental brain research. Experimentelle Hirnforschung. Experimentation cerebrale*, 85, 300-13.

- CHESTER, R., COSTA, M. L., SHEPSTONE, L., COOPER, A. & DONELL, S. T. 2008. Eccentric calf muscle training compared with therapeutic ultrasound for chronic Achilles tendon pain-A pilot study. *Manual Therapy*, 13, 484-491.
- CHILD, S., BRYANT, A. L., CLARK, R. A. & CROSSLEY, K. M. 2010. Mechanical properties of the achilles tendon aponeurosis are altered in athletes with achilles tendinopathy. *The American journal of sports medicine*, 38, 1885-93.
- CODAMOTION, C. 2010. CODA motion user manual.
- COLLIANDER, E. B., DUDLEY, G. A. & TESCH, P. A. 1988. Skeletal muscle fiber type composition and performance during repeated bouts of maximal, concentric contractions. *European journal of applied physiology and occupational physiology*, 58, 81-6.
- COOK, J. L. & PURDAM, C. R. 2009. Is tendon pathology a continuum? A pathology model to explain the clinical presentation of load-induced tendinopathy. *British journal of sports medicine*, 43, 409-16.
- COSTA, M. L., SHEPSTONE, L., DONELL, S. T. & THOMAS, T. L. 2005. Shock wave therapy for chronic Achilles tendon pain: a randomized placebo-controlled trial. *Clinical orthopaedics and related research*, 440, 199-204.
- COUPPE, C., KONGSGAARD, M., AAGAARD, P., HANSEN, P., BOJSEN-MOLLER, J., KJAER, M. & MAGNUSSON, S. P. 2008. Habitual loading results in tendon hypertrophy and increased stiffness of the human patellar tendon. *Journal of Applied Physiology*, 105, 805-810.
- COURVILLE, X. F., COE, M. P. & HECHT, P. J. 2009. Current Concepts Review: Noninsertional Achilles Tendinopathy. *Foot & Ankle International*, 30, 1132-1142.
- CRAMER, J., HOUSH, T., WEIR, J., JOHNSON, G., BERNING, J., PERRY, S. & BULL, A. 2004. Gender, muscle, and velocity comparisons of mechanomyographic and electromyographic responses during isokinetic muscle actions. *Scand J Med Sci Sports*, 14, 116-27.
- CREANEY, L., WALLACE, A., CURTIS, M. & CONNELL, D. 2011. Growth factor-based therapies provide additional benefit beyond physical therapy in resistant elbow tendinopathy: a prospective, single-blind, randomised trial of autologous blood injections versus platelet-rich plasma injections. *British journal of sports medicine*, 45, 966-71.
- CRESSWELL, A. G., LOSCHER, W. N. & THORSTENSSON, A. 1995. Influence of gastrocnemius muscle length on triceps surae torque development and electromyographic activity in man. *Experimental brain research. Experimentelle Hirnforschung. Experimentation cerebrale*, 105, 283-90.
- CROISIER, J. L., FORTHOMME, B., FOIDART-DESSALLE, M., GODON, B. & CRIELAARD, J. M. 2001. Treatment of recurrent tendinitis by isokinetic eccentric exercises. *Isokinetics and Exercise Science*, 9, 133-141.
- CSAPO, R., MAGANARIS, C. N., SEYNNES, O. R. & NARICI, M. V. 2010. On muscle, tendon and high heels. *The Journal of experimental biology*, 213, 2582-8.
- CUI, L., MAAS, H., PERREAULT, E. J. & SANDERCOCK, T. G. 2009. In situ estimation of tendon material properties: differences between muscles of the feline hindlimb. *Journal of biomechanics*, 42, 679-85.
- CUNNINGHAM, D. J. & ROMANES, G. J. 1986. Cunningham's manual of practical anatomy. *Oxford : Oxford University Press.*, v.1. Upper and lower limbs.
- DE JONGE, S., DE VOS, R. J., VAN SCHIE, H. T. M., VERHAAR, J. A. N., WEIR, A. & TOL, J. L. 2010. One-year follow-up of a randomised controlled trial on added splinting to eccentric exercises in chronic midportion Achilles tendinopathy. *British Journal of Sports Medicine*, 44, 673-677.
- DE JONGE, S., DE VOS, R. J., WEIR, A., VAN SCHIE, H. T., BIERMA-ZEINSTRAS, S. M., VERHAAR, J. A., WEINANS, H. & TOL, J. L. 2011a. One-Year Follow-up of Platelet-Rich Plasma Treatment in Chronic Achilles Tendinopathy: A Double-Blind Randomized Placebo-Controlled Trial. *The American journal of sports medicine*, 39, 1623-9.

- DE JONGE, S., VAN DEN BERG, C., DE VOS, R. J., VAN DER HEIDE, H. J., WEIR, A., VERHAAR, J. A., BIERMA-ZEINSTRAS, S. M. & TOL, J. L. 2011b. Incidence of midportion Achilles tendinopathy in the general population. *British journal of sports medicine*, 45, 1026-8.
- DE VOS, R. J., HEIJBOER, M. P., WEINANS, H., VERHAAR, J. A. & VAN SCHIE, J. T. 2012. Tendon structure's lack of relation to clinical outcome after eccentric exercises in chronic midportion Achilles tendinopathy. *J Sport Rehabil*, 21, 34-43.
- DE VOS, R. J., WEIR, A., COBBEN, L. P. J. & TOL, J. L. 2007a. The value of power Doppler ultrasonography in Achilles tendinopathy - A prospective study. *American Journal of Sports Medicine*, 35, 1696-1701.
- DE VOS, R. J., WEIR, A., VAN SCHIE, H. T. M., BIERMA-ZEINSTRAS, S. M. A., VERHAAR, J. A. N., WEINANS, H. & TOL, J. L. 2010. Platelet-Rich Plasma Injection for Chronic Achilles Tendinopathy A Randomized Controlled Trial. *Jama-Journal of the American Medical Association*, 303, 144-149.
- DE VOS, R. J., WEIR, A., VISSER, R. J. A., DE WINTER, T. & TOL, J. L. 2007b. The additional value of a night splint to eccentric exercises in chronic midportion Achilles tendinopathy: a randomised controlled trial. *British Journal of Sports Medicine*, 41, -.
- DEL BUONO, A., BATTERY, L., DENARO, V., MACCAURO, G. & MAFFULLI, N. 2011a. Tendinopathy and inflammation: some truths. *International journal of immunopathology and pharmacology*, 24, 45-50.
- DEL BUONO, A., PAPALIA, R., DENARO, V., MACCAURO, G. & MAFFULLI, N. 2011b. Platelet rich plasma and tendinopathy: state of the art. *International journal of immunopathology and pharmacology*, 24, 79-83.
- DIMITROV, V. G., ARABADZHIEV, T. I., DIMITROVA, N. A. & DIMITROV, G. V. 2012. The spectral changes in EMG during a second bout eccentric contraction could be due to adaptation in muscle fibres themselves: a simulation study. *European journal of applied physiology*, 112, 1399-409.
- DORAL, M. N., ALAM, M., BOZKURT, M., TURHAN, E., ATAY, O. A., DONMEZ, G. & MAFFULLI, N. 2010. Functional anatomy of the Achilles tendon. *Knee surgery, sports traumatology, arthroscopy : official journal of the ESSKA*, 18, 638-43.
- ELLIOTT, D. H. 1965. Structure and Function of Mammalian Tendon. *Biological reviews of the Cambridge Philosophical Society*, 40, 392-421.
- ENOKA, R. M. 1996. Eccentric contractions require unique activation strategies by the nervous system. *Journal of applied physiology*, 81, 2339-46.
- FAHLSTROM, M., JONSSON, P., LORENTZON, R. & ALFREDSON, H. 2003. Chronic Achilles tendon pain treated with eccentric calf-muscle training. *Knee Surg Sports Traumatol Arthrosc*, 11, 327-333.
- FARRIS, D. J. & SAWICKI, G. S. 2012. Human medial gastrocnemius force-velocity behavior shifts with locomotion speed and gait. *Proceedings of the National Academy of Sciences of the United States of America*, 109, 977-82.
- FARRIS, D. J., TREWARTHA, G. & MCGUIGAN, M. P. 2011. Could intra-tendinous hyperthermia during running explain chronic injury of the human Achilles tendon? *Journal of biomechanics*, 44, 822-6.
- FARRIS, D. J., TREWARTHA, G. & MCGUIGAN, M. P. 2012. The effects of a 30-min run on the mechanics of the human Achilles tendon. *European journal of applied physiology*, 112, 653-60.
- FARTHING, J. P. & CHILIBECK, P. D. 2003. The effects of eccentric and concentric training at different velocities on muscle hypertrophy. *Eur J Appl Physiol*, 89, 578-86.
- FINNI, T., HODGSON, J. A., LAI, A. M., EDGERTON, V. R. & SINHA, S. 2003. Nonuniform strain of human soleus aponeurosis-tendon complex during submaximal voluntary contractions in vivo. *Journal of applied physiology*, 95, 829-37.



- FINNOFF, J. T., FOWLER, S. P., LAI, J. K., SANTRACH, P. J., WILLIS, E. A., SAYEED, Y. A. & SMITH, J. 2011. Treatment of Chronic Tendinopathy with Ultrasound-Guided Needle Tenotomy and Platelet-Rich Plasma Injection. *PM & R : the journal of injury, function, and rehabilitation*.
- FLINT, D., PUGH, S. & CALLAGHAN, M. 2009. Eccentric Exercise in the Treatment of Achilles Tendinopathy. *Emergency Medicine Journal*, 26, 815-818.
- FRANZ, J. R. & KRAM, R. 2012. The effects of grade and speed on leg muscle activations during walking. *Gait & Posture*, 35, 143-147.
- FREDBERG, U., BOLVIG, L. & ANDERSEN, N. T. 2008. Prophylactic training in asymptomatic soccer players with ultrasonographic abnormalities in Achilles and patellar tendons - The Danish super league study. *American Journal of Sports Medicine*, 36, 451-460.
- FRIDEN, J. & LIEBER, R. L. 1995. Biomechanical injury to skeletal muscle from repetitive loading: Eccentric contractions and vibrations. *Repetitive Motion Disorders of the Upper Extremity*, 301-312.
- FRIEDRICH, T., SCHMIDT, W., JUNGMICHEL, D., HORN, L. C. & JOSTEN, C. 2001. Histopathology in rabbit Achilles tendon after operative tenolysis (longitudinal fiber incisions). *Scandinavian Journal of Medicine & Science in Sports*, 11, 4-8.
- FRIESENBICHLER, B., STIRLING, L. M., FEDEROLF, P. & NIGG, B. M. 2011. Tissue vibration in prolonged running. *J Biomech*, 44, 116-20.
- FUKASHIRO, S., KOMI, P. V., JARVINEN, M. & MIYASHITA, M. 1995. In vivo Achilles tendon loading during jumping in humans. *European journal of applied physiology and occupational physiology*, 71, 453-8.
- FUKUNAGA, T., KAWAKAMI, Y., KUBO, K. & KANEHISA, H. 2002. Muscle and tendon interaction during human movements. *Exercise and sport sciences reviews*, 30, 106-10.
- FURIA, J. P. 2008. High-energy extracorporeal shock wave therapy as a treatment for chronic noninsertional Achilles tendinopathy. *The American journal of sports medicine*, 36, 502-8.
- GARDIN, A., MOVIN, T., SVENSSON, L. & SHALABI, A. 2010. The long-term clinical and MRI results following eccentric calf muscle training in chronic Achilles tendinosis. *Skeletal Radiol*, 39, 435-442.
- GRASSME, R., STEGEMAN, D. F., DROST, G., SCHUMANN, N. P. & SCHOLLE, H. 2003. Selective spatial information from surface EMG after temporal filtering: the application to interference EMG using cross-covariance analysis. *Clinical neurophysiology : official journal of the International Federation of Clinical Neurophysiology*, 114, 2338-46.
- GRIFFIN, J. W. 1987. Differences in elbow flexion torque measured concentrically, eccentrically, and isometrically. *Physical therapy*, 67, 1205-8.
- GRIGG, N. L., WEARING, S. C., O'TOOLE, J. M. & SMEATHERS, J. E. 2012. Achilles Tendinopathy Modulates Force Frequency Characteristics of Eccentric Exercise. *Medicine and science in sports and exercise*.
- GRIGG, N. L., WEARING, S. C. & SMEATHERS, J. E. 2009. Eccentric calf muscle exercise produces a greater acute reduction in Achilles tendon thickness than concentric exercise. *British Journal of Sports Medicine*, 43, 280-283.
- GROOD, E. S. & SUNTAY, W. J. 1983. A joint coordinate system for the clinical description of three-dimensional motions: application to the knee. *Journal of biomechanical engineering*, 105, 136-44.
- GRUBER, M., LINNAMO, V., STROJNIK, V., RANTALAINEN, T. & AVELA, J. 2009. Excitability at the motoneuron pool and motor cortex is specifically modulated in lengthening compared to isometric contractions. *Journal of neurophysiology*, 101, 2030-40.
- GUIMARAES, A. C., HERZOG, W., HULLIGER, M., ZHANG, Y. T. & DAY, S. 1994. EMG-force relationship of the cat soleus muscle studied with distributed and non-periodic stimulation of ventral root filaments. *The Journal of experimental biology*, 186, 75-93.
- HALLIDAY, A. M. & REDFEARN, J. W. 1956. An analysis of the frequencies of finger tremor in healthy subjects. *J Physiol*, 134, 600-11.

- HATFIELD, D. L., KRAEMER, W. J., SPIERING, B. A., HAKKINEN, K., VOLEK, J. S., SHIMANO, T., SPREUWENBERG, L. P., SILVESTRE, R., VINGREN, J. L., FRAGALA, M. S., GOMEZ, A. L., FLECK, S. J., NEWTON, R. U. & MARESH, C. M. 2006a. The impact of velocity of movement on performance factors in resistance exercise. *Journal of strength and conditioning research / National Strength & Conditioning Association*, 20, 760-6.
- HATFIELD, D. L., KRAEMER, W. J., VOLEK, J. S., RUBIN, M. R., GREBIEN, B., GOMEZ, A. L., FRENCH, D. N., SCHEETT, T. P., RATAMESS, N. A., SHARMAN, M. J., MCGUIGAN, M. R., NEWTON, R. U. & HAKKINEN, K. 2006b. The effects of carbohydrate loading on repetitive jump squat power performance. *Journal of strength and conditioning research / National Strength & Conditioning Association*, 20, 167-71.
- HEDAYATPOUR, N. & FALLA, D. 2012. Non-uniform muscle adaptations to eccentric exercise and the implications for training and sport. *Journal of electromyography and kinesiology : official journal of the International Society of Electrophysiological Kinesiology*, 22, 329-33.
- HEDAYATPOUR, N., FALLA, D., ARENDT-NIELSEN, L. & FARINA, D. 2008. Sensory and electromyographic mapping during delayed-onset muscle soreness. *Medicine and science in sports and exercise*, 40, 326-34.
- HEDAYATPOUR, N., FALLA, D., ARENDT-NIELSEN, L. & FARINA, D. 2010. Effect of delayed-onset muscle soreness on muscle recovery after a fatiguing isometric contraction. *Scandinavian journal of medicine & science in sports*, 20, 145-53.
- HENRIKSEN, M., AABOE, J., BLIDDAL, H. & LANGBERG, H. 2009. Biomechanical characteristics of the eccentric Achilles tendon exercise. *Journal of Biomechanics*, 42, 2702-2707.
- HERMENS, H. J., BOON, K. L. & ZILVOLD, G. 1986. The clinical use of surface EMG. *Acta Belg Med Phys*, 9, 119-30.
- HERMENS, H. J., FRERIKS, B., DISSELHORST-KLUG, C. & RAU, G. 2000. Development of recommendations for SEMG sensors and sensor placement procedures. *J Electromyogr Kinesiol*, 10, 361-74.
- HERRINGTON, L. & MCCULLOCH, R. 2007. The role of eccentric training in the management of Achilles tendinopathy: A pilot study. *Physical Therapy in Sport*, 8, 191-196.
- HESS, G. P., CAPIELLO, W. L., POOLE, R. M. & HUNTER, S. C. 1989. Prevention and Treatment of Overuse Tendon Injuries. *Sports Medicine*, 8, 371-384.
- HILL, A. V. 1970. First and Last Experiments in Muscle Mechanics. *Cambridge, UK: Cambridge Univ. Press*, 23-37.
- HOF, A. L. 1998. In vivo measurement of the series elasticity release curve of human triceps surae muscle. *Journal of biomechanics*, 31, 793-800.
- HOF, A. L. 2003. Muscle mechanics and neuromuscular control. *Journal of biomechanics*, 36, 1031-8.
- HOFFMAN, A. H., ROBICHAUD II, D. R., DUQUETTE, J. J. & GRIGG, P. 2005. Determining the effect of hydration upon the properties of ligaments using pseudo Gaussian stress stimuli. *Journal of biomechanics*, 38, 1636-1642.
- HOLTERMANN, A., ROELEVELD, K. & KARLSSON, J. S. 2005. Inhomogeneities in muscle activation reveal motor unit recruitment. *Journal of electromyography and kinesiology : official journal of the International Society of Electrophysiological Kinesiology*, 15, 131-7.
- HORTOBAGYI, T. & KATCH, F. I. 1990. Eccentric and concentric torque-velocity relationships during arm flexion and extension. Influence of strength level. *European journal of applied physiology and occupational physiology*, 60, 395-401.
- HOWELL, J. N., FUGLEVAND, A. J., WALSH, M. L. & BIGLAND-RITCHIE, B. 1995. Motor unit activity during isometric and concentric-eccentric contractions of the human first dorsal interosseus muscle. *Journal of neurophysiology*, 74, 901-4.
- HUMPHREY, J., CHAN, O., CRISP, T., PADHIAR, N., MORRISSEY, D., TWYLCROSS-LEWIS, R., KING, J. & MAFFULLI, N. 2010. The short-term effects of high volume image guided injections in resistant non-insertional Achilles tendinopathy. *Journal of Science and Medicine in Sport*, 13, 295-298.

- JAMIESON, E. B., WALMSLEY, R. & MURPHY, T. R. 1971. Jamieson's illustrations of regional anatomy. Section 7, Lower limb. *Edinburgh [Teviot Place, Edinburgh] : Churchill Livingstone.*
- JARVINEN, T. A., KANNUS, P., MAFFULLI, N. & KHAN, K. M. 2005. Achilles tendon disorders: etiology and epidemiology. *Foot and ankle clinics*, 10, 255-66.
- JARVINEN, T. A., KANNUS, P., PAAVOLA, M., JARVINEN, T. L., JOZSA, L. & JARVINEN, M. 2001. Achilles tendon injuries. *Current opinion in rheumatology*, 13, 150-5.
- JONES, D., ROUND, J. & DE HAAN, A. 2004. Chapter 1 - Structure of the muscle fibre. *Skeletal Muscle from Molecules to Movement*. Edinburgh: Churchill Livingstone.
- JONSSON, P., ALFREDSON, H., SUNDING, K., FAHLSTROM, M. & COOK, J. 2008. New regimen for eccentric calf-muscle training in patients with chronic insertional Achilles tendinopathy: results of a pilot study. *British Journal of Sports Medicine*, 42, 746-749.
- JOYCE, G. C. & RACK, P. M. 1974. The effects of load and force on tremor at the normal human elbow joint. *J Physiol*, 240, 375-96.
- JOZSA, L. & KANNUS, P. 1997. Human tendons: anatomy, physiology and pathology. *Champaign, IL: Human Kinetics.*
- KADER, D., SAXENA, A., MOVIN, T. & MAFFULLI, N. 2002. Achilles tendinopathy: some aspects of basic science and clinical management. *British Journal of Sports Medicine*, 36, 239-49.
- KANE, T. P., ISMAIL, M. & CALDER, J. D. 2008. Topical glyceryl trinitrate and noninsertional Achilles tendinopathy: a clinical and cellular investigation. *The American journal of sports medicine*, 36, 1160-3.
- KANNUS, P. 1997. Etiology and pathophysiology of chronic tendon disorders in sports. *Scandinavian Journal of Medicine & Science in Sports*, 7, 78-85.
- KANNUS, P. 2000. Structure of the tendon connective tissue. *Scandinavian journal of medicine & science in sports*, 10, 312-20.
- KANNUS, P. & JOZSA, L. 1991. Histopathological changes preceding spontaneous rupture of a tendon. A controlled study of 891 patients. *The Journal of bone and joint surgery. American volume*, 73, 1507-25.
- KASTELIC, J., GALESKI, A. & BAER, E. 1978. Multicomposite Structure of Tendon. *Connective Tissue Research*, 6, 11-23.
- KEARNEY, R. & COSTA, M. L. 2010. Insertional Achilles Tendinopathy Management: A Systematic Review. *Foot & Ankle International*, 31, 689-694.
- KELLIS, E. & BALTZOPOULOS, V. 1995. Isokinetic eccentric exercise. *Sports medicine*, 19, 202-22.
- KELLIS, E. & BALTZOPOULOS, V. 1998. Muscle activation differences between eccentric and concentric isokinetic exercise. *Med Sci Sports Exerc*, 30, 1616-23.
- KER, R. F. 1981. Dynamic tensile properties of the plantaris tendon of sheep (*Ovis aries*). *The Journal of experimental biology*, 93, 283-302.
- KHAN, K. M., COOK, J. L., BONAR, F., HARCOURT, P. & ASTROM, M. 1999. Histopathology of common tendinopathies. Update and implications for clinical management. *Sports Medicine*, 27, 393-408.
- KHAN, K. M., COOK, J. L., MAFFULLI, N. & KANNUS, P. 2000. Where is the pain coming from in tendinopathy? It may be biochemical, not only structural, in origin. *British Journal of Sports Medicine*, 34, 81-3.
- KHAN, K. M., FORSTER, B. B., ROBINSON, J., CHEONG, Y., LOUIS, L., MACLEAN, L. & TAUNTON, J. E. 2003. Are ultrasound and magnetic resonance imaging of value in assessment of Achilles tendon disorders? A two year prospective study. *British journal of sports medicine*, 37, 149-53.
- KINDERMANN, W., BONING, D., SCHMITT, H., NIESS, A., STEINACKER, J. M. & FLEISCHER, S. 2010. German Sports Medicine in 2009. *Deutsche Zeitschrift Fur Sportmedizin*, 61, 181-189.
- KINGMA, J. J., DE KNIKKER, R., WITTINK, H. M. & TAKKEN, T. 2007. Eccentric overload training in patients with chronic Achilles tendinopathy: a systematic review. *Br J Sports Med*, 41.

- KINUGASA, R., KAWAKAMI, Y. & FUKUNAGA, T. 2005. Muscle activation and its distribution within human triceps surae muscles. *Journal of applied physiology*, 99, 1149-56.
- KINUGASA, R., KAWAKAMI, Y., SINHA, S. & FUKUNAGA, T. 2011. Unique spatial distribution of in vivo human muscle activation. *Experimental physiology*, 96, 938-48.
- KIRKENDALL, D. T. & GARRETT, W. E. 1997. Function and biomechanics of tendons. *Scandinavian Journal of Medicine & Science in Sports*, 7, 62-66.
- KJAER, M., LANGBERG, H. & MAGNUSSON, P. 2003. [Overuse injuries in tendon tissue: insight into adaptation mechanisms]. *Ugeskrift for laeger*, 165, 1438-43.
- KLEINE, B. U., SCHUMANN, N. P., STEGEMAN, D. F. & SCHOLLE, H. C. 2000. Surface EMG mapping of the human trapezius muscle: the topography of monopolar and bipolar surface EMG amplitude and spectrum parameters at varied forces and in fatigue. *Clinical neurophysiology : official journal of the International Federation of Clinical Neurophysiology*, 111, 686-93.
- KNOBLOCH, K. 2007. Eccentric training in Achilles tendinopathy: is it harmful to tendon microcirculation? *British Journal of Sports Medicine*, 41, -.
- KNOBLOCH, K. 2009. Eccentric Training and the Science Behind. *Medicine and Science in Sports and Exercise*, 41, 251-251.
- KNOBLOCH, K., SCHREIBMUELLER, L., KRAEMER, R., JAGODZINSKI, M., VOGT, P. M. & REDEKER, J. 2010. Gender and eccentric training in Achilles mid-portion tendinopathy. *Knee Surgery Sports Traumatology Arthroscopy*, 18, 648-655.
- KNOBLOCH, K., SCHREIBMUELLER, L., LONGO, U. G. & VOGT, P. M. 2008a. Eccentric exercises for the management of tendinopathy of the main body of the Achilles tendon with or without an AirHeel Brace. A randomized controlled trial. B: Effects of compliance. *Disability and Rehabilitation*, 30, 1692-1696.
- KNOBLOCH, K., YOON, U. & VOGT, P. M. 2008b. Acute and overuse injuries correlated to hours of training in master running athletes. *Foot & ankle international / American Orthopaedic Foot and Ankle Society [and] Swiss Foot and Ankle Society*, 29, 671-6.
- KNOBLOCK, K., KRAEMER, R., JAGODZINSKI, M., ZEICHEN, J., MELLER, R. & VOGT, P. M. 2007. Eccentric training decreases paratendon capillary blood flow and preserves paratendon oxygen saturation in chronic achilles tendinopathy. *Journal of Orthopaedic & Sports Physical Therapy*, 37, 269-276.
- KOMI, P. V., FUKASHIRO, S. & JARVINEN, M. 1992. Biomechanical loading of Achilles tendon during normal locomotion. *Clinics in sports medicine*, 11, 521-31.
- KON, E., FILARDO, G., DELCOGLIANO, M., LO PRESTI, M., RUSSO, A., BONDI, A., MARTINO, A., CENACCHI, A., FORNASARI, P. M. & MARCACCI, M. 2009. Platelet-rich plasma: New clinical application A pilot study for treatment of jumper's knee. *Injury-International Journal of the Care of the Injured*, 40, 598-603.
- KONGSGAARD, M., KOVANEN, V., AAGAARD, P., DOESSING, S., HANSEN, P., LAURSEN, A. H., KALDAU, N. C., KJAER, M. & MAGNUSSON, S. P. 2009. Corticosteroid injections, eccentric decline squat training and heavy slow resistance training in patellar tendinopathy. *Scandinavian Journal of Medicine & Science in Sports*, 19, 790-802.
- KORSTANJE, J. W., SELLES, R. W., STAM, H. J., HOVIUS, S. E. & BOSCH, J. G. 2010. Development and validation of ultrasound speckle tracking to quantify tendon displacement. *Journal of biomechanics*, 43, 1373-9.
- KOUNTOURIS, A. & COOK, J. 2007. Rehabilitation of Achilles and patellar tendinopathies. *Best Practice & Research in Clinical Rheumatology*, 21, 295-316.
- KUBO, K., KANEHISA, H. & FUKUNAGA, T. 2002a. Effects of resistance and stretching training programmes on the viscoelastic properties of human tendon structures in vivo. *The Journal of physiology*, 538, 219-26.
- KUBO, K., KANEHISA, H. & FUKUNAGA, T. 2003. Gender differences in the viscoelastic properties of tendon structures. *European journal of applied physiology*, 88, 520-6.

- KUBO, K., KAWAKAMI, Y., KANEHISA, H. & FUKUNAGA, T. 2002b. Measurement of viscoelastic properties of tendon structures in vivo. *Scandinavian journal of medicine & science in sports*, 12, 3-8.
- KUES, J., ROTHSTEIN, J. & LAMB, R. 1994. The relationships among knee extensor torques produced during maximal voluntary contractions under various test conditions. *Phys Ther*, 74, 674-83.
- KULIG, K., LEDERHAUS, E. S., REISCHL, S., ARYA, S. & BASHFORD, G. 2009. Effect of Eccentric Exercise Program for Early Tibialis Posterior Tendinopathy. *Foot & Ankle International*, 30, 877-885.
- LAIDLAW D., Y. G. H., ALEXANDER A. L., GMITRO A. F., UNGER E. C., ENOKA R. M. 1994. Nonhomogeneous and task-dependent activation of first dorsal interosseus muscle. *Soc. Neurosci. Abstr.* 20:386.
- LANGBERG, H., ELLINGSGAARD, H., MADSEN, T., JANSSON, J., MAGNUSSON, S. P., AAGAARD, P. & KJAER, M. 2007. Eccentric rehabilitation exercise increases peritendinous type I collagen synthesis in humans with Achilles tendinosis. *Scandinavian Journal of Medicine & Science in Sports*, 17, 61-66.
- LASTAYO, P. C., WOOLF, J. M., LEWEK, M. D., SNYDER-MACKLER, L., REICH, T. & LINDSTEDT, S. L. 2003. Eccentric muscle contractions: their contribution to injury, prevention, rehabilitation, and sport. *The Journal of orthopaedic and sports physical therapy*, 33, 557-71.
- LAVAGNINO, M., ARNOCKY, S. P., TIAN, T. & VAUPEL, Z. 2003. Effect of amplitude and frequency of cyclic tensile strain on the inhibition of MMP-1 mRNA expression in tendon cells: an in vitro study. *Connective tissue research*, 44, 181-7.
- LICHTWARK, G. A. & WILSON, A. M. 2005a. Effects of series elasticity and activation conditions on muscle power output and efficiency. *The Journal of experimental biology*, 208, 2845-53.
- LICHTWARK, G. A. & WILSON, A. M. 2005b. In vivo mechanical properties of the human Achilles tendon during one-legged hopping. *The Journal of experimental biology*, 208, 4715-25.
- LOH, E. Y., AGUR, A. M. & MCKEE, N. H. 2003. Intramuscular innervation of the human soleus muscle: a 3D model. *Clinical anatomy*, 16, 378-82.
- LONGO, U. G., RONGA, M. & MAFFULLI, N. 2009. Achilles tendinopathy. *Sports medicine and arthroscopy review*, 17, 112-26.
- LORAM, I. D., MAGANARIS, C. N. & LAKIE, M. 2006. Use of ultrasound to make noninvasive in vivo measurement of continuous changes in human muscle contractile length. *Journal of applied physiology*, 100, 1311-23.
- LUMLEY, J. S. P. 2008. *Surface anatomy: the anatomical basis of clinical examination*, Edinburgh, Churchill Livingstone.
- MAFFULLI, N., KHAN, K. M. & PUDDU, G. 1998. Overuse tendon conditions: time to change a confusing terminology. *Arthroscopy*, 14, 840-3.
- MAFFULLI, N. & LONGO, U. G. 2008. How do eccentric exercises work in tendinopathy? *Rheumatology*, 47, 1444-1445.
- MAFFULLI, N., LONGO, U. G., LOPPINI, M. & DENARO, V. 2010. Current treatment options for tendinopathy. *Expert Opinion on Pharmacotherapy*, 11, 2177-86.
- MAFFULLI, N., LONGO, U. G., MAFFULLI, G. D., KHANNA, A. & DENARO, V. 2011a. Achilles tendon ruptures in elite athletes. *Foot & ankle international / American Orthopaedic Foot and Ankle Society [and] Swiss Foot and Ankle Society*, 32, 9-15.
- MAFFULLI, N., LONGO, U. G., SPIEZIA, F. & DENARO, V. 2011b. Aetiology and prevention of injuries in elite young athletes. *Medicine and sport science*, 56, 187-200.
- MAFFULLI, N., SHARMA, P. & LUSCOMBE, K. L. 2004. Achilles tendinopathy: aetiology and management. *Journal of the Royal Society of Medicine*, 97, 472-6.
- MAFFULLI, N., TESTA, V., CAPASSO, G., OLIVA, F., PANNI, A. S., LONGO, U. G. & KING, J. B. 2008a. Surgery for chronic Achilles tendinopathy produces worse results in women. *Disability and rehabilitation*, 30, 1714-20.
- MAFFULLI, N., WALLEY, G., SAYANA, M. K., LONGO, U. G. & DENARO, V. 2008b. Eccentric calf muscle training in athletic patients with Achilles tendinopathy. *Disabil Rehabil*, 30, 1677-1684.

- MAFFULLI, N., WONG, J. & ALMEKINDERS, L. C. 2003. Types and epidemiology of tendinopathy. *Clinics in Sports Medicine*, 22, 675-92.
- MAFI, N., LORENTZON, R. & ALFREDSON, H. 2001. Superior short-term results with eccentric calf muscle training compared to concentric training in a randomized prospective multicenter study on patients with chronic Achilles tendinosis. *Knee Surg Sports Traumatol Arthrosc*, 9, 42-7.
- MAFI N, L. R., ALFREDSON H. 2001. Superior short-term results with eccentric calf muscle training compared to concentric training in a randomized prospective multicenter study on patients with chronic Achilles tendinosis. *Knee Surg Sports Traumatol Arthrosc.*, 9, 42-7.
- MAGANARIS, C. N. 2002. Tensile properties of in vivo human tendinous tissue. *Journal of biomechanics*, 35, 1019-27.
- MAGANARIS, C. N., NARICI, M. V. & MAFFULLI, N. 2008. Biomechanics of the Achilles tendon. *Disability and rehabilitation*, 30, 1542-7.
- MAGANARIS, C. N. & PAUL, J. P. 1999. In vivo human tendon mechanical properties. *J Physiol*, 521 Pt 1, 307-13.
- MAGANARIS, C. N. & PAUL, J. P. 2002. Tensile properties of the in vivo human gastrocnemius tendon. *Journal of biomechanics*, 35, 1639-46.
- MAGNUSSON, R. A., DUNN, W. R. & THOMSON, A. B. 2009. Nonoperative Treatment of Midportion Achilles Tendinopathy: A Systematic Review. *Clinical Journal of Sport Medicine*, 19, 54-64.
- MAGNUSSON, S. P., HANSEN, P., AAGAARD, P., BROND, J., DYHRE-POULSEN, P., BOJSEN-MOLLER, J. & KJAER, M. 2003. Differential strain patterns of the human gastrocnemius aponeurosis and free tendon, in vivo. *Acta physiologica Scandinavica*, 177, 185-95.
- MAGNUSSON, S. P., NARICI, M. V., MAGANARIS, C. N. & KJAER, M. 2008. Human tendon behaviour and adaptation, in vivo. *Journal of Physiology-London*, 586, 71-81.
- MAHIEU, N. N., MCNAIR, P., COOLS, A., D'HAEN, C., VANDERMEULEN, K. & WITVROUW, E. 2008. Effect of eccentric training on the plantar flexor muscle-tendon tissue properties. *Med Sci Sports Exerc*, 40, 117-23.
- MALM, C., NYBERG, P., ENGSTROM, M., SJODIN, B., LENKEI, R., EKBLUM, B. & LUNDBERG, I. 2000. Immunological changes in human skeletal muscle and blood after eccentric exercise and multiple biopsies. *J Physiol*, 529 Pt 1, 243-62.
- MARSDEN, C. D., FOLEY, T. H., OWEN, D. A. & MCALLISTER, R. G. 1967a. Peripheral beta-adrenergic receptors concerned with tremor. *Clin Sci*, 33, 53-65.
- MARSDEN, C. D., MEADOWS, J. C., LANGE, G. W. & WATSON, R. S. 1967b. Effect of deafferentation on human physiological tremor. *Lancet*, 2, 700-2.
- MCAULEY, J. H. & MARSDEN, C. D. 2000. Physiological and pathological tremors and rhythmic central motor control. *Brain*, 123 ( Pt 8), 1545-67.
- MCGOWAN, C. P., DUARTE, H. A., MAIN, J. B. & BIEWENER, A. A. 2006. Effects of load carrying on metabolic cost and hindlimb muscle dynamics in guinea fowl (*Numida meleagris*). *Journal of applied physiology*, 101, 1060-9.
- MCMAHON, T. A. & CHENG, G. C. 1990. The mechanics of running: how does stiffness couple with speed? *Journal of biomechanics*, 23 Suppl 1, 65-78.
- MEI-DAN, O., LIPPI, G., SANCHEZ, M., ANDIA, I. & MAFFULLI, N. 2010. Autologous platelet-rich plasma: a revolution in soft tissue sports injury management? *The Physician and sportsmedicine*, 38, 127-35.
- MERLETTI, R., BOTTER, A., TROIANO, A., MERLO, E. & MINETTO, M. A. 2009. Technology and instrumentation for detection and conditioning of the surface electromyographic signal: state of the art. *Clinical biomechanics*, 24, 122-34.
- MEYER, A., TUMILTY, S. & BAXTER, G. D. 2009. Eccentric exercise protocols for chronic non-insertional Achilles tendinopathy: how much is enough? *Scandinavian Journal of Medicine & Science in Sports*, 19, 609-615.

- MOLLER, A., ASTRON, M. & WESTLIN, N. 1996. Increasing incidence of Achilles tendon rupture. *Acta Orthop Scand*, 67, 479-81.
- MOORE, M. J. & DE BEAUX, A. 1987. A quantitative ultrastructural study of rat tendon from birth to maturity. *Journal of anatomy*, 153, 163-9.
- MORITANI, T., MURAMATSU, S. & MURO, M. 1987. Activity of motor units during concentric and eccentric contractions. *Am J Phys Med*, 66, 338-50.
- MORRISSEY, D., ROSKILLY, A., TWYLCROSS-LEWIS, R., ISINKAYE, T., SCREEN, H., WOLEDGE, R. & BADER, D. 2011. The effect of eccentric and concentric calf muscle training on Achilles tendon stiffness. *Clinical rehabilitation*, 25, 238-47.
- MURAMATSU, T., MURAOKA, T., TAKESHITA, D., KAWAKAMI, Y., HIRANO, Y. & FUKUNAGA, T. 2001. Mechanical properties of tendon and aponeurosis of human gastrocnemius muscle in vivo. *Journal of applied physiology*, 90, 1671-8.
- MURAOKA, T., MURAMATSU, T., FUKUNAGA, T. & KANEHISA, H. 2005. Elastic properties of human Achilles tendon are correlated to muscle strength. *J Appl Physiol*, 99, 665-9.
- NARDONE, A., ROMANO, C. & SCHIEPPATI, M. 1989. Selective recruitment of high-threshold human motor units during voluntary isotonic lengthening of active muscles. *J Physiol*, 409, 451-71.
- NG, B. H., CHOU, S. M., LIM, B. H. & CHONG, A. 2004. Strain rate effect on the failure properties of tendons. *Proc Inst Mech Eng H*, 218, 203-6.
- NICOLLE, S. & PALIERNE, J. F. 2010. Dehydration effect on the mechanical behaviour of biological soft tissues: Observations on kidney tissues. *Journal of the Mechanical Behavior of Biomedical Materials*, 3, 630-635.
- NIGG, B. M. 1997. Impact forces in running. *Curr Opin Orthop* 8, 43-47.
- NIGG, B. M. & HERZOG, W. 2007. Biomechanics of the musculo-skeletal system. *John Wiley & Sons*, (3rd ed).
- NORREGAARD, J., LARSEN, C. C., BIELER, T. & LANGBERG, H. 2007. Eccentric exercise in treatment of Achilles tendinopathy. *Scandinavian Journal of Medicine & Science in Sports*, 17, 133-138.
- NOSAKA, K., SAKAMOTO, K., NEWTON, M. & SACCO, P. 2001. The repeated bout effect of reduced-load eccentric exercise on elbow flexor muscle damage. *European journal of applied physiology*, 85, 34-40.
- NOYES, F. R., DELUCAS, J. L. & TORVIK, P. J. 1974. Biomechanics of anterior cruciate ligament failure: an analysis of strain-rate sensitivity and mechanisms of failure in primates. *The Journal of bone and joint surgery. American volume*, 56, 236-53.
- O'BRIEN, M. 1992. Functional anatomy and physiology of tendons. *Clinics in Sports Medicine*, 11, 505-20.
- OHBERG, L., LORENTZON, R. & ALFREDSON, H. 2004. Eccentric training in patients with chronic Achilles tendinosis: normalised tendon structure and decreased thickness at follow up. *British journal of sports medicine*, 38, 8-11; discussion 11.
- ONO, T., OKUWAKI, T. & FUKUBAYASHI, T. 2010. Differences in activation patterns of knee flexor muscles during concentric and eccentric exercises. *Research in sports medicine*, 18, 188-98.
- PAGENSTERT, G., LEUMANN, A., FRIGG, A. & VALDERRABANO, V. 2010. Achilles tendon ruptures and tibialis anterior tendon ruptures. *Orthopedist*, 39, 1135-1147.
- PAOLONI, J. A., APPELYARD, R. C., NELSON, J. & MURRELL, G. A. 2004. Topical glyceryl trinitrate treatment of chronic noninsertional achilles tendinopathy. A randomized, double-blind, placebo-controlled trial. *The Journal of bone and joint surgery. American volume*, 86-A, 916-22.
- PAOLONI, J. A., APPELYARD, R. C., NELSON, J. & MURRELL, G. A. 2005. Topical glyceryl trinitrate application in the treatment of chronic supraspinatus tendinopathy: a randomized, double-blinded, placebo-controlled clinical trial. *The American journal of sports medicine*, 33, 806-13.

- PAOLONI, J. A. & MURRELL, G. A. 2007. Three-year followup study of topical glyceryl trinitrate treatment of chronic noninsertional Achilles tendinopathy. *Foot & ankle international / American Orthopaedic Foot and Ankle Society [and] Swiss Foot and Ankle Society*, 28, 1064-8.
- PARK, D. Y., RUBENSON, J., CARR, A., MATTSON, J., BESIER, T. & CHOU, L. B. 2011. Influence of stretching and warm-up on Achilles tendon material properties. *Foot & ankle international / American Orthopaedic Foot and Ankle Society [and] Swiss Foot and Ankle Society*, 32, 407-13.
- PARRY, D. A., BARNES, G. R. & CRAIG, A. S. 1978. A comparison of the size distribution of collagen fibrils in connective tissues as a function of age and a possible relation between fibril size distribution and mechanical properties. *Proceedings of the Royal Society of London. Series B, Containing papers of a Biological character. Royal Society*, 203, 305-21.
- PASCHALIS, V., KOUTEDAKIS, Y., JAMURTAS, A. Z., MOUGIOS, V. & BALTZOPOULOS, V. 2005. Equal volumes of high and low intensity of eccentric exercise in relation to muscle damage and performance. *Journal of strength and conditioning research / National Strength & Conditioning Association*, 19, 184-8.
- PEARSON, S. J., BURGESS, K. & ONAMBELE, G. N. 2007. Creep and the in vivo assessment of human patellar tendon mechanical properties. *Clinical biomechanics*, 22, 712-7.
- PEERS, K. H. E. & LYSENS, R. J. J. 2005. Patellar tendinopathy in athletes - Current diagnostic and therapeutic recommendations. *Sports Medicine*, 35, 71-87.
- PELTONEN, J., CRONIN, N. J., AVELA, J. & FINNI, T. 2010. In vivo mechanical response of human Achilles tendon to a single bout of hopping exercise. *The Journal of experimental biology*, 213, 1259-65.
- PETERSEN, W., WELP, R. & ROSENBAUM, D. 2007. Chronic Achilles tendinopathy - A prospective randomized study comparing the therapeutic effect of eccentric training, the AirHeel brace, and a combination of both. *American Journal of Sports Medicine*, 35, 1659-1667.
- PFEFER, M. T., COOPER, S. R. & UHL, N. L. 2009. Chiropractic Management of Tendinopathy: A Literature Synthesis. *Journal of Manipulative and Physiological Therapeutics*, 32, 41-52.
- POLLOCK, R. D., MARTIN, F. C. & NEWHAM, D. J. 2012. Whole-body vibration in addition to strength and balance exercise for falls-related functional mobility of frail older adults: a single-blind randomized controlled trial. *Clinical rehabilitation*, 26, 915-23.
- POLLOCK, R. D., WOLEDGE, R. C., MILLS, K. R., MARTIN, F. C. & NEWHAM, D. J. 2010. Muscle activity and acceleration during whole body vibration: effect of frequency and amplitude. *Clinical biomechanics*, 25, 840-6.
- PORTNEY, L. G. & WATKINS, M. P. 2009. Foundations of Clinical Research Application to Practice. *Third edition, Prentice Hall.*, 416 - 424.
- QI, L., WAKELING, J. M. & FERGUSON-PELL, M. 2011a. Spectral properties of electromyographic and mechanomyographic signals during dynamic concentric and eccentric contractions of the human biceps brachii muscle. *Journal of electromyography and kinesiology : official journal of the International Society of Electrophysiological Kinesiology*, 21, 1056-63.
- QI, L., WAKELING, J. M., GREEN, A., LAMBRECHT, K. & FERGUSON-PELL, M. 2011b. Spectral properties of electromyographic and mechanomyographic signals during isometric ramp and step contractions in biceps brachii. *Journal of electromyography and kinesiology : official journal of the International Society of Electrophysiological Kinesiology*, 21, 128-35.
- REES, J. D., LICHTWARK, G. A., WOLMAN, R. L. & WILSON, A. M. 2008. The mechanism for efficacy of eccentric loading in Achilles tendon injury; an in vivo study in humans. *Rheumatology*, 47, 1493-1497.
- REEVES, N. & NARICI, M. 2003. Behavior of human muscle fascicles during shortening and lengthening contractions in vivo. *J Appl Physiol*, 95, 1090-6.
- REEVES, N. D., MAGANARIS, C. N., FERRETTI, G. & NARICI, M. V. 2005. Influence of 90-day simulated microgravity on human tendon mechanical properties and the effect of resistive countermeasures. *Journal of applied physiology*, 98, 2278-86.



- REEVES, N. D., MAGANARIS, C. N. & NARICI, M. V. 2003a. Effect of strength training on human patella tendon mechanical properties of older individuals. *The Journal of physiology*, 548, 971-81.
- REEVES, N. D., NARICI, M. V. & MAGANARIS, C. N. 2003b. Strength training alters the viscoelastic properties of tendons in elderly humans. *Muscle & nerve*, 28, 74-81.
- REEVES, N. D., NARICI, M. V. & MAGANARIS, C. N. 2004. In vivo human muscle structure and function: adaptations to resistance training in old age. *Exp Physiol*, 89, 675-89.
- REID, D., MCNAIR, P. J., JOHNSON, S., POTTS, G., WITVROUW, E. & MAHIEU, N. 2012. Electromyographic analysis of an eccentric calf muscle exercise in persons with and without Achilles tendinopathy. *Physical Therapy in Sport*, 13, 150-155.
- RICHARDS, J., THEWLIS, D., SELFE, J., CUNNINGHAM, A. & HAYES, C. 2008. A biomechanical investigation of a single-limb squat: Implications for lower extremity rehabilitation exercise. *Journal of Athletic Training*, 43, 477-482.
- RICHARDS, P. J., MCCALL, I. W., DAY, C., BELCHER, J. & MAFFULLI, N. 2010. Longitudinal microvascularity in Achilles tendinopathy (power Doppler ultrasound, magnetic resonance imaging time-intensity curves and the Victorian Institute of Sport Assessment-Achilles questionnaire): a pilot study. *Skeletal Radiology*, 39, 509-521.
- RIGBY, B. J., HIRAI, N., SPIKES, J. D. & EYRING, H. 1959. The Mechanical Properties of Rat Tail Tendon. *J Gen Physiol*, 43, 265-83.
- RILEY, G. 2004. The pathogenesis of tendinopathy. A molecular perspective. *Rheumatology*, 43, 131-142.
- RILEY, G. P., HARRALL, R. L., CONSTANT, C. R., CHARD, M. D., CAWSTON, T. E. & HAZLEMAN, B. L. 1994. Tendon degeneration and chronic shoulder pain: changes in the collagen composition of the human rotator cuff tendons in rotator cuff tendinitis. *Ann Rheum Dis*, 53, 359-66.
- ROBINSON, J. M., COOK, J. L., PURDAM, C., VISENTINI, P. J., ROSS, J., MAFFULLI, N., TAUNTON, J. E. & KHAN, K. M. 2001. The VISA-A questionnaire: a valid and reliable index of the clinical severity of Achilles tendinopathy. *British journal of sports medicine*, 35, 335-41.
- RODGERS, K. L. & BERGER, R. A. 1974. Motor-unit involvement and tension during maximum, voluntary concentric, eccentric, and isometric contractions of the elbow flexors. *Med Sci Sports*, 6, 253-9.
- ROIG, M., O'BRIEN, K., KIRK, G., MURRAY, R., MCKINNON, P., SHADGAN, B. & REID, W. D. 2009. The effects of eccentric versus concentric resistance training on muscle strength and mass in healthy adults: a systematic review with meta-analysis. *British journal of sports medicine*, 43, 556-68.
- ROMPE, J. D., FURIA, J. & MAFFULLI, N. 2009. Eccentric loading versus eccentric loading plus shock-wave treatment for midportion achilles tendinopathy: a randomized controlled trial. *The American journal of sports medicine*, 37, 463-70.
- ROMPE, J. D., NAFE, B., FURIA, J. P. & MAFFULLI, N. 2007. Eccentric loading, shock-wave treatment, or a wait-and-see policy for tendinopathy of the main body of tendo achillis - A randomized controlled trial. *American Journal of Sports Medicine*, 35, 374-383.
- ROOS, E. M., ENGSTROM, M., LAGERQUIST, A. & SODERBERG, B. 2004. Clinical improvement after 6 weeks of eccentric exercise in patients with mid-portion Achilles tendinopathy - a randomized trial with 1-year follow-up. *Scandinavian Journal of Medicine & Science in Sports*, 14, 286-295.
- ROWE, V., HEMMINGS, S., BARTON, C., MALLIARAS, P., MAFFULLI, N. & MORRISSEY, D. 2012. Conservative management of midportion achilles tendinopathy: a mixed methods study, integrating systematic review and clinical reasoning. *Sports medicine*, 42, 941-67.
- RUBIN, C., TURNER, A. S., BAIN, S., MALLINCKRODT, C. & MCLEOD, K. 2001. Anabolism. Low mechanical signals strengthen long bones. *Nature*, 412, 603-4.
- SASAKI, K. & NEPTUNE, R. R. 2006. Muscle mechanical work and elastic energy utilization during walking and running near the preferred gait transition speed. *Gait & posture*, 23, 383-90.

- SATYENDRA, L. & BYL, N. 2006. Effectiveness of physical therapy for Achilles tendinopathy: An evidence based review of eccentric exercises. *Isokinetics and Exercise Science*, 14, 71-80.
- SAYANA, M. K. & MAFFULLI, N. 2007. Eccentric calf muscle training in non-athletic patients with Achilles tendinopathy. *J Sci Med Sport*, 10, 52-58.
- SCHOLLE, H. C., SCHUMANN, N. P., BIEDERMANN, F., STEGEMAN, D. F., GRASSME, R., ROELEVELD, K., SCHILLING, N. & FISCHER, M. S. 2001. Spatiotemporal surface EMG characteristics from rat triceps brachii muscle during treadmill locomotion indicate selective recruitment of functionally distinct muscle regions. *Experimental brain research. Experimentelle Hirnforschung. Experimentation cerebrale*, 138, 26-36.
- SCHOLLE, H. C., STRUPPLER, A., ANDERS, C. & SCHUMANN, N. P. 1992. [Control of isometric muscle contraction in muscle hypotonia of central origin: EMG mapping analysis]. *EEG-EMG Zeitschrift fur Elektroenzephalographie, Elektromyographie und verwandte Gebiete*, 23, 178-83.
- SCOTT, A., DANIELSON, P., ABRAHAM, T., FONG, G., SAMPAIO, A. V. & UNDERHILL, T. M. 2011. Mechanical force modulates scleraxis expression in bioartificial tendons. *J Musculoskeletal Neuronal Interact*, 11, 124-32.
- SCOTT, S. H. & LOEB, G. E. 1995. Mechanical properties of aponeurosis and tendon of the cat soleus muscle during whole-muscle isometric contractions. *J Morphol*, 224, 73-86.
- SEGAL, R. L., WOLF, S. L., DECAMP, M. J., CHOPP, M. T. & ENGLISH, A. W. 1991. Anatomical partitioning of three multiarticular human muscles. *Acta anatomica*, 142, 261-6.
- SELVANETTI, A., CIPOLLA, M. & PUDDU, G. 1997. Overuse tendon injuries: Basic science and classification. *Operative Techniques in Sports Medicine*, 5, 110-117.
- SHALABI, A., KRISTOFFERSEN-WIBERG, M., ASPELIN, P. & MOVIN, T. 2004a. Immediate Achilles tendon response after strength training evaluated by MRI. *Medicine and Science in Sports and Exercise*, 36, 1841-1846.
- SHALABI, A., KRISTOFFERSEN-WILBERG, M., SVENSSON, L., ASPELIN, P. & MOVIN, T. 2004b. Eccentric training of the gastrocnemius-soleus complex in chronic Achilles tendinopathy results in decreased tendon volume and intratendinous signal as evaluated by MRI. *American Journal of Sports Medicine*, 32, 1286-1296.
- SHAMPO, M. A. & KYLE, R. A. 1992. Medical mythology: Achilles. *Mayo Clinic proceedings. Mayo Clinic*, 67, 651.
- SHARMA, P. & MAFFULLI, N. 2005. Tendon injury and tendinopathy: healing and repair. *The Journal of bone and joint surgery. American volume*, 87, 187-202.
- SHEPSTONE, T. N., TANG, J. E., DALLAIRE, S., SCHUENKE, M. D., STARON, R. S. & PHILLIPS, S. M. 2005. Short-term high- vs. low-velocity isokinetic lengthening training results in greater hypertrophy of the elbow flexors in young men. *Journal of applied physiology*, 98, 1768-76.
- SILBERNAGEL, K. G., BRORSSON, A. & LUNDBERG, M. 2011. The majority of patients with Achilles tendinopathy recover fully when treated with exercise alone: a 5-year follow-up. *The American journal of sports medicine*, 39, 607-13.
- SILBERNAGEL, K. G., GUSTAVSSON, A., THOMEE, R. & KARLSSON, J. 2006. Evaluation of lower leg function in patients with Achilles tendinopathy. *Knee Surgery Sports Traumatology Arthroscopy*, 14, 1207-1217.
- SILBERNAGEL, K. G., THOMEE, R., THOMEE, P. & KARLSSON, J. 2001. Eccentric overload training for patients with chronic Achilles tendon pain--a randomised controlled study with reliability testing of the evaluation methods. *Scand J Med Sci Sports*, 11, 197-206.
- SLATER, H., THERIAULT, E., RONNINGEN, B. O., CLARK, R. & NOSAKA, K. 2010. Exercise-induced mechanical hypoalgesia in musculotendinous tissues of the lateral elbow. *Manual Therapy*, 15, 66-73.
- SMITH, C. W., YOUNG, I. S. & KEARNEY, J. N. 1996. Mechanical properties of tendons: changes with sterilization and preservation. *Journal of biomechanical engineering*, 118, 56-61.

- SMITH, R. K., BIRCH, H., PATTERSON-KANE, J., FIRTH, E. C., WILLIAMS, L., CHERDCHUTHAM, W., VAN WEEREN, W. R. & GOODSHIP, A. E. 1999. Should equine athletes commence training during skeletal development?: changes in tendon matrix associated with development, ageing, function and exercise. *Equine Vet J Suppl*, 30, 201-9.
- SPOOR, C. W. & VAN LEEUWEN, J. L. 1992. Knee muscle moment arms from MRI and from tendon travel. *J Biomech*, 25, 201-6.
- STANISH, W. D., RUBINOVICH, R. M. & CURWIN, S. 1986. Eccentric exercise in chronic tendinitis. *Clin Orthop Relat Res.*, 208, 65-8.
- STASINOPOULOS, D. & STASINOPOULOS, I. 2004. Comparison of effects of exercise programme, pulsed ultrasound and transverse friction in the treatment of chronic patellar tendinopathy. *Clinical rehabilitation*, 18, 347-52.
- STASINOPOULOS, D., STASINOPOULOS, I., PANTELIS, M. & STASINOPOULOU, K. 2009. Comparing the Effects of Exercise Program and Low-Level Laser Therapy with Exercise Program and Polarized Polychromatic Non-coherent Light (Bioptron Light) on the Treatment of Lateral Elbow Tendinopathy. *Photomedicine and Laser Surgery*, 27, 513-520.
- STAUBER, W. T. 1989. Eccentric action of muscles: physiology, injury, and adaptation. *Exercise and sport sciences reviews*, 17, 157-85.
- STAUDENMANN, D., KINGMA, I., DAFFERTSHOFER, A., STEGEMAN, D. F. & VAN DIEEN, J. H. 2009. Heterogeneity of muscle activation in relation to force direction: a multi-channel surface electromyography study on the triceps surae muscle. *Journal of electromyography and kinesiology : official journal of the International Society of Electrophysiological Kinesiology*, 19, 882-95.
- STERGIOULAS, A., STERGIOULA, M., AARSKOG, R., LOPES-MARTINS, R. A. B. & BJORDAL, J. M. 2008. Effects of low-level laser therapy and eccentric exercises in the treatment of recreational athletes with chronic achilles tendinopathy. *American Journal of Sports Medicine*, 36, 881-887.
- STILES, R. N. & RANDALL, J. E. 1967. Mechanical factors in human tremor frequency. *Journal of applied physiology*, 23, 324-30.
- SUGISAKI, N., KAWAKAMI, Y., KANEHISA, H. & FUKUNAGA, T. 2011. Effect of muscle contraction levels on the force-length relationship of the human Achilles tendon during lengthening of the triceps surae muscle-tendon unit. *Journal of biomechanics*, 44, 2168-71.
- SUN, Y. L., THORESON, A. R., CHA, S. S., ZHAO, C., AN, K. N. & AMADIO, P. C. 2010. Temporal response of canine flexor tendon to limb suspension. *Journal of applied physiology*, 109, 1762-8.
- SUSSMILCH-LEITCH, S. P., COLLINS, N. J., BIALOCERKOWSKI, A. E., WARDEN, S. J. & CROSSLEY, K. M. 2012. Physical therapies for Achilles tendinopathy: systematic review and meta-analysis. *Journal of foot and ankle research*, 5, 15.
- TAKAI, S., WOO, S. L., HORIBE, S., TUNG, D. K. & GELBERMAN, R. H. 1991. The effects of frequency and duration of controlled passive mobilization on tendon healing. *J Orthop Res*, 9, 705-13.
- TALLON, C., MAFFULLI, N. & EWEN, S. W. B. 2001. Ruptured Achilles tendons are significantly more degenerated than tendinopathic tendons. *Medicine & Science in Sports & Exercise*, 33, 1983-1990.
- TAN, S. C. & CHAN, O. 2008. Achilles and patellar tendinopathy: Current understanding of pathophysiology and management. *Disability and Rehabilitation*, 30, 1608-1615.
- TAYLOR, N. A., COTTER, J. D., STANLEY, S. N. & MARSHALL, R. N. 1991. Functional torque-velocity and power-velocity characteristics of elite athletes. *European journal of applied physiology and occupational physiology*, 62, 116-21.
- THEIS, N., MOHAGHEGHI, A. A. & KORFF, T. 2012. Method and strain rate dependence of Achilles tendon stiffness. *J Electromyogr Kinesiol*, 22, 947-53.
- THORPE, C. T., CLEGG, P. D. & BIRCH, H. L. 2010. A review of tendon injury: why is the equine superficial digital flexor tendon most at risk? *Equine Vet J*, 42, 174-80.

- THORPE, C. T., UDEZE, C. P., BIRCH, H. L., CLEGG, P. D. & SCREEN, H. R. 2012. Specialization of tendon mechanical properties results from interfascicular differences. *Journal of the Royal Society, Interface / the Royal Society*, 9, 3108-17.
- TUMILTY, S., MUNN, J., ABBOTT, J. H., MCDONOUGH, S., HURLEY, D. A., BASFORD, J. R. & BAXTER, G. D. 2010. Laser Therapy in the Treatment of Achilles Tendinopathy: A Randomised Controlled Trial. *Laser Florence 2009: A Gallery through the Laser Medicine World*, 1226, 163-169.
- TUMILTY, S., MUNN, J., ABBOTT, J. H., MCDONOUGH, S., HURLEY, D. A. & BAXTER, G. D. 2008. Laser therapy in the treatment of Achilles tendinopathy: A pilot study. *Photomedicine and Laser Surgery*, 26, 25-30.
- VACZI, M., TIHANYI, J., HORTOBAGYI, T., RACZ, L., CSENDE, Z., COSTA, A. & PUCSOK, J. 2011. Mechanical, biochemical, and electromyographic responses to short-term eccentric-concentric knee extensor training in humans. *Journal of strength and conditioning research / National Strength & Conditioning Association*, 25, 922-32.
- VAILAS, A. C., TIPTON, C. M., LAUGHLIN, H. L., TCHENG, T. K. & MATTHES, R. D. 1978. Physical-Activity and Hypophysectomy on Aerobic Capacity of Ligaments and Tendons. *Journal of Applied Physiology*, 44, 542-546.
- VAN DIJK, C. N., VAN STERKENBURG, M. N., WIEGERINCK, J. I., KARLSSON, J. & MAFFULLI, N. 2011. Terminology for Achilles tendon related disorders. *Knee surgery, sports traumatology, arthroscopy : official journal of the ESSKA*, 19, 835-41.
- VERSCHUEREN, S. M., ROELANTS, M., DELECLUSE, C., SWINNEN, S., VANDERSCHUEREN, D. & BOONEN, S. 2004. Effect of 6-month whole body vibration training on hip density, muscle strength, and postural control in postmenopausal women: a randomized controlled pilot study. *J Bone Miner Res*, 19, 352-9.
- VISENTINI, P. J., KHAN, K. M., COOK, J. L., KISS, Z. S., HARCOURT, P. R. & WARK, J. D. 1998. The VISA score: an index of severity of symptoms in patients with jumper's knee (patellar tendinosis). Victorian Institute of Sport Tendon Study Group. *Journal of science and medicine in sport / Sports Medicine Australia*, 1, 22-8.
- VOGEL, H. G. 1983. Age dependence of mechanical properties of rat tail tendons (hysteresis experiments). *Aktuelle Gerontol*, 13, 22-7.
- WAGGETT, A. D., RALPHS, J. R., KWAN, A. P., WOODNUTT, D. & BENJAMIN, M. 1998. Characterization of collagens and proteoglycans at the insertion of the human Achilles tendon. *Matrix biology : journal of the International Society for Matrix Biology*, 16, 457-70.
- WAKAHARA, T., KANEHISA, H., KAWAKAMI, Y. & FUKUNAGA, T. 2007. Fascicle behavior of medial gastrocnemius muscle in extended and flexed knee positions. *Journal of biomechanics*, 40, 2291-8.
- WAKAHARA, T., KANEHISA, H., KAWAKAMI, Y. & FUKUNAGA, T. 2009. Effects of knee joint angle on the fascicle behavior of the gastrocnemius muscle during eccentric plantar flexions. *Journal of electromyography and kinesiology : official journal of the International Society of Electrophysiological Kinesiology*, 19, 980-7.
- WAKAHARA, T., MIYAMOTO, N., SUGISAKI, N., MURATA, K., KANEHISA, H., KAWAKAMI, Y., FUKUNAGA, T. & YANAI, T. 2012. Association between regional differences in muscle activation in one session of resistance exercise and in muscle hypertrophy after resistance training. *European journal of applied physiology*, 112, 1569-76.
- WAKELING, J. M., NIGG, B. M. & ROZITIS, A. I. 2002a. Muscle activity damps the soft tissue resonance that occurs in response to pulsed and continuous vibrations. *J Appl Physiol*, 93, 1093-103.
- WAKELING, J. M., PASCUAL, S. A. & NIGG, B. M. 2002b. Altering muscle activity in the lower extremities by running with different shoes. *Med Sci Sports Exerc*, 34, 1529-32.
- WAKELING, J. M., VON TSCHARNER, V., NIGG, B. M. & STERGIOU, P. 2001. Muscle activity in the leg is tuned in response to ground reaction forces. *J Appl Physiol*, 91, 1307-17.
- WANG, J. H. 2006. Mechanobiology of tendon. *Journal of biomechanics*, 39, 1563-82.

- WANG, J. H., GUO, Q. & LI, B. 2011. Tendon Biomechanics and Mechanobiology-A Minireview of Basic Concepts and Recent Advancements. *Journal of hand therapy : official journal of the American Society of Hand Therapists*.
- WANG, J. H., JIA, F., YANG, G., YANG, S., CAMPBELL, B. H., STONE, D. & WOO, S. L. 2003. Cyclic mechanical stretching of human tendon fibroblasts increases the production of prostaglandin E2 and levels of cyclooxygenase expression: a novel in vitro model study. *Connective tissue research*, 44, 128-33.
- WANG, N., BUTLER, J. P. & INGBER, D. E. 1993. Mechanotransduction across the cell surface and through the cytoskeleton. *Science*, 260, 1124-7.
- WARDEN, S. J., METCALF, B. R., KISS, Z. S., COOK, J. L., PURDAM, C. R., BENNELL, K. L. & CROSSLEY, K. M. 2008. Low-intensity pulsed ultrasound for chronic patellar tendinopathy: a randomized, double-blind, placebo-controlled trial. *Rheumatology*, 47, 467-471.
- WASIELEWSKI, N. J. & KOTSKO, K. M. 2007. Does eccentric exercise reduce pain and improve strength in physically active adults with symptomatic lower extremity tendinosis? A systematic review. *Journal of Athletic Training*, 42, 409-421.
- WELLS, P. N. 1987. The prudent use of diagnostic ultrasound. *Ultrasound in medicine & biology*, 13, 391-400.
- WESTGAARD, R. H. & DE LUCA, C. J. 1999. Motor unit substitution in long-duration contractions of the human trapezius muscle. *Journal of neurophysiology*, 82, 501-4.
- WESTH, E., KONGSGAARD, M., BOJSEN-MOLLER, J., AAGAARD, P., HANSEN, M., KJAER, M. & MAGNUSSON, S. P. 2008. Effect of habitual exercise on the structural and mechanical properties of human tendon, in vivo, in men and women. *Scandinavian Journal of Medicine & Science in Sports*, 18, 23-30.
- WESTING, S. H., CRESSWELL, A. G. & THORSTENSSON, A. 1991. Muscle activation during maximal voluntary eccentric and concentric knee extension. *European journal of applied physiology and occupational physiology*, 62, 104-8.
- WESTING, S. H., SEGER, J. Y., KARLSON, E. & EKBLUM, B. 1988. Eccentric and concentric torque-velocity characteristics of the quadriceps femoris in man. *European journal of applied physiology and occupational physiology*, 58, 100-4.
- WESTING, S. H., SEGER, J. Y. & THORSTENSSON, A. 1990. Effects of electrical stimulation on eccentric and concentric torque-velocity relationships during knee extension in man. *Acta physiologica Scandinavica*, 140, 17-22.
- WIJESEKERA, N. T., CALDER, J. D. & LEE, J. C. 2011. Imaging in the assessment and management of Achilles tendinopathy and paratendinitis. *Semin Musculoskelet Radiol*, 15, 89-100.
- WILLBERG, L., SUNDING, K., FORSSBLAD, M., FAHLSTROM, M. & ALFREDSON, H. 2011. Sclerosing polidocanol injections or arthroscopic shaving to treat patellar tendinopathy/jumper's knee? A randomised controlled study. *British Journal of Sports Medicine*, 45, 411-5.
- WILLBERG, L., SUNDING, K., OHBERG, L., FORSSBLAD, M., FAHLSTROM, M. & ALFREDSON, H. 2008. Sclerosing injections to treat midportion Achilles tendinosis: a randomised controlled study evaluating two different concentrations of Polidocanol. *Knee surgery, sports traumatology, arthroscopy : official journal of the ESSKA*, 16, 859-64.
- WILLIAMS, J. G. 1986. Achilles tendon lesions in sport. *Sports Medicine*, 3, 114-35.
- WOLEDGE, R. C., CURTIN, N. A. & HOMSHER, E. 1985. Energetic aspects of muscle contraction. *Monogr Physiol Soc*, 41, 1-357.
- WOLF, S. L. & KIM, J. H. 1997. Morphological analysis of the human tibialis anterior and medial gastrocnemius muscles. *Acta anatomica*, 158, 287-95.
- WOODLEY, B. L., NEWSHAM-WEST, R. J. & BAXTER, G. D. 2007. Chronic tendinopathy: effectiveness of eccentric exercise. *British Journal of Sports Medicine*, 41, 188-198.
- WREN, T. A., YERBY, S. A., BEAUPRE, G. S. & CARTER, D. R. 2001. Mechanical properties of the human achilles tendon. *Clinical biomechanics*, 16, 245-51.

- WU, G. & REN, X. 2009. Speed effect of selected Tai Chi Chuan movement on leg muscle activity in young and old practitioners. *Clinical Biomechanics*, 24, 415-421.
- WU, G., SIEGLER, S., ALLARD, P., KIRTLEY, C., LEARDINI, A., ROSENBAUM, D., WHITTLE, M., D'LIMA, D. D., CRISTOFOLINI, L., WITTE, H., SCHMID, O. & STOKES, I. 2002. ISB recommendation on definitions of joint coordinate system of various joints for the reporting of human joint motion--part I: ankle, hip, and spine. International Society of Biomechanics. *Journal of biomechanics*, 35, 543-8.
- WU, J. J. 2006. Quantitative constitutive behaviour and viscoelastic properties of fresh flexor tendons. *Int J Artif Organs*, 29, 852-7.
- WYNDOW, N., COWAN, S. M., WRIGLEY, T. V. & CROSSLEY, K. M. 2012. Triceps surae activation is altered in male runners with Achilles tendinopathy. *J Electromyogr Kinesiol*.
- YAMAMOTO, N. & HAYASHI, K. 1998. Mechanical properties of rabbit patellar tendon at high strain rate. *Bio-medical materials and engineering*, 8, 83-90.
- YELLAND, M. J., SWEETING, K. R., LYFTOGT, J. A., NG, S. K., SCUFFHAM, P. A. & EVANS, K. A. 2011. Prolotherapy injections and eccentric loading exercises for painful Achilles tendinosis: a randomised trial. *British journal of sports medicine*, 45, 421-8.
- YORK, G. & KIM, Y. 1999. Ultrasound processing and computing: review and future directions. *Annual review of biomedical engineering*, 1, 559-88.
- YOUNG, M. A., COOK, J. L., PURDAM, C. R., KISS, Z. S. & ALFREDSON, H. 2005. Eccentric decline squat protocol offers superior results at 12 months compared with traditional eccentric protocol for patellar tendinopathy in volleyball players. *Br J Sports Med*, 39, 102-5.
- YU, J., PARK, D. & LEE, G. 2012. Effect of Eccentric Strengthening on Pain, Muscle Strength, Endurance, and Functional Fitness Factors in Male Patients with Achilles Tendinopathy. *American journal of physical medicine & rehabilitation / Association of Academic Physiatrists*.
- ZAJAC, F. E. 1989. Muscle and tendon: properties, models, scaling, and application to biomechanics and motor control. *Critical reviews in biomedical engineering*, 17, 359-411.
- ZWERVER, J., BREDEWEG, S. W. & HOF, A. L. 2007. Biomechanical analysis of the single-leg decline squat. *British Journal of Sports Medicine*, 41, 264-268.

## **Appendix I**



Queen Mary, University of London

Room E16  
Queen's Building  
Queen Mary University of London  
Mile End Road  
London E1 4NS

**Queen Mary Research Ethics Committee**

Hazel Covill  
Research Ethics Administrator

Tel: +44 (0) 20 7882 2207

Email: [h.covill@qmul.ac.uk](mailto:h.covill@qmul.ac.uk)

c/o Dr Dylan Morrissey  
Centre for Sports and Exercise Medicine  
Mile End Hospital  
Bancroft Road  
Mile End.

29<sup>th</sup> July 2009

To Whom It May Concern:

**Re: QMREC2008/85 – Modelling eccentric and concentric loading of the triceps sura before and after training: an observation in normal subjects**

The above study was approved by The Queen Mary Research Ethics Committee on the 14<sup>th</sup> January 2009. A protocol amendment (concerning increased participant groups and methodological refinement) was conditionally approved by the Committee on the 8<sup>th</sup> July 2009. Full approval was ratified by Chair's Action on the 29<sup>th</sup> July 2009.

(N.B. An updated title for this study being *Comparing Achilles tendon stiffness during eccentric and concentric movement: An in vivo study in normal subjects*).

This approval is valid for a period of two years, (if the study is not started before this date then the applicant will have to reapply to the Committee).

Yours faithfully

A handwritten signature in black ink, appearing to read "E. Hall".

Ms Elizabeth Hall – QMREC Chair.

Patron: Her Majesty the Queen  
Incorporated by Royal  
Charter as Queen Mary  
and Westfield College,  
University of London





**Centre for Sport and Exercise Medicine**

Barts and the London School of Medicine and Dentistry

Mann Ward

The Mile End Hospital

Bancroft Road

London E1 4DG

Telephone: +44 (0)20 7223 8839

Fax: +44 (0)20 8983 6500

**Information sheet**

**Research study** : Modelling eccentric and concentric loading of triceps surae complex

**Information for participants**

We would like to invite you to be part of this research project. You should only agree to take part if you want to. If you choose not to take part there won't be any disadvantages for you.

Please read the following information carefully before you decide to take part; this will tell you why the research is being done and what you will be asked to do if you take part. Please ask if there is anything that is not clear or if you would like more information.

If you decide to take part you will be asked to sign the attached form to say that you agree.

You are still free to withdraw at any time and without giving a reason.

Details of study

Tendons link muscle to bone and allow us to move. In some people, for reasons we don't completely understand, certain tendons can become painful and stiff. We call this a tendinopathy. Exercise programs have been developed to help reduce this pain and stiffness and appear to work well. The way these exercises work and their effects on tendons are not very well understood at the moment. We are trying to model these special exercises to investigate Achilles tendon stiffness at various points. We are doing this in people with normal tendons first. We hope to use this information for a better understanding of exercise treatments and to maybe help develop better treatments in the future.

What will you have to do?

- Your Achilles tendon will be measured in terms of cross sectional area, length and elongation by an ultrasound scan. This requires placing ultrasound probe on skin to take images (the same type used to image babies in mother's womb). The activity of your muscle will be measured using a technique called EMG to see how much your muscle contract during exercise. This technique simply requires attachment of electrodes with double-sided sticky tape on your right leg. To study motion of the lower limb during exercise marker will be placed on your skin allowing your movement to be tracked.
- You will need to bare your right leg until knee.
- This is highly non-invasive study and does not involve any radiation.

- We will make the measurements during the movement. We will ask you to repeat each movement for three times to ensure that our measurements are accurate.
- The complete procedure will take only an hour.

There are no personal benefits to being involved in this study.

All personal information will be kept confidential and filed securely within the Department of Sports and Exercise Medicine, QMUL. This will comply with the Data Protection Act 1998. In the event of you suffering any adverse effects as a consequence of your participation in this study, you will be compensated through Queen Mary University of London's 'No Fault Compensation Scheme.'

If you would like further information about this study please feel free to contact at:

If you do decide to take part you will be given this information sheet to keep and be asked to sign a consent form.

**Consent**

Please complete this form after you have read the Information Sheet and/or listened to an explanation about the research.

Title of Study: Modelling eccentric and concentric loading of the triceps surae

Queen Mary Research Ethics Committee Ref: \_\_\_\_\_

. • Thank you for considering taking part in this research. The person organizing the research must explain the project to you before you agree to take part.

. • If you have any questions arising from the Information Sheet or explanation already given to you, please ask the researcher before you decide whether to join in. You will be given a copy of this Consent Form to keep and refer to at any time.

. • *I understand that if I decide at any other time during the research that I no longer wish to participate in this project, I can notify the researchers involved and be withdrawn from it immediately.*

. • *I consent to the processing of my personal information for the purposes of this research study. I understand that such information will be treated as strictly confidential and handled in accordance with the provisions of the Data Protection Act 1998.*

**Participant's Statement:**

I \_\_\_\_\_ agree that the research project named above has been explained to me to my satisfaction and I agree to take part in the study. I have read both the notes written above and the Information Sheet about the project, and understand what the research study involves.

Signed:

Date:

**Investigator's Statement:**

I \_\_\_\_\_ confirm that I have carefully explained the nature, demands and any foreseeable risks (where applicable) of the proposed research to the volunteer.

Signed: Date:

## **Appendix II**

## 1) Matlab code for tracking the MTJ junction

```

function res=YellowThreeAuto(FNo)
File= ['F:\SpeedStudyL1\Video' int2str(FNo) '.mat'];
CFile=['F:\SpeedStudyL1\AllFiles\Coda' int2str(FNo) '.mat'] ;
figure(1); clf; figure(2); clf; figure(3); clf; figure(4); clf;
hlab=text(0, 0.7, {'Dock This figure' 'Context sensitive instructions will
be shown here'}, 'Units', 'normalized');
set(hlab, 'EdgeColor', 'b'); axis off;

AA=[]; II=[];
load(File, 'Vid', 'AA', 'II', 'FrameRate')
load(CFile, 'TT')
TTvid=round(TT*FrameRate);
if ~isempty(II)
    figure(3); clf; plot(II(:,1), '.');xlim([1 size(Vid,3)]);
    hold on; plot([1 1]*TTvid(1), ylim, 'g',[1 1]*TTvid(2), ylim, 'g')
    set(hlab, 'String', '.....
    {' Click on the frame at which you want to start' })
    [x y]=ginput(1); fs=round(x);
else
    fs=2;
end
Vid=Vid(:,1:300,:); % cut off the bottom of the pictures to speed up and
increase radon contrast
[XX YY FF]= size(Vid); mYY=round(YY/2); mXX=round(XX/2);
but=1;
%% look for good starting frame
while but==1
if fs<1; fs=1; end% don't run off LHs
    pic=Vid(:, :, fs)';
    figure(1); clf; image(cat(3,pic,pic,pic));hold on; plot([1 1]*XX/2,
ylim, 'r'); text(10,10, int2str(fs), 'Color', 'y');
    set(hlab, 'String', '.....
    {' Left click to change frame no. Advance if right of red line,
Retard if left of red line',....
' Right click to use this frame'})
    [x,y,but]=ginput(1); if x>mean(xlim); fs=fs+1; else fs=fs-1; end
if ~isempty(lastwarn); [msgstr msgid] = lastwarn; warning('off', msgid);
end%#ok<ASGLU>
end

%% mark two points on proto yellow line
TwoDots
kk=4;
%% frame loop goes through the movie finding a pair of lines for each frame
tic
Free=0;
flist=[fs:FF fs:-1:1];
f=0;
while f>=0 && f<=length(flist)-1;
    f=f+1;
if flist(f)==fs; Atarg=AtargS; Itarg=ItargS; Ath=3; Ith=3; DelI=12; end

    pic=Vid(:, :, flist(f))'; figure(1); clf; image(cat(3,pic,pic,pic)); hold
on; title(flist(f))
    but=1; UseTop=0; UseBot=0;
if Free>0;
    Free=Free-1;
    FindTwoLines

```

```

        drawnow
else
while ~isempty(but)
    FindTwoLines
        set(hlab, 'String', .....
            {' Left click if you want to remark the line', .....
            ' "8" on keypad to move line up', .....
            ' "2" on keypad to move line down', .....
            ' Up Arrow to move red up to white', .....
            ' Down Arrow to move red down to white', .....
            ' Left Arrow to rotate counterclockwise', .....
            ' Right Arrow to rotate clockwise', .....
            ' + on keypad to run auto for 10 frames', .....
            ' - on keypad to move back 10 frames', .....
            ' "s" to save and quit'})
        [x y but]=ginput(1);

if isempty(but); continue; end
switch but
case 1 % Left button
                TwoDots; Atarg=AtargS; Itarg=ItargS;
case 56 % eight key
                Itarg=Itarg+3;
case 50 % two key
                Itarg=Itarg-3;
case 3 % Right button
                TwoDots; Atarg=AtargS; Itarg=ItargS;
case 31 % Up arrow key
if UseBot; UseBot=0; else UseTop=1; UseBot=0; end
case 30 % Down arrow key
if UseTop; UseTop=0; else UseBot=1; UseTop=0; end
case 28 % right arrow key
                Atarg=Atarg+1;
case 29 % Left arrow key
                Atarg=Atarg-1;
case 115 % s for save
break
case 43
                Free=10; but=[]; %#ok<NASGU>% Plus key. runs auto for
10 points
case 45
                f=f-11; but=[]; % Minus key; goes back 10 points

end
end
if but==115; break; end
end
    %% prepare for next frame
    Atarg=AA(flist(f),1); if Atarg<93; Atarg=93; end
    Itarg=II(flist(f),1); % target for first line next round
    DelI=DelInext; if DelI<10; DelI=8; end; if DelI<13; DelI=13; end
    figure(3); clf; plot(II(:,1), '.');xlim([1 size(Vid,3)]); hold on;
plot([flist(f) flist(f)], ylim, 'r')
    hold on; plot([1 1]*TTvid(1), ylim, 'g',[1 1]*TTvid(2), ylim, 'g')

    save(File, 'AA', 'II', '-append')

end
save(File, 'AA', 'II', '-append')
res=1;

```

```

function FindTwoLines
    pic=Vid(:,:,flist(f))';
    figure(2); clf; image(cat(3,pic,pic,pic)); hold on;
    disp([flist(f) Atarg, Ath, Itarg, Ith, kk, but, UseTop, UseBot])
    %% find first lines
    [A1 I1 R]= FindLinesY(pic, Atarg, Ath, Itarg, Ith, kk);
    %% find other lines about 12 pixel above and below the first and
parallel to it
    Atarg2=mean(A1); Itargdw=mean(I1)-DelI; Itargup=mean(I1)+DelI;
Ith=3;
    [Adw Idw Rdw]= FindLinesY(pic, Atarg2, 1, Itargup, 7, kk);
    [Aup Iup Rup]= FindLinesY(pic, Atarg2, 1, Itargdw, 7, kk);
    A=A1; I=I1; DelInext=(abs(mean(Aup-A))+abs(mean(Aup-A)))/2;
if UseTop; A=Aup; I=Iup; end
if UseBot; A=Adw; I=Idw; end
    %% Draw the lines
    rub=DrawLines(XX, YY, mean(A1), mean(I1), 'w', 1);
    rub=DrawLines(XX, YY, mean(Adw), mean(Idw), 'w', 1);
    rub=DrawLines(XX, YY, mean(Aup), mean(Iup), 'w', 1);
    rub=DrawLines(XX, YY, mean(A), mean(I), 'r', 1); %#ok<NASGU>

    %% save the results (now only one value)
    AA(flist(f),1)=mean(A); II(flist(f),1)=mean(I); %#ok<*SAGROW>

end

function TwoDots
for q=1:2
    set(hlab, 'String',.....
        {' Mark two points well spaced on the line you want to use',....
' (Either left or right click is OK)'});
        [x(q) y(q)]=ginput(1);
        plot(x(q), y(q), '+r')
end
    AtargS=90+round((180/pi)*atan2(abs(diff(y)), abs(diff(x))));
ItargS=mYY-(y(1)+(diff(y)/diff(x))*(mXX-x(1)));
end

end

function res=GreenThreeAuto(FNo)
File= ['F:\SpeedStudyL1\Video' int2str(FNo) '.mat'];
CFile=['F:\SpeedStudyL1\AllFiles\Coda' int2str(FNo) '.mat'] ;
figure(1); clf; figure(2); clf; figure(3); clf;
AA=[]; II=[]; XMs=[]; YMs=[];
load(File, 'Vid', 'AA', 'II', 'XMs', 'YMs', 'FrameRate')
load(CFile, 'TT')
TTvid=round(TT*FrameRate);
if ~isempty(XMs)
    figure(3); clf; plot(XMs, '.');xlim([1 size(Vid,3)]);
    hold on; plot([1 1]*TTvid(1), ylim, 'g',[1 1]*TTvid(2), ylim, 'g')
    [x y]=ginput(1); fs=round(x);
else
    fs=2;
end
Vid=Vid(:,1:300,:); % cut off the bottom of the pictures to speed up and
increase radon contrast
[XX YY FF]= size(Vid); mYY=round(YY/2); mXX=round(XX/2);

```



```

but=1;
%% look for good starting frame
while but==1
if fs<1; fs=1; end% don't run off LHs
    pic=Vid(:, :, fs)';
    figure(1); clf; imshow(pic, []); hold on; plot([1 1]*XX/2, ylim, 'r');
text(10,10, int2str(fs), 'Color', 'y');
    [IntY SlpY]=DrawLines(XX,YY, AA(fs,1), II(fs,1), 'y', 1);
    [x,y,but]=ginput(1); if x>mean(xlim); fs=fs+1; else fs=fs-1; end
if ~isempty(lastwarn); [msgstr msgid] = lastwarn; warning('off', msgid);
end%#ok<ASGLU>
end

%% get init Xlim
[Xlim rub]=ginput(1);
Ylim=15+round(YY-(IntY+SlpY*Xlim));
AtargS=75; ItargS=0; IthS=4;
corner=pic(1:Ylim,1:round(Xlim)); [YYc XXc]=size(corner);
mYY=round(YYc/2); mXX=round(XXc/2);
figure(2); clf; imshow(corner, []); hold on;
TwoDots

kk=4;
%% frame loop goes through the movie finding a pair of lines for each frame

Free=0;
flist=[fs:FF fs:-1:1];
f=0;
while f>=0 && f<=length(flist)-1;
    f=f+1;
    Ath=4; Ith=4;
if flist(f)==fs; Atarg=AtargS; Itarg=ItargS; Ith=IthS; DelI=12; end
    pic=Vid(:, :, flist(f))'; figure(1); clf; imshow(pic, []); hold on;
title(flist(f))

    but=1; UseTop=0; UseBot=0;
if Free>0;
    Free=Free-1;
    FindTwoLines
    drawnow
else
while ~isempty(but)
    FindTwoLines
    figure(2)
    [x y but]=ginput(1);
if isempty(but); continue; end
switch but
case 1 % Left button
    TwoDots; Atarg=AtargS; Itarg=ItargS;
case 56 % eight key
    Itarg=Itarg+3;
case 50 % two key
    Itarg=Itarg-3;
case 3 % Right button
    TwoDots; Atarg=AtargS; Itarg=ItargS;
case 31 % Up arrow key
if UseBot; UseBot=0; else UseTop=1; UseBot=0; end
case 30 % Down arrow key
if UseTop; UseTop=0; else UseBot=1; UseTop=0; end
case 28 % right arrow key

```

```

                Atarg=Atarg+1;
case 29 % Left arrow key
                Atarg=Atarg-1;
case 115 % S for save
break
case 43
                Free=10; but=[]; %#ok<NASGU>% Plus key. runs auto for
10 points
case 45
                f=f-11; but=[]; % Minus key; goes back 10p oints
end
end
                save(File, 'XMs', 'YMs', '-append')
if but==115; break; end
end
        %% prepare for next frame
if flist(f)<FF; [IntY SlpY]=DrawLines (XX,YY, AA(flist(f)+1,1),
II(flist(f)+1,1), 'y', 0); end
        Xlim=XM-40;
if Xlim<100; Xlim=100; end
if Xlim>XX; Xlim=XX; end
        Ylim=15+round(YY-(IntY+SlpY*Xlim));
        Atarg=mean(A); if Atarg>93; Atarg=93; end
        Itarg=mean(I); % target for first line next round
        DelI=DelInext; if DelI<7; DelI=7; end; if DelI>13; DelI=13; end
figure(3); clf; plot(XMs, '.');xlim([1 size(Vid,3)]); hold on;
plot([flist(f) flist(f)], ylim, 'r')
        hold on; plot([1 1]*TTvid(1), ylim, 'g',[1 1]*TTvid(2), ylim, 'g')
        save(File, 'XMs', '-append')
end

res=1;

function FindTwoLines
pic=Vid(:, :, flist(f))';
corner=pic(1:Ylim,1:round(Xlim));[YYc XXc]=size(corner);
mYY=round(YYc/2); mXX=round(XXc/2);
figure(2); clf; imshow(corner, []); hold on;
disp([flist(f) Atarg, Ath, Itarg, Ith, kk, but, UseTop, UseBot])
%% find first lines
[A1 I1 R]= FindLinesY(corner, Atarg, Ath, Itarg, Ith, kk);
%% find other lines about 12 pixel above and below the first and
parallel to it
        Atarg2=mean(A1); Itargdw=mean(I1)-DelI; Itargup=mean(I1)+DelI;
Ith=3;
        [Adw Idw Rdw]= FindLinesY(pic, Atarg2, 1, Itargup, 7, kk);
        [Aup Iup Rup]= FindLinesY(pic, Atarg2, 1, Itargdw, 7, kk);
        A=A1; I=I1; DelInext=(abs(mean(Aup-A))+abs(mean(Aup-A)))/2;
if UseTop; A=Aup; I=Iup; end
if UseBot; A=Adw; I=Idw; end
        %% Draw the lines
rub=DrawLines (XXc, YYc, mean(A1), mean(I1), 'w', 1);
rub=DrawLines (XXc, YYc, mean(Adw), mean(Idw), 'w', 1);
rub=DrawLines (XXc, YYc, mean(Aup), mean(Iup), 'w', 1);
[Ints SlpS]=DrawLines (XXc, YYc, A, I, 'g', 1); %#ok<NASGU>
IntsG=Ints+(YY-YYc);
figure(1);
clf; imshow(pic, []); hold on
[rub1 rub2]=DrawLines (XX,YY, AA(flist(f),1), II(flist(f),1), 'y',
1);
for k=1:kk

```

```

        plot([0 XXc],YY-[IntsG(k) IntsG(k)+Slps(k)*XXc], ':g')
end
[XM YM]=FindCrossY(YY, IntsG, Slps, IntY, SlpY, 1);
%% save the results (now only one value)
XMs(flist(f))=XM; YMs(flist(f))=YM; %#ok<*SAGROW>

end

function TwoDots
for q=1:2
    [x(q) y(q)]=ginput(1);
    plot(x(q), y(q), '+r')
end
    AtargS=90-round((180/pi)*atan2(diff(y), diff(x)));
ItargS=mYY-(y(1)+(diff(y)/diff(x))*(mXX-x(1)));
end

end

```

**2 Matlab code for testing and optimising the Fast Fourier transform (FFT). The FFT was used to compute the digital Fourier transform and then its power was computed.**

```
% clear
Fs = 1000; % Sample frequency (Hz)
t = (0:2047)/Fs; % ~3 sec sample
XX = (1.33)*sin(2*pi*15.66*t) ... % ~15 Hz component
    + (1.71)*sin(2*pi*41.4*(t-2)) ... % ~40 Hz component
    + (0.354)*randn(size(t)); % Gaussian noise;
%XX=x;
VarX=var(XX)
% Use fft to compute the DFT Four and its Power:
Npoints = length(XX); % Window length
Fi=Fs/Npoints; % interval of frequency
represented by each point in the fourier
Freq = (0:Npoints/2-1)*Fi; % Frequency scale for the fourier
Four = fft(XX); % DFT

% this scaling gives a consistent value for Amp so that the Power
% sums without further scaling to give the correct total variance
% therefore the Amp terms will be independent of the sampling
% frequency because the variance is independent of the sampling
% frequency
Scale=sqrt(2)/Npoints;
Amp=abs(Four)*Scale; % amplitude of the DFT
Power=Amp.^2; % Power of the DFT
Varcurve=cumsum(Power(1:Npoints/2));
SF=max(Varcurve)
figure(2); clf
%plot(Freq,Varcurve, '-b', [0 50], VarX*[1 1], 'r')
plot(Power)
xlim([0 50])
```

**3 Matlab code for testing the effect of smoothing on the resulting FFT output on an EMG signal.**

```
Time=0:0.001:4; % signal time
Freq=10; % frequency
Amp=5+0.1*sin(Time*Freq*2*pi); % Amplitude of input signal
EMG=Amp.*sin(Time*184*2*pi); % Input EMG signal
windowSize = 121; % or 121; smoothing filter window size
Fs=1000; % Sampling frequency
sEMG=filter(ones(1,windowSize)/windowSize,1,abs(EMG)); % smooth EMG
Ebit=sEMG;
L=length(Ebit); % length of signal
Tbit=Time; % time
pp=polyfit(Tbit, Ebit, 1); yy=polyval(pp,Tbit); % polynomial fit
Ebit=Ebit-yy;
Four = fft(Ebit); Scale=sqrt(2)/L;% taking fast Fourier transform
Amp=abs(Four(1:round(L/2)))*Scale; % Rectification
Power=Amp.^2; % power calculation
Fi=Fs/L; Freq = (1:round(L/2))*Fi; %
CumPow=cumsum(Power); %cumulative sum of power
figure(1); clf
plot(EMG); hold on
grid on;
xlabel('Frequency Hz'); ylabel('Amplitude of fourier terms')
plot(Freq(6:500), Amp(6:500)); hold on
grid on;
xlabel('time (ms)'); ylabel('EMG (mv)')
```



